

# **Zooming in on Platelets in Hemostatic Disorders**

**Maurice Swinkels**

The research described in this thesis was performed at the Department of Hematology, Erasmus University Medical Center, Rotterdam, The Netherlands.

ISBN: 978-94-6496-039-6

Cover: Inge Snoeren (design) and Maurice Swinkels (images)

Design: Inge Snoeren

Printing: Gildeprint

© Maurice Swinkels, 2024.

# Zooming in on Platelets in Hemostatic Disorders

## Inzoomen op bloedplaatjes in hemostatische ziektes

Proefschrift

ter verkrijging van de graad van doctor aan de  
Erasmus Universiteit Rotterdam  
op gezag van de  
rector magnificus

Prof.dr. A.L. Bredenoord

en volgens besluit van het College voor Promoties.  
De openbare verdediging zal plaatsvinden op

woensdag 20 maart 2024 om 13:00 uur

door

Maurice Wilhelmus Josephus Swinkels  
geboren te Asten.

## **Promotiecommissie:**

**Promotoren:** Prof.dr. F.W.G. Leebeek  
Prof.dr. J.J. Voorberg

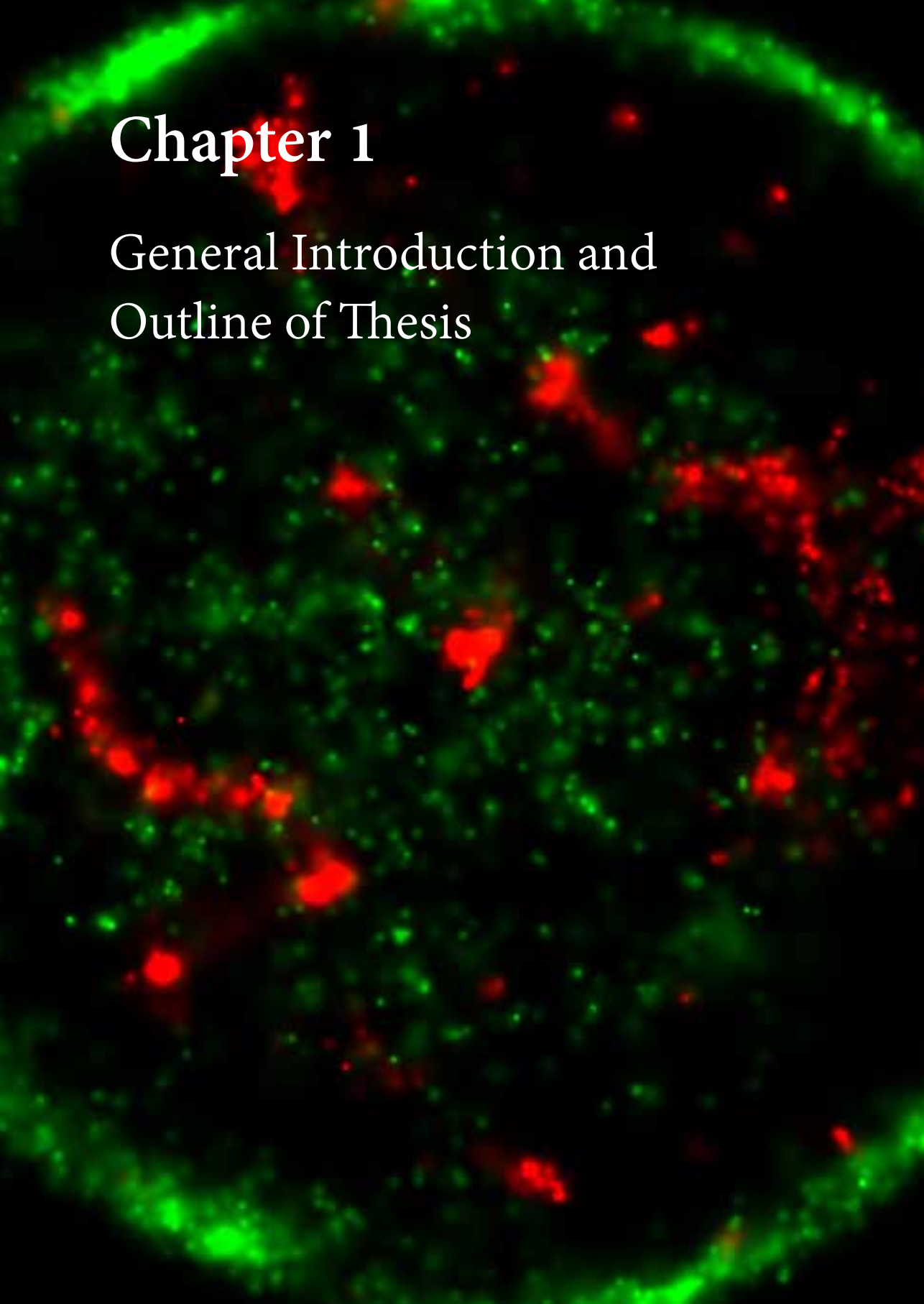
**Overige leden:** Prof.dr. M.P.M. de Maat  
Dr. J.M.E.M. Cosemans  
Prof.dr. A.W. Langerak

**Copromotoren:** Dr. A.J.G. Jansen  
Dr.ir. R. Bierings

# Table of Contents

<i>Chapter 1</i> - General introduction and outline of thesis	8
<b>Part 1: Platelets in ITP: Opportunities and Challenges</b>	
<i>Chapter 2</i> - Emerging concepts in immune thrombocytopenia	20
<i>Chapter 3</i> - COVID-19 vaccination in patients with immune thrombocytopenia	50
<b>Part 2: Platelet and VWF: Key Partners in Disease and Health</b>	
<i>Chapter 4</i> - Platelet degranulation and bleeding phenotype in a large cohort of Von Willebrand disease patients	68
<i>Chapter 5</i> - Quantitative 3D microscopy highlights altered von Willebrand factor $\alpha$ -granule storage in patients with von Willebrand disease with distinct pathogenic mechanisms	82
<i>Chapter 6</i> - Quantitative super-resolution imaging of platelet degranulation reveals differential release of VWF and VWF propeptide from alpha-granules	118
<i>Chapter 7</i> - General discussion and conclusion	150
<i>Chapter 8</i> - Summary	164
<b>Appendices</b>	
List of publications	172
About the author	173
PhD portfolio	174
Dankwoord	176



A fluorescence microscopy image of a cell. The cell is roughly circular and shows a bright green ring along its periphery, likely representing the plasma membrane. The interior of the cell is filled with numerous small green spots and several larger, bright red spots, which could represent different organelles or protein localizations. The background is black.

# Chapter 1

General Introduction and  
Outline of Thesis

## Introduction

### **Platelets and hemostasis - "Once Upon a Time in the Bloodstream"**

A variety of highly specialized cells circulate in blood, that have diverse roles in physiology such as the transportation of oxygen, hemostasis, wound healing and the identification and neutralization of pathogens as part of the immune system.

Platelets are anuclear and one of the smallest cellular components of the bloodstream, yet they are essential for their role in hemostasis and have also been implicated in immunity [1]. Platelets are produced by their precursor megakaryocytes, polynuclear cells residing in the bone marrow that bud off individual platelets into the bloodstream [2]. Platelet production is maintained by thrombopoietin (TPO) produced in the liver, of which levels are regulated by the number of platelets in the circulation [3]. This delicate balance is maintained while platelets circulate for 7-10 days in the bloodstream and are eventually cleared by the liver and spleen under homeostatic conditions [4,5]. As platelets age, they gradually release their granular contents, undergo morphological changes, become procoagulant, and in general are losing some of their functional properties compared to newly produced platelets [6-8].

The process of hemostasis initiates with platelets being recruited to the site of tissue injury, where the subendothelial layer of the damaged vessel wall will be exposed (Figure 1)[1]. Here, exposed collagen fibrils and von Willebrand Factor (VWF), a large adhesive glycoprotein, facilitate platelet adhesion. VWF has ligand binding sites for both collagen and platelet glycoprotein (GP) Iba and is essential for initial platelet plug formation [9]. At this time, platelets also activate and secrete a large array of hemostatic proteins and molecules from their secretory granules, such as VWF and fibrinogen. [10]. Ultimately, platelets aggregate through fibrinogen- and VWF-cross linked GP IIb/IIIa receptors and form an adhesive blood clot [1]. These collective steps are termed primary hemostasis, and are greatly dependent on the adequate functioning of platelets, collagen and VWF. The release of tissue factor initiates secondary hemostasis, a series of serine proteases (coagulation factors) that trigger the step-wise activation of prothrombin to thrombin [11]. Thrombin cleaves fibrinogen into fibrin, which forms a dense fibrillar network that overlays and stabilizes platelet plugs. Exposed phosphatidyl serine on the surface of activated platelets provides an important driver of pro-coagulant pathways, thereby integrating primary and secondary hemostasis. Once wound healing is initiated and a wound is sufficiently sealed, fibrinolysis and platelet-driven clot retraction facilitate dissolution of the fibrin-enriched platelet plug to restore the physiological function of the repaired vessel wall [11,12]. Depending on the type of blood vessel and (patho)physiological source of tissue injury, other blood cells and proteins are involved in the hemostatic process, but this falls outside the scope of this thesis.

### **Von Willebrand Factor - "A Platelet's Best Friend"**

As outlined above, VWF provides a crucial component for the adhesion of blood platelets

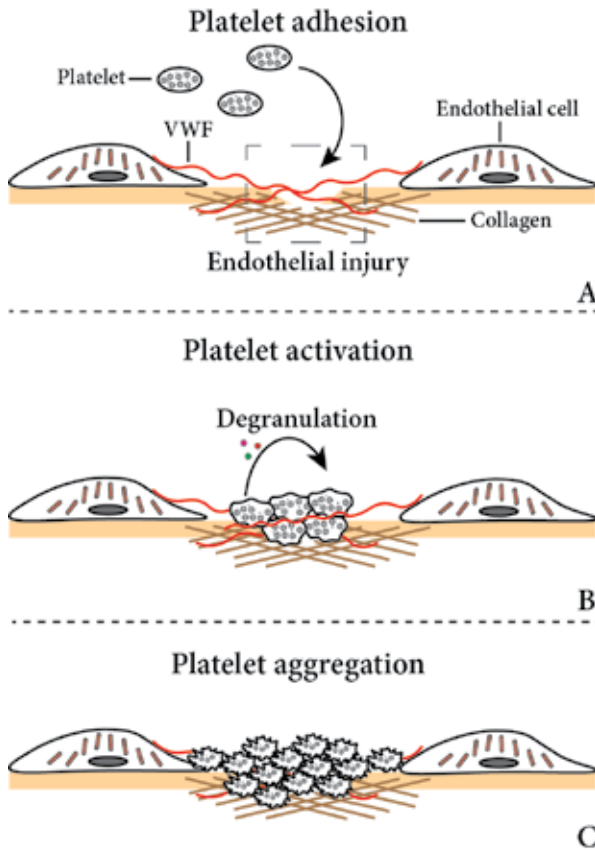


Figure 1. Platelets and their central role in primary hemostasis.

Platelet adhesion (1A) is the initial step in hemostasis where circulating platelets adhere to exposed collagen fibrils and VWF at sites of endothelial injury. Subsequently, platelets activate, change shape and secrete granular contents (1B). Degranulated, activated platelets rapidly aggregate, thereby quickly sealing off sites of vascular injury to prevent leaking of blood into the underlying tissues (1C).

at sites of vascular injury. VWF is synthesized by endothelial cells and megakaryocytes and packaged in secretory organelles: Weibel-Palade bodies (WPBs) in endothelial cells and alpha-granules in platelets [13]. Additionally, circulating levels of VWF are maintained through basal secretion of WPBs by endothelial cells [14].

Our current knowledge of VWF biosynthesis primarily stems from endothelial cells, where VWF is processed through various steps into large, high-molecular-weight multimers in WPBs [9]. VWF is first dimerized in the endoplasmic reticulum (ER), after which a pre-protein is cleaved off in the Golgi, the VWF propeptide (VWFpp) [15]. The mature VWF protein then multimerizes and is condensed in large tubules that are packaged in WPBs. Meanwhile, VWFpp remains non-covalently associated to VWF and is co-packaged into WPBs as an integral part of the tubules [9]. Upon exocytosis from WPBs,

VWF and VWFpp undergo divergent fates in the circulation, where the extracellular function of VWFpp is still unknown [16].

The leading assumption is that a similar process of VWF biosynthesis takes place in megakaryocytes, where VWF is packaged eccentrically in alpha-granules into tubule-like structures that are shorter in length (Figure 2) [17,18]. It is however unclear how VWFpp is processed in megakaryocytes, where it is stored in platelets, and if concomitant VWF- and VWFpp release occurs in platelets.

### Platelet alpha-granule cargo - *"I Can't Carry It For You, But I Can Carry You"*

The process of platelet degranulation and the release of cargo from secretory organelles like alpha-granules into sites of thrombus formation is one of the key cellular functions of platelets [10,19]. Besides VWF and fibrinogen, alpha-granules also contain chemokines, growth factors, angiogenic mediators and many other proteins involved in acute hemostatic and immunological responses (Figure 2). Another secretory organelle in platelets is the dense-granule, which particularly contains small signalling molecules (serotonin, histamine, ADP, ATP and polyphosphate). Formation and maturation of these key organelles occurs in the megakaryocyte, and cargo for granules is recruited primarily by biosynthetic pathways, but occasionally by endocytosis in case of fibrinogen and coagulation factor V [20,21].

Platelet secretion, or degranulation, of alpha-granule cargo is one of the main parameters used in diagnostic laboratories to assess platelet function [19,10]. One such cargo protein to assess is platelet factor 4 (PF4), a small chemokine which is synthesized only by the megakaryocyte-lineage. In the circulation, it is therefore solely found inside platelet alpha-granules [22]. This makes its detection in plasma a sensitive correlative marker for platelet cargo release [22]. Nevertheless, the precise contributions of platelet-derived cargo molecules in hemostasis are unclear.

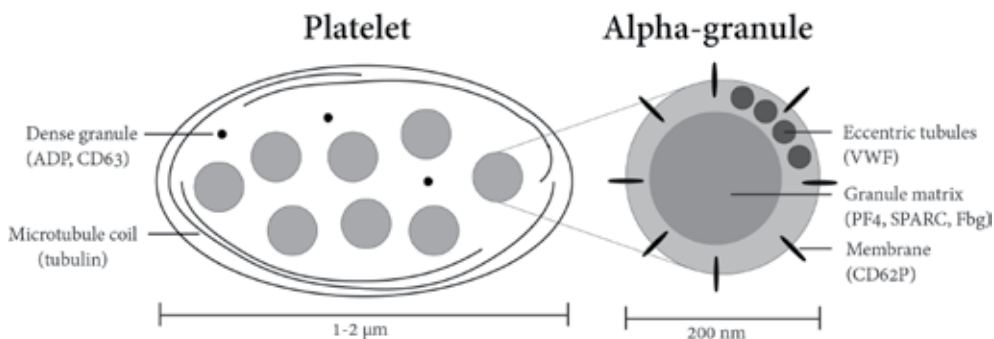


Figure 2. Platelet- and alpha-granule ultrastructure.

Platelets (1-2 μm in diameter) contain a microtubule coil and various secretory organelles, the most abundant ones being alpha- and dense granules. Alpha-granules (200 nm in diameter) contain eccentric nanodomains with VWF, and a condensed granule matrix with various proteins including PF4, SPARC and fibrinogen. Alpha-granular membranes contain CD62P.

### **Differential release of alpha-granule cargo - "We Are Not Here Because We Are Free, We Are Here Because We Are Not Free"**

Several models have been postulated in an effort to capture the biological mechanisms underlying release of platelet alpha-granule cargo, considering that several proteins with opposing functions reside in alpha-granules [19]. Early studies analyzed the differential localization of pro- and antiangiogenic proteins, and identified subsets of alpha-granules exclusively containing one or the other [23,24]. Similarly, VWF and fibrinogen were identified in different subsets of alpha-granules [23]. From these data, it was suggested that different subsets of alpha-granules would be able to facilitate the differential release of alpha-granule cargo. However, higher-resolution quantitative light- and advanced electron microscopy techniques have now shown that it is instead a stochastic distribution of cargo that is present in alpha-granules, with no evidence for granule subsets [25,26]. Significant controversy on this topic remains, as a recent paper has identified alpha-granule subsets in megakaryocytes [27].

An alternative model for the differential release of alpha-granule cargo is based on different modes of exocytosis or as a result of different release kinetics [28,29]. In a parallel with endothelial cell WPBs, which share several of the proteins stored in alpha-granules, several modes of release are employed by endothelial cells resulting in the release of different cargo molecules [14]. One example is the "kiss-and-run"-mode, where a small fusion pore is formed that triggers release of smaller proteins like chemokines but impairs the release of large bulky proteins like VWF [30].

### **Hemostatic disorders - "All It Takes Is a Little Push"**

Diseases that affect components of the hemostatic system leading to its dysfunction are collectively termed hemostatic disorders. Depending on the defect, this may lead to thrombosis in case of increased activation of coagulation, or spontaneous bleeding or excessive blood loss in response to hemostatic challenges such as trauma in case of reduced coagulation. Defects in platelets, as a central player of the hemostatic system, can be identified in various hemostatic disorders and can be classified into defects that affect platelet numbers (thrombocytopenia or thrombocytosis), platelet function (thrombocytopathy) or a related hemostatic component that affects its interaction with platelets [31,32].

### **Immune Thrombocytopenia - "The B and T Cells Send Their Regards"**

Immune thrombocytopenia (ITP) is a hemostatic disorder characterized by reduced platelet numbers ( $<150 \times 10^9/L$ ) [33,34]. Patients with ITP may suffer from bleedings which can present with bruising, petechiae due to bleeding from small vessels in the skins, nose and gum bleeds as well as excessive menstrual bleeding [35]. ITP is characterized by autoimmune reactivity towards platelets either by autoantibodies generated by B cells or by platelet reactive cytotoxic T cells. Autoreactive cells may trigger both platelet clearance and/or disrupt platelet production by megakaryocytes, depending on the mechanism of action [34]. The current diagnostic regimen is incapable of separating these two mechanisms, and

it is therefore difficult to predict the therapeutic response of patients to various treatment options. Two frequently used treatments are: immunosuppressive drugs that downregulate B and T cell responses, and TPO-receptor agonists that stimulate platelet production [33]. In recent years, novel treatment regimens have primarily focused on downstream targets of platelet clearance that are promising, but also difficult to predict [36,37].

Demystifying the pathological mechanisms underlying ITP is complicated by the fact that platelets are increasingly acknowledged as immune cells [38,39], and that there are few biological studies that have employed patient-derived autoreactive T or B cells to study the anti-platelet response. While there is no clear association between immunity-related genes (e.g. HLA) and ITP, numerous pro-inflammatory markers and immune cell subsets have been correlated to ITP status [33,34]. However, it is unknown precisely why platelets are targeted. One of the triggers to expose platelet antigens which may lead to ITP, is an infection from bacterial or viral origin [33,34]. Although vaccination against such pathogens protects individuals, it has also been suggested that vaccination poses as an additional trigger for ITP. Additionally, numerous studies have reported lower platelets counts in ITP patients as a result of vaccination events [33,34]. However, it is not clear under which conditions vaccinations lead to lower platelet counts in ITP patients, how these platelets counts fluctuate over time, and if ITP patients are at additional risk after vaccination.

### **Von Willebrand Disease – “*The Dark Side of the Bloodstream*”**

Impaired adhesion of platelets is a hallmark of Von Willebrand Disease (VWD), the most-common inherited bleeding disorder [40]. VWD is characterized by a deficiency or a defect in VWF, which subsequently leads to impaired or sub-optimal adhesion of platelets to sites of vascular injury. Diagnosis of VWD is based on circulating VWF in plasma, and is subdivided by quantitative defects (type 1 and 3) and qualitative defects (type 2) that impair the physiological function of VWF (Figure 3) [41]. Qualitative defects are: lack of high-molecular weight multimers (type 2A); gain-of-function to bind GPIIb/IIIa on platelets (type 2B); loss-of-function to bind GPIIb/IIIa on platelets (type 2M) or loss-of-function to stabilize and/or interact with coagulation factor VIII (type 2N) [41]. Type 1 is generally the mildest form with reduced levels of VWF due to enhanced clearance or reduced synthesis, while type 3 is the most severe where there is a complete absence of VWF in the circulation [40].

Apart from functional defects, aberrant intracellular trafficking within endothelial cells may also result in reduced levels of VWF and/or lack of high molecular weight VWF multimers in the circulation. (Figure 3). Yet, the levels of circulating VWF are not always associated with the severity of bleeding phenotypes found in patients with VWD [42,43]. At present, the functional role and storage of platelet VWF in patients with VWD has not been extensively studied. There is also limited information with respect to the contribution of platelet VWF to the bleeding phenotype in VWD patients. A recent report by Bowman and co-workers provided evidence for discrepant platelet and plasma von Willebrand factor levels in a VWD patient which resulted in a milder

bleeding phenotype which was attributed to the release of functional VWF from platelets [44].

The WiN (Willebrand in the Netherlands) study is a nation-wide cohort study which was initiated and coordinated by the Erasmus University Medical Center [45]. Over 800 patients with VWD from all hemophilia treatment centers in the Netherlands were included in this study. Many VWF parameters like VWF circulatory levels, function and mutations in the VWF gene have been analyzed and associated with clinical outcomes (such as age, bleeding, response to treatment) [42,46–48]. Additional associations with endothelial markers have been investigated [49], but not yet with platelet markers. In an ongoing prospective follow-up study (WiN-Pro), previous WiN patients and newly diagnosed VWD patients are included and VWF- and clinical parameters are examined prospectively.

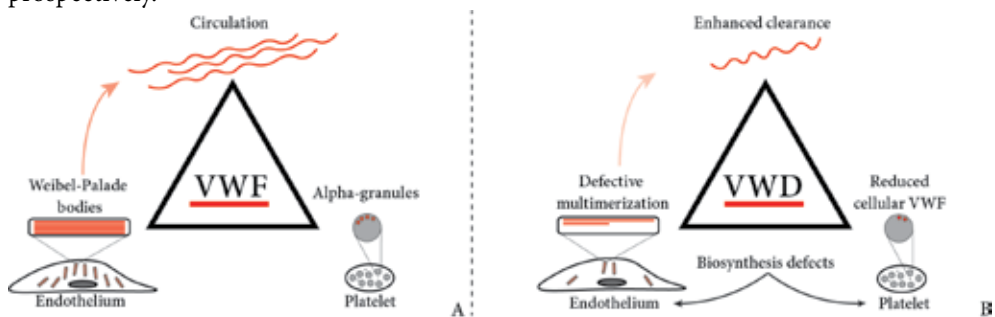


Figure 3. VWF sources and cellular VWF deficiencies that can occur in VWD.

VWF stems from three components to maintain hemostasis: endothelial Weibel-Palade bodies, platelet alpha-granules, and circulatory VWF that is derived from endothelial basal release (arrow, 3A). Various sub-types of VWD hallmark cellular defects in VWF, which can affect multiple VWF components (3B).

### Quantitative Super-resolution Microscopy - "Fluorescent Platelets and How to Find Them"

A related open question is how platelet-derived VWF is dysregulated in VWD types that affect VWF biosynthesis. Previous studies on this topic have depended on high-resolution qualitative- (electron microscopy) or quantitative bulk- techniques (ELISA) to analyze VWF in VWD patient platelets [50–54]. However, quantitative studies that assess granule heterogeneity and subcellular localization of VWF in VWD platelets are lacking. Considering that platelets gradually release granule content and undergo morphological changes during aging, quantitative microscopical tools are necessary to fully understand the intracellular dynamics of platelet VWF [6,55].

With the development of 'super-resolution' imaging techniques reaching resolutions below the diffraction limit of light (250 nm) [56], it becomes possible to quantitatively assess platelet alpha-granules (200 nm in diameter) and their cargo, such as VWF. One of these is Structured Illumination Microscopy (SIM): by using multiple illumination patterns and advanced reconstruction algorithms, resolution is improved to approximately 100 nm

in XY and 250 nm in Z [57]. One of the main advantages of SIM is that it is capable of imaging large fields of view (up to several hundreds of platelets), allowing quantification of data on a relatively large microscopical dataset for selective patient studies [56,57]. So far, no SIM-based studies have been performed on platelets of VWD patients.

### **High-throughput analysis of platelet images - "One Ring to Encircle Them All and in Darkness Quantify Them"**

A typical hallmark of platelets is a marginal band of tubulin that is formed during budding from megakaryocyte proplatelet extensions [58,59]. Considering the high spatial density of tubulin strands in this ring, it is an ideal protein to stain and to use in imaging software to segment individual platelets [60]. Using this marginal band as segmentation tool, other stainings can then be included to study VWF and other alpha-granule components.

Further analysis with imaging software includes thresholding, segmentation and analysis of stained 3D structures to identify individual VWF- and other cargo containing structures and their exact volume, shape and position per platelet across hundreds of platelets [61]. As such, this methodology allows large scale 3D quantification of platelet alpha-granule cargo proteins across multiple individuals.

## **Scope and aims of this thesis:**

### **Part 1: Platelets in ITP: Opportunities and Challenges**

In chapter 2, we review key concepts of ITP pathophysiology, and a novel model focusing on potential triggers for ITP is presented. The hypothesis of this model is that a chronic anti-platelet response is likely triggered through an exposure of platelet antigens in combination with a loss of immune tolerance. Emerging concepts that warrant further investigation, that will help to better define the pathophysiology of ITP, are also suggested in this chapter.

In chapter 3, the aim is to investigate potential vaccination-triggered events in ITP patients, with a focus on COVID-19 vaccination. The leading hypothesis is that platelet counts fluctuate over time as a result of vaccination and that close monitoring is needed in ITP subgroups. To address this question, a prospective study of ITP patients (in comparison to healthy donors) was performed, in which platelet counts were monitored at different time-points both before- and after COVID-19 vaccination.

### **Part 2: Platelet and VWF: Key Partners in Disease and Health**

The second part of this thesis concentrates on the platelet-VWF axis in hemostasis and how this functions in the pathological condition of VWD and in platelet physiology.

In chapter 4, the aim is to examine the contribution of platelet degranulation in a large cohort of VWD patients. The hypothesis is that platelet degranulation may be altered in

VWD subtypes. Plasma samples of VWD patients from the WiN study will be assessed for PF4 plasma levels as a measure for platelet degranulation and correlated to VWF- and clinical parameters, as part of an explorative approach to determine the potential role of platelet cargo release in VWD.

In chapter 5, the aim is to develop a methodology based on SIM imaging to quantitatively study platelet granular structures. The hypothesis is that this methodology is capable of stratifying different VWF biosynthesis defects in platelets. As part of the WiN-Pro study, platelets samples from selective VWD patients were studied in order to better understand how VWF defects lead to VWF alterations in platelets.

In chapter 6, the aim is to study the role of platelet-derived VWF and its VWFpp in hemostasis. localization and release of VWF and its cleaved propeptide VWFpp in platelets. The hypothesis is that VWF and VWFpp are localized in a similar nanodomain of the alpha-granule, but differentially released from platelets. Localization and release of VWF and its cleaved propeptide VWFpp are studied in resting and stimulated platelets using the quantitative imaging methodology from Chapter 5.

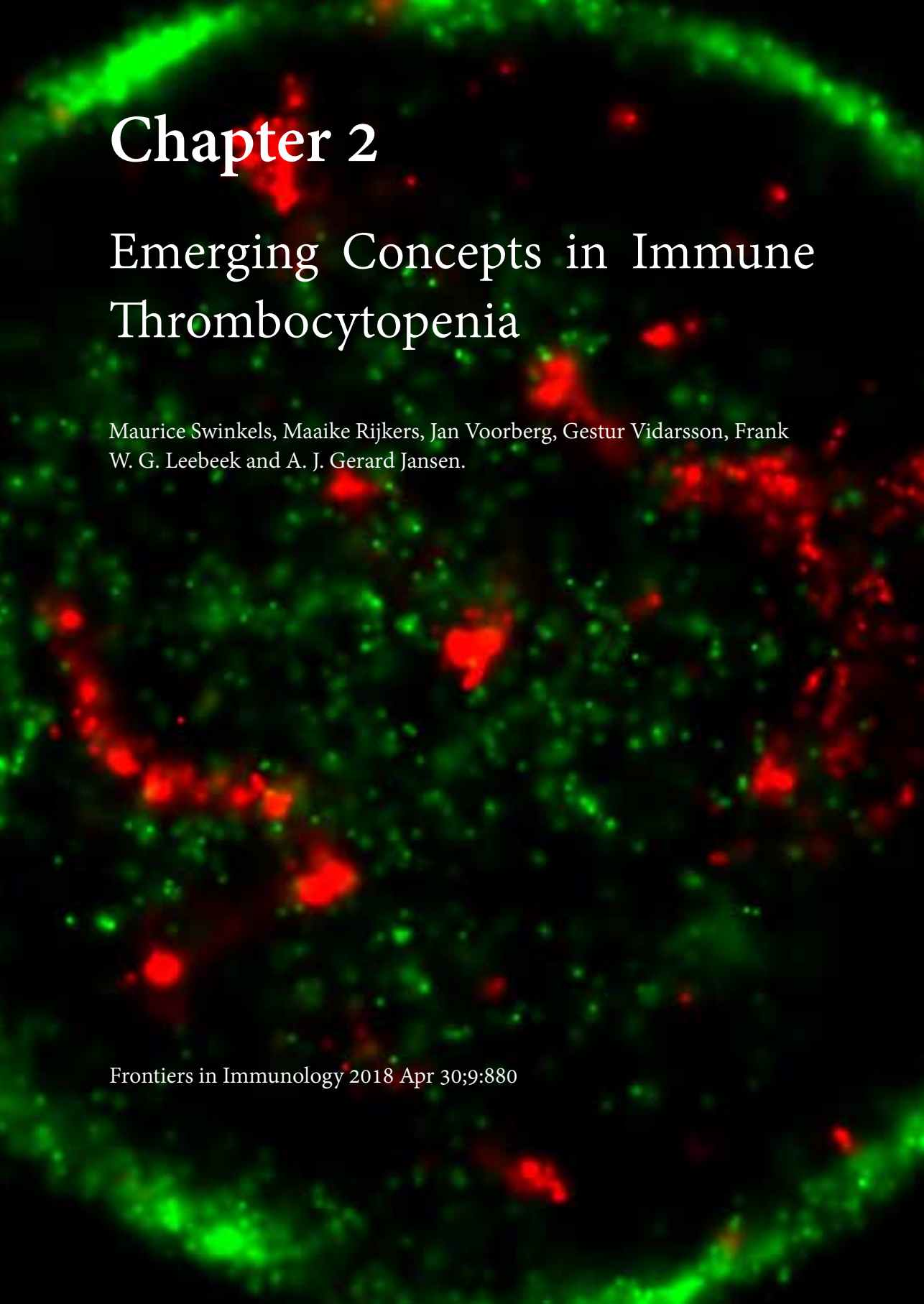
Finally, in chapter 7, a general discussion is provided that covers the role of platelets in the described hemostatic disorders. Where are the opportunities for future research and applications?

## References

1. Broos K, Feys HB, De Meyer SF, Vanhoorelbeke K, Deckmyn H. Platelets at work in primary hemostasis. *Blood Rev* 2011; 25: 155–67.
2. Grozovsky R, Giannini S, Falet H, Hoffmeister KM. Regulating billions of blood platelets: Glycans and beyond. *Blood* 2015; 126: 1877–84.
3. Grozovsky R, Begonja AJ, Liu K, Visner G, Hartwig JH, Falet H, Hoffmeister KM. The Ashwell-Morell receptor regulates hepatic thrombopoietin production via JAK2-STAT3 signaling. *Nat Med* 2015; 21: 47–54.
4. Li R, Hoffmeister KM, Falet H. Glycans and the platelet life cycle. *Platelets* 2016; 27: 505–11.
5. Hoffmeister KM, Falet H. Platelet clearance by the hepatic Ashwell-Morrell receptor: mechanisms and biological significance. *Thromb Res* 2016; 141: S68–72.
6. Shrivastava M. The platelet storage lesion. *Transfus Apher Sci* 2009; 41: 105–13.
7. Rijkers M, Van Den Eshof BL, Van Der Meer PF, Van Alphen FPJ, De Korte D, Leebeek FWG, Meijer AB, Voorberg J, Jansen AJG. Monitoring storage induced changes in the platelet proteome employing label free quantitative mass spectrometry. *Sci Rep* 2017; .
8. Rijkers M, van der Meer PF, Bontekoe IJ, Daal BB, de Korte D, Leebeek FWG, Voorberg J, Jansen AJG. Evaluation of the role of the GPIb-IX-V receptor complex in development of the platelet storage lesion. *Vox Sang* 2016; .
9. Springer TA. Von Willebrand factor, Jedi knight of the bloodstream. *Blood* 2014; 124: 1412–25.
10. Heijnen H, van der Sluijs P. Platelet secretory behaviour: As diverse as the granules... or not? *J Thromb Haemost* 2015; 13: 2141–51.
11. Versteeg HH, Heemskerk JWM, Levi M, Reitsma PH. New Fundamentals in hemostasis. *Physiol Rev* 2013; 93: 327–58.
12. Sorrentino S, Studt JD, Medalia O, Tanuj Sapra K. Roll, adhere, spread and contract: Structural mechanics of platelet function. *Eur J Cell Biol* 2015; 94: 129–38.
13. Karampini E, Bierings R, Voorberg J. Orchestration of Primary Hemostasis by Platelet and Endothelial Lysosome-Related Organelles. *Arterioscler Thromb Vasc Biol* 2020; 40: 1441–53.
14. Schillemans M, Karampini E, Kat M, Bierings R. Exocytosis of Weibel–Palade bodies: how to unpack a vascular emergency kit. *J Thromb Haemost* 2019; 17: 6–18.
15. Haberichter SL. Von Willebrand factor propeptide: Biology and clinical utility. *Blood* 2015; 126: 1753–61.
16. Wagner DD, Fay PJ, Sporn LA, Sinha S, Lawrence SO, Marder VJ. Divergent fates of von Willebrand factor and its propolypeptide (von Willebrand antigen II) after secretion from endothelial cells. *Proc Natl Acad Sci U S A* 1987; 84: 1955–9.
17. Van Nispen Tot Pannerden H, De Haas F, Geerts W, Posthuma G, Van Dijk S, Heijnen HFG. The platelet interior revisited: Electron tomography reveals tubular  $\alpha$ -granule subtypes. *Blood* 2010; 116: 1147–56.
18. Cramer EM, Meyer D, Le Menn R, Breton-Gorius J. Eccentric localization of von Willebrand factor in an internal structure of platelet  $\alpha$ -granule resembling that of Weibel–Palade bodies. *Blood* 1985; 66: 710–3.
19. Yadav S, Storrie B. The cellular basis of platelet secretion: Emerging structure/function relationships. *Platelets Taylor & Francis*; 2017; 28: 108–18.
20. Harrison P, Wilbourn B, Debili N, Vainchenker W, Breton-Gorius J, Lawrie AS, Masse JM, Savidge GF, Cramer EM. Uptake of plasma fibrinogen into the alpha granules of human megakaryocytes and platelets. *J Clin Invest* 1989; 84: 1320–4.
21. Suehiro Y, Veljkovic DK, Fuller N, Motomura Y, Massé JM, Cramer EM, Hayward CPM. Endocytosis and storage of plasma factor V by human megakaryocytes. *Thromb Haemost* 2005; 94: 585–92.
22. Slungaard A. Platelet factor 4: A chemokine enigma. *Int J Biochem Cell Biol* 2005; 37: 1162–7.
23. Sehgal S, Storrie B. Evidence that differential packaging of the major platelet granule proteins von Willebrand factor and fibrinogen can support their differential release. *J Thromb Haemost* 2007; 5: 2009–16.
24. Italiano JE, Richardson JL, Patel-Hett S, Battinelli E, Zaslavsky A, Short S, Ryeom S, Folkman J, Klement GL. Angiogenesis is regulated by a novel mechanism: Pro- and antiangiogenic proteins are organized into separate platelet  $\alpha$  granules and differentially released. *Blood* 2008; 111: 1227–33.
25. Kamykowski J, Carlton P, Sehgal S, Storrie B. Quantitative immunofluorescence mapping reveals little functional coclustering of proteins within platelet  $\alpha$ -granules. *Blood* 2011; 118: 1370–3.

26. Pokrovskaya ID, Yadav S, Rao A, McBride E, Kamykowski JA, Zhang G, Aronova MA, Leapman RD, Storrle B. 3D ultrastructural analysis of  $\alpha$ -granule, dense granule, mitochondria, and canalicular system arrangement in resting human platelets. *Res Pract Thromb Haemost* 2020; 4: 72–85.
27. Battinelli EM, Thon JN, Okazaki R, Peters CG, Vijey P, Wilkie AR, Noetzli LJ, Flaumenhaft R, Italiano JE. Megakaryocytes package contents into separate  $\alpha$ -granules that are differentially distributed in platelets. *Blood Adv* 2019; 3: 3092–8.
28. Eckly A, Rinckel JY, Proamer F, Ulas N, Joshi S, Whiteheart SW, Gachet C. Respective contributions of single and compound granule fusion to secretion by activated platelets. *Blood* 2016; 128: 2538–49.
29. Jonnalagadda D, Izu LT, Whiteheart SW. Platelet secretion is kinetically heterogeneous in an agonist-responsive manner. *Blood* 2012; 120: 5209–16.
30. Babich V, Knipe L, Hewlett L, Meli A, Dempster J, Hannah MJ, Carter T. Differential effect of extracellular acidosis on the release and dispersal of soluble and membrane proteins secreted from the Weibel-Palade body. *J Biol Chem* 2009; 284: 12459–68.
31. Lentaigne C, Freson K, Laffan MA, Turro E, Ouwehand WH. Inherited platelet disorders: Toward DNA-based diagnosis. *Blood* 2016; 127: 2814–23.
32. Casari C, Bergmeier W. Acquired platelet disorders. *Thromb Res* 2016; 141: S73–5.
33. Zufferey A, Kapur R, Semple JW. Pathogenesis and therapeutic mechanisms in immune thrombocytopenia (ITP). *J Clin Med* 2017; 6.
34. Cines DB, Cuker A, Semple JW. Pathogenesis of immune thrombocytopenia. *Press Medicale* 2014; 43.
35. DeLoughery TG. Immune Thrombocytopenia. *Hemost Thromb Fourth Ed* 2019; : 73–9.
36. Rodeghiero F. Recent progress in ITP treatment. *Int J Hematol Japan*; 2023; 117: 316–30.
37. Jiang D, Al-Samkari H, Panch SR. Changing Paradigms in ITP Management: Newer Tools for an Old Disease. *Transfus Med Rev United States*; 2022; 36: 188–94.
38. Semple JW, Italiano JE, Freedman J. Platelets and the immune continuum. *Nat Rev Immunol* 2011; 11: 264–74.
39. Nelson VS, Jolink ATC, Amini SN, Zwaginga JJ, Netelenbos T, Semple JW, Porcelijn L, de Haas M, Schipperus MR, Kapur R. Platelets in ITP: Victims in charge of their own fate? *Cells* 2021; 10.
40. De Gopegui RR, Feldman BF. von Willebrand's disease. *Comp Clin Path* 1997; 7: 187–96.
41. de Jong A, Eikenboom J. Von Willebrand disease mutation spectrum and associated mutation mechanisms. *Thromb Res* 2017; 159: 65–75.
42. de Wee EM, Sanders Y V, Mauser-Bunschoten EP, van der Bom JG, Degenaar-Dujardin MEL, Eikenboom J, de Goede-Bolder A, Laros-van Gorkom BAP, Meijer K, Hamulyák K, Nijziel MR, Fijnvandraat K, Leebeek FWG. Determinants of bleeding phenotype in adult patients with moderate or severe von Willebrand disease. *Thromb Haemost* 2012; 108: 683–92.
43. Flood VH, Christopherson PA, Gill JC, Friedman KD, Haberichter SL, Bellissimo DB, Udani RA, Dasgupta M, Hoffmann RG, Ragni M V, Shapiro AD, Lusher JM, Lentz SR, Abshire TC, Leissing C, Hoots WK, Manco-Johnson MJ, Gruppo RA, Boggio LN, Montgomery KT, et al. Clinical and laboratory variability in a cohort of patients diagnosed with type 1 VWD in the United States. *Blood* 2016; 127: 2481–8.
44. Bowman ML, Pluthero FG, Tuttle A, Casey L, Li L, Christensen H, Robinson KS, Lillcrap D, Kahr WHA, James P. Discrepant platelet and plasma von Willebrand factor in von Willebrand disease patients with p.Pro-2808Leufs\*24. *J Thromb Haemost* 2017; 15: 1403–11.
45. De Wee EM, Mauser-Bunschoten EP, Van der Bom AG, Eikenboom JCJ, Fijn van Draat KJ, De Goede-Bolder A, Meijer K, Nováková I, Plug I, Leebeek FWG. Willebrand in the Netherlands: WiN Study. Background and Study Design. *Blood* 2008; 112: 4510–4510.
46. Sanders YV, Van Der Bom JG, Cnossen MH, De Maat MPM, Laros-van Gorkom BAP, Fijnvandraat KJ, Meijer K, Mauser-Bunschoten E, Eikenboom HJC, Leebeek FWG. Genetic variations determine von Willebrand factor levels in patients with von Willebrand disease from the WiN study. *J Thromb Haemost* 2013; 11: 116.
47. Sanders Y V, Giezenaar MA, Laros-van Gorkom BAP, Meijer K, van der Bom JG, Cnossen MH, Nijziel MR, Ypma PF, Fijnvandraat K, Eikenboom J, Mauser-Bunschoten EP, Leebeek FWG, Middeldorp S, Kors A, Zweegman S, de Meris J, Jonkers MH, Dors N, Nijziel MR, Meijer K, et al. Von Willebrand disease and aging: An evolving phenotype. *J Thromb Haemost* 2014; 12: 1066–75.

48. Atiq F, Schütte LM, Looijen AEM, Boender J, Cnossen MH, Eikenboom J, de Maat MPM, Kruij MJHA, Leebeek FWG. Von Willebrand factor and factor VIII levels after desmopressin are associated with bleeding phenotype in type 1 VWD. *Blood Adv* 2019; 3: 4147–54.
49. Groeneveld DJ, Sanders Y V, Adelmeijer J, Mauser-Bunschoten EP, Van Der Bom JG, Cnossen MH, Fijnvandraat K, Laros-Van Gorkom BAP, Meijer K, Lisman T, Eikenboom J, Leebeek FWG. Circulating Angiogenic Mediators in Patients with Moderate and Severe von Willebrand Disease: A Multicentre Cross-Sectional Study. *Thromb Haemost* 2018; 118: 152–60.
50. Nurden P, Chretien F, Poujol C, Winckler J, Borel-Derlon A, Nurden A. Platelet ultrastructural abnormalities in three patients with type 2B von Willebrand disease. *Br J Haematol* 2000; 110: 704–14.
51. Nurden P, Debili N, Vainchenker W, Bobe R, Bredoux R, Corvazier E, Combrie R, Fressinaud E, Meyer D, Nurden AT, Enouf J. Impaired megakaryocytopoiesis in type 2B von Willebrand disease with severe thrombocytopenia. *Blood* 2006; 108: 2587–95.
52. Nurden P, Nurden AT, La Marca S, Punzo M, Baronciani L, Federici AB. Platelet morphological changes in 2 patients with von Willebrand disease type 3 caused by large homozygous deletions of the von Willebrand factor gene. *Haematologica* 2009; 94: 1627–9.
53. Nurden P, Gobbi G, Nurden A, Enouf J, Youlyouz-Marfak I, Carubbi C, La Marca S, Punzo M, Baronciani L, De Marco L, Vitale M, Federici AB. Abnormal VWF modifies megakaryocytopoiesis: Studies of platelets and megakaryocyte cultures from patients with von Willebrand disease type 2B. *Blood* 2010; 115: 2649–56.
54. Casonato A, Cattini MG, Daidone V, Pontara E, Bertomoro A, Prandoni P. Diagnostic value of measuring platelet von Willebrand factor in von willebrand disease. *PLoS One* 2016; 11.
55. Rijkers M, Van Den Eshof BL, Van Der Meer PF, Van Alphen FPJ, De Korte D, Leebeek FWG, Meijer AB, Voorberg J, Jansen AJG. Monitoring storage induced changes in the platelet proteome employing label free quantitative mass spectrometry. *Sci Rep* 2017; 7.
56. Schermelleh L, Ferrand A, Huser T, Eggeling C, Sauer M, Biehlmaier O, Drummen GPC. Super-resolution microscopy demystified. *Nat Cell Biol* 2019; 21: 72–84.
57. Wu Y, Shroff H. Faster, sharper, and deeper: structured illumination microscopy for biological imaging. *Nat Methods* 2018; 15: 1011–9.
58. Diagouraga B, Grichine A, Fertin A, Wang J, Khochbin S, Sadoul K. Motor-driven marginal band coiling promotes cell shape change during platelet activation. *J Cell Biol* 2014; 204: 177–85.
59. Machlus KR, Thon JN, Italiano JE. Interpreting the developmental dance of the megakaryocyte: A review of the cellular and molecular processes mediating platelet formation. *Br J Haematol* 2014; 165: 227–36.
60. Westmoreland D, Shaw M, Grimes W, Metcalf DJ, Burden JJ, Gomez K, Knight AE, Cutler DF. Super-resolution microscopy as a potential approach to diagnosis of platelet granule disorders. *J Thromb Haemost* 2016; 14: 839–49.
61. Schindelin J, Arganda-Carreras I, Frise E, Kaynig V, Longair M, Pietzsch T, Preibisch S, Rueden C, Saalfeld S, Schmid B, Tinevez JY, White DJ, Hartenstein V, Eliceiri K, Tomancak P, Cardona A. Fiji: An open-source platform for biological-image analysis. *Nat Methods* 2012; 9: 676–82.

A fluorescence microscopy image of a cell, showing a bright green ring-like structure at the top and bottom edges, and numerous red and green spots scattered throughout the interior. The background is dark.

# Chapter 2

## Emerging Concepts in Immune Thrombocytopenia

Maurice Swinkels, Maaïke Rijkers, Jan Voorberg, Gestur Vidarsson, Frank W. G. Leebeek and A. J. Gerard Jansen.

## Abstract

Immune thrombocytopenia (ITP) is an autoimmune disease defined by low platelet counts which presents with an increased bleeding risk. Several genetic risk factors (e.g., poly-morphisms in immunity-related genes) predispose to ITP. Autoantibodies and cytotoxic CD8+ T cells (Tc) mediate the anti-platelet response leading to thrombocytopenia. Both effector arms enhance platelet clearance through phagocytosis by splenic macrophages or dendritic cells and by induction of apoptosis. Meanwhile, platelet production is inhibited by CD8+ Tc targeting megakaryocytes in the bone marrow. CD4+ T helper cells are important for B cell differentiation into autoantibody secreting plasma cells. Regulatory Tc are essential to secure immune tolerance, and reduced levels have been implicated in the development of ITP. Both Fc $\gamma$ -receptor-dependent and -independent pathways are involved in the etiology of ITP. In this review, we present a simplified model for the pathogenesis of ITP, in which exposure of platelet surface antigens and a loss of tolerance are required for development of chronic anti-platelet responses. We also suggest that infections may comprise an important trigger for the development of auto-immunity against platelets in ITP. Post-translational modification of autoantigens has been firmly implicated in the development of autoimmune disorders like rheumatoid arthritis and type 1 diabetes. Based on these findings, we propose that post-translational modifications of platelet antigens may also contribute to the pathogenesis of ITP.

Keywords: immune thrombocytopenia, immune thrombocytopenic purpura, autoantibodies, CD8+ T cells, autoimmunity, ITP

## Introduction

Immune thrombocytopenia (ITP) is an autoimmune disease characterized by low platelet counts and increased bleeding risk [1-4]. The initial event(s) leading to anti-platelet autoimmunity remains unclear, but strong evidence exists that autoantibodies and autoreactive CD8+ cytotoxic T cells (Tc) trigger enhanced platelet destruction and impair platelet production by megakaryocytes (MKs) in the bone marrow. We will briefly discuss the clinical aspects of this heterogeneous disease, followed by an overview of the mechanisms and pathways by which autoreactive B and Tc engage in anti-platelet immunity, with a particular focus on their specificity for platelet autoantigens. We will postulate a general model for ITP pathophysiology and finally highlight opportunities in ITP research, which can be derived from studies on other autoimmune diseases.

### Epidemiology and Clinical Features

Immune thrombocytopenia is a diagnosis of exclusion: patients who develop thrombocytopenia (defined as platelet counts below 100,000 platelets per microliter) with no clear underlying cause are currently diagnosed with (isolated) primary ITP [1,4]. Secondary ITP is defined as an ITP induced by other diseases or treatments. These include autoimmune disorders, lymphoproliferative disorders, infectious agents, transfusion, or induction by drugs, accounting in total for 20% of ITP cases (5,6). In total, the incidence of ITP is approximately 1.9–6.4 per 100,000 children/year and 3.3–3.9 per 100,000 adults/year [6-8], and this number is increasing [6,9]. ITP can be classified in a transient form termed newly diagnosed ITP (up until 3 months), or persistent ITP (up until 12 months) that is more prevalent in children, or a chronic form (longer than 12 months) that does not resolve on itself and is more prevalent in adult patients [1,6,7]. The acronym “ITP” should not be confused with the outdated definition of “idiopathic thrombocytopenic purpura” that has been used previously [1,4]. ITP is no longer considered an idiopathic disease and a proportion of patients do not present with purpura (see below). In this review, we discuss both adult and pediatric ITP studies and highlight discrepancies between both groups where necessary.

Bleeding symptoms in ITP patients typically present as either a mild form, such as bleeding in skin and mucosal regions, or a more severe, life-threatening form, such as bleeding in gastrointestinal or intracranial areas [6,10]. Patients with ITP have varying platelet counts as a result of the disease. Those with platelet counts above 50,000 per microliter rarely bleed, but below this “threshold” value, there are large differences in clinical phenotypes between patients that are as of yet unexplained [2,3,10]. Platelet function testing appears successful in predicting bleeding risk in patients [11-13]. However, no clear-cut diagnostic tools exist as associations between biomarkers and ITP remain limited, and no markers exist that may predict treatment responses [2,3]. The most common therapeutic options are based on immunosuppression [by corticosteroids, intravenous immunoglobulin (IVIg),

or rituximab], or stimulation of platelet production [by thrombopoietin receptor agonists (TPO-RAs), see below].

### **Platelet Life Cycle**

On average, the human body produces around 100 billion platelets per day resulting in a concentration of ~150,000–400,000 platelets per microliter blood [14]. Platelets circulate for approximately 7–10 days, slowly undergoing age-related changes in morphology, activation, and surface receptor density [15–18]. Platelets are produced by MKs in the bone marrow [19]. MKs are polynuclear cells that protrude extensions in the blood, termed proplatelets, and eventually bud off platelets from these extensions [20,21]. Recent findings show that MKs may also reside in the lung, facilitating platelet production in lung tissues [22], although the relevance of platelet production at this site is currently unclear.

Thrombopoietin (TPO) is the key hormone responsible for platelet production. It is primarily synthesized in the liver and promotes MKs to produce platelets in the bone marrow via the TPO receptor, Mpl [23–25]. As newly made TPO is released in the bloodstream by hepatocytes, it is also incorporated into circulating platelets via Mpl. This constitutes an inhibitory feedback loop in which platelet counts inversely correlate with the amount of TPO reaching the bone marrow to stimulate new platelet production [23,26]. Recent evidence suggests that the Ashwell-Morrell receptor (AMR) on hepatocytes plays an important role in this physiological process. Normally, as platelets age terminal sialic acid is gradually lost from the surface, which exposes the underlying galactose residues. This allows for their clearance by the AMR [27]. AMR-mediated platelet clearance triggers hepatic TPO transcription and translation, and new TPO is released [27]. Several other physiological clearance mechanisms exist that control platelet numbers, such as platelet apoptosis [28] and possibly phagocytosis by  $\alpha M\beta 2$  integrins on hepatic and splenic macrophages [for a review, see Ref. [29]].

In ITP, this normal platelet life cycle is disturbed by autoantibodies and platelet-reactive CD8+ Tc as summarized in Figure 1. Autoantibodies and CD8+ Tc may interfere with multiple aspects of the platelet life cycle, including their production and clearance that result in thrombocytopenia. In such thrombocytopenic conditions, the small amount of circulating Mpl-containing platelets often leads to high TPO levels [30,31]. Interestingly, only slightly elevated TPO levels are observed in ITP; likely because platelets with incorporated TPO are rapidly cleared [31]. Therefore, one of the therapeutic options for ITP patients involves stimulation of the TPO receptor on MKs by TPO-RAs, which proves to be successful in many patients [32]. Not all patients are equally responsive to TPO-RAs and poor responders likely suffer from a prolonged autoimmune response against platelets that cannot be resolved by increasing the platelet production.

### **Genetic Risk Factors**

As mentioned, autoreactive B and Tc have been firmly implicated in the pathophysiology of ITP. Consequently, many studies have reported associations

between ITP and single nucleotide polymorphisms (SNP) in immunity-related genes. Polymorphisms in genes encoding specific cyto- or chemokines, such as interleukin (IL)-1, IL-2, IL-4, IL-6, IL-10, IL-17, TNF- $\alpha$ , TGF- $\beta$ , and IFN- $\gamma$ , have been associated with ITP [33-37]. Several studies have also investigated whether specific HLA class I or II alleles are elevated in patients with ITP [38-45]; current findings suggest that polymorphic sites within the HLA locus are not linked to ITP as studies have reported both significant and nonsignificant findings [37-44]. The variation in studies could potentially be explained by small sample size, ethnic variability, or differences in diagnosis, yet does not allow to reach a consensus. New biomarkers such as miRNAs regulating levels of cytokines or other immune components are also increasingly recognized as potential risk factors for ITP [46]. Classically, polymorphisms in Fc $\gamma$  receptors (Fc $\gamma$ Rs) have been associated with the onset and pathogenesis of ITP [47-54] and are therefore further discussed below. Most of the reported association studies performed in ITP patients were conducted in small cohorts and in specific ethnic subgroups, and thus should be interpreted with caution. Additionally, many of the identified associations are not found in all patients and are commonly observed in other autoimmune diseases as well and are therefore general predisposing factors and not specific for ITP. Advances in (epi)genomics are likely to identify additional genetic risk factors for the development of ITP [55,56].

### **Environmental Risk Factors**

For a long time, the occurrence of specific infections has been associated with ITP, particularly in children [5-7]. Some of the most occurring and most studied infectious agents are *Helicobacter pylori* [57,58], Hepatitis C virus [59,60] and human immunodeficiency virus [61-67]. Evidence also exists for Cytomegalovirus [68,69], Epstein Barr Virus [69], and some other viruses [70,71]. Although individual cases of ITP have been reported after vaccination, this is exceedingly rare [72,73]. One of the suggested mechanisms by which infections lead to autoimmunity is the occurrence of molecular mimicry. In this case, viral proteins resemble platelet receptors to evade the immune system [74]. In case of an immune response against these viral proteins, cross reactivity may occur against platelet receptors, which subsequently lead to autoantibodies specific for both the viral protein and platelet receptors. This could explain the initiation of ITP in some cases [60-63, 66], which can be resolved by clearance of the infectious agent after which autoantibodies diminish [57,58]. Besides a transient decrease in platelet counts, infections sometimes elicit strong immune responses that can perpetuate and develop into chronic ITP, resulting in sustained platelet clearance.

Toll-like receptors are present on various innate immune cells, including platelets, and are suggested to mediate some of the microbial-platelet interactions that can trigger and/or aggravate autoimmunity [75]. Immune-mediated thrombocytopenia may also occur as a result of other autoimmune diseases, drugs, transfusion, and in lymphoproliferative disorders [76,77]. Often, these cases are also diagnosed as secondary ITP, but may greatly differ in etiology. As our review focuses on primary ITP, we refer readers to Ref. [77] for more information on the underlying pathophysiology of these forms of secondary ITP.

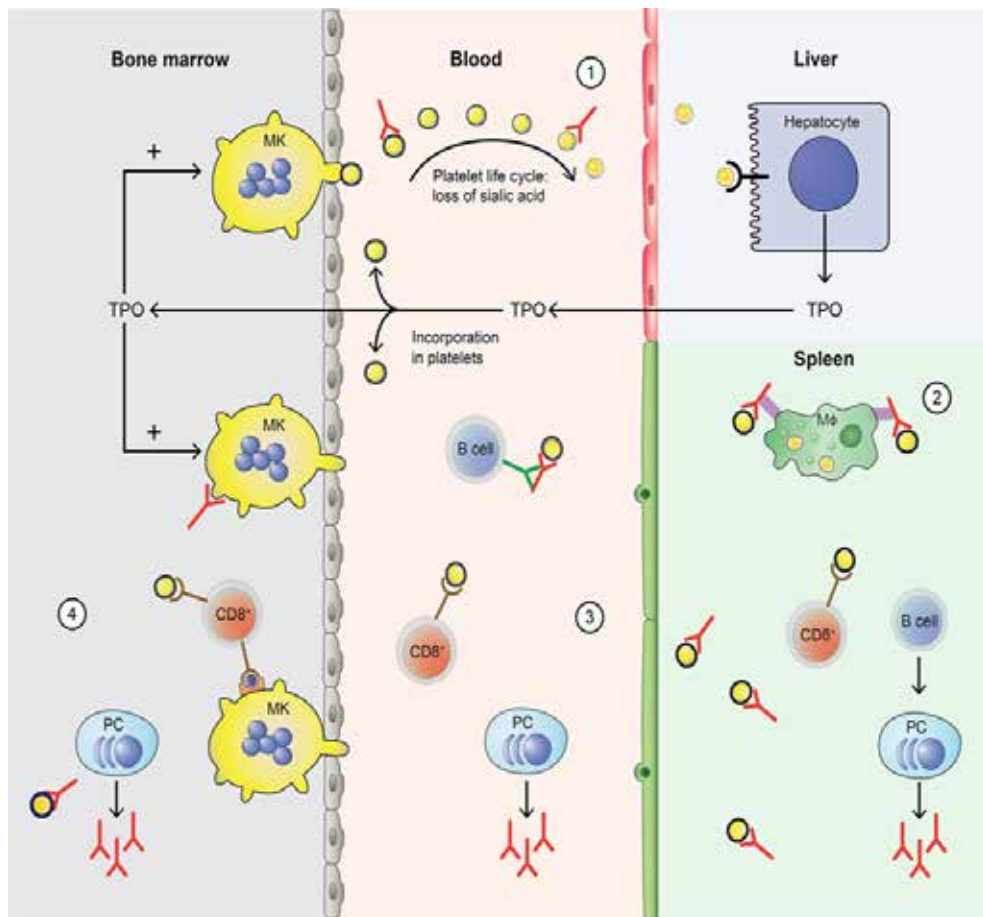


Figure 1. Disturbance of the platelet life cycle in immune thrombocytopenia (ITP).

(1) Platelets (yellow) are normally produced by megakaryocytes (MKs, yellow) in the bone marrow. Aging platelets undergo apoptosis but also gradually lose terminal sialic acid from the surface (indicated by black circles). This allows for their clearance in the liver. Liver-mediated platelet clearance triggers hepatic TPO transcription and translation, and new TPO is released. This process is disrupted by autoantibodies in ITP, which are hypothesized to enhance platelet desialylation leading to enhanced clearance. (2) Macrophages (M $\phi$ , green) can phagocytose platelets; meanwhile, platelet antigens are presented in the spleen to immune cells, such as CD4+ T helper (Th) cells. With CD4+ T cell help, B cells (B cell, dark blue) are able to differentiate into platelet-reactive plasma cells (PC, light blue) that can secrete autoantibodies (red). Cytotoxic T cells (Tc) (CD8+, red) can directly lyse platelets. (3) In peripheral blood, plasma cells and cytotoxic Tc further induce autoimmune responses against platelets. Cytotoxic Tc may also induce desialylation leading to enhanced clearance. In addition, platelet-reactive memory B cells may be present in the blood. (4) Plasma cells and cytotoxic Tc are also present in the bone marrow, where they can inhibit platelet production by targeting MKs.

## Etiology

### Autoantibodies

In approximately 60% of all ITP patients, autoantibodies are found, predominantly against platelet glycoprotein (GP)IIb/IIIa (~70%) and/or the GPIb-IX-V complex (~25%) [78-81]. Antibodies against GPIa-IIa or GPVI are also detected in sporadic cases (~5%) [80,82,83]. While it is not entirely clear how autoantibodies against platelet antigens are generated, their effect on platelet clearance and production have now been fully elucidated (Figure 1). When microbial-antigens mimicking platelet autoantigens, or the platelet antigens themselves, are presented to B cells, these can develop into autoantibody-secreting plasma cells. The spleen has been implied as an organ where immune cells are primarily presented with platelet autoantigens, and where platelet clearance takes place most [84, 85]. Particularly splenic macrophages and dendritic cells (DCs) can present platelet antigens to T helper (Th) cells that provide help to B cells that differentiate into antibody-secreting plasma cells [86,87]. Plasma cells secreting platelet-reactive autoantibodies are present in peripheral blood and bone marrow, where they can further generate autoantibodies that can sequester platelets and MKs [88-90]. In addition, memory B cells activated in the spleen are also released in the circulation (Figure 2)[85]. Autoantibodies accelerate platelet clearance by removal via splenic macrophages and DCs [87], complement deposition [91-93] and platelet apoptosis [94], or by inhibiting megakaryocytic platelet production [88-90].

### Autoantibody and B Cell Classification

Initial studies investigating autoantibodies in ITP identified high levels of platelet-associated IgGs (PAIgGs) in nearly all patients, and they were soon thought to be the causative factor of the autoimmune response. However, it was found that PAIgGs bound nonspecifically to platelets and were detected in other non-ITPs as well [95], likely because platelets themselves can bind circulating IgG via FcγRIIa [96]. PAIgGs thus proved to be a poor predictor of the disease [for a review, see Ref. [95]]. Although it is interesting that PAIgGs levels are higher in ITP and other thrombocytopenic patients (consisting of different IgG subclasses compared to healthy individuals), their usefulness in investigating ITP remains limited and can be largely subscribed to the state of thrombocytopenia rather than the autoimmune conditions. Following the introduction of the MAIPA and immunobead assays in 1987 [79,97], investigators were able to detect and further study platelet-specific autoantibodies in ITP [98,99].

Most autoantibodies found in chronic ITP patients are of the IgG class, but IgM and sporadically IgA antibodies are also detected [100-102]. IgM antibodies were shown to fix complement on platelets which could facilitate clearance, but this has not been further investigated; IgG autoantibodies seem to be the main mediator of antibody-driven autoimmunity [100]. Most prevalent are IgGs of the IgG1 subclass, and while IgG2, IgG3, and IgG4 subclass autoantibodies can be also found in patients, they are often accompanied by IgG1 antibodies [103,104]. Autoantibody allotypes and Fc-glycosylation are important determinants in antibody-mediated immunity and immunological disorders related to ITP

[105-107], yet have been scarcely investigated.

In the majority of ITP patients, B cells producing platelet-binding antibodies have been identified in clinical samples from different sources, such as peripheral blood, spleen, and bone marrow [108-115]. However, not all patients have platelet-reactive B cells [108,109,112-114], suggesting that B cell independent autoimmune mechanisms (such as CD8+ T cell mediated auto-immunity) exist. A landmark study by Roark and co-workers employed repertoire cloning to clone platelet autoantibodies from the spleen of two patients with chronic ITP [110]. Sequence analysis of Ig heavy chain arrangements revealed that these anti-platelet antibodies evolved from a restricted number of B cell clones and provided evidence for extensive modification of heavy chain segments by somatic hypermutation [110]. Overall, these findings provide evidence for a CD4+

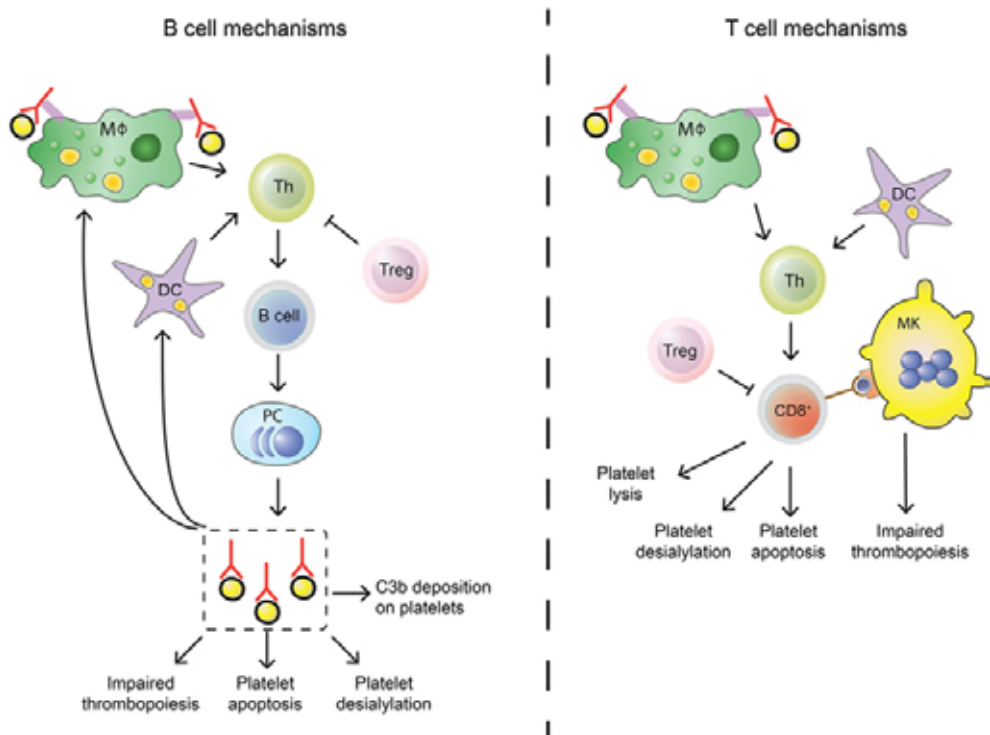


Figure 2. Differences in B cell and T cell mechanisms in immune thrombocytopenia (ITP).

B cells (left) differ from cytotoxic T cells (Tc) (right) in their autoimmune response against platelets in ITP. Stimulation of the adaptive immune response is similar: splenic macrophages (green) and dendritic cells (DCs, purple) can phagocytose platelet fragments to present to T helper (Th, light green) cells. Th cells are able to induce B cell development into antibody secreting plasma cells and can also stimulate cytotoxic Tc effector mechanisms. This process is regulated by regulatory Tc (Treg, pink), but regulatory T cell levels are imbalanced in ITP patients which leads to insufficient control of the autoimmune response. Shared effector functions of B cell-produced autoantibodies and cytotoxic Tc include impairing thrombopoiesis by targeting megakaryocytes (MKs), inducing platelet apoptosis and enhancing platelet desialylation. Autoantibodies can further stimulate C3b deposition on platelets to initiate complement activation, while cytotoxic Tc can directly lyse platelets.

T cell-driven antigen-specific response in patients with ITP. Evidence for the selective incorporation of the VH3-30 variable heavy chain gene segment was noted in this study providing additional evidence for a restricted, oligoclonal B cell response targeting a limited number of epitopes on platelet antigens in ITP patients [110].

### Autoepitope Specificity of Antibodies

As the predominant source of epitopes for autoantibodies in ITP, the GPIIb/IIIa receptor, or integrin  $\alpha$ IIB $\beta$ 3, has been studied most frequently. Reports have shown that autoantibodies can bind epitopes in both the extracellular- and cytoplasmic domain of GPIIb/IIIa [80,116]. However, autoantibodies targeting the cytoplasmic domain are likely to be generated during platelet destruction rather than being pathogenic, but their significance remains unclear [80]. Subsequent studies have shown that autoantibodies particularly bind to the IIB subunit [117,118], or contradictory, the IIIa subunit of the dimer [119]. Eventually, several investigators have demonstrated that specific portions of the protein are preferred autoepitopes in ITP, often near ligand binding sites [81,120]. The vitronectin ( $\alpha$ v $\beta$ 3) receptor shares the  $\beta$ 3 integrin with GPIIb/IIIa and was shown to be an important autoantigen in ITP as well [121]. However, this has not been further investigated.

Less is known about relevant autoepitopes on GP complex Ib-IX-V, although most antibodies are directed against the GPIb part of the receptor complex [78,98,122]. Interestingly, patients with autoantibodies against GPIb are often less responsive to immunosuppressive therapy with corticosteroids or IVIg when compared to patients with GPIIb/IIIa autoantibodies [122-124]. This could be explained by specific epitopes on GPIb, relative receptor abundance on the platelet surface or differences between both protein complexes.

### B Cell Help by CD4+ T Cells

B cells require help by CD4+ Tc to efficiently develop into anti-body-secreting plasma cells (Figure 2). As the development of autoantibodies is a hallmark of ITP, several studies have explored the involvement of CD4+ Tc in the pathogenesis of ITP. Initial observational studies showed that cytokines necessary for Th functions (such as IL-2, IL-10, IFN- $\gamma$ ) are increased in ITP patients [125,126]. Further evidence came from studies that identified a T cell imbalance in ITP: patients have a disturbed Th1/Th2 subset ratio, which trends toward a Th1 phenotype [127-129]. Both rituximab and splenectomy seemed to resolve this polarization in responding patients, indicating the importance of balancing different populations of CD4+ Tc in ITP [128,130]. Pioneering work by Kuwana and co-workers have provided firm evidence for the presence of auto-reactive CD4+ Tc that target epitopes on GPIIb/IIIa [131,132].

Recently, pro-inflammatory Th17 cells have emerged as a critical player in development of autoimmunity [133]. Higher levels of Th17 cells were observed in several ITP cohorts [134,135], but not in all studies [136]. Several studies have found higher levels of both Th1 and Th17, compared to Th2 [137-141]. The potential involvement of another subset

of Th cells, Th22, was also investigated in ITP. Th22 cells typically promote protective and regenerative responses with predominant effects on epithelial cells [142-144]. Increased levels IL-22 and elevated levels of the Th22 T cell subset have been observed in patients with ITP suggesting a role for this population of Tc in ITP pathogenesis [145, 146]. In line with its established role in B cell help, splenic follicular Th (TFH) cells have also been implicated in the pathogenesis of ITP [147]. These findings show that multiple Th populations including Th1/Th17/Th22/TFH contribute to the pathogenesis of ITP [127,129,135,137, 145-147]. We anticipate that the observed skewing toward Th1/Th17/Th22/TFH populations is not specific for ITP as similar Th polarization profiles are observed in other autoimmune diseases.

### CD8+ T Cells

Besides autoreactive B cells, CD8+ Tc have also been implicated in ITP pathogenesis [126, 148, 149]. Evidence from association studies shows that patients with ITP more often present with polymorphisms in CD8+ related cytokines [126,150,151], have increased granzyme levels [152], and have imbalanced ratios of CD8+ Tc cell subsets [137,140]. As CD8+ Tc are also dependent on help of CD4+ Th cells to efficiently perform effector functions, the polarization of CD4+ Th cells probably also affects the CD8+ Tc cell response [137,140].

T cells are part of cell-mediated immunity and have different effector functions compared to antibody-secreting B cells. In ITP, B cells and Tc thus elicit different forms of anti-platelet immunity (Figure 2). CD8+ Tc have been shown to directly lyse platelets [148, 153-155], induce platelet apoptosis [153], and inhibit thrombopoiesis by MKs [156]. CD8+ Tc can further inhibit platelet production by inhibiting MK apoptosis [157].

Increased levels of CD8+ Tc were found in patients without autoantibodies [154], suggesting that CD8+ Tc cell-mediated autoimmunity can be elicited separately from autoantibody-mediated autoimmunity. Evidence of a T cell response separate from antibody-mediated autoimmunity was further shown in ITP patients who did not respond to the anti-CD20+ B cell-depleting antibody rituximab, in whom increased levels of splenic CD8+ Tc were detected [158]. In contrast, CD8+ Tc were found to be protective and required for effective steroid therapy in a murine model of ITP, although these findings are counterintuitive and not supported by observations in other autoimmune diseases [159].

It is unclear how the B cell depletion and repopulation effects of rituximab alter T cell subsets in responding patients. Possibly, the altered cytokine environment as a result of B cell depletion affects T cell subsets, as the B-T cell interplay is essential in a systemic autoimmune response [160]. A recent study showed that rituximab could suppress murine CD8+ T-cell mediated immune responses [161], suggesting that B cells may regulate the CD8+ T-cell response in ITP. In fact, ITP patients present with lower levels of regulatory B cells [162]. However, the effect of rituximab treatment in ITP remains difficult to interpret as B cell depletion may also affect CD20+ regulatory B cells, which can secrete IL-10 and

other suppressive cytokines to induce immune tolerance [163], as suggested previously.

As of yet, the target peptides expressed on MHC class I recognized by platelet specific CD8<sup>+</sup> Tc have not been identified. Interestingly, no clear HLA association is found in ITP patients [38-45], as opposed to other autoimmune diseases. In *H.pylori*-mediated ITP, HLA associations were also unclear [114,164]. Platelets are capable of presenting non-renewable MK-derived peptides on MHC class I, and it is likely that these peptides are being recognized by CD8<sup>+</sup> Tc that develop in patients with ITP [165]. More recently, it was proposed that platelets have the propensity to activate naïve CD8<sup>+</sup> Tc and that platelets can present pathogen-derived peptides in the context of MHC class I [166]. In this context, it is interesting to note that following dengue infection the MHC class I density on platelets increases, suggesting an active role of platelets in combatting infections [166,167]. Under resting conditions, platelets do not express MHC class II molecules on their surface, but several reports suggested platelets to express MHCII complexes during infection [164,168]. Whether antigen presentation on MHC class I by platelets has a role in the pathogenesis of ITP has not been demonstrated. In view of the established role of CD8<sup>+</sup> Tc in this autoimmune disorder, this will be an interesting area for further research.

### Regulatory T Cells

Tregs are a crucial checkpoint to limit immunity and secure immune tolerance. As such, they are important regulators that keep both B- and T cell-mediated autoimmunity in check (Figure 2). The importance of Tregs for the pathogenesis of ITP is evidenced by their reduced numbers and function in patients [169-173]. The pivotal role of immune regulation in ITP, particularly by Tregs, was further shown by phenotypic and Treg profiling studies of treated versus untreated ITP patients. Treatment with corticosteroids and/or rituximab in responding patients both improved Treg levels as well as their activity [130, 174-178], indicating that loss of tolerance is essential for the pathogenesis of ITP. In an experimental murine model of ITP, Tregs were retained in the thymus. This was resolved by IVIg treatment, which normalized Tregs in the periphery [179]. Additionally, transferring retained thymocytes delayed the onset of ITP, suggesting Tregs actively prevent ITP development at least in mice [179]. Interestingly, TPO-RAs improved Treg activity indicating that platelets could directly or indirectly play a regulatory role in ITP by affecting Treg levels [175]. As such, it is clear that ITP patients present with lower Treg levels which are restored upon successful treatment (see above). However, it is still unclear whether restoring Treg functionality directly alleviates the disease or is simply a marker of restored immune tolerance. Potentially involved pathways are further discussed below.

Tregs can interact with DCs to induce a tolerogenic phenotype. Two studies found that the interplay between Tregs and DCs is impaired in ITP [178,180]. As Treg levels are lower in ITP, this leads to a reduced expression of immunomodulatory enzyme indoleamine 2,3-dioxygenase 1 (IDO1) by DCs, and increased levels of mature DCs that can present (auto)antigens to other immune cells [178, 180]. The important role of tolerance induction by DCs in ITP was further suggested by another study, in which IVIg was shown to

mediate its effect via DCs in a murine model [181]. The interplay between Tregs and DCs and immunomodulation via IL-10 is not only important in ITP but was also found essential in antibody-mediated acute lung injury [182,183]. As such, the Treg-DC-axis may be particularly important in autoantibody-mediated ITP, but this remains to be investigated.

### **Other immune Cells**

Several other immune cells may modulate autoimmune responses in ITP but have been investigated sparsely. Neutrophils have been found to line MKs in ITP bone marrow [184], but their role in ITP has not been further investigated. A subset of CD16+ monocytes derived from patients with ITP has shown to promote the proliferation of IFN- $\gamma$ + CD4+ Tc [185]. Shifts in the balance of inhibitory and activating Fc $\gamma$ R were observed on monocytes following treatment with high-dose corticosteroid dexamethason as well as following H.pylori eradication in ITP [186, 187] (further discussed below). Additionally, they were found to be involved in T cell development [185]. Both increased and decreased levels of NK cells have been found in ITP patients [188-190]. The significance of these observations is unclear since NK cells are not able to lyse platelets [148].

Finally, platelets themselves may be able to affect the autoimmune response in ITP, as they are increasingly recognized as mediators of immunity and inflammation [for a recent review, see Ref. [191]]. Evidence for such an autoregulatory loop was found in ITP patients responding to TPO-RAs, who not only had increased platelet counts but also correlating higher TGF- $\beta$  plasma levels [175]. Presumably, increased plasma TGF- $\beta$  levels derive from an increased platelet mass [175]. Furthermore, TPO-RAs reduced both autoantibody and T cell responses in a mouse model, which also lead to elevated TGF- $\beta$  plasma levels [192]. Interestingly, TPO-RAs may induce remission in a subset of patients whom then no longer needed therapy to maintain platelet levels [193–195]. This would imply that immune tolerance can be restored in certain patient subsets by enhancing platelet numbers. Another mechanism by which platelets regulate immune responses occurs via CD40L. Activated Tc can stimulate B cell proliferation and differentiation via CD40L interactions with CD40 on B cells [196]. Platelets normally express CD40L only upon activation, but higher baseline levels are observed in ITP patients [13]. Furthermore, activated platelets from ITP patients were shown to stimulate autoreactive B cells by CD40L [197]. Interestingly, CD40L inhibition was successful in suppressing T cell-assisted B cell-mediated autoantibody production in ITP, even in treatment of refractory ITP [198, 199]. However, whether this is similarly successful affecting a potential B cell- platelet interaction remains unknown.

## **Pathways Involved in Platelet Clearance**

### **Fc $\gamma$ R-Mediated eradication of Platelets**

Fc $\gamma$ R have long been implicated in ITP etiology. These receptors are differentially expressed on immune cells and are the primary receptor for IgG. Fc $\gamma$ R mediate different

functions, including phagocytosis, antibody dependent cellular cytotoxicity, and release of cytokines [reviewed in detail in Ref. [96]]. Most FcγRs are involved in activating the immune system, whereas FcγRIIb is the only inhibitory FcγR. Platelets only express FcγRIIa on their surface, while myeloid cells, such as granulocytes, monocytes, macrophages, and DCs express several FcγRs [96]. In liver and particularly spleen, monocytes and macrophages have been suggested to bind and phagocytose Ig-opsonized platelets by FcγRs, explicitly contributing to platelet clearance and autoantigen presentation [85, 87]. As such, polymorphisms in several FcγRs have been associated with ITP [47-54]. The low affinity FcγRIIa, FcγRIIIb on granulocytes, and FcγRIIIa on NK cells, monocytes, and macrophages all contain SNP that affect binding affinity to IgG (200).

For FcγRIIa, one polymorphism at position 131 (R/H, with H having higher affinity) most strongly or exclusively affects IgG2 binding [200], and the higher-affinity allele was found to be associated with ITP [48, 51-54]. However, these studies had inconsistent outcomes. A recent meta-analysis indicated that the R131H polymorphism might be associated with a subgroup of childhood-onset ITP, but this should be interpreted with caution [54]. In accordance with the notion that FcγRIIIa+ splenic monocytes are particularly important for the clearance of platelets, only the higher affinity-allele of the FcγRIIIa polymorphism at position 158 [F/V, with 158 V having higher affinity for IgG1 and IgG3 [200]] has been found to be associated with ITP [48, 50-53]. Intriguingly, one study found that a polymorphism in the transmembrane region of the inhibitory FcγRIIb (232I/T) is associated with the onset of newly diagnosed ITP in children [49]. This polymorphism (232T) has been found to negatively affect the capacity of this receptor to downregulate immune responses [201] and could point at an immunomodulatory role of FcγRIIb. Intriguingly, eradication of *H.pylori* (a potential molecular mimicry causative of the onset of ITP) was found to shift monocyte FcγR expression toward an inhibitory FcγRIIb phenotype [187]. Finally, the FcγRIIc has also been associated with ITP [50]. FcγRIIc is a pseudogene in most individuals, but having FcγRIIc most likely predisposes individuals to stronger immune responses [202,203]. While the extracellular IgG-binding domain of FcγRIIc is identical to the inhibitory FcγRIIb, the intracellular tail is identical to FcγRIIa and contains an activating motif [202]. Due to the proposed expression of FcγRIIc on B cells, it may downregulate the negative feedback provided by FcγRIIb [202]. Interestingly, FcγRs are known to crosstalk with Toll-like receptors, particularly during bacterial infections. This leads to T cell polarization [204], but it is unclear if this crosstalk is in any way relevant for platelets and/or in the context of ITP. Considering the strong correlation with infections in the onset of ITP, investigating the FcγR-TLR crosstalk could be interesting.

Additional evidence that FcγR-mediated pathways are important in ITP pathogenesis was shown by the therapeutic use of IVIg, which may bind FcγRs by its Fc-portion [205], and is one of the successful cornerstone treatments for ITP to rapidly increase platelet counts. It was recently shown that IVIg does not modulate FcγR expression directly but inhibits the phagocytic capabilities of splenic macrophages [206]. In addition, a previous pilot

study has also shown that Syk-inhibitors, which affect downstream FcγR signaling, can improve ITP [207]. While IVIg does not work in all patients, the efficacy may be predicted by specific FcγR poly-morphisms [208]. As such, various FcγR polymorphisms provide the most compelling evidence that genetics may affect ITP, both by predicting higher risk of disease development and treatment outcomes. In addition, the role of FcγRs on platelets and other immune cells has now been firmly implicated in ITP pathogenesis. Nevertheless, FcγR-independent mechanisms may exist as well.

### **FcγR-independent eradication of Platelets**

A recent study has implicated a FcγR-independent pathway in an experimental mouse model [209], which was hypothesized to occur simultaneously aside FcγR-mediated clearance by splenic macrophages. Autoreactive antibodies against GPIb were hypothesized to induce platelet activation and degranulation, which leads to sialidase release [210]. This induces desialylation of platelet membrane glycans, which can subsequently lead to recognition of platelets by the AMR in the liver thereby accelerating platelet clearance [27,209]. Interestingly, there are a few cases of ITP patients with abnormal platelet surface sialic acid levels [211,212]. Oseltamivir, which is a sialidase inhibitor used to treat influenza, has been found to increase platelet sialic acid content [213] and in two cases was successful in ameliorating thrombocytopenia whereas conventional therapy was not [212,214]. Platelet desialylation was also found to correlate with non-responsiveness to first-line therapies in ITP [215]. Finally, CD8+ Tc have also been suggested to induce platelet desialylation and to facilitate platelet clearance similar to the earlier mentioned mechanisms [155]. While the importance of sialic acid in the platelet life cycle has long been established [14], it is unclear whether the experimental findings in mice can be translated to a human and/or clinical setting. Ongoing studies are needed to establish the importance of platelet desialylation in ITP.

### **C-Reactive Protein and Reactive Oxygen Species**

Recently, a role for inflammatory acute-phase protein C-reactive protein (CRP) has also been implied in ITP pathogenesis [216]. CRP levels were elevated in ITP patients and enhanced platelet phagocytosis in presence of anti-platelet antibodies in vitro and in vivo. This effect was ameliorated by IVIg treatment, suggesting that this mechanism may at least in part be mediated via FcγRs [216]. Phosphorylcholine, a CRP ligand present on cell surfaces, was exposed after antibody-induced oxidative stress. Oxidative stress induced by ITP autoantibodies has also been shown in two separate studies on ITP [217,218] and appears to be a suitable biomarker for ITP [219]. Additionally, the pathophysiological role of reactive oxygen species has long been implied in a model of HIV-initiated ITP [64,65,67]. In this model, reactive oxygen species induced by platelet antibodies were able to directly lyse platelets, leading to platelet fragmentation. This appears to involve the platelet NADPH pathway and is complement independent [65]. Interestingly, treating platelets with dexamethasone was shown to inhibit NADPH oxidase components that partially prevented induction of reactive oxygen species [67]. Further studies will be required to elucidate the exact role of CRP, oxidative stress, and autoantibodies or autoreactive CD8+ Tc in ITP.

## Model for ITP Pathogenesis

As knowledge on the pathogenesis of ITP develops, definitions become outdated, and lines between primary and secondary ITP are beginning to blur. In other autoimmune diseases, infections are increasingly recognized as one of the primary initiating events that can lead to an autoimmune response. This is not the case for ITP, where it is regarded as a secondary form. However, even in what is called primary ITP, there must be some sort of initiating event that triggers the autoimmune response and exposes platelet antigens. This initiating event will obviously still have consequences for clinical treatment of ITP, whether it is an infection, blood transfusion, drug, or an unknown other trigger. Nonetheless, infections should no longer simply be regarded as a secondary form considering their potential as an initiating event or trigger to expose platelet antigens.

The number of people developing ITP directly after an infection is small, which suggests that additional factors have to be present during an infection to develop persistent autoimmunity. Individuals with a known autoimmune disease are more prone to develop ITP, indicating that dysregulation of immune homeostasis may contribute to the onset of ITP. Interestingly, most pediatric patients only develop transient thrombocytopenia, which is eventually resolved when the viral antigen is cleared. Meanwhile, similar to other autoimmune disorders, chronic ITP is more prevalent in adult patients, and the incidence increases with age. Based on the currently available data, we propose a simplified model of ITP in which both exposure of platelet antigens and loss of tolerance are required to induce ITP (Figure 3). The specific type of trigger likely determines whether a CD4+ T cell-assisted B cell response develops or whether CD8+ Tc targeting platelets are induced. Transient forms of ITP may develop if insufficient CD4+ T cell help is available for the generation of class-switched, fully affinity matured, strongly binding anti-platelet antibodies. Such antibodies are likely produced by bone marrow-residing plasma cells in a fully developed CD4+ T cell-assisted B cell response. We furthermore propose that platelet directed CD8+ T cell responses develop following presentation of pathogen-derived peptides on MHC class I that may evoke the formation of CD8+Tc that (cross) react with peptides presented on MHC class I on platelets.

## Future Research

### Emerging Concepts and Opportunities to Unravel the Pathogenesis of ITP

Limited information is available on the autoantigens in ITP and their importance for recognition by immune cells once bound by autoantibodies. Epitopes targeted by platelet autoantibodies seem to differ between patients, coinciding with different responses to therapy and different bleeding phenotypes. The molecular basis for the variable bleeding diathesis in patients with ITP has not yet been fully elucidated. Investigators have primarily made use of ITP sera or plasmas to study the role of autoantibodies. However, these can contain multiple autoantibodies, some potentially undetected by the current methods.

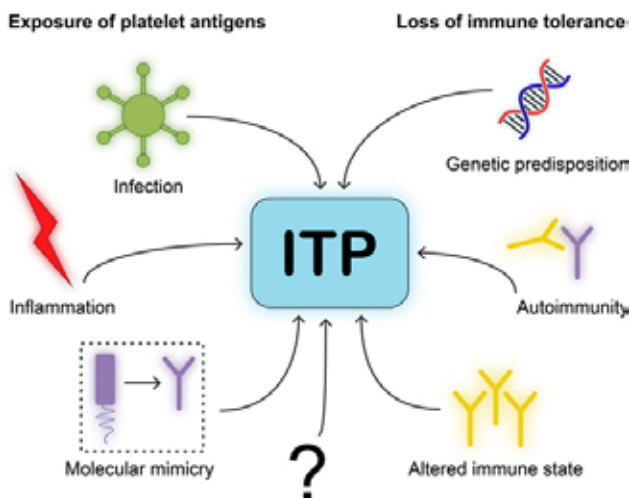


Figure 3. Model for immune thrombocytopenia (ITP) pathogenesis.

We postulate a simplified model for the pathogenesis of ITP. One, neo-epitopes on platelet antigens need to be exposed to immune cells. This requires an initiating event or trigger, such as infection, inflammation, or molecular mimicry of viral antigens to resemble platelet glycoproteins. Two, immune cells will need to be able to develop self-reactivity due to loss of immune tolerance. This requires either genetic disposition in immune related-genes, autoimmunity by comorbidities that implies a central dysfunction in tolerance, or an altered immune state such as after organ transplantation.

Similar to the elegant studied by Roark and co-workers [110], specific autoantibodies should be isolated to further study their effects on platelets, possibly combining characteristics like subclass characterization, epitope specificity, and glycosylation patterns.

### ITP versus Other Autoimmune Diseases: Lessons to Be Learnt

In other autoimmune disorders such as rheumatoid arthritis, systemic lupus erythematosus, or type 1 diabetes, it has been shown that post-translational modifications of autoantigens can elicit the formation of CD4+ T cell responses as well as create neo-epitopes that are recognized by B cells. In view of the common mechanisms involved in loss of tolerance against self, these findings may open novel avenues for dissecting pathways contributing to the onset of ITP.

Evidence has been obtained for post-translational modifications of platelet proteins. Phosphorylation and particularly glycosylation of platelets have been well studied [29,210,220,221], and the importance of platelet glycans is increasingly appreciated. Furthermore, platelets and peripheral blood contain different glycosyltransferases to modify platelet glycans [221], but their relevance in normal platelet physiology is still unclear and their potential relevance for the onset of ITP has not been established. A role for desialylation triggered by platelet autoantibodies or CD8+ Tc has been postulated, but it is unknown if this can also lead to the generation of neo-epitopes on the platelet surface [155,209]. Recently, it was also shown that formation of oxidative stress induced neo-epitopes on platelets promotes binding of the acute phase protein CRP resulting in

enhanced phagocytosis of IgG-coated platelets [216]. It is unclear whether the auto-antibodies found in ITP patients are able to recognize such neo-epitopes in similar fashion.

Besides post-translational modifications, platelet membranes are highly dynamic with respect to the expression of cell-surface receptors. GP expression on the platelet surface is tightly regulated by different metalloproteases, such as ADAM10 and ADAM17 that facilitate receptor shedding [222,223]. Additionally, platelet granules release their content to rapidly increase receptor density on the membrane, such as the well-established activation marker P-selectin [223]. These processes are important in both health and disease [224]; however, it is unknown if the dynamic shuffling of receptors on the platelet surface is in any way relevant to formation of neo-epitopes in ITP.

The difference between post-translational modifications in other autoimmune diseases and ITP is that most of the modifications mentioned above are induced by autoantibodies in ITP, while modifications in for example the autoantigens that are implicated in rheumatoid arthritis precede the formation of autoantibodies [225-227] and are postulated to be one of the key events that triggers their generation. In fact, infection-induced post-translational modifications of target proteins, such as citrullination of fibrin, are thought to initiate a continuous inflammatory environment, which eventually leads to autoimmunity [225-227]. Interestingly, the autoantigens in rheumatoid arthritis are usually located on “static” long-lived cartilage and/or joint proteins, such as fibrin. This is different in ITP, where the autoantigens are located on GPs on platelets that have a limited lifespan. Currently, no information is available with respect to the potential of post-translational modifications of platelet antigens to trigger autoimmune responses. In view of the prominent role of post-translational modifications in the onset of autoimmunity, we speculate that this will provide a novel and interesting avenue for future research to dissect the mechanisms that contribute to the onset of ITP.

## Conclusion

We suggest a simplified model of ITP in which both exposure of platelet antigens and loss of tolerance are required for the onset of ITP, thereby promoting CD4+ T cell-assisted B cell responses against platelets. Additionally, we propose that infections resulting in the presentation of pathogen-derived peptides on MHC class I may induce the formation of CD8+ Tc that (cross) react with peptides presented on MHC class I on platelets. Specific triggers likely determine the type of autoimmune response against platelets. We speculate that post-translational modifications of platelet antigens harbor potential to generate neo-epitopes that trigger autoimmune responses in ITP, as they do in other autoimmune disorders. Future studies interrogating these hypotheses may yield novel insights into the mechanisms that underlie the development of ITP.

## Author Contributions

MS wrote the manuscript. MR, JV, GV, FL and AJ provided input, made suggestions for improvement, and approved the final version for submission.

## Acknowledgments

We would like to thank Egied Simons (Department of Hematology, Erasmus Medical Centre, Rotterdam) for his help in digitalizing Figures 1-3.

## Funding

Supported by grant PPOC-2013-019 and PPOC-2015-024P (Netherlands Ministry of Health). AJGJ is supported by a Clinical Fellowship of the European Hematology Association.

## References

1. Rodeghiero F, Stasi R, Gernsheimer T, Michel M, Provan D, Arnold DM, et al. Standardization of terminology, definitions and outcome criteria in immune thrombocytopenic purpura of adults and children: report from an international working group. *Blood* (2009) 113(11):2386–93. doi:10.1182/ blood-2008-07-162503
2. Provan D, Stasi R, Newland AC, Blanchette VS, Bolton-Maggs P, Bussel JB, et al. International consensus report on the investigation and management of primary immune thrombocytopenia. *Blood* (2010) 115(2):168–86. doi:10.1182/ blood-2009-06-225565
3. Neunert C, Lim W, Crowther M, Cohen A, Solberg L Jr, Crowther MA, et al. The American Society of Hematology 2011 evidence-based practice guideline for immune thrombocytopenia. *Blood* (2011) 117(16):4190–207. doi:10.1182/ blood-2010-08-302984
4. Michel M. Immune thrombocytopenia nomenclature, consensus reports, and guidelines: what are the consequences for daily practice and clinical research? *Semin Hematol* (2013) 50(Suppl 1):S50–4. doi:10.1053/j.seminhematol.2013.03.008
5. Cines DB, Bussel JB, Liebman HA, Luning Prak ET. The ITP syndrome: pathogenic and clinical diversity. *Blood* (2009) 113(26):6511–21. doi:10.1182/ blood-2009-01-129155
6. Moulis G, Palmaro A, Montastruc JL, Godeau B, Lapeyre-Mestre M, Sailler L. Epidemiology of incident immune thrombocytopenia: a nationwide population-based study in France. *Blood* (2014) 124(22):3308–15. doi:10.1182/ blood-2014-05-578336
7. Terrell DR, Beebe LA, Vesely SK, Neas BR, Segal JB, George JN. The incidence of immune thrombocytopenic purpura in children and adults: a critical review of published reports. *Am J Hematol* (2010) 85(3):174–80. doi:10.1002/ ajh.21616
8. Bennett CM, Neunert C, Grace RF, Buchanan G, Imbach P, Vesely SK, et al. Predictors of remission in children with newly diagnosed immune thrombocytopenia: data from the Intercontinental Cooperative ITP Study Group Registry II participants. *Pediatr Blood Cancer* (2018) 65(1):e26736. doi:10.1002/ pbc.26736
9. An R, Wang PP. Length of stay, hospitalization cost, and in-hospital mortality in US adult inpatients with immune thrombocytopenic purpura, 2006-2012. *Vasc Health Risk Manag* (2017) 13:15–21. doi:10.2147/ VHRM.S123631
10. Neunert C, Noroozi N, Norman G, Buchanan GR, Goy J, Nazi I, et al. Severe bleeding events in adults and children with primary immune thrombocytopenia: a systematic review. *J Thromb Haemost* (2015) 13(3):457–64. doi:10.1111/ jth.12813
11. Panzer S, Rieger M, Vormittag R, Eichelberger B, Dunkler D, Pabinger I. Platelet function to estimate the bleeding risk in autoimmune thrombocytopenia. *Eur J Clin Invest* (2007) 37(10):814–9. doi:10.1111/j.1365-2362.2007.01855.x
12. Greene LA, Chen S, Seery C, Imahiyerobo AM, Bussel JB. Beyond the platelet count: immature platelet

- fraction and thromboelastometry correlate with bleeding in patients with immune thrombocytopenia. *Br J Haematol* (2014) 166(4):592–600. doi:10.1111/bjh.12929
13. Frelinger AL III, Grace RF, Gerrits AJ, Berny-Lang MA, Brown T, Carmichael SL, et al. Platelet function tests, independent of platelet count, are associated with bleeding severity in ITP. *Blood* (2015) 126(7):873–9. doi:10.1182/blood-2015-02-628461
  14. Li R, Hoffmeister KM, Falet H. Glycans and the platelet life cycle. *Platelets* (2016) 27(6):505–11. doi:10.3109/09537104.2016.1171304
  15. Shrivastava M. The platelet storage lesion. *Transfus Apher Sci* (2009) 41(2):105–13. doi:10.1016/j.transci.2009.07.002
  16. Devine DV, Serrano K. The platelet storage lesion. *Clin Lab Med* (2010) 30(2):475–87. doi:10.1016/j.cll.2010.02.002
  17. Rijkers M, van den Eshof BL, van der Meer PF, van Alphen FPJ, de Korte D, Leebeek FWG, et al. Monitoring storage induced changes in the platelet proteome employing label free quantitative mass spectrometry. *Sci Rep* (2017) 7(1):11045. doi:10.1038/s41598-017-11643-w
  18. Rijkers M, van der Meer PF, Bontekoe IJ, Daal BB, de Korte D, Leebeek FW, et al. Evaluation of the role of the GPIb-IX-V receptor complex in development of the platelet storage lesion. *Vox Sang* (2016) 111(3):247–56. doi:10.1111/vox.12416
  19. Stegner D, vanEeuwijk JMM, Angay O, Gorelashvili MG, Semeniak D, Pinnecker J, et al. Thrombopoiesis is spatially regulated by the bone marrow vasculature. *Nat Commun* (2017) 8(1):127. doi:10.1038/s41467-017-00201-7
  20. Italiano JE Jr, Lecine P, Shivdasani RA, Hartwig JH. Blood platelets are assembled principally at the ends of proplatelet processes produced by differentiated megakaryocytes. *J Cell Biol* (1999) 147(6):1299–312. doi:10.1083/jcb.147.6.1299
  21. Thon JN, Montalvo A, Patel-Hett S, Devine MT, Richardson JL, Ehrlicher A, et al. Cytoskeletal mechanics of proplatelet maturation and platelet release. *J Cell Biol* (2010) 191(4):861–74. doi:10.1083/jcb.201006102
  22. Lefrançais E, Ortiz-Munoz G, Caudrillier A, Mallavia B, Liu F, Sayah DM, et al. The lung is a site of platelet biogenesis and a reservoir for haematopoietic progenitors. *Nature* (2017) 544(7648):105–9. doi:10.1038/nature21706
  23. Gurney AL, Carver-Moore K, de Sauvage FJ, Moore MW. Thrombocytopenia in c-mpl-deficient mice. *Science* (1994) 265(5177):1445–7. doi:10.1126/science.8073287
  24. Alexander WS, Roberts AW, Nicola NA, Li R, Metcalf D. Deficiencies in progenitor cells of multiple hematopoietic lineages and defective megakaryocytopoiesis in mice lacking the thrombopoietic receptor c-Mpl. *Blood* (1996) 87(6):2162–70.
  25. Varghese LN, Defour JP, Pecquet C, Constantinescu SN. The thrombopoietin receptor: structural basis of traffic and activation by ligand, mutations, agonists, and mutated calreticulin. *Front Endocrinol* (2017) 8:59. doi:10.3389/fendo.2017.00059
  26. de Sauvage FJ, Carver-Moore K, Luoh SM, Ryan A, Dowd M, Eaton DL, et al. Physiological regulation of early and late stages of megakaryocytopoiesis by thrombopoietin. *J Exp Med* (1996) 183(2):651–6. doi:10.1084/jem.183.2.651
  27. Grozovsky R, Begonja AJ, Liu K, Visner G, Hartwig JH, Falet H, et al. The Ashwell-Morell receptor regulates hepatic thrombopoietin production via JAK2-STAT3 signaling. *Nat Med* (2015) 21(1):47–54. doi:10.1038/nm.3770
  28. Mason KD, Carpinelli MR, Fletcher JI, Collinge JE, Hilton AA, Ellis S, et al. Programmed anuclear cell death delimits platelet life span. *Cell* (2007) 128(6):1173–86. doi:10.1016/j.cell.2007.01.037
  29. Grozovsky R, Giannini S, Falet H, Hoffmeister KM. Regulating billions of blood platelets: glycans and beyond. *Blood* (2015) 126(16):1877–84. doi:10.1182/blood-2015-01-569129
  30. Tahara T, Usuki K, Sato H, Ohashi H, Morita H, Tsumura H, et al. A sensitive sandwich ELISA for measuring thrombopoietin in human serum: serum thrombopoietin levels in healthy volunteers and in patients with haemopoietic disorders. *Br J Haematol* (1996) 93(4):783–8. doi:10.1046/j.1365-2141.1996.d01-1741.x
  31. Kosugi S, Kurata Y, Tomiyama Y, Tahara T, Kato T, Tadokoro S, et al. Circulating thrombopoietin level in chronic immune thrombocytopenic purpura. *Br J Haematol* (1996) 93(3):704–6. doi:10.1046/j.1365-2141.1996.d01-1702.x

32. Rodeghiero F, Carli G. Beyond immune thrombocytopenia: the evolving role of thrombopoietin receptor agonists. *Ann Hematol* (2017) 96(9):1421–34. doi:10.1007/s00277-017-2953-6
33. Wu KH, Peng CT, Li TC, Wan L, Tsai CH, Lan SJ, et al. Interleukin 4, interleukin 6 and interleukin 10 polymorphisms in children with acute and chronic immune thrombocytopenic purpura. *Br J Haematol* (2005) 128(6):849–52. doi:10.1111/j.1365-2141.2005.05385.x
34. Emmerich F, Bal G, Barakat A, Milz J, Muhle C, Martinez-Gamboa L, et al. High-level serum B-cell activating factor and promoter polymorphisms in patients with idiopathic thrombocytopenic purpura. *Br J Haematol* (2007) 136(2):309–14. doi:10.1111/j.1365-2141.2006.06431.x
35. Rocha AM, De Souza C, Rocha GA, De Melo FF, Saraiva IS, Clementino NC, et al. IL1RN VNTR and IL2-330 polymorphic genes are independently associated with chronic immune thrombocytopenia. *Br J Haematol* (2010) 150(6):679–84. doi:10.1111/j.1365-2141.2010.08318.x
36. Pehlivan M, Okan V, Sever T, Balci SO, Yilmaz M, Babacan T, et al. Investigation of TNF-alpha, TGF-beta 1, IL-10, IL-6, IFN-gamma, MBL, GPIA, and IL1A gene polymorphisms in patients with idiopathic thrombocytopenic purpura. *Platelets* (2011) 22(8):588–95. doi:10.3109/09537104.2011.577255
37. Saitoh T, Tsukamoto N, Koiso H, Mitsui T, Yokohama A, Handa H, et al. Interleukin-17F gene polymorphism in patients with chronic immune thrombocytopenia. *Eur J Haematol* (2011) 87(3):253–8. doi:10.1111/j.1600-0609.2011.01651.x
38. Kuwana M, Kaburaki J, Pandey JP, Murata M, Kawakami Y, Inoko H, et al. HLA class II alleles in Japanese patients with immune thrombocytopenic purpura. Associations with anti-platelet glycoprotein autoantibodies and responses to splenectomy. *Tissue Antigens* (2000) 56(4):337–43. doi:10.1034/j.1399-0039.2000.560405.x
39. Leung AY, Hawkins BR, Chim CS, Kwong YY, Liang RH. Genetic analysis of HLA-typing in Chinese patients with idiopathic thrombocytopenic purpura. *Haematologica* (2001) 86(2):221–2.
40. Stanworth SJ, Turner DM, Brown J, McCloskey D, Brown C, Provan D, et al. Major histocompatibility complex susceptibility genes and immune thrombocytopenic purpura in Caucasian adults. *Hematology* (2002) 7(2):119–21. doi:10.1080/10245330290028605
41. El Neanaey WA, Barakat SS, Ahmed MA, El Nabie WM, Ahmed ME. The relation between HLA-DRB1 alleles and the outcome of therapy in children with idiopathic thrombocytopenic purpura. *Egypt J Immunol* (2005) 12(2):29–38.
42. Hopkins LM, Davis JM, Buchli R, Vangundy RS, Schwartz KA, Gerlach JA. MHC class I-associated peptides identified from normal platelets and from individuals with idiopathic thrombocytopenic purpura. *Hum Immunol* (2005) 66(8):874–83. doi:10.1016/j.humimm.2005.06.004
43. Maia MH, Peixoto Rde L, de Lima CP, Magalhaes M, Sena L, Costa Pdo S, et al. Predisposition to idiopathic thrombocytopenic purpura maps close to the major histocompatibility complex class I chain-related gene A. *Hum Immunol* (2009) 70(3):179–83. doi:10.1016/j.humimm.2009.01.011
44. Negi RR, Bhoria P, Pahuja A, Saikia B, Varma N, Malhotra P, et al. Investigation of the possible association between the HLA antigens and idiopathic thrombocytopenic purpura (ITP). *Immunol Invest* (2012) 41(2):117–28. doi:10.3109/08820139.2011.593218
45. Ho WL, Lu MY, Hu FC, Lee CC, Huang LM, Jou ST, et al. Clinical features and major histocompatibility complex genes as potential susceptibility factors in pediatric immune thrombocytopenia. *J Formos Med Assoc* (2012) 111(7):370–9. doi:10.1016/j.jfma.2011.06.025
46. Jernas M, Hou Y, Stromberg Celind F, Shao L, Nookaew I, Wang Q, et al. Differences in gene expression and cytokine levels between newly diagnosed and chronic pediatric ITP. *Blood* (2013) 122(10):1789–92. doi:10.1182/blood-2013-05-502807
47. Foster CB, Zhu S, Erichsen HC, Lehrnbecher T, Hart ES, Choi E, et al. Polymorphisms in inflammatory cytokines and Fcgamma receptors in childhood chronic immune thrombocytopenic purpura: a pilot study. *Br J Haematol* (2001) 113(3):596–9. doi:10.1046/j.1365-2141.2001.02807.x
48. Carcao MD, Blanchette VS, Wakefield CD, Stephens D, Ellis J, Matheson K, et al. Fcgamma receptor IIa and IIIa polymorphisms in childhood immune thrombocytopenic purpura. *Br J Haematol* (2003) 120(1):135–41. doi:10.1046/j.1365-2141.2003.04033.x
49. Bruin M, Bierings M, Uiterwaal C, Revesz T, Bode L, Wiesman ME, et al. Platelet count, previous infection and FCGR2B genotype predict development of chronic disease in newly diagnosed idiopathic thrombocytopenia in childhood: results of a prospective study. *Br J Haematol* (2004) 127(5):561–7. doi:10.1111/

j.1365-2141.2004.05235.x

50. Breunis WB, van Mirre E, Bruin M, Geissler J, de Boer M, Peters M, et al. Copy number variation of the activating FCGR2C gene predisposes to idiopathic thrombocytopenic purpura. *Blood* (2008) 111(3):1029–38. doi:10.1182/blood-2007-03-079913
51. Amorim DM, Silveira Vda S, Scrideli CA, Queiroz RG, Tone LG. Fcγ receptor gene polymorphisms in childhood immune thrombocytopenic purpura. *J Pediatr Hematol Oncol* (2012) 34(5):349–52. doi:10.1097/MPH.0b013e3182580908
52. Eyada TK, Farawela HM, Khorshied MM, Shaheen IA, Selim NM, Khalifa IA. FcγRIIa and FcγRIIIa genetic polymorphisms in a group of pediatric immune thrombocytopenic purpura in Egypt. *Blood Coagul Fibrinolysis* (2012) 23(1):64–8. doi:10.1097/MBC.0b013e31832834ddf2f
53. Papagianni A, Economou M, Tragiannidis A, Karatza E, Samarah F, Gombakis N, et al. FcγRIIa and FcγRIIIa polymorphisms in childhood primary immune thrombocytopenia: implications for disease pathogenesis and outcome. *Blood Coagul Fibrinolysis* (2013) 24(1):35–9. doi:10.1097/MBC.0b013e318328359b-c3b
54. Wang D, Hu SL, Cheng XL, Yang JY. FCGR2A rs1801274 polymorphism is associated with risk of childhood-onset idiopathic (immune) thrombocytopenic purpura: evidence from a meta-analysis. *Thromb Res* (2014) 134(6):1323–7. doi:10.1016/j.thromres.2014.10.003
55. Simeoni I, Stephens JC, Hu F, Deevi SV, Megy K, Bariana TK, et al. A high-throughput sequencing test for diagnosing inherited bleeding, thrombotic, and platelet disorders. *Blood* (2016) 127(23):2791–803. doi:10.1182/blood-2015-12-688267
56. Bariana TK, Ouwehand WH, Guerrero JA, Gomez K; BRIDGE Bleeding, Thrombotic and Platelet Disorders and ThromboGenomics Consortia. Dawning of the age of genomics for platelet granule disorders: improving insight, diagnosis and management. *Br J Haematol* (2017) 176(5):705–20. doi:10.1111/bjh.14471
57. Takahashi T, Yujiri T, Shinohara K, Inoue Y, Sato Y, Fujii Y, et al. Molecular mimicry by *Helicobacter pylori* CagA protein may be involved in the pathogenesis of *H. pylori*-associated chronic idiopathic thrombocytopenic purpura. *Br J Haematol* (2004) 124(1):91–6. doi:10.1046/j.1365-2141.2003.04735.x
58. Stasi R, Sarpatwari A, Segal JB, Osborn J, Evangelista ML, Cooper N, et al. Effects of eradication of *Helicobacter pylori* infection in patients with immune thrombocytopenic purpura: a systematic review. *Blood* (2009) 113(6):1231–40. doi:10.1182/blood-2008-07-167155
59. Rajan SK, Espina BM, Liebman HA. Hepatitis C virus-related thrombocytopenia: clinical and laboratory characteristics compared with chronic immune thrombocytopenic purpura. *Br J Haematol* (2005) 129(6):818–24. doi:10.1111/j.1365-2141.2005.05542.x
60. Zhang W, Nardi MA, Borkowsky W, Li Z, Karpatkin S. Role of molecular mimicry of hepatitis C virus protein with platelet GPIIIa in hepatitis C-related immunologic thrombocytopenia. *Blood* (2009) 113(17):4086–93. doi:10.1182/blood-2008-09-181073
61. Hohmann AW, Booth K, Peters V, Gordon DL, Comacchio RM. Common epitope on HIV p24 and human platelets. *Lancet* (1993) 342(8882):1274–5. doi:10.1016/0140-6736(93)92363-X
62. Bettaieb A, Oksenhendler E, Duedari N, Bierling P. Cross-reactive antibodies between HIV-gp120 and platelet gpIIIa (CD61) in HIV-related immune thrombocytopenic purpura. *Clin Exp Immunol* (1996) 103(1):19–23. doi:10.1046/j.1365-2249.1996.917606.x
63. Dominguez V, Gevorkian G, Govezensky T, Rodriguez H, Viveros M, Cocho G, et al. Antigenic homology of HIV-1 GP41 and human platelet glycoprotein GPIIIa (integrin beta3). *J Acquir Immune Defic Syndr Hum Retrovirol* (1998) 17(5):385–90. doi:10.1097/00042560-199804150-00001
64. Nardi M, Tomlinson S, Greco MA, Karpatkin S. Complement-independent, peroxide-induced antibody lysis of platelets in HIV-1-related immune thrombocytopenia. *Cell* (2001) 106(5):551–61. doi:10.1016/S0092-8674(01)00477-9
65. Nardi M, Feinmark SJ, Hu L, Li Z, Karpatkin S. Complement-independent Ab-induced peroxide lysis of platelets requires 12-lipoxygenase and a platelet NADPH oxidase pathway. *J Clin Invest* (2004) 113(7):973–80. doi:10.1172/JCI20726
66. Li Z, Nardi MA, Karpatkin S. Role of molecular mimicry to HIV-1 peptides in HIV-1-related immunologic thrombocytopenia. *Blood* (2005) 106(2):572–6. doi:10.1182/blood-2005-01-0243
67. Nardi MA, Gor Y, Feinmark SJ, Xu F, Karpatkin S. Platelet particle formation by anti GPIIIa49-66 Ab,

- Ca<sup>2+</sup> ionophore A23187, and phorbol myristate acetate is induced by reactive oxygen species and inhibited by dexamethasone blockade of platelet phospholipase A<sub>2</sub>, 12-lipoxygenase, and NADPH oxidase. *Blood* (2007) 110(6):1989–96. doi:10.1182/blood-2006-10-054064
68. DiMaggio D, Anderson A, Bussel JB. Cytomegalovirus can make immune thrombocytopenic purpura refractory. *Br J Haematol* (2009) 146(1):104–12. doi:10.1111/j.1365-2141.2009.07714.x
69. Wu Z, Zhou J, Wei X, Wang X, Li Y, Peng B, et al. The role of Epstein-Barr virus (EBV) and cytomegalovirus (CMV) in immune thrombocytopenia. *Hematology* (2013) 18(5):295–9. doi:10.1179/1607845413Y.0000000084
70. Wright JF, Blanchette VS, Wang H, Arya N, Petric M, Semple JW, et al. Characterization of platelet-reactive antibodies in children with varicella-as-associated acute immune thrombocytopenic purpura (ITP). *Br J Haematol* (1996) 95(1):145–52. doi:10.1046/j.1365-2141.1996.d01-1872.x
71. Musaji A, Cormont F, Thirion G, Cambiaso CL, Coutelier JP. Exacerbation of autoantibody-mediated thrombocytopenic purpura by infection with mouse viruses. *Blood* (2004) 104(7):2102–6. doi:10.1182/blood-2004-01-0310
72. Mantadakis E, Farmaki E, Buchanan GR. Thrombocytopenic purpura after measles-mumps-rubella vaccination: a systematic review of the literature and guidance for management. *J Pediatr* (2010) 156(4):623–8. doi:10.1016/j.jpeds.2009.10.015
73. Grimaldi-Bensouda L, Michel M, Aubrun E, Leighton P, Viallard JF, Adoue D, et al. A case-control study to assess the risk of immune thrombocytopenia associated with vaccines. *Blood* (2012) 120(25):4938–44. doi:10.1182/blood-2012-05-431098
74. Rose NR. Negative selection, epitope mimicry and autoimmunity. *Curr Opin Immunol* (2017) 49:51–5. doi:10.1016/j.coi.2017.08.014
75. Aslam R, Speck ER, Kim M, Crow AR, Bang KW, Nestel FP, et al. Platelet toll-like receptor expression modulates lipopolysaccharide-induced thrombocytopenia and tumor necrosis factor- $\alpha$  production in vivo. *Blood* (2006) 107(2):637–41. doi:10.1182/blood-2005-06-2202
76. Aster RH, Bougie DW. Drug-induced immune thrombocytopenia. *N Engl J Med* (2007) 357(6):580–7. doi:10.1056/NEJMra066469
77. Cines DB, Liebman H, Stasi R. Pathobiology of secondary immune thrombocytopenia. *Semin Hematol* (2009) 46(1 Suppl 2):S2–14. doi:10.1053/j.seminhematol.2008.12.005
78. van Leeuwen EF, van der Ven JT, Engelfriet CP, von dem Borne AE. Specificity of autoantibodies in autoimmune thrombocytopenia. *Blood* (1982) 59(1):23–6.
79. McMillan R, Tani P, Millard F, Berchtold P, Renshaw L, Woods VL Jr. Platelet-associated and plasma anti-glycoprotein autoantibodies in chronic ITP. *Blood* (1987) 70(4):1040–5.
80. He R, Reid DM, Jones CE, Shulman NR. Spectrum of Ig classes, specificities, and titers of serum anti-glycoproteins in chronic idiopathic thrombocytopenic purpura. *Blood* (1994) 83(4):1024–32.
81. Kiyomizu K, Kashiwagi H, Nakazawa T, Tadokoro S, Honda S, Kanakura Y, et al. Recognition of highly restricted regions in the beta-propeller domain of  $\alpha$ IIb by platelet-associated anti- $\alpha$ IIb $\beta$ 3 autoantibodies in primary immune thrombocytopenia. *Blood* (2012) 120(7):1499–509. doi:10.1182/blood-2012-02-409995
82. Beer JH, Rabaglio M, Berchtold P, von Felten A, Clemetson KJ, Tsakiris DA, et al. Autoantibodies against the platelet glycoproteins (GP) IIb/IIIa, Ia/IIa, and IV and partial deficiency in GPIV in a patient with a bleeding disorder and a defective platelet collagen interaction. *Blood* (1993) 82(3):820–9.
83. Boylan B, Chen H, Rathore V, Paddock C, Salacz M, Friedman KD, et al. Anti-GPVI-associated ITP: an acquired platelet disorder caused by autoantibody-mediated clearance of the GPVI/Fc $\gamma$  chain complex from the human platelet surface. *Blood* (2004) 104(5):1350–5. doi:10.1182/blood-2004-03-0896
84. Najean Y, Rain JD, Billotey C. The site of destruction of autologous <sup>111</sup>In-labelled platelets and the efficiency of splenectomy in children and adults with idiopathic thrombocytopenic purpura: a study of 578 patients with 268 splenectomies. *Br J Haematol* (1997) 97(3):547–50. doi:10.1046/j.1365-2141.1997.832723.x
85. Kuwana M, Okazaki Y, Kaburaki J, Kawakami Y, Ikeda Y. Spleen is a primary site for activation of platelet-reactive T and B cells in patients with immune thrombocytopenic purpura. *J Immunol* (2002) 168(7):3675–82. doi:10.4049/jimmunol.168.7.3675
86. Catani L, Fagioli ME, Tazzari PL, Ricci F, Curti A, Rovito M, et al. Dendritic cells of immune

- thrombocytopenic purpura (ITP) show increased capacity to present apoptotic platelets to T lymphocytes. *Exp Hematol* (2006) 34(7):879–87. doi:10.1016/j.exphem.2006.03.009
87. Kuwana M, Okazaki Y, Ikeda Y. Splenic macrophages maintain the anti-platelet autoimmune response via uptake of opsonized platelets in patients with immune thrombocytopenic purpura. *J Thromb Haemost* (2009) 7(2):322–9. doi:10.1111/j.1538-7836.2008.03161.x
88. Chang M, Nakagawa PA, Williams SA, Schwartz MR, Imfeld KL, Buzby JS, et al. Immune thrombocytopenic purpura (ITP) plasma and purified ITP monoclonal autoantibodies inhibit megakaryocytopoiesis in vitro. *Blood* (2003) 102(3):887–95. doi:10.1182/blood-2002-05-1475
89. McMillan R, Wang L, Tomer A, Nichol J, Pistillo J. Suppression of in vitro megakaryocyte production by antiplatelet autoantibodies from adult patients with chronic ITP. *Blood* (2004) 103(4):1364–9. doi:10.1182/blood-2003-08-2672
90. Lev PR, Grodzielski M, Goette NP, Glembofsky AC, Espasandin YR, Pierdominici MS, et al. Impaired proplatelet formation in immune thrombocytopenia: a novel mechanism contributing to decreased platelet count. *Br J Haematol* (2014) 165(6):854–64. doi:10.1111/bjh.12832
91. Tsubakio T, Tani P, Curd JG, McMillan R. Complement activation in vitro by antiplatelet antibodies in chronic immune thrombocytopenic purpura. *Br J Haematol* (1986) 63(2):293–300. doi:10.1111/j.1365-2141.1986.tb05552.x
92. Peerschke EI, Andemariam B, Yin W, Bussel JB. Complement activation on platelets correlates with a decrease in circulating immature platelets in patients with immune thrombocytopenic purpura. *Br J Haematol* (2010) 148(4):638–45. doi:10.1111/j.1365-2141.2009.07995.x
93. Najaoui A, Bakchoul T, Stoy J, Bein G, Rummel MJ, Santoso S, et al. Autoantibody-mediated complement activation on platelets is a common finding in patients with immune thrombocytopenic purpura (ITP). *Eur J Haematol* (2012) 88(2):167–74. doi:10.1111/j.1600-0609.2011.01718.x
94. Goette NP, Glembofsky AC, Lev PR, Grodzielski M, Contrufo G, Pierdominici MS, et al. Platelet apoptosis in adult immune thrombocytopenia: insights into the mechanism of damage triggered by auto-antibodies. *PLoS One* (2016) 11(8):e0160563. doi:10.1371/journal.pone.0160563
95. George JN. Platelet immunoglobulin G: its significance for the evaluation of thrombocytopenia and for understanding the origin of alpha-granule proteins. *Blood* (1990) 76(5):859–70.
96. Nagelkerke SQ, Kuijpers TW. Immunomodulation by IVIg and the role of Fc-gamma receptors: classic mechanisms of action after all? *Front Immunol* (2014) 5:674. doi:10.3389/fimmu.2014.00674
97. Kiefel V, Santoso S, Weisheit M, Mueller-Eckhardt C. Monoclonal anti-body-specific immobilization of platelet antigens (MAIPA): a new tool for the identification of platelet-reactive antibodies. *Blood* (1987) 70(6):1722–6.
98. Fujisawa K, Tani P, O'Toole TE, Ginsberg MH, McMillan R. Different specificities of platelet-associated and plasma autoantibodies to platelet GPIIb-IIIa in patients with chronic immune thrombocytopenic purpura. *Blood* (1992) 79(6):1441–6.
99. Crossley A, Calvert JE, Taylor PR, Dickinson AM. A comparison of monoclonal antibody immobilization of platelet antigen (MAIPA) and immunobead methods for detection of GPIIb/IIIa antiplatelet antibodies in immune thrombocytopenic purpura. *Transfus Med* (1997) 7(2):127–34. doi:10.1046/j.1365-3148.1997.d01-15.x
100. Cines DB, Wilson SB, Tomaski A, Schreiber AD. Platelet antibodies of the IgM class in immune thrombocytopenic purpura. *J Clin Invest* (1985) 75(4):1183–90. doi:10.1172/JCI111814
101. Winiarski J. IgG and IgM antibodies to platelet membrane glycoprotein antigens in acute childhood idiopathic thrombocytopenic purpura. *Br J Haematol* (1989) 73(1):88–92. doi:10.1111/j.1365-2141.1989.tb00225.x
102. Nishioka T, Yamane T, Takubo T, Ohta K, Park K, Hino M. Detection of various platelet-associated immunoglobulins by flow cytometry in idiopathic thrombocytopenic purpura. *Cytometry B Clin Cytom* (2005) 68(1):37–42. doi:10.1002/cyto.b.20067
103. Chan H, Moore JC, Finch CN, Warkentin TE, Kelton JG. The IgG subclasses of platelet-associated autoantibodies directed against platelet glycoproteins IIB/IIIa in patients with idiopathic thrombocytopenic purpura. *Br J Haematol* (2003) 122(5):818–24. doi:10.1046/j.1365-2141.2003.04509.x
104. Hymes K, Schur PH, Karpatkin S. Heavy-chain subclass of round antiplatelet IgG in autoimmune

thrombocytopenic purpura. *Blood* (1980) 56(1):84–7.

105. Vidarsson G, Dekkers G, Rispens T. IgG subclasses and allotypes: from structure to effector functions. *Front Immunol* (2014) 5:520. doi:10.3389/fimmu.2014.00520

106. Sonneveld ME, Natunen S, Sainio S, Koeleman CA, Holst S, Dekkers G, et al. Glycosylation pattern of anti-platelet IgG is stable during pregnancy and predicts clinical outcome in alloimmune thrombocytopenia. *Br J Haematol* (2016) 174(2):310–20. doi:10.1111/bjh.14053

107. Sonneveld ME, de Haas M, Koeleman C, de Haan N, Zeerleder SS, Ligthart PC, et al. Patients with IgG1-anti-red blood cell autoantibodies show aberrant Fc-glycosylation. *Sci Rep* (2017) 7(1):8187. doi:10.1038/s41598-017-08654-y

108. Christie DJ, Sauro SC, Fairbanks KD, Kay NE. Detection of clonal platelet antibodies in immunologically-mediated thrombocytopenias: association with circulating clonal/oligoclonal B cells. *Br J Haematol* (1993) 85(2):277–84. doi:10.1111/j.1365-2141.1993.tb03167.x

109. Kim J, Park CJ, Chi HS, Kim MJ, Seo JJ, Moon HN, et al. Idiopathic thrombo-cytopenic purpura: better therapeutic responses of patients with B- or T-cell clonality than patients without clonality. *Int J Hematol* (2003) 78(5):461–6. doi:10.1007/BF02983822

110. Roark JH, Bussel JB, Cines DB, Siegel DL. Genetic analysis of autoantibodies in idiopathic thrombocytopenic purpura reveals evidence of clonal expansion and somatic mutation. *Blood* (2002) 100(4):1388–98.

111. Stockelberg D, Hou M, Jacobsson S, Kutti J, Wadenvik H. Evidence for a light chain restriction of glycoprotein Ib/IX and IIb/IIIa reactive antibodies in chronic idiopathic thrombocytopenic purpura (ITP). *Br J Haematol* (1995) 90(1):175–9. doi:10.1111/j.1365-2141.1995.tb03397.x

112. Stockelberg D, Hou M, Jacobsson S, Kutti J, Wadenvik H. Light chain-restricted autoantibodies in chronic idiopathic thrombocytopenic purpura, but no evidence for circulating clone B-lymphocytes. *Ann Hematol* (1996) 72(1):29–34. doi:10.1007/BF00663013

113. van der Harst D, de Jong D, Limpens J, Kluin PM, Rozier Y, van Ommen GJ, et al. Clonal B-cell populations in patients with idiopathic thrombocytopenic purpura. *Blood* (1990) 76(11):2321–6.

114. Veneri D, De Matteis G, Solero P, Federici F, Zanuso C, Guizzardi E, et al. Analysis of B- and T-cell clonality and HLA class II alleles in patients with idiopathic thrombocytopenic purpura: correlation with *Helicobacter pylori* infection and response to eradication treatment. *Platelets* (2005) 16(5):307–11. doi:10.1080/09537100400028685

115. Voelkerding KV, Sandhaus LM, Belov L, Frenkel L, Ettinger LJ, Raska K Jr. Clonal B-cell proliferation in an infant with congenital HIV infection and immune thrombocytopenia. *Am J Clin Pathol* (1988) 90(4):470–4. doi:10.1093/ajcp/90.4.470

116. Fujisawa K, O'Toole TE, Tani P, Loftus JC, Plow EF, Ginsberg MH, et al. Autoantibodies to the presumptive cytoplasmic domain of platelet glycoprotein IIIa in patients with chronic immune thrombocytopenic purpura. *Blood* (1991) 77(10):2207–13.

117. Kosugi S, Tomiyama Y, Honda S, Kato H, Kiyoi T, Kashiwagi H, et al. Platelet-associated anti-GPIIb-IIIa autoantibodies in chronic immune thrombocytopenic purpura recognizing epitopes close to the ligand-binding site of glycoprotein (GP) IIb. *Blood* (2001) 98(6):1819–27. doi:10.1182/blood.V98.6.1819

118. McMillan R, Lopez-Dee J, Loftus JC. Autoantibodies to alpha(IIb)beta(3) in patients with chronic immune thrombocytopenic purpura bind primarily to epitopes on alpha(IIb). *Blood* (2001) 97(7):2171–2. doi:10.1182/blood.V97.7.2171

119. Kekomaki R, Dawson B, McFarland J, Kunicki TJ. Localization of human platelet autoantigens to the cysteine-rich region of glycoprotein IIIa. *J Clin Invest* (1991) 88(3):847–54. doi:10.1172/JCI115386

120. McMillan R, Wang L, Lopez-Dee J, Jiu S, Loftus JC. Many alphaIIb beta3 autoepitopes in chronic immune thrombocytopenic purpura are localized to alphaIIb between amino acids L1 and Q459. *Br J Haematol* (2002) 118(4):1132–6. doi:10.1046/j.1365-2141.2002.03751.x

121. Kosugi S, Tomiyama Y, Honda S, Kashiwagi H, Shiraga M, Tadokoro S, et al. Anti-alphaIIb beta3 antibodies in chronic immune thrombocytopenic purpura. *Thromb Haemost* (2001) 85(1):36–41. doi:10.1055/s-0037-1612660

122. Berchtold P, Wenger M. Autoantibodies against platelet glycoproteins in autoimmune thrombocytopenic purpura: their clinical significance and response to treatment. *Blood* (1993) 81(5):1246–50.

123. Zeng Q, Zhu L, Tao L, Bao J, Yang M, Simpson EK, et al. Relative efficacy of steroid therapy in immune thrombocytopenia mediated by anti-platelet GPIIb/IIIa versus GPIIb/IIIa antibodies. *Am J Hematol* (2012) 87(2):206–8. doi:10.1002/ajh.22211
124. Peng J, Ma SH, Liu J, Hou Y, Liu XM, Niu T, et al. Association of autoantibody specificity and response to intravenous immunoglobulin G therapy in immune thrombocytopenia: a multicenter cohort study. *J Thromb Haemost* (2014) 12(4):497–504. doi:10.1111/jth.12524
125. Semple JW, Freedman J. Increased antiplatelet T helper lymphocyte reactivity in patients with autoimmune thrombocytopenia. *Blood* (1991) 78(10):2619–25.
126. Semple JW, Milev Y, Cosgrave D, Mody M, Hornstein A, Blanchette V, et al. Differences in serum cytokine levels in acute and chronic autoimmune thrombocytopenic purpura: relationship to platelet phenotype and antiplatelet T-cell reactivity. *Blood* (1996) 87(10):4245–54.
127. Ogawara H, Handa H, Morita K, Hayakawa M, Kojima J, Amagai H, et al. High Th1/Th2 ratio in patients with chronic idiopathic thrombocytopenic purpura. *Eur J Haematol* (2003) 71(4):283–8. doi:10.1034/j.1600-0609.2003.00138.x
128. Panitsas FP, Mouzaki A. Effect of splenectomy on type-1/type-2 cytokine gene expression in a patient with adult idiopathic thrombocytopenic purpura (ITP). *BMC Blood Disord* (2004) 4(1):4. doi:10.1186/1471-2326-4-4
129. Wang T, Zhao H, Ren H, Guo J, Xu M, Yang R, et al. Type 1 and type 2 T-cell profiles in idiopathic thrombocytopenic purpura. *Haematologica* (2005) 90(7):914–23.
130. Stasi R, Del Poeta G, Stipa E, Evangelista ML, Trawinska MM, Cooper N, et al. Response to B-cell depleting therapy with rituximab reverts the abnormalities of T-cell subsets in patients with idiopathic thrombocytopenic purpura. *Blood* (2007) 110(8):2924–30. doi:10.1182/blood-2007-02-068999
131. Kuwana M, Kaburaki J, Ikeda Y. Autoreactive T cells to platelet GPIIb-IIIa in immune thrombocytopenic purpura. Role in production of anti-platelet autoantibody. *J Clin Invest* (1998) 102(7):1393–402. doi:10.1172/JCI4238
132. Kuwana M, Kaburaki J, Kitasato H, Kato M, Kawai S, Kawakami Y, et al. Immunodominant epitopes on glycoprotein IIb-IIIa recognized by autoreactive T cells in patients with immune thrombocytopenic purpura. *Blood* (2001) 98(1):130–9. doi:10.1182/blood.V98.1.130
133. Chen X, Oppenheim JJ. Th17 cells and Tregs: unlikely allies. *J Leukoc Biol* (2014) 95(5):723–31. doi:10.1189/jlb.1213633
134. Ma D, Zhu X, Zhao P, Zhao C, Li X, Zhu Y, et al. Profile of Th17 cytokines (IL-17, TGF-beta, IL-6) and Th1 cytokine (IFN-gamma) in patients with immune thrombocytopenic purpura. *Ann Hematol* (2008) 87(11):899–904. doi:10.1007/s00277-008-0535-3
135. Guo ZX, Chen ZP, Zheng CL, Jia HR, Ge J, Gu DS, et al. The role of Th17 cells in adult patients with chronic idiopathic thrombocytopenic purpura. *Eur J Haematol* (2009) 82(6):488–9. doi:10.1111/j.1600-0609.2009.01229.x
136. Sollazzo D, Trabaneli S, Curti A, Vianelli N, Lemoli RM, Catani L. Circulating CD4+CD161+CD196+ Th17 cells are not increased in immune thrombocytopenia. *Haematologica* (2011) 96(4):632–4. doi:10.3324/haematol.2010.038638
137. Zhang J, Ma D, Zhu X, Qu X, Ji C, Hou M. Elevated profile of Th17, Th1 and Tc1 cells in patients with immune thrombocytopenic purpura. *Haematologica* (2009) 94(9):1326–9. doi:10.3324/haematol.2009.007823
138. Zhu X, Ma D, Zhang J, Peng J, Qu X, Ji C, et al. Elevated interleukin-21 correlated to Th17 and Th1 cells in patients with immune thrombocytopenia. *J Clin Immunol* (2010) 30(2):253–9. doi:10.1007/s10875-009-9353-1
139. Rocha AM, Souza C, Rocha GA, de Melo FF, Clementino NC, Marino MC, et al. The levels of IL-17A and of the cytokines involved in Th17 cell commitment are increased in patients with chronic immune thrombocytopenia. *Haematologica* (2011) 96(10):1560–4. doi:10.3324/haematol.2011.046417
140. Hu Y, Ma DX, Shan NN, Zhu YY, Liu XG, Zhang L, et al. Increased number of Tc17 and correlation with Th17 cells in patients with immune thrombocytopenia. *PLoS One* (2011) 6(10):e26522. doi:10.1371/journal.pone.0026522
141. Ji L, Zhan Y, Hua F, Li F, Zou S, Wang W, et al. The ratio of Treg/Th17 cells correlates with the disease activity of primary immune thrombocytopenia. *PLoS One* (2012) 7(12):e50909. doi:10.1371/journal.

pone.0050909

142. Eyerich K, Dimartino V, Cavani A. IL-17 and IL-22 in immunity: driving protection and pathology. *Eur J Immunol* (2017) 47(4):607–14. doi:10.1002/eji.201646723
143. Eyerich S, Eyerich K, Cavani A, Schmidt-Weber C. IL-17 and IL-22: siblings, not twins. *Trends Immunol* (2010) 31(9):354–61. doi:10.1016/j.it.2010.06.004
144. Eyerich S, Eyerich K, Pennino D, Carbone T, Nasorri F, Pallotta S, et al. Th22 cells represent a distinct human T cell subset involved in epidermal immunity and remodeling. *J Clin Invest* (2009) 119(12):3573–85. doi:10.1172/JCI40202
145. Cao J, Chen C, Zeng L, Li L, Li X, Li Z, et al. Elevated plasma IL-22 levels correlated with Th1 and Th22 cells in patients with immune thrombo-cytopenia. *Clin Immunol* (2011) 141(1):121–3. doi:10.1016/j.clim.2011.05.003
146. Hu Y, Li H, Zhang L, Shan B, Xu X, Li H, et al. Elevated profiles of Th22 cells and correlations with Th17 cells in patients with immune thrombocytopenia. *Hum Immunol* (2012) 73(6):629–35. doi:10.1016/j.humimm.2012.04.015
147. Audia S, Rossato M, Santeogoets K, Spijkers S, Wichers C, Bekker C, et al. Splenic TFH expansion participates in B-cell differentiation and antiplatelet-antibody production during immune thrombocytopenia. *Blood* (2014) 124(18):2858–66. doi:10.1182/blood-2014-03-563445
148. Olsson B, Andersson PO, Jernas M, Jacobsson S, Carlsson B, Carlsson LM, et al. T-cell-mediated cytotoxicity toward platelets in chronic idiopathic thrombocytopenic purpura. *Nat Med* (2003) 9(9):1123–4. doi:10.1038/nm921
149. Ware RE, Howard TA. Phenotypic and clonal analysis of T lymphocytes in childhood immune thrombocytopenic purpura. *Blood* (1993) 82(7):2137–42.
150. Shenoy S, Mohanakumar T, Chatila T, Tersak J, Duffy B, Wang R, et al. Defective apoptosis in lymphocytes and the role of IL-2 in autoimmune hematologic cytopenias. *Clin Immunol* (2001) 99(2):266–75. doi:10.1006/clim.2001.5017
151. Olsson B, Andersson PO, Jacobsson S, Carlsson L, Wadenvik H. Disturbed apoptosis of T-cells in patients with active idiopathic thrombocytopenic purpura. *Thromb Haemost* (2005) 93(1):139–44. doi:10.1160/TH04-06-0385
152. Olsson B, Jernas M, Wadenvik H. Increased plasma levels of granzymes in adult patients with chronic immune thrombocytopenia. *Thromb Haemost* (2012) 107(6):1182–4. doi:10.1160/TH12-01-0012
153. Zhang F, Chu X, Wang L, Zhu Y, Li L, Ma D, et al. Cell-mediated lysis of autologous platelets in chronic idiopathic thrombocytopenic purpura. *Eur J Haematol* (2006) 76(5):427–31. doi:10.1111/j.1600-0609.2005.00622.x
154. Zhao C, Li X, Zhang F, Wang L, Peng J, Hou M. Increased cytotoxic T-lymphocyte-mediated cytotoxicity predominant in patients with idiopathic thrombocytopenic purpura without platelet autoantibodies. *Haematologica* (2008) 93(9):1428–30. doi:10.3324/haematol.12889
155. Qiu J, Liu X, Li X, Zhang X, Han P, Zhou H, et al. CD8(+) T cells induce platelet clearance in the liver via platelet desialylation in immune thrombo-cytopenia. *Sci Rep* (2016) 6:27445. doi:10.1038/srep27445
156. Olsson B, Ridell B, Carlsson L, Jacobsson S, Wadenvik H. Recruitment of T cells into bone marrow of ITP patients possibly due to elevated expression of VLA-4 and CX3CR1. *Blood* (2008) 112(4):1078–84. doi:10.1182/blood-2008-02-139402
157. Li S, Wang L, Zhao C, Li L, Peng J, Hou M. CD8+ T cells suppress autologous megakaryocyte apoptosis in idiopathic thrombocytopenic purpura. *Br J Haematol* (2007) 139(4):605–11. doi:10.1111/j.1365-2141.2007.06737.x
158. Audia S, Samson M, Mahevas M, Ferrand C, Trad M, Ciudad M, et al. Preferential splenic CD8(+) T-cell activation in rituximab-nonresponder patients with immune thrombocytopenia. *Blood* (2013) 122(14):2477–86. doi:10.1182/blood-2013-03-491415
159. Ma L, Simpson E, Li J, Xuan M, Xu M, Baker L, et al. CD8+ T cells are predominantly protective and required for effective steroid therapy in murine models of immune thrombocytopenia. *Blood* (2015) 126(2):247–56. doi:10.1182/blood-2015-03-635417
160. Shlomchik MJ, Craft JE, Mamula MJ. From T to B and back again: positive feedback in systemic autoimmune disease. *Nat Rev Immunol* (2001) 1(2):147–53. doi:10.1038/35100573

161. Guo L, Kapur R, Aslam R, Speck ER, Zufferey A, Zhao Y, et al. CD20+ B-cell depletion therapy suppresses murine CD8+ T-cell-mediated immune thrombocytopenia. *Blood* (2016) 127(6):735–8. doi:10.1182/blood-2015-06-655126
162. Li X, Zhong H, Bao W, Boulad N, Evangelista J, Haider MA, et al. Defective regulatory B-cell compartment in patients with immune thrombocytopenia. *Blood* (2012) 120(16):3318–25. doi:10.1182/blood-2012-05-432575
163. Mauri C, Menon M. Human regulatory B cells in health and disease: therapeutic potential. *J Clin Invest* (2017) 127(3):772–9. doi:10.1172/JCI85113
164. Veneri D, Gottardi M, Guizzardi E, Zanuso C, Krampera M, Franchini M. Idiopathic thrombocytopenic purpura, *Helicobacter pylori* infection, and HLA class II alleles. *Blood* (2002) 100(5):1925–6; author reply 6–7. doi:10.1182/blood-2002-05-1348
165. Gouttefangeas C, Diehl M, Keilholz W, Hornlein RF, Stevanovic S, Rammensee HG. Thrombocyte HLA molecules retain nonrenewable endogenous peptides of megakaryocyte lineage and do not stimulate direct alloreactivity in vitro. *Blood* (2000) 95(10):3168–75.
166. Chapman LM, Aggrey AA, Field DJ, Srivastava K, Ture S, Yui K, et al. Platelets present antigen in the context of MHC class I. *J Immunol* (2012) 189(2):916–23. doi:10.4049/jimmunol.1200580
167. Trugilho MRO, Hottz ED, Brunoro GVF, Teixeira-Ferreira A, Carvalho PC, Salazar GA, et al. Platelet proteome reveals novel pathways of platelet activation and platelet-mediated immunoregulation in dengue. *PLoS Pathog* (2017) 13(5):e1006385. doi:10.1371/journal.ppat.1006385
168. Boshkov LK, Kelton JG, Halloran PF. HLA-DR expression by platelets in acute idiopathic thrombocytopenic purpura. *Br J Haematol* (1992) 81(4):552–7. doi:10.1111/j.1365-2141.1992.tb02991.x
169. Fahim NM, Monir E. Functional role of CD4+CD25+ regulatory T cells and transforming growth factor-beta1 in childhood immune thrombocytopenic purpura. *Egypt J Immunol* (2006) 13(1):173–87.
170. Sakakura M, Wada H, Tawara I, Nobori T, Sugiyama T, Sagawa N, et al. Reduced Cd4+Cd25+ T cells in patients with idiopathic thrombocytopenic purpura. *Thromb Res* (2007) 120(2):187–93. doi:10.1016/j.thromres.2006.09.008
171. Liu B, Zhao H, Poon MC, Han Z, Gu D, Xu M, et al. Abnormality of CD4(+) CD25(+) regulatory T cells in idiopathic thrombocytopenic purpura. *Eur J Haematol* (2007) 78(2):139–43. doi:10.1111/j.1600-0609.2006.00780.x
172. Yu J, Heck S, Patel V, Levan J, Yu Y, Bussel JB, et al. Defective circulating CD25 regulatory T cells in patients with chronic immune thrombocytopenic purpura. *Blood* (2008) 112(4):1325–8. doi:10.1182/blood-2008-01-135335
173. Zhang XL, Peng J, Sun JZ, Liu JJ, Guo CS, Wang ZG, et al. De novo induction of platelet-specific CD4(+) CD25(+) regulatory T cells from CD4(+) CD25(-) cells in patients with idiopathic thrombocytopenic purpura. *Blood* (2009) 113(11):2568–77. doi:10.1182/blood-2008-03-148288
174. Stasi R, Cooper N, Del Poeta G, Stipa E, Laura Evangelista M, Abruzzese E, et al. Analysis of regulatory T-cell changes in patients with idiopathic thrombocytopenic purpura receiving B cell-depleting therapy with rituximab. *Blood* (2008) 112(4):1147–50. doi:10.1182/blood-2007-12-129262
175. Bao W, Bussel JB, Heck S, He W, Karpoff M, Boulad N, et al. Improved regulatory T-cell activity in patients with chronic immune thrombocytopenia treated with thrombopoietic agents. *Blood* (2010) 116(22):4639–45. doi:10.1182/blood-2010-04-281717
176. Audia S, Samson M, Guy J, Janikashvili N, Fraszczak J, Trad M, et al. Immunologic effects of rituximab on the human spleen in immune thrombocytopenia. *Blood* (2011) 118(16):4394–400. doi:10.1182/blood-2011-03-344051
177. Li Z, Mou W, Lu G, Cao J, He X, Pan X, et al. Low-dose rituximab combined with short-term glucocorticoids up-regulates Treg cell levels in patients with immune thrombocytopenia. *Int J Hematol* (2011) 93(1):91–8. doi:10.1007/s12185-010-0753-z
178. Ling Y, Cao X, Yu Z, Ruan C. Circulating dendritic cells subsets and CD4+Foxp3+ regulatory T cells in adult patients with chronic ITP before and after treatment with high-dose dexamethasone. *Eur J Haematol* (2007) 79(4):310–6. doi:10.1111/j.1600-0609.2007.00917.x
179. Aslam R, Hu Y, Gebremeskel S, Segel GB, Speck ER, Guo L, et al. Thymic retention of CD4+CD25+FoxP3+ T regulatory cells is associated with their peripheral deficiency and thrombocytopenia in a murine model of

- immune thrombocytopenia. *Blood* (2012) 120(10):2127–32. doi:10.1182/blood-2012-02-413526
180. Catani L, Sollazzo D, Trabanelli S, Curti A, Evangelisti C, Polverelli N, et al. Decreased expression of indoleamine 2,3-dioxygenase 1 in dendritic cells contributes to impaired regulatory T cell development in immune thrombocytopenia. *Ann Hematol* (2013) 92(1):67–78. doi:10.1007/s00277-012-1556-5
181. Siragam V, Crow AR, Brinc D, Song S, Freedman J, Lazarus AH. Intravenous immunoglobulin ameliorates ITP via activating Fc gamma receptors on dendritic cells. *Nat Med* (2006) 12(6):688–92. doi:10.1038/nm1416
182. Kapur R, Kim M, Rebetz J, Rondina MT, Porcelijn L, Semple JW. Low levels of interleukin-10 in patients with transfusion-related acute lung injury. *Ann Transl Med* (2017) 5(16):339. doi:10.21037/atm.2017.04.37
183. Kapur R, Kim M, Aslam R, McVey MJ, Tabuchi A, Luo A, et al. T regulatory cells and dendritic cells protect against transfusion-related acute lung injury via IL-10. *Blood* (2017) 129(18):2557–69. doi:10.1182/blood-2016-12-758185
184. Houwerzijl EJ, Blom NR, van der Want JJ, Esselink MT, Koornstra JJ, Smit JW, et al. Ultrastructural study shows morphologic features of apoptosis and para-apoptosis in megakaryocytes from patients with idiopathic thrombocytopenic purpura. *Blood* (2004) 103(2):500–6. doi:10.1182/blood-2003-01-0275
185. Zhong H, Bao W, Li X, Miller A, Seery C, Haq N, et al. CD16+ monocytes control T-cell subset development in immune thrombocytopenia. *Blood* (2012) 120(16):3326–35. doi:10.1182/blood-2012-06-434605
186. Liu XG, Ma SH, Sun JZ, Ren J, Shi Y, Sun L, et al. High-dose dexamethasone shifts the balance of stimulatory and inhibitory Fc gamma receptors on monocytes in patients with primary immune thrombocytopenia. *Blood* (2011) 117(6):2061–9. doi:10.1182/blood-2010-07-295477
187. Asahi A, Nishimoto T, Okazaki Y, Suzuki H, Masaoka T, Kawakami Y, et al. Helicobacter pylori eradication shifts monocyte Fc gamma receptor balance toward inhibitory Fc gammaRIIB in immune thrombocytopenic purpura patients. *J Clin Invest* (2008) 118(8):2939–49. doi:10.1172/JCI34496
188. Semple JW, Bruce S, Freedman J. Suppressed natural killer cell activity in patients with chronic autoimmune thrombocytopenic purpura. *Am J Hematol* (1991) 37(4):258–62. doi:10.1002/ajh.2830370409
189. Garcia-Suarez J, Prieto A, Reyes E, Manzano L, Merino JL, Alvarez-Mon M. Severe chronic autoimmune thrombocytopenic purpura is associated with an expansion of CD56+ CD3- natural killer cells subset. *Blood* (1993) 82(5):1538–45.
190. Ebbo M, Audonnet S, Grados A, Benarous L, Mahevas M, Godeau B, et al. NK cell compartment in the peripheral blood and spleen in adult patients with primary immune thrombocytopenia. *Clin Immunol* (2017) 177:18–28. doi:10.1016/j.clim.2015.11.005
191. Koupounova M, Clancy L, Corkrey HA, Freedman JE. Circulating platelets as mediators of immunity, inflammation, and thrombosis. *Circ Res* (2018) 122(2):337–51. doi:10.1161/CIRCRESAHA.117.310795
192. Nishimoto T, Numajiri M, Nakazaki H, Okazaki Y, Kuwana M. Induction of immune tolerance to platelet antigen by short-term thrombopoietin treatment in a mouse model of immune thrombocytopenia. *Int J Hematol* (2014) 100(4):341–4. doi:10.1007/s12185-014-1661-4
193. Ghadaki B, Nazi I, Kelton JG, Arnold DM. Sustained remissions of immune thrombocytopenia associated with the use of thrombopoietin receptor agonists. *Transfusion* (2013) 53(11):2807–12. doi:10.1111/trf.12139
194. Thachil J, Salter I, George JN. Complete remission of refractory immune thrombocytopenia (ITP) with a short course of Romiplostim. *Eur J Haematol* (2013) 91(4):376–7. doi:10.1111/ejh.12165
195. Mahevas M, Fain O, Ebbo M, Roudot-Thoraval F, Limal N, Khellaf M, et al. The temporary use of thrombopoietin-receptor agonists may induce a pro-longed remission in adult chronic immune thrombocytopenia. Results of a French observational study. *Br J Haematol* (2014) 165(6):865–9. doi:10.1111/bjh.12888
196. Grewal IS, Flavell RA. CD40 and CD154 in cell-mediated immunity. *Annu Rev Immunol* (1998) 16:111–35. doi:10.1146/annurev.immunol.16.1.111
197. Solanilla A, Pasquet JM, Viillard JE, Contin C, Grosset C, Dechanet-Merville J, et al. Platelet-associated CD154 in immune thrombocytopenic purpura. *Blood* (2005) 105(1):215–8. doi:10.1182/blood-2003-07-2367
198. Kuwana M, Nomura S, Fujimura K, Nagasawa T, Muto Y, Kurata Y, et al. Effect of a single injection of humanized anti-CD154 monoclonal antibody on the platelet-specific autoimmune response in patients with immune thrombocytopenic purpura. *Blood* (2004) 103(4):1229–36. doi:10.1182/blood-2003-06-2167
199. Kuwana M, Kawakami Y, Ikeda Y. Suppression of autoreactive T-cell response to glycoprotein IIb/IIIa by blockade of CD40/CD154 interaction: implications for treatment of immune thrombocytopenic purpura. *Blood*

- (2003) 101(2):621–3. doi:10.1182/blood-2002-07-2157
200. Bruhns P, Iannascoli B, England P, Mancardi DA, Fernandez N, Jorieux S, et al. Specificity and affinity of human Fcγ receptors and their poly-morphic variants for human IgG subclasses. *Blood* (2009) 113(16):3716–25. doi:10.1182/blood-2008-09-179754
201. Kono H, Kyogoku C, Suzuki T, Tsuchiya N, Honda H, Yamamoto K, et al. FcγRIIB Ile232Thr transmembrane polymorphism associated with human systemic lupus erythematosus decreases affinity to lipid rafts and attenuates inhibitory effects on B cell receptor signaling. *Hum Mol Genet* (2005) 14(19):2881–92. doi:10.1093/hmg/ddi320
202. Li X, Wu J, Ptacek T, Redden DT, Brown EE, Alarcon GS, et al. Allelic- dependent expression of an activating Fc receptor on B cells enhances humoral immune responses. *Sci Transl Med* (2013) 5(216):216ra175. doi:10.1126/scitranslmed.3007097
203. Stegmann TC, Veldhuisen B, Nagelkerke SQ, Winkelhorst D, Schonewille H, Verduin EP, et al. RhIg-prophylaxis is not influenced by FCGR2/3 polymorphisms in red blood cell clearance. *Blood* (2017) 129(8):1045–8. doi:10.1182/blood-2016-05-716365
204. van Egmond M, Vidarsson G, Bakema JE. Cross-talk between pathogen recognizing toll-like receptors and immunoglobulin Fc receptors in immunity. *Immunol Rev* (2015) 268(1):311–27. doi:10.1111/imr.12333
205. Schwab I, Nimmerjahn F. Intravenous immunoglobulin therapy: how does IgG modulate the immune system? *Nat Rev Immunol* (2013) 13(3):176–89. doi:10.1038/nri3401
206. Audia S, Santeogoets K, Laarhoven AG, Vidarsson G, Facy O, Ortega- Deballon P, et al. Fcγ receptor expression on splenic macrophages in adult immune thrombocytopenia. *Clin Exp Immunol* (2017) 188(2):275–82. doi:10.1111/cei.12935
207. Podolanczuk A, Lazarus AH, Crow AR, Grossbard E, Bussel JB. Of mice and men: an open-label pilot study for treatment of immune thrombocytopenic purpura by an inhibitor of Syk. *Blood* (2009) 113(14):3154–60. doi:10.1182/blood-2008-07-166439
208. Heitink-Polle KMJ, Laarhoven AG, Bruin MCA, Veldhuisen B, Nagelkerke SQ, Kuijpers T, et al. Fcγ receptor polymorphisms are associated with susceptibility to and recovery from pediatric immune thrombocytopenia. *Blood* (2016) 128(22):867.
209. Li J, van der Wal DE, Zhu G, Xu M, Yougbare I, Ma L, et al. Desialylation is a mechanism of Fc-independent platelet clearance and a therapeutic target in immune thrombocytopenia. *Nat Commun* (2015) 6:7737. doi:10.1038/ncomms8737
210. Jansen AJ, Josefsson EC, Rumjantseva V, Liu QP, Falet H, Bergmeier W, et al. Desialylation accelerates platelet clearance after refrigeration and initiates GPIIb/IIIa metalloproteinase-mediated cleavage in mice. *Blood* (2012) 119(5):1263–73. doi:10.1182/blood-2011-05-355628
211. Li J, Callum JL, Lin Y, Zhou Y, Zhu G, Ni H. Severe platelet desialylation in a patient with glycoprotein Ib/IX antibody-mediated immune thrombocytopenia and fatal pulmonary hemorrhage. *Haematologica* (2014) 99(4):e61–3. doi:10.3324/haematol.2013.102897
212. Shao L, Wu Y, Zhou H, Qin P, Ni H, Peng J, et al. Successful treatment with oseltamivir phosphate in a patient with chronic immune thrombocytopenia positive for anti-GPIIb/IX autoantibody. *Platelets* (2015) 26(5):495–7. doi:10.3109/09537104.2014.948838
213. Jansen AJ, Peng J, Zhao HG, Hou M, Ni H. Sialidase inhibition to increase platelet counts: a new treatment option for thrombocytopenia. *Am J Hematol* (2015) 90(5):E94–5. doi:10.1002/ajh.23953
214. Alioglu B, Tasar A, Ozen C, Selver B, Dallar Y. An experience of oseltamivir phosphate (tamiflu) in a pediatric patient with chronic idiopathic thrombocytopenic purpura: a case report. *Pathophysiol Haemost Thromb* (2010) 37(2–4):55–8. doi:10.1159/000321379
215. Tao L, Zeng Q, Li J, Xu M, Wang J, Pan Y, et al. Platelet desialylation correlates with efficacy of first-line therapies for immune thrombocytopenia. *J Hematol Oncol* (2017) 10(1):46. doi:10.1186/s13045-017-0413-3
216. Kapur R, Heitink-Polle KM, Porcelijn L, Bentlage AE, Bruin MC, Visser R, et al. C-reactive protein enhances IgG-mediated phagocyte responses and thrombocytopenia. *Blood* (2015) 125(11):1793–802. doi:10.1182/blood-2014-05-579110
217. Zhang B, Lo C, Shen L, Sood R, Jones C, Cusmano-Ozog K, et al. The role of vanin-1 and oxidative stress-related pathways in distinguishing acute and chronic pediatric ITP. *Blood* (2011) 117(17):4569–79. doi:10.1182/blood-2010-09-304931

218. Jin CQ, Dong HX, Cheng PP, Zhou JW, Zheng BY, Liu F. Antioxidant status and oxidative stress in patients with chronic ITP. *Scand J Immunol* (2013) 77(6):482–7. doi:10.1111/sji.12048
219. Elsalakawy WA, Ali MA, Hegazy MG, Farweez BA. Value of vanin-1 assessment in adult patients with primary immune thrombocytopenia. *Platelets* (2014) 25(2):86–92. doi:10.3109/09537104.2013.782484
220. Prensler T, Lewandrowski U, Sickmann A, Zahedi RP. Phosphoproteome analysis of the platelet plasma membrane. *Methods Mol Biol* (2011) 728:279–90. doi:10.1007/978-1-61779-068-3\_19
221. Lee-Sundlov MM, Ashline DJ, Hanneman AJ, Grozovsky R, Reinhold VN, Hoffmeister KM, et al. Circulating blood and platelets supply glycosyltransferases that enable extrinsic extracellular glycosylation. *Glycobiology* (2017) 27(2):188–98. doi:10.1093/glycob/cww108
222. Fong KP, Barry C, Tran AN, Traxler EA, Wannemacher KM, Tang HY, et al. Deciphering the human platelet sheddome. *Blood* (2011) 117(1):e15–26. doi:10.1182/blood-2010-05-283838
223. Andrews RK, Gardiner EE. Basic mechanisms of platelet receptor shedding. *Platelets* (2017) 28(4):319–24. doi:10.1080/09537104.2016.1235690
224. Au AE, Josefsson EC. Regulation of platelet membrane protein shedding in health and disease. *Platelets* (2017) 28(4):342–53. doi:10.1080/09537104.2016.1203401
225. Doyle HA, Mamula MJ. Post-translational protein modifications in antigen recognition and autoimmunity. *Trends Immunol* (2001) 22(8):443–9. doi:10.1016/S1471-4906(01)01976-7
226. Zavala-Cerna MG, Martinez-Garcia EA, Torres-Bugarin O, Rubio-Jurado B, Riebeling C, Nava A. The clinical significance of posttranslational modification of autoantigens. *Clin Rev Allergy Immunol* (2014) 47(1):73–90. doi:10.1007/s12016-014-8424-0
227. Klareskog L, Ronnelid J, Lundberg K, Padyukov L, Alfredsson L. Immunity to citrullinated proteins in rheumatoid arthritis. *Annu Rev Immunol* (2008) 26:651–75. doi:10.1146/annurev.immunol.26.021607.090244

Conflict of Interest Statement: AJ has received travel funding for hematological conferences from Novartis, not specifically for the subject of the manuscript. FL has received an unrestricted grant outside the submitted work from CSL Behring and Shire, and is a consultant for UniQure, NovoNordisk, and Shire, of which the fees go to Erasmus University. JV is a consultant for BioTest. The other authors report no conflict of interest.

# Chapter 3

## COVID-19 Vaccination in Patients with Immune Thrombocytopenia

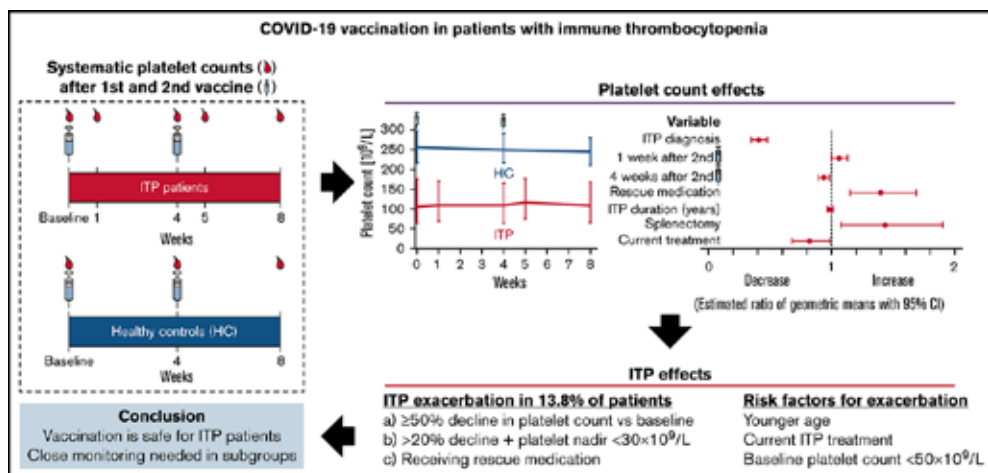
Chantal Visser, Maurice Swinkels, Erik D. van Werkhoven, F. Nanne Croles, Heike S. Noordzij-Nooteboom, Matthijs Eefting, Suzanne M. Last-Koopmans, Cecile Idink, Peter E. Westerweel, Bart Santbergen, Pieter A. Jobse, Fazil Baboe, RECOVAC-IR Consortium, Peter A. W. te Boekhorst, Frank W. G. Leebeek, Mark-David Levin, Marieke J. H. A. Kruip, and A. J. Gerard Jansen.

## Abstract

Immune thrombocytopenia (ITP) is an acquired autoimmune disorder that is characterized by low platelet count and increased bleeding risk. COVID-19 vaccination has been described as a risk factor for de novo ITP, but the effects of COVID-19 vaccination in patients with ITP are unknown. We aimed to investigate the effects of COVID-19 vaccination in patients with ITP on platelet count, bleeding complications, and ITP exacerbation ( $\geq 50\%$  decline in platelet count, or nadir platelet count,  $< 30 \times 10^9/L$  with a  $> 20\%$  decrease from baseline, or use of rescue therapy). Platelet counts in patients with ITP and healthy controls were collected immediately before and 1 and 4 weeks after the first and second vaccinations. Linear mixed-effects modeling was applied to analyze platelet counts over time. We included 218 patients with ITP (50.9% female; mean age, 55 years; and median platelet count,  $106 \times 10^9/L$ ) and 200 healthy controls (60.0% female; mean age, 58 years; median platelet count,  $256 \times 10^9/L$ ). Platelet counts decreased by 6.3% after vaccination. We did not observe any difference in decrease between the groups. Thirty patients with ITP (13.8%; 95% confidence interval [CI], 9.5-19.1) had an exacerbation and 5 (2.2%; 95% CI, 0.7-5.3) suffered from a bleeding event. Risk factors for ITP exacerbation were platelet count  $< 50 \times 10^9/L$  (odds ratio [OR], 5.3; 95% CI, 2.1-13.7), ITP treatment at time of vaccination (OR, 3.4; 95% CI, 1.5-8.0), and age (OR, 0.96 per year; 95% CI, 0.94-0.99). Our study highlights the safety of COVID-19 vaccination in patients with ITP and the importance of the close monitoring of platelet counts in a subgroup of patients with ITP. Patients with ITP with exacerbation responded well on therapy.

### Key Points:

- A decrease in platelet count after SARS-CoV-2 vaccination is similar in patients with ITP and healthy controls.
- Risk factors for exacerbation of ITP after SARS-CoV-2 vaccination include low platelet count, younger age, and current therapy.



## Introduction

Vaccination against severe acute respiratory syndrome coronavirus 2 (SARS-CoV-2) is critical to control the COVID-19 pandemic. The European Medicines Agency has authorized 4 vaccines for use in the European Union: the BNT162b2 (Comirnaty) vaccine, the messenger RNA (mRNA)-1273 (Spikevax) vaccine, the ChAdOx1-S (Vaxzevria) vaccine, and the Ad26.COV2.S (Johnson & Johnson) vaccine [1-4]. Reports of serious adverse events, including vaccine-associated immune thrombocytopenia (ITP), thrombosis, and the rare occurrence of vaccine induced immune thrombotic thrombocytopenia, has led to the restrictive use of the ChAdOx1-S and Ad26.COV2.S vaccines [5,6].

ITP is an acquired autoimmune disorder that is characterized by low platelet count ( $<100 \times 10^9/L$ ), resulting from platelet destruction and impaired platelet production, that leads to increased bleeding risk [7]. ITP is likely to arise from defective immune tolerance in addition to a possible triggering event [7]. COVID-19 infection has recently been identified as a risk factor for ITP development [8], and a large population study showed a small increased risk for de novo ITP after the ChAdOx1-S vaccine but not after the BNT162b2 vaccine [9]. These findings illustrate that immunological events like infection and vaccination in the COVID-19 pandemic could be an important risk factor in the development and exacerbation of ITP.

Exacerbation of thrombocytopenia in patients with ITP after COVID-19 vaccination has been described in retrospective studies, but a systematic evaluation of platelet counts over time is missing [10-13]. Therefore, it is still unclear how COVID-19 vaccination affects patients with ITP over time, if and when thrombocytopenia develops, and when they are at risk for bleeding.

To gain a better understanding of the effect of COVID-19 vaccination in patients with ITP, we systematically monitored platelet counts, bleeding events, and ITP exacerbations in routine clinical practice.

## Methods

### Trial design and oversight

We conducted a multicenter observational study across 9 participating hospitals in The Netherlands. The study was designed and conducted in accordance with the Declaration of Helsinki. The medical ethical committee of Erasmus MC and the local research committees approved the study protocol and amendments (MEC-2021-0238). Erasmus MC was the sponsor, served as the coordinating center, and was responsible for maintenance of the database, validation and analyses of data, and trial coordination.

## Participants and procedures

Adult patients with a history of ITP, according to Rodeghiero et al [14], and who received  $\geq 1$  COVID-19 vaccination were enrolled. Patients were scheduled to receive 2 vaccinations,  $\sim 4$  weeks apart. Without existing guidelines about how to monitor patients with ITP after COVID-19 vaccination, we decided to measure platelet counts at baseline, followed by measurements 1 and 4 weeks after the first and second vaccinations as part of routine clinical practice. Data on platelet counts of healthy controls were obtained at baseline, as well as at 4 weeks after the first and the second mRNA-1273 vaccinations, from the Renal patients COVID-19 VACcination Immune Response (RECOVAC IR) study (Central Committee on Research Involving Human Subjects, NL76215.012.21)[15]. Healthy controls included the partner, sibling, or household member of the patient included in the RECOVAC IR study [15].

## Objectives and outcomes

The primary objective was to study platelet dynamics in patients with ITP after COVID-19 vaccination. Secondary outcomes were symptomatic bleeding (defined as World Health Organization [WHO] bleeding  $\geq$  grade 2) and exacerbation of ITP (defined as the development of any of the following:  $\geq 50\%$  decline in platelet count compared with baseline,  $>20\%$  decline in platelet count compared with baseline and a platelet nadir  $<30 \times 10^9/L$ , or need for rescue medication). Rescue medication was defined as treatment change at the discretion of the treating physician (ie, switch to other ITP medication, start new ITP medication, addition of concomitant ITP medication, or intensification of current ITP treatment), all independently of change in platelet count and vaccine-specific and nonspecific adverse events. Finally, risk factors for ITP exacerbation were studied.

## Statistical analyses

Descriptive statistics are expressed as median and interquartile range (IQR), mean and standard deviation, or counts with percentages. Characteristics of patients with ITP and healthy controls were compared using Fisher's test or Wilcoxon's rank-sum test with continuity correction. To identify the effect of COVID-19 vaccination over time while taking into account intrasubject variability, a linear mixed effects model was applied to the log-transformed platelet count. After log transformation, platelet count was closer to a normal distribution, allowing for a better model fit. The exponentiated model coefficients can be interpreted as ratios of the geometric means and percentage differences. A random intercept per patient was included. In this model, time was considered a grouped variable, and no interaction between time and ITP status was included because of the lack of interaction ( $P=.78$  of the interaction term). We corrected the model using fixed effects for age, sex, duration of ITP, presence of any treatment at the start of vaccination, receiving any previous ITP treatment, splenectomy, rescue medication, and treatment in an academic center. Rescue medication was treated as a time-varying covariate. It was set to 0 at the start and at 1 after the first date of rescue medication. A Friedman test was performed in the subgroups of patients with ITP grouped by baseline platelet count with steps of  $50 \times 10^9/L$  platelets. The 95% confidence intervals (CIs) of the crude percentages of patients with

exacerbation and bleeding were calculated using the Clopper-Pearson method. A logistic regression model was created to identify risk factors for exacerbation. All other statistical analyses were performed with IBM SPSS Statistics 25 and R version 4.1.1. with package lme4.

## Results

### Patient characteristics

We included 218 patients with ITP (50.9% female) aged 55 (17) years and 200 healthy controls (60.0% female) aged 58 (13) years between 1 February 2021 and 16 July 2021 (Table 1). All healthy controls received the same vaccine (mRNA-1273 vaccines)[15], but patients with ITP received 3 different types of vaccines: 201 (92.2%) received the mRNA-1273 vaccine, 16 (7.3%) received the BNT162b2 vaccine, and 1 (0.5%) received the ChAdOx1-S vaccine (supplemental Figure 1). Of the patients with ITP, 213 (97.7%) received both vaccinations. Reasons for not receiving the second vaccination were death from esophageal varices bleeding (n=1), deemed unsafe by treating physician (n=2), or prior infection with SARS-CoV-2 virus (n=2). Healthy controls and patients with ITP had similar baseline characteristics, with the exception of a small difference in mean age (58.2 and 55.2 years, respectively;  $P=.047$ ) and median baseline platelet count ( $256 \times 10^9/L$  and  $106 \times 10^9/L$  respectively;  $P=.001$ ) (Table 1). One hundred and ninety-six (89.9%) patients with ITP had primary ITP for a median duration (IQR) of 5.8 (10.6) years. One hundred and thirty-six (62.4%) patients had chronic ITP, and 69 (31.7%) were in remission. Sixty-four (29.5%) patients with ITP were receiving ITP treatment at the time of first vaccination. Sixteen (7.3%) patients with ITP had used rescue medication in the 6 months prior to COVID-19 vaccination.

### COVID-19 vaccination and platelet count response

During our study, a decrease in platelet count was observed in 55% (n=120) of patients with ITP and 63% (n=126) of healthy controls (Figure 1A). In patients with ITP grouped by baseline platelet count, no significant difference in the decrease in platelet count over time was found, with the exception of patients with ITP with baseline platelet counts  $>150 \times 10^9/L$  (Figure 1B). A large variability in platelet counts was observed across patients with ITP (intraclass correlation, 0.75; Figure 2).

In the mixed-effects analysis, a significant (6.3%) decrease in platelet count compared with baseline was found 4 weeks after the second vaccination (Figure 3; supplemental Table 1). We corrected for age, sex, duration of ITP, current treatment, receiving any prior ITP treatment, splenectomy, rescue medication, and treatment in an academic center. We did not observe any difference in the decrease between the groups.

Factors significantly associated with decreased platelet counts were longer duration of ITP (defined as years between ITP diagnosis and COVID-19 vaccination) and the presence of

	Patients with ITP (N=218)			Healthy controls (N=200)
	All patients with ITP (N=218)	Patients with ITP without exacerbation* (n=188)	Patients with ITP with exacerbation* (n=30)	
Age, y <sup>†</sup>	55.2 ± 16.8	56.7 ± 16.4	46.3 ± 11.7	58.2 ± 13.4
Females	111 (50.9)	97 (51.6)	14 (46.7)	120 (60.0)
Baseline platelet count, median (IQR), ×10 <sup>9</sup> /L	106 (110)	108 (108)	84 (143)	256 (83)
<b>ITP classification‡</b>				
Primary ITP	196 (89.9)	168 (89.4)	28 (93.3)	
Secondary ITP	21 (9.6)	20 (10.6)	2 (6.7)	
Duration of ITP, median (IQR), y	5.8 (10.6)	6.0 (10.4)	4.8 (14.9)	
<b>ITP duration*</b>				
Newly diagnosed	1 (0.5)	1 (0.5)	0 (0.0)	
Persistent	11 (5.0)	9 (4.8)	2 (6.7)	
Chronic	136 (62.4)	115 (61.2)	21 (70.0)	
Remission	69 (31.7)	63 (33.5)	6 (20.0)	
Unknown	1 (0.5)	0 (0.0)	1 (3.3)	
Prior splenectomy	27 (12.4)	22 (11.7)	5 (16.7)	
Prior ITP treatment§	138 (63.6)	114 (60.6)	24 (80.0)	
Rescue medication in 6 mo prior to COVID-19 vaccination <sup>¶</sup>	16 (7.3)	5 (2.7)	11 (36.7)	
<b>Current therapy</b>				
Glucocorticoids	16 (7.4)	15 (8.0)	1 (3.3)	
Rituximab	1 (0.5)	0 (0)	1 (3.3)	
TPO-RAs				
Eltrombopag	25 (11.5)	20 (10.6)	5 (16.7)	
Romiplostim	16 (7.4)	7 (3.7)	9 (30.0)	
Other	6 (2.8)	6 (3.2)	0 (0.0)	

Table 1. Characteristics of patients with ITP and healthy controls

TPO-RAs, thrombopoietin receptor agonists.

Unless otherwise noted, data are n (%).

\*Exacerbation is defined as the development of any of the following: ≥50% decline in platelet count compared with baseline, >20% decline in platelet count compared with baseline and a platelet nadir < 30x10<sup>9</sup>/L, or use of rescue medication. Rescue medication was defined as any treatment change by discretion of the treating physician (ie, switch to other ITP medication, start of new ITP medication, addition of concomitant ITP medication, or intensification of current ITP treatment).

†Data are mean ± standard deviation.

‡According to the definition of Rodeghiero and colleagues [14].

§Defined as having ≥1 therapy before COVID-19 vaccination.

¶Defined as any treatment change by discretion of the treating physician (ie, switch to other ITP medication, start of new ITP medication, addition of concomitant ITP medication, or intensification of current ITP treatment).

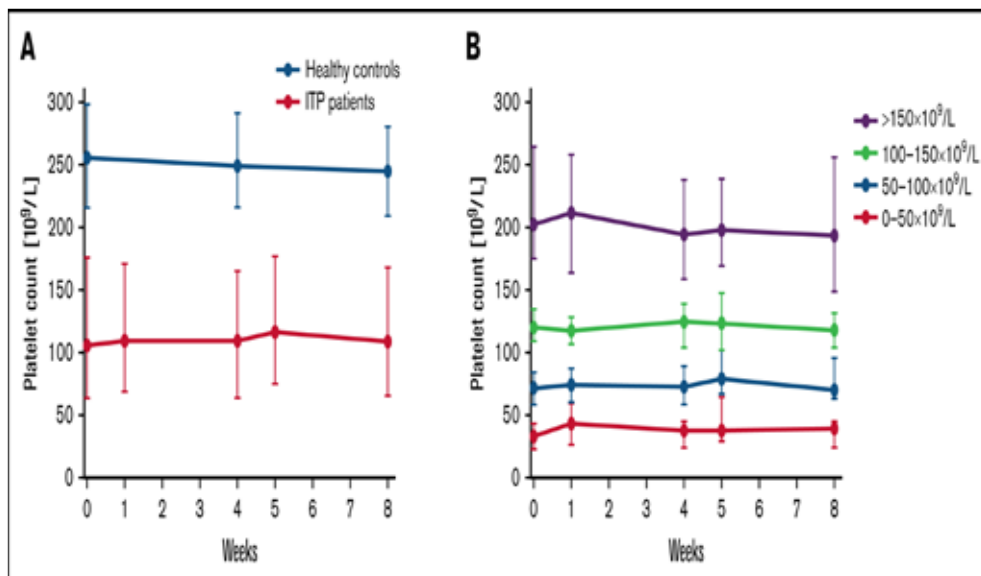


Figure 1. Platelet counts of patients with ITP and healthy controls after COVID-19 vaccination.

(A) Platelet counts of patients with ITP and healthy controls over the entire study period. Platelet counts are median ±IQR. No significant difference in platelet count over time was observed between the 2 groups. (B) Platelet counts for patients with ITP grouped by baseline platelet count. Absolute platelet counts are median ±IQR.

current treatment. In contrast, previous splenectomy was associated with increased platelet counts (Figure 3; supplemental Table 1).

### ITP exacerbation and complications after COVID-19 vaccination

Thirty (13.8%; 95% CI, 9.5-19.1) patients with ITP experienced an exacerbation during the study period (Table 1). Eighteen (8.3%) patients had a ≥50% decline in platelet count compared with baseline, 18 (8.3%) patients had a >20% decline in platelet count compared with baseline and a platelet nadir < 30x10<sup>9</sup>/L, and 15 (6.9%) patients received rescue medication after COVID-19 vaccination (Table 2). Eleven (36.7%) of these 30 patients with ITP needed rescue medication 6 months prior to COVID-19 vaccination compared with 5 (2.7%) of the patients with ITP without exacerbation (Table 1). Of the 30 patients with exacerbation, 16 experienced it after their first vaccination, and 3 of these patients did not receive the second vaccination. Individual platelet counts of patients with ITP with rescue medication and a significant decrease in platelet count are shown in supplemental Figure 2A and supplemental Figure 2B, respectively. Six (2.8%) patients began ITP treatment after COVID-19 vaccination: 3 received glucocorticoids only, 1

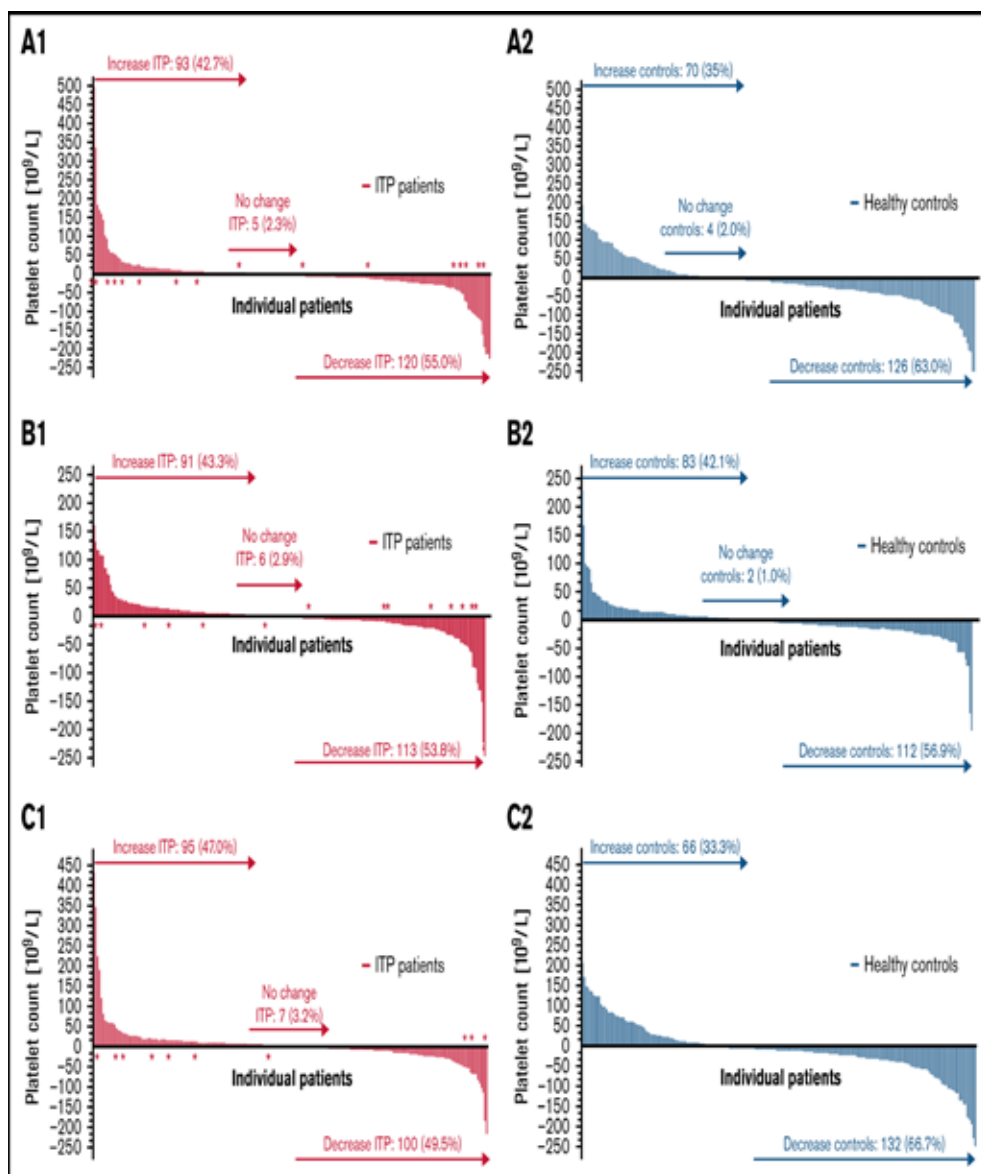


Figure 2. Individual changes in platelet count after both COVID-19 vaccinations in patients with ITP and in healthy controls.

The absolute difference in platelet count is shown per individual in patients with ITP (red) and healthy controls (blue), absolute differences between baseline and 4 weeks after the second vaccination (A1- A2), between baseline and the second vaccination (B1- B2), and between the second vaccination and 4 weeks after the second vaccination (C1-C2). Every bar represents 1 subject. A positive change in absolute platelet count means an increase in platelet count after COVID-19 vaccination, whereas a negative change represents a decrease.

\*Subject received rescue medication during the study period.

received glucocorticoids with IV immunoglobulin (IVIG), 1 received IVIG, and 1 received eltrombopag. Six (2.8%) patients required intensification of current treatment with TPO RA and 1 (0.5%) switched to another TPO RA. Of these seven patients 4 used romiplostim and 3 used eltrombopag (Table 2).

Rescue medication resulted in a complete response in 7 (46.7%) patients and a partial response in 2 (13.3%) patients. One patient (6.7%) did not respond to rescue medication, and 5 (33.3%) patients had no recorded response.

Bleeding complications occurred in 5 (2.3%) patients with ITP and in 0 (0.0%) healthy controls (Table 2). The first patient experienced 2 bleeding complications after the first COVID-19 vaccination. Two weeks after the COVID-19 vaccination, the patient experienced hematuria with a platelet count  $<3 \times 10^9/L$ . The second bleeding was a vitreous hemorrhage and occurred 3 weeks after the first COVID-19 vaccination (platelet count,  $7 \times 10^9/L$ ). The second patient experienced several episodes of bleeding during the study period with epistaxis, oral mucosal bleeding, and urogenital bleeding. This patient had a baseline platelet count  $<3 \times 10^9/L$  and received a red blood cell transfusion and additional IVIG as the result of a severe epistaxis episode. The third patient had a bleeding event after elective vascular surgery and received a red blood cell transfusion in combination with platelet transfusion. The platelet count was  $75 \times 10^9/L$ , and the

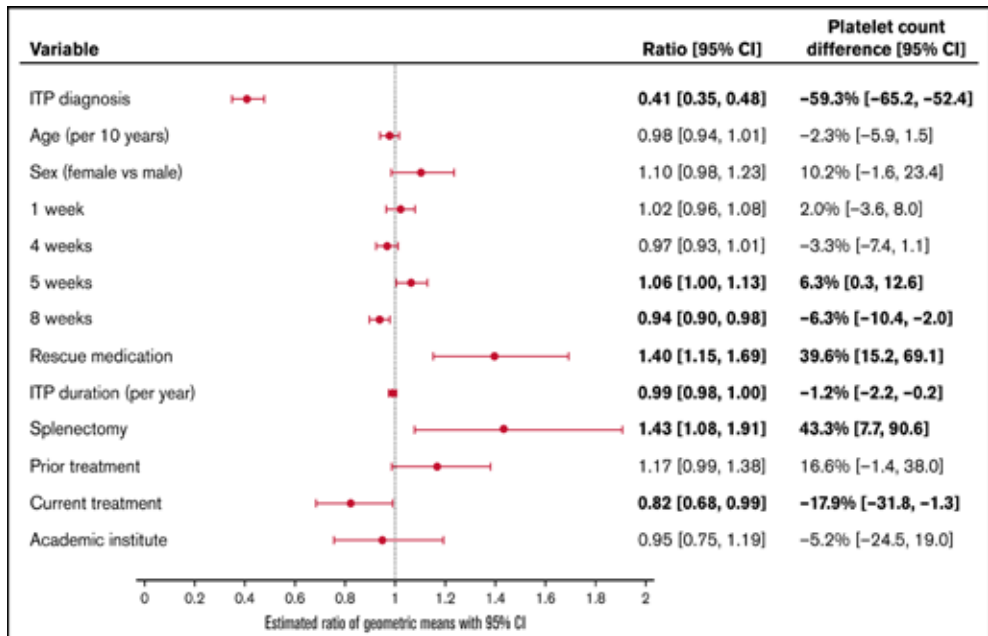


Figure 3. Effect of COVID-19 vaccination on platelet count.

Forest plot for estimated ratios of geometric means with 95% CI for the effect on platelet count. Time points 1 week, 4 weeks, 5 weeks, and 8 weeks after the first COVID-19 vaccination are compared with T=0 (baseline), ITP diagnosis is the comparison of patients vs healthy subjects, and other variables are reported as comparisons of yes vs no. \*Percentage difference and 95% CI were calculated from the ratio of geometric means.

patient did not experience any decrease in platelet count after COVID-19 vaccination. The fourth patient had a spontaneous cerebellar bleeding 3 weeks after the first vaccination with a platelet count of  $104 \times 10^9/L$ . This patient did not experience a decrease in platelet count after COVID-19 vaccination. The patient was treated with additional platelet transfusion and corticosteroids. The fifth patient had a fatal esophageal bleeding 2 weeks after the first COVID-19 vaccination. This patient experienced a decrease in platelet count to  $14 \times 10^9/L$  after COVID-19 vaccination, for which the dosage of romiplostim was increased. However, the patient had a normal platelet count of  $175 \times 10^9/L$  at the time of bleeding. Despite endoscopic intervention and additional platelet transfusion, the patient died from ongoing bleeding. The most common side effects after COVID-19 vaccination in patients with ITP were local tenderness and swelling at the site of vaccination ( $n=15$ ; 29.4%) and myalgia and arthralgia ( $n=13$ ; 25.5%). Fever was reported more often after the second vaccination (supplemental Table 2).

### **Risk factors for ITP exacerbation after COVID-19 vaccination**

Risk factors for exacerbation of ITP after vaccination were baseline platelet count  $< 50 \times 10^9/L$  (odds ratio [OR], 5.33; 95% CI, 2.07-13.73), ITP treatment at start of COVID-19 vaccination (OR, 3.44; 95% CI, 1.47-8.04), and younger age (OR, 0.96 per year; 95% CI, 0.94-0.99) (supplemental Table 3). Although a longer duration of ITP was associated with a decrease in platelet counts over the entire study, in our logistic regression model it did not increase the risk of exacerbation. The type of vaccine was not associated with the risk of exacerbation, but the sample size might have been too small to detect differences between groups. The presence of antiplatelet antibodies also was not associated with exacerbation risk. However, the presence of antiplatelet antibodies was recorded in only 4.6% of patients with ITP, so our sample size might have been too small to detect differences.

## **Discussion**

We systematically investigated the effects of COVID-19 vaccination on platelet count in a large study of patients with ITP compared with healthy controls. Only 3 of 218 patients experienced problems after the first vaccination that prohibited completion of the series. COVID-19 vaccination led to a significant (6.3%) decrease in platelet counts in patients with ITP and healthy controls. Of the patients with ITP, 13.8% exhibited an exacerbation following vaccination. Risk factors for exacerbation were baseline platelet count  $< 50 \times 10^9/L$ , having ITP treatment at the start of COVID-19 vaccination, and/or younger age. Nearly all patients with ITP had a (complete) response after rescue medication.

Thrombocytopenia (platelet count  $< 100 \times 10^9/L$ ) after vaccination has been described in children, with an incidence rate of 0.087 to 2.6 per 100 000 dose [16]. After COVID-19 vaccination in adults, the incidence rate of thrombocytopenia was reported to be 1.13 to 1.33 per 100000 ChAdOx1-S doses [9,17,18]. In our study, 63% of healthy controls experienced decreased platelet counts 4 weeks after the second vaccination, but only 1 (0.5%) had a platelet count  $< 100 \times 10^9/L$ .

	Total (n=218)	After first vaccination (n=218)	After second vaccination (n=213)	Healthy controls (n=200)
<b>Bleeding</b>	5 (2.3)	5 (2.3)	0 (0.0)	0 (0.0)
WHO grade 2	2 (0.9)	2 (0.9)	0 (0.0)	
WHO grade 3	1 (0.5)	1 (0.5)	0 (0.0)	
WHO grade 4	2 (0.9)	2 (0.9)	0 (0.0)	
<b>Exacerbation</b>	30 (13.8)	16 (7.3)	14 (6.6)	2 (1.0)
≥50% decline in platelet count compared with baseline	18 (8.3)	8 (3.7)	10 (4.7)	2 (1.0)
>20% decline in platelet count compared with baseline and platelet nadir < 30 × 10 <sup>9</sup> /L	18 (8.3)	6 (2.8)	12 (5.6)	0 (0.0)
<b>Use of rescue medication</b>	15 (6.9)	8 (3.7)	6 (2.8)	0 (0.0)
Intensification of treatment	6 (2.8)	4 (1.8)	1 (0.5)	
Addition of extra medication	4 (1.8)	2 (0.9)	2 (0.9)	
Switch medication	1 (0.5)	1 (0.5)	0 (0.0)	
Start new medication	4 (1.8)	1 (0.5)	3 (1.4)	
<b>Transfusion</b>	4 (1.8)	4 (1.8)	0 (0.0)	0 (0.0)
Red blood cell transfusion	3 (1.4)	3 (1.4)	0 (0.0)	
Platelet transfusion	2 (0.9)	2 (0.9)	0 (0.0)	

Table 2. Complications after COVID-19 vaccination in patients with ITP.

All data are n (%).

In 2 small studies, a decrease in platelet counts was reported in 12% to 32% of the patients with ITP after COVID-19 vaccination [10,11]. This is in line with our observed decrease in 55% of patients with ITP after COVID-19 vaccination. In contrast, a study of 92 patients with ITP who mostly received the BNT162b2 vaccine did not report a decreased platelet count after the first and second vaccinations [12]. In our mixed-effects model, we observed a significant (6.3%) decrease in platelet counts in patients with ITP after COVID-19 vaccination. Because there is a high degree of inter- and intraindividual variability in platelet counts over time, we systemically measured patients over a longer observation period and corrected for inter- and intraindividual variability. We hypothesize that this

systematic approach to monitor platelet count is essential to draw conclusions about their changes following COVID-19 vaccination.

In our study, 13.8% of patients with ITP experienced an exacerbation, defined as development of any of the following:  $\geq 50\%$  decline in platelet count compared with baseline,  $>20\%$  decline in platelet count compared with baseline and a platelet nadir  $<30 \times 10^9/L$ , or a need for rescue medication. Other observational studies found comparable incidences between 12% and 25% [11-13]. In our study, 6.9% of our patients required rescue medication compared with 8.7% in the study by Crickx et al [12]. In other autoimmune diseases, exacerbation of symptoms after COVID-19 vaccination has been described anecdotally, with rapid remission after glucocorticoids [19,20]. However, in a single-center study of 26 patients with chronic inflammatory diseases, no patient experienced a disease flare [21]. Furthermore, a large cohort study did not show any significant difference in the exacerbation of autoimmune rheumatic disease compared with non-autoimmune rheumatic disease after COVID-19 vaccination [22].

Based on our current understanding, we speculate that ITP stems from a propensity to autoimmunity in combination with a triggering event, such as infection or vaccination [7]. Intriguingly, in our systematic evaluation of platelet counts in patients with ITP and healthy individuals, we found that both groups had significantly decreased platelet counts as a result of COVID-19 vaccination. This suggests that exacerbation or development of thrombocytopenia because of (COVID-19) vaccination might be unrelated to ITP, as evidenced by the fact that we could not find an interaction between platelet counts over time and whether a subject had ITP. This observation is also underscored by the high degree of interindividual variability in patients with ITP and healthy controls, suggesting no universal mechanism leading to lower or higher platelet counts. We also did not find a correlation between platelet counts and anti-SARS-CoV-2 immunoglobulin G levels in the healthy controls (data not shown), suggesting that, at least in healthy individuals, changes in platelet count are unrelated to vaccine response. On the other hand, we found a significant negative association between platelet counts and ITP duration, as well as between platelet counts and current ITP treatment. Also, patients with ITP with exacerbation needed more frequent rescue medication prior to COVID-19 vaccination compared with patients with ITP without exacerbation. These data may suggest that the hardest-to-treat patients with chronic ITP are more susceptible to develop thrombocytopenia after vaccination in comparison with a group not currently requiring treatment for ITP.

Additionally, previous splenectomy was positively associated with platelet counts over time, signifying that this potential lack of acute immune response is directly favorable for platelet counts in these individuals. To summarize, it remains unclear whether COVID-19 vaccination has a differential effect on patients with ITP and healthy controls. Our associative findings warrant further investigation to firmly establish whether patients with ITP are more prone to platelet count changes resulting from COVID-19 vaccination.

Our study aimed to provide a better understanding of the effect of COVID-19 vaccination in patients with ITP. The strengths of this study are the prospective and systematic evaluation of real-world data on platelet counts, bleeding complications, and the need for rescue medication in patients with ITP. Furthermore, we used a healthy control group to interpret results from patients with ITP accordingly. However, there are also some limitations. First, almost all patients with ITP received the mRNA vaccine, so caution is warranted when generalizing our results to other vaccines. Still, mRNA vaccines are the most frequently used globally, with >80% of European vaccine recipients and >90% of US vaccine recipients getting this type of vaccine [23,24]. One patient with ITP received the adenoviral vector vaccine (ChAdOx1-S vaccine) without any significant changes in platelet count. Although thrombocytopenia after COVID-19 vaccination is primarily associated with ChAdOx1-S vaccination, conclusions cannot be made with regard to ChAdOx1-S vaccination in patients with ITP [9]. Second, although we cannot exclude that exacerbation after COVID-19 vaccination is due to a natural course of ITP, half of the patients with ITP with exacerbation did not require treatment for ITP before COVID-19 vaccination. In these patients, COVID-19 vaccination seems to be a plausible cause of exacerbation. Third, we did not assess anti-SARS-CoV-2 immunoglobulin G levels in patients with ITP as a measure of vaccine response, so no firm conclusions can be made about the direct effect of COVID-19 vaccination on platelet count; however, no association between platelet count and antibody levels was noted in healthy controls. Finally, platelet count and bleeding complications in healthy controls were obtained from the RECOVAC IR study. Because bleeding complications were not a primary outcome in this study, their underestimation might have occurred, although bleeding scores were similar (eg, WHO criteria National Cancer Institute's Common Terminology Criteria  $\geq$  grade 2). Also, the RECOVAC-IR study did not measure platelet count 1 week after each COVID-19 vaccination. A temporary decrease in platelet counts may be missed in healthy volunteers. In contrast, however, we observed an increase in overall platelet count in patients with ITP 1 week after the first and second vaccinations.

To conclude, our study highlights the safety of COVID-19 vaccination in patients with ITP and the importance of close monitoring of platelet counts in a subgroup of patients with ITP. Patients with ITP with an exacerbation responded well to therapy.

### Authorship

Contribution: H.N.N., M.E., S.M.L.K., C.I., M.D.L., and A.J.G.J. designed the study protocol; C.V. and E.D.v.W. analyzed data; E.D.v.W. created the linear mixed-effects model; F.N.C., H.N.N., M.E., S.M.L.K., C.I., P.E.W., B.S., P.A.J., F.B., P.A.W.t.B., F.W.G.L., M.J.H.A.K., and A.J.G.J. enrolled and treated patients; the RECOVACIR Consortium provided data for healthy controls; and C.V., M.S., and A.J.G.J. wrote the manuscript. All authors reviewed and provided feedback on the drafts and approved the final manuscript for submission.

Conflict-of-interest disclosure: P.A.W.t.B. received speaker's fee from, and is a member of the advisory boards for, Novartis and Sanofi. F.W.G.L. has received research support from

CSL Behring and Shire/Takeda for performing the Willebrand in the Netherlands study; has acted as a consultant for uniQure, Novo Nordisk, and Shire/Takeda in exchange for fees paid to the institution; has received travel support from Sobi; and is member of the Data Safety Monitoring Board for a study sponsored by Roche. M.J.H.A.K. has received unrestricted grants, paid to the department for research outside of the scope of this work, from Bayer and Daiichi Sankyo and has received a speaker's fee, paid to the department, from Bayer. A.J.G.J. has received speaker's fees from, and has had travel costs paid by, 3SBio, Amgen, and Novartis; has served on an international advisory board for Novartis; and has received research funding from CSL Behring. The remaining authors declare no competing financial interests.

A complete list of the members of the RECOVAC-IR Consortium appears in the supplemental Appendix.

ORCID profiles: C.V., 0000-0002-2025-1734; M.S., 0000-0002-6667-9031; E.D.v.W., 0000-0001-7469-7427; F.N.C., 0000-0001-7722-1862; P.E.W., 0000-0002-0746-7039; P.A.W.t.B., 0000-0002-3566-5016; M.-D.L., 0000-0003-2139-3547; M.J.H.A.K., 0000-0002-0265-4871; A.J.G.J., 0000-0002-2612-1420.

## References

1. Polack FP, Thomas SJ, Kitchin N, et al; C4591001 Clinical Trial Group. Safety and efficacy of the BNT162b2 mRNA Covid-19 vaccine. *N Engl J Med.* 2020;383(27):2603-2615.
2. Baden LR, El Sahly HM, Essink B, et al; COVE Study Group. Efficacy and safety of the mRNA-1273 SARS-CoV-2 vaccine. *N Engl J Med.* 2021;384(5):403-416.
3. Folegatti PM, Ewer KJ, Aley PK, et al; Oxford COVID Vaccine Trial Group. Safety and immunogenicity of the ChAdOx1 nCoV-19 vaccine against SARS-CoV-2: a preliminary report of a phase 1/2, single-blind, randomised controlled trial [published correction appears in *Lancet.* 2020;396(10263):E89]. *Lancet.* 2020;396(10249):467-478.
4. Sadoff J, Gray G, Vandebosch A, et al; ENSEMBLE Study Group. Safety and efficacy of single-dose Ad26.COV2.S vaccine against Covid-19. *N Engl J Med.* 2021;384(23):2187-2201.
5. Greinacher A, Thiele T, Warkentin TE, Weisser K, Kyrle PA, Eichinger S. Thrombotic thrombocytopenia after ChAdOx1 nCov-19 vaccination. *N Engl J Med.* 2021;384(22):2092-2101.
6. Muir KL, Kallam A, Koepsell SA, Gundabolu K. Thrombotic thrombocytopenia after Ad26.COV2.S vaccination. *N Engl J Med.* 2021;384(20):1964-1965.
7. Swinkels M, Rijkers M, Voorberg J, Vidarsson G, Leebeek FWG, Jansen AJG. Emerging concepts in immune thrombocytopenia. *Front Immunol.* 2018;9:880.
8. Bomhof G, Mutsaers PGNJ, Leebeek FWG, et al. COVID-19-associated immune thrombocytopenia. *Br J Haematol.* 2020;190(2):e61-e64.
9. Simpson CR, Shi T, Vasileiou E, et al. First-dose ChAdOx1 and BNT162b2 COVID-19 vaccines and thrombocytopenic, thromboembolic and hemorrhagic events in Scotland. *Nat Med.* 2021;27(7):1290-1297.
10. Platelet Disorder Support Association. Results from the ITP Natural History Study. <https://pdsa.org/images/COVID-19-survey-results.pdf>. Accessed 14 September 2021.
11. Kuter DJ. Exacerbation of immune thrombocytopenia following COVID-19 vaccination. *Br J Haematol.* 2021;195(3):365-370.
12. Crickx E, Moulis G, Ebbo M, et al. Safety of anti-SARS-CoV-2 vaccination for patients with immune thrombocytopenia. *Br J Haematol.* 2021;

195(5):703-705.

13. Lee EJ, Beltrami Moreira M, Al-Samkari H, et al. SARS-CoV-2 vaccination and immune thrombocytopenia in de novo and pre-existing ITP patients [published online ahead of print 9 Sep 2021]. *Blood*.
14. Rodeghiero F, Stasi R, Gernsheimer T, et al. Standardization of terminology, definitions and outcome criteria in immune thrombocytopenic purpura of adults and children: report from an international working group. *Blood*. 2009;113(11):2386-2393.
15. Kho MML, Reinders MEJ, Baan CC, et al; RECOVAC Collaborators. The RECOVAC IR study: the immune response and safety of the mRNA-1273 COVID-19 vaccine in patients with chronic kidney disease, on dialysis or living with a kidney transplant. *Nephrol Dial Transplant*. 2021;36(9): 1761-1764.
16. Perricone C, Ceccarelli F, Neshor G, et al. Immune thrombocytopenic purpura (ITP) associated with vaccinations: a review of reported cases. *Immunol Res*. 2014;60(2-3):226-235.
17. Hippisley-Cox J, Patone M, Mei XW, et al. Risk of thrombocytopenia and thromboembolism after Covid-19 vaccination and SARS-CoV-2 positive testing: self-controlled case series study. *BMJ*. 2021;374:n1931.
18. Lee EJ, Cines DB, Gernsheimer T, et al. Thrombocytopenia following Pfizer and Moderna SARS-CoV-2 vaccination. *Am J Hematol*. 2021;96(5): 534-537.
19. Niebel D, Ralser-Isselstein V, Jaschke K, Braegelmann C, Bieber T, Wenzel J. Exacerbation of subacute cutaneous lupus erythematosus following vaccination with BNT162b2 mRNA vaccine. *Dermatol Ther (Heidelb)*. 2021;34(4):e15017.
20. Kulkarni R, Sollecito TP. COVID-19 vaccination: possible short-term exacerbations of oral mucosal diseases. *Int J Dermatol*. 2021;60(9):e335-e336.
21. Geisen UM, Berner DK, Tran F, et al. Immunogenicity and safety of anti-SARS-CoV-2 mRNA vaccines in patients with chronic inflammatory conditions and immunosuppressive therapy in a monocentric cohort. *Ann Rheum Dis*. 2021;80(10):1306-1311.
22. Cherian S, Paul A, Ahmed S, et al. Safety of the ChAdOx1 nCoV-19 and the BBV152 vaccines in 724 patients with rheumatic diseases: a postvaccination cross-sectional survey. *Rheumatol Int*. 2021;41(8):1441-1445.
23. European Centre for Disease Prevention and Control. COVID-19 vaccine tracker. <https://gap.ecdc.europa.eu/public/extensions/COVID-19/vaccinetracker.html#distribution-tab>. Accessed 9 Jan 2021.
24. Our World in Data. Statistics and research: coronavirus (COVID-19) vaccinations. <https://ourworldindata.org/covid-vaccinations>. Accessed 9 Jul 2021.

## Appendix

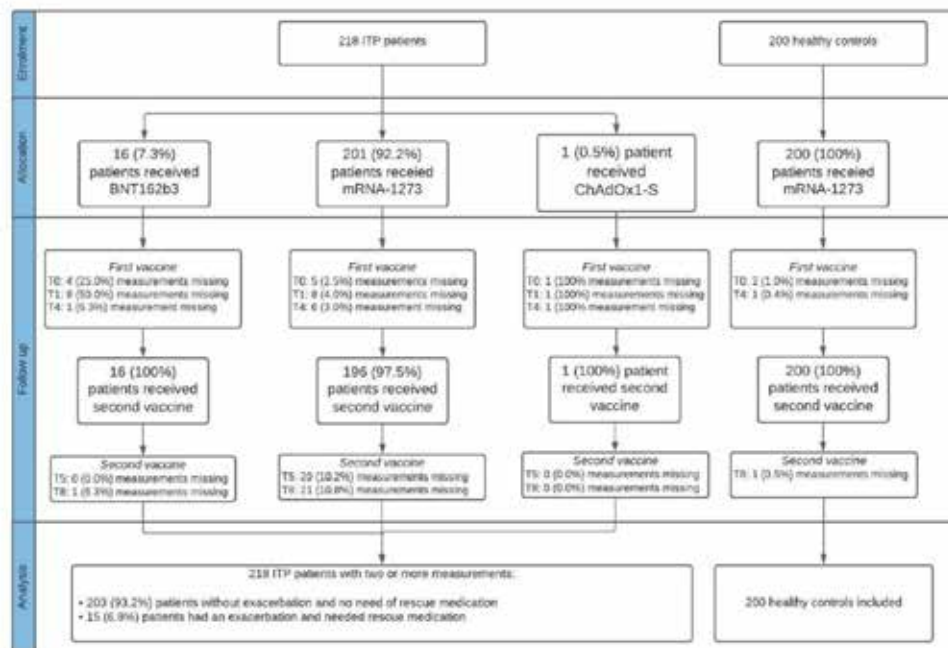


Figure S1. CONSORT Flow Diagram.

Consort diagram of ITP patients and healthy controls describing enrolment, type of vaccine, follow-up and analysis. Data of healthy controls were obtained from the RECOVAC IR study.<sup>14</sup> T0= baseline, T1= 1 week after first COVID-19 vaccination, T4= the moment of the second COVID-19 vaccination, T5= 1 week after second COVID-19 vaccination and T8= 4 weeks after second COVID-19 vaccination.

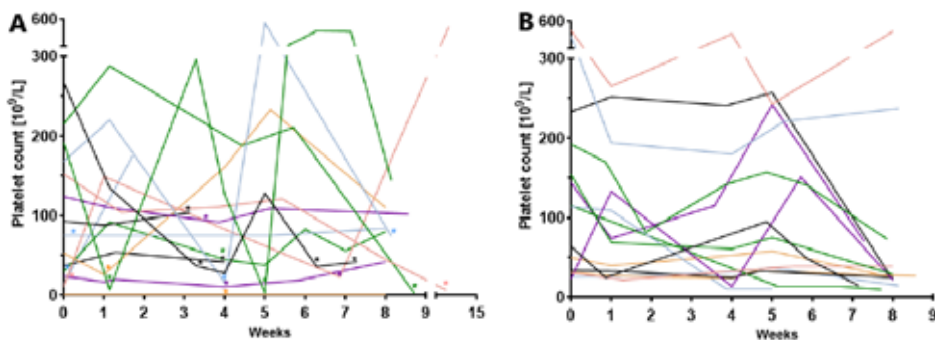


Figure S2. Platelet counts of ITP patients with an exacerbation after COVID-19 vaccination.

Absolute platelet counts after COVID-19 vaccination of 30 ITP patients with an exacerbation defined as use of rescue medication (A) or significant decrease in platelet count (B). Rescue medication is defined as treatment change at the discretion of the treating physician, i. e. to switch to other ITP medication, start of new ITP medication, the addition of concomitant ITP medication or intensification of current ITP treatment. Significant decrease in platelet count is defined as either a  $\geq 50\%$  decline in platelet count from baseline or  $>20\%$  decline in platelet count from baseline and a platelet nadir  $<30 \times 10^9/L$ , but did not receive rescue medication. Every line represents one individual patient. \* Time of rescue medication as described above.

	Association with log platelet count (coefficient $\beta$ )	Ratio of mean platelet count ( $e^\beta$ )	Platelet count difference (percentage)
<b>Intercept</b>	5.63 (5.38—5.88)		
<b>ITP diagnosis</b>	-0.90 (-1.05—0.74)	0.41 (0.35—0.48)	<b>-59.3%</b> (-65.2—52.4)
<b>Age (per 10 years)</b>	-0.02 (-0.06—0.01)	0.98 (0.94—1.01)	-2.3% (-5.9—1.5)
<b>Sex (female vs. male)</b>	0.10 (-0.02—0.21)	1.10 (0.98—1.23)	10.2% (-1.6—23.4)
<b>Time since 1st vaccination</b>			
<b>1 week</b>	0.02 (-0.04—0.08)	1.02 (0.96—1.08)	2.0% (-3.6—8.0)
<b>4 weeks</b>	-0.03 (-0.08—0.01)	0.97 (0.93—1.01)	-3.3% (-7.4—1.1)
<b>5 weeks</b>	0.06 (0.003—0.12)	1.06 (1.00—1.13)	<b>6.3%</b> (0.3—12.6)
<b>8 weeks</b>	-0.07 (-0.11—0.02)	0.94 (0.90—0.98)	<b>-6.3%</b> (-10.4—2.0)
<b>Use of rescue medication**</b>	0.33 (0.14—0.53)	1.40 (1.15—1.69)	<b>39.6%</b> (15.2—69.1)
<b>ITP duration (per year)</b>	-0.01 (-0.02—0.002)	0.99 (0.98—1.00)	-1.2% (-2.2—0.2)
<b>Splenectomy</b>	0.36 (0.07—0.64)	1.43 (1.08—1.91)	<b>43.3%</b> (7.7—90.6)
<b>Prior treatment</b>	0.15 (-0.01—0.32)	1.17 (0.99—1.38)	16.6% (-1.4—38.0)
<b>Current treatment</b>	-0.20 (-0.38—0.01)	0.82 (0.68—0.99)	<b>-17.9%</b> (-31.8—1.3)
<b>Academic institute</b>	-0.05 (-0.28—0.17)	0.95 (0.75—1.19)	-5.2% (-24.5—19.0)

Table S1. Effect of COVID-19 vaccination on platelet count\*.

\* Estimates with 95% confidence intervals from a linear mixed-effects model with random intercept per patient. Time points T=1, 4, 5 and 8 weeks are compared with T=0 (baseline); ITP diagnosis is the comparison of patients versus healthy subjects; other variables are reported as comparisons of yes versus no.

\*\* Rescue medication is defined as treatment change at the discretion of the treating physician, i. e. to switch to other ITP medication, start of new ITP medication, the addition of concomitant ITP medication or intensification of current ITP treatment.

	Total (N=51)	After first vaccination (N=27)	After second vaccination (N=24)
<b>Side effect</b>			
Local tenderness/ Swelling	15 (29.4)	10 (37.0)	5 (20.8)
Fatigue	7 (13.7)	4 (14.8)	3 (12.5)
Fever	7 (13.7)	1 (3.7)	6 (25.0)
Lymphadenopathy	1 (2.0)	1 (3.7)	0 (0.0)
Headache	6 (11.7)	2 (7.4)	4 (16.7)
Myalgia/arthralgia	13 (25.5)	8 (26.6)	5 (20.8)
Nausea/vomiting	2 (3.9)	1 (3.7)	1 (4.2)

Table S2. Documented side effects after COVID-19 vaccination in ITP patients\*.

\* Data are presented as number (percentage)

	OR	CI
Platelet count <50x10 <sup>9</sup> /L	5.33	2.07-13.73
Current treatment	3.44	1.47 - 8.04
Age	0.96	0.94 - 0.99

Table S3. Risk factors for ITP exacerbation after COVID-19 vaccination.

OR, Odds ratio calculated by multivariable logistic regression; CI, 95% confidence interval.

# Chapter 4

## Platelet Degranulation and Bleeding Phenotype in a Large Cohort of VWD Patients

Maurice Swinkels, Ferdows Atiq, Petra E. Bürgisser, Iris van Moort, Karina Meijer, Jeroen Eikenboom, Karin Fijnvandraat, Karin P. M. van Galen, Joke de Meris, Saskia E. M. Schols, Johanna G. van der Bom, Marjon H. Cnossen, Jan Voorberg, Frank W. G. Leebeek, Ruben Bierings, A. J. Gerard Jansen, WiN study group

British Journal of Haematology 2022 May; 197(4): 497–501

## Abstract

Von Willebrand disease (VWD) is a bleeding disorder caused by quantitative (type 1 or 3) or qualitative (type 2A/2B/2M/2N) defects of circulating von Willebrand factor (VWF). Circulating VWF levels not always fully explain bleeding phenotypes, suggesting a role for alternative factors, like platelets. Here, we investigated platelet factor 4 (PF4) in a large cohort of patients with VWD. PF4 levels were lower in type 2B and current bleeding phenotype was significantly associated with higher PF4 levels, particularly in type 1 VWD. Based on our findings we speculate that platelet degranulation and cargo release may play a role across VWD subtypes.

Keywords: bleeding disorders, platelet activation, platelet factor 4, VWD, VWF

## Introduction

Von Willebrand disease (VWD) is the most common inherited bleeding disorder, characterized by a deficiency of von Willebrand factor (VWF)[1]. VWF is a large, multimeric protein that interacts with many haemostatic components, collagen, surface receptors on platelets, coagulation factor VIII (FVIII) and other ligands [2]. VWD is classified in subtypes based on VWF defects that are quantitative (reduction of VWF levels in type 1; or absence of VWF in type 3) or qualitative (in type 2 VWD). Type 2 VWD can be further subdivided into: defects in multimerization or enhanced proteolytic cleavage by ADAMTS13 (Type 2A), enhanced interaction with platelet GPIb (Type 2B), defective binding to platelet GPIb or collagen (Type 2M) or defective binding and stabilization of FVIII (Type 2N). This classification is based on diagnostic assays that determine function and quantity of VWF in the circulation [1].

However, VWD patients with similar circulating VWF levels can have variable bleeding phenotypes [3,4], suggesting that additional disease modifiers, such as release of VWF and other haemostatic cargo from platelets may be of importance in VWD. Platelet factor 4 (PF4) is a platelet-specific chemokine that can be sensitively measured in plasma after platelet cargo release. This cargo release from platelet alpha granules, or degranulation, is part of the platelet activation process [5].

In the current study, our aim is to explore the degree of platelet degranulation across a large population of VWD patients. We hypothesize that platelet degranulation could be an additional determinant of the bleeding phenotype in VWD. We first quantified PF4 levels across VWD subtypes and in relation to VWF parameters. Next, we investigated whether PF4 levels are associated with the bleeding phenotype in VWD patients.

## Methods

### Patients

Adult patients with VWD were included in the 'Willebrand in the Netherlands' (WiN) study [3,6,7]. Patients were included in 2007–2009 and citrated plasma samples were stored at time of inclusion at  $-80^{\circ}\text{C}$ . Inclusion criteria were: (1) haemorrhagic symptoms or family history of VWD; and (2) one historically lowest measured value of VWF antigen (VWF:Ag) or ristocetin cofactor activity  $\leq 0.3$  IU/ml and/or FVIII coagulant activity (FVIII:C)  $\leq 0.40$  IU/ml (for type 2N VWD). Exclusion criteria were treatment with blood products prior to inclusion ( $<72$  h) and pregnancy. The study was in accordance with the Declaration of Helsinki and approved by the Medical Ethical committees of the participating centres. Written informed consent was obtained from all study participants.

## Clinical data and bleeding phenotype

Clinical parameters in the WiN study have been described previously [3,6,7]. Bleeding scores were assessed using the self-administered version of the condensed Tostetto bleeding score, while current bleeding phenotype was defined as bleeding episodes that required haemostatic treatment in the year prior to inclusion [8,9]. Platelet counts of type 2B patients were collected from patient files. Thrombocytopenia was defined as platelet counts below  $150 \times 10^9/L$ . Persistent thrombocytopenia was defined as thrombocytopenia throughout the total follow-up period based on available platelet count data in medical files. Intermittent thrombocytopenia was defined as platelet counts that fluctuated between reference values  $150\text{--}400 \times 10^9/L$  and below  $150 \times 10^9/L$ .

## Plasma measurements and statistics

Measurements of VWF parameters and PF4 in plasma, as well as statistics are described in the Supporting information.

## Results

### PF4 levels are lower in type 2B VWD

Plasma PF4 was measured in a total of 594 VWD patients (Table S1; Figure S1). We found that PF4 levels differed across VWD subtypes ( $p < 0.0001$ , Figure 1). PF4 levels in type 2B VWD patients [63.2 (32.1–115.4) ng/ml] were lower compared to type 1 VWD patients [110 (70.7–160.7) ng/ml,  $p=0.0003$ ].

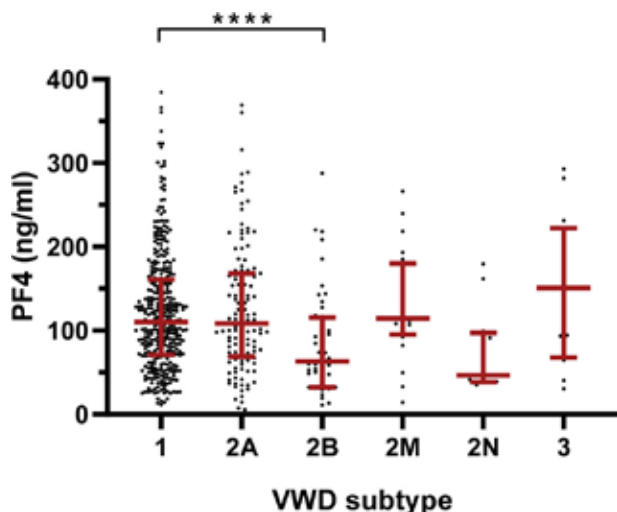


Figure 1. Platelet factor 4 (PF4) levels in the von Willebrand disease (VWD) cohort.

Distribution of PF4 plasma levels in ng/ml are shown per subtype of VWD. Subtypes are type 1 (n=368), type 2A (n=125), type 2B (n=50), type 2M (n=20), type 2N (n=12) and type 3 (n=19). Data shown as median  $\pm$  interquartile range. \*\*\*\*,  $p < 0.0001$ .

### Potential determinants of PF4 plasma levels in type 2A and 2B VWD

In the total VWD population, we found no association between PF4 and VWF:Ag, VWF activity, or VWF collagen binding (data not shown). We found a small negative correlation between PF4 levels and VWF propeptide/VWF:Ag ratio in VWD patients ( $r=-0.083$ ,  $p=0.043$ ) which was primarily attributable to type 2A patients ( $r=-0.214$ ,  $p=0.017$ ). In line with this observation, we found a positive correlation between PF4 and VWF:Ag levels in type 2A VWD patients ( $r=0.229$ ,  $p=0.010$ ).

A further, explorative, analysis of PF4 levels in types 2A and 2B showed that levels may be associated with specific mutations (Figure S2A,B). We found significantly lower PF4 levels in type 2B patients with persistent thrombocytopenia when compared to patients with intermittent thrombocytopenia or normal platelet counts (Figure S2C).

### PF4 levels associate with bleeding requiring treatment in VWD patients

Finally, we investigated whether PF4 levels were associated with bleeding phenotype in VWD patients (Figure 2A). PF4 was not associated with total bleeding score [ $\beta=0.02$  ( $-0.52;0.56$ ),  $p=0.940$ ]. However, we found that PF4 levels in the total VWD cohort were positively associated with the current bleeding phenotype [odds ratio (OR) 1.21 (1.02;1.43),  $p=0.029$ ]. Similarly, the third and fourth PF4 quartiles contained a higher proportion of patients who experienced recent bleeding (Q1=28.7%, Q2=23.1%, Q3=34.5%, Q4=38.0%; Figure 2A).

When VWD types were analysed separately we only found a significant association between PF4 and current bleeding phenotype in patients with type 1 VWD [OR 1.40 (1.10–1.79),  $p=0.007$ ]. Descriptive data are further shown in Figure 2B.

## Discussion

In this study, we measured PF4 levels in a large and well-defined cohort of VWD patients aiming to investigate platelet degranulation in VWD. We found that PF4 levels were positively associated with the current bleeding phenotype, mainly in type 1 VWD patients. We also identified that type 2B VWD patients, particularly those with persistent thrombocytopenia, had lower PF4 levels in comparison to type 1 VWD patients. Associations between PF4, VWF levels and VWF mutations suggest that platelet degranulation could play role in type 2A and 2B VWD. In conclusion, our associative findings highlight a potential association between PF4 levels, as a measure for platelet degranulation, and current bleeding phenotype in VWD patients.

The role of platelets and their cargo release in the pathophysiology and phenotype of VWD patients is largely unknown, as there have been no large cohort association studies until now. We found that PF4 levels were positively associated with a current bleeding phenotype, particularly in type 1 VWD. Considering that bleeding in type 1 VWD patients is also determined by factors other than VWF [3,4,10,11], our data suggest that platelet

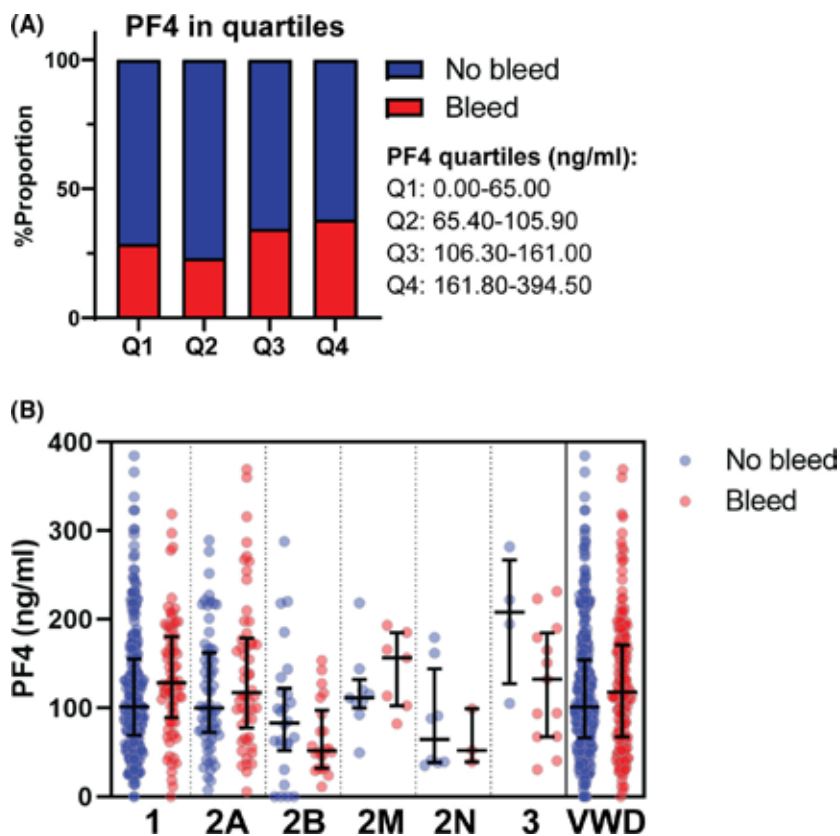


Figure 2. Platelet factor 4 (PF4) levels in relation to current bleeding phenotype in the von Willebrand disease (VWD) cohort.

PF4 plasma levels were related to bleeding that required treatment in the year prior to inclusion. For this analysis, PF4 was subdivided into quartiles: 0.00–65.00 ng/ml (Q1), 65.40–105.90 ng/ml (Q2), 106.30–161.00 ng/ml (Q3) and 161.80–394.50 ng/ml (Q4). The proportion of patients with no bleeding (no bleed, blue) versus bleeding (bleed, red) were plotted across the four quartiles of PF4 levels (A). Bleeding versus PF4 levels are also plotted per subtype and total population (B). Data are shown as proportion (A) and median  $\pm$  interquartile range (B).

cargo release may be of particular interest in this subtype. Elevated PF4 levels may be indicative of partial pre-release of platelet cargo or constitutive platelet activation, suggesting platelets may no longer fully function during primary haemostasis. This might explain the increasing bleeding tendency in patients with higher PF4 levels, but mechanistic studies are required to further elucidate this.

We also found that PF4 levels were lower in type 2B compared to type 1 VWD, especially in those with persistent thrombocytopenia. Possibly, this indicates that the continuous consumption of platelets [12] (capable of releasing PF4) in some of these patients leads to lower PF4 levels. Platelet degranulation itself could also be affected, as PF4 levels in type 2B patients without thrombocytopenia were also lower than in type 1 VWD.

A final explanation for lower PF4 levels in type 2B may be due to megakaryocytic defects in type 2B patients, which could directly affect PF4 synthesis [13].

In the current study, we also identified a positive correlation between PF4 and VWF levels in type 2A VWD patients. A recent *in vitro* study has demonstrated that VWF and PF4 may interact under specific conditions, possibly at the A2 domain of VWF, and that this interaction may affect ADAMTS13-mediated cleavage of VWF [14]. Intriguingly, we found that type 2A patients with A2 mutations had high PF4 levels, which might indicate a similar interaction *in vivo*. We did not find an association between ADAMTS13 activity and PF4 levels (data not shown), but the assay for ADAMTS13 activity is not suited to determine how PF4 affects ADAMTS13-mediated VWF proteolysis [15]. Thus, our data cannot decisively answer if PF4 plays a role in VWF interactions and ADAMTS13-mediated proteolysis *in vivo* yet, but suggests this could ultimately be relevant to type 2A patients.

One limitation of the current study was that platelet degranulation was measured based solely on a plasma marker. Ideally, a parallel approach would also measure platelet cell surface activation markers, but this requires fresh platelet samples. Finally, another limitation is that we had no access to a healthy control dataset that was matched to the patient population. A prospective follow-up study that includes both VWD and healthy subjects would be very useful to further elucidate the role of platelet degranulation in VWD.

In conclusion, we evaluated PF4 plasma levels as a marker of platelet degranulation in a large cohort of VWD patients. Our findings suggest that platelet degranulation may be associated with current bleeding phenotype in type 1 VWD, and VWF levels and mutations in type 2A and 2B VWD. Further mechanistic and prospective studies on the role of platelet cargo in the pathophysiology of VWD will be needed to elucidate the associations generated in this study.

### Acknowledgements

This work was supported by grants from the Landsteiner Stichting voor Bloedtransfusie Research (LSBR-1707)(Ruben Bierings), the Netherlands Organization for Scientific Research (NWO NWA.1160.18.038) (Ruben Bierings and Iris van Moort) and an EHA Clinical Research Fellowship (A. J. Gerard Jansen). The WiN study was supported (in part) by research funding from the Dutch Haemophilia Foundation (Stichting Haemophilia) (Frank W. G. Leebeek) and CSL Behring (Frank W. G. Leebeek, unrestricted grant).

### Conflict of Interest

F.W.G. Leebeek received research support from CSL Behring and Shire for performing the Willebrand in the Netherlands (WiN) study, and is consultant for uniQure, Biomarin, Novo Nordisk and Shire, of which the fees go to the institution. F. Atiq received the CSL Behring-Heimburger Award 2018, and a travel grant from Sobi. I. van Moort received the CSL Behring-Heimburger Award 2021. A. J. G. Jansen received speaker fees

and travel cost payments from 3SBio, Amgen and Novartis, is on the international advisory board at Novartis and received research support from Sanofi, Argenx and CSL Behring. J. Eikenboom received research support from CSL Behring and he has been a teacher on educational activities of Roche. K. P. M. van Galen received unrestricted research support from CSL Behring and Bayer. J. G. van der Bom has received unrestricted research/educational funding for various projects from the following companies: Bayer Schering Pharma, Baxter, CSL Behring, Novo Nordisk, and Pfizer. In addition, she has been a consultant to Baxter and Pfizer, and she has been a teacher on educational activities of Bayer Schering Pharma. M. H. Cnossen has received unrestricted research/educational and travel funding from the following companies: Pfizer, Baxter, Bayer Schering Pharma, CSL Behring, Novo Nordisk and Novartis, and serves as a member on steering boards of Roche and Bayer of which fees go to the institution. K. Fijnvandraat is a member of the European Haemophilia Treatment and Standardization Board sponsored by Baxter, has received unrestricted research grants from CSL Behring and Bayer, and has given lectures at educational symposiums organized by Pfizer, Bayer and Baxter. K. Meijer received speaker fees from Alexion, Bayer and CSL Behring, fees for participation in trial steering committee for Bayer, consulting fees from Unique, and fees for participation in data monitoring and endpoint adjudication committee for Octapharma. S. Schols received travel grants from Bayer and Takeda and consultancy grants from Takeda and Novo Nordisk. None of the other authors has a conflict of interest to declare.

### **Author Contributions**

Maurice Swinkels, Petra E. Bürgisser, Iris van Moort performed experiments. Maurice Swinkels and Ferdows Atiq analysed data. Ferdows Atiq retrieved data from patients files. Karina Meijer, Jeroen Eikenboom, Karin Fijnvandraat, Karin P. M. van Galen, Joke de Meris, Saskia E. M. Schols, Johanna G. van der Bom and Marjon H. Cnossen provided essential patient material for the study. Maurice Swinkels, Jan Voorberg, Frank W. G. Leebeek, Ruben Bierings and A. J. Gerard Jansen designed the research and wrote the paper. All authors critically revised and approved of the final version of the manuscript.

### **Win Study Group Members**

Academic Medical Centre, Amsterdam: K. Fijnvandraat, M. Coppens. The Netherlands Haemophilia Society: J. de Meris. Maxima Medical Centre, Eindhoven: L. Nieuwenhuizen. University Medical Centre Groningen, Groningen: K. Meijer, R. Y. J. Tamminga. HagaZiekenhuis, The Hague: P. F. Ypma. Leiden University Medical Centre, Leiden: H. C. J. Eikenboom, J. G. van der Bom, F. J. W. Smiers. Maastricht University Medical Centre, Maastricht: B. Granzen, F. Moenen. Radboud University Medical Centre, Nijmegen: P. Brons, S. E. M. Schols. Erasmus University Medical Centre, Rotterdam: F. W. G. Leebeek (principal investigator), M. H. Cnossen, F. Atiq, C. B. van Kwawegen. Van Creveld Clinic, University Medical Centre Utrecht, Utrecht: K. P. M. van Galen.

**ORCID**Maurice Swinkels <https://orcid.org/0000-0002-6667-9031>Ferdows Atiq <https://orcid.org/0000-0002-3769-9148>Karin P. M. van Galen <https://orcid.org/0000-0003-3251-8595>Jan Voorberg <https://orcid.org/0000-0003-4585-2621>Frank W. G. Leebeek <https://orcid.org/0000-0001-5677-1371>Ruben Bierings <https://orcid.org/0000-0002-1205-9689>A. J. Gerard Jansen <https://orcid.org/0000-0002-2612-1420>**References**

1. Leebeek FW, Eikenboom JC. Von Willebrand's disease. *N Engl J Med.* 2016;375(21):2067–80.
2. Springer TA. von Willebrand factor, Jedi knight of the bloodstream. *Blood.* 2014;124(9):1412–25.
3. de Wee EM, Sanders YV, Mauser-Bunschoten EP, van der Bom JG, Degenaar-Dujardin ME, Eikenboom J, et al. Determinants of bleeding phenotype in adult patients with moderate or severe von Willebrand disease. *Thromb Haemost.* 2012;108(4):683–92.
4. Flood VH, Christopherson PA, Gill JC, Friedman KD, Haberichter SL, Bellissimo DB, et al. Clinical and laboratory variability in a cohort of patients diagnosed with type 1 VWD in the United States. *Blood.* 2016;127(20):2481–8.
5. Karampini E, Bierings R, Voorberg J. Orchestration of primary hemostasis by platelet and endothelial lysosome-related organelles. *Arterioscler Thromb Vasc Biol.* 2020;40(6):1441–53.
6. Sanders YV, Eikenboom J, de Wee EM, van der Bom JG, Cnossen MH, Degenaar-Dujardin ME, et al. Reduced prevalence of arterial thrombosis in von Willebrand disease. *J Thromb Haemost.* 2013;11(5):845–54.
7. Sanders YV, Groeneveld D, Meijer K, Fijnvandraat K, Cnossen MH, van der Bom JG, et al. von Willebrand factor propeptide and the phenotypic classification of von Willebrand disease. *Blood.* 2015;125(19):3006–13.
8. Tosetto A, Rodeghiero F, Castaman G, Goodeve A, Federici AB, Batlle J, et al. A quantitative analysis of bleeding symptoms in type 1 von Willebrand disease: results from a multicenter European study (MCMDM-1 VWD). *J Thromb Haemost.* 2006;4(4):766–73.
9. Bowman M, Mundell G, Grabell J, Hopman WM, Rapson D, Lillicrap D, et al. Generation and validation of the condensed MCMDM-1 VWD bleeding questionnaire for von Willebrand disease. *J Thromb Haemost.* 2008;6(12):2062–6.
10. Atiq F, Fijnvandraat K, van Galen KPM, Laros-VanGorkom BAP, Meijer K, de Meris J, et al. BMI is an important determinant of VWF and FVIII levels and bleeding phenotype in patients with von Willebrand disease. *Am J Hematol.* 2019;94(8):E201–E5.
11. Atiq F, Schutte LM, Looijen AEM, Boender J, Cnossen MH, Eikenboom J, et al. von Willebrand factor and factor VIII levels after desmopressin are associated with bleeding phenotype in type 1 VWD. *Blood Adv.* 2019;3(24):4147–54.
12. de Jong A, Eikenboom J. Von Willebrand disease mutation spectrum and associated mutation mechanisms. *Thromb Res.* 2017;159:65–75.
13. Nurden AT, Federici AB, Nurden P. Altered megakaryocytopoiesis in von Willebrand type 2B disease. *J Thromb Haemost.* 2009;7(Suppl1):277–81.
14. Nazy I, Elliott TD, Arnold DM. Platelet factor 4 inhibits ADAMTS13 activity and regulates the multimeric distribution of von Willebrand factor. *Br J Haematol.* 2020;190(4):594–8.
15. Boender J, Nederlof A, Meijer K, Mauser-Bunschoten EP, Cnossen MH, Fijnvandraat K, et al. ADAMTS-13 and bleeding phenotype in von Willebrand disease. *Res Pract Thromb Haemost.* 2020;4(8):1331–9.

# Appendix

## Supplementary Methods

### Diagnostic laboratory measurements

In the WiN study, plasma levels of VWF antigen (VWF:Ag), VWF activity (measured by VWF monoclonal antibody assay, VWF:Ab), VWF collagen binding capacity (VWF:CB) and FVIII:C were centrally measured in samples obtained at inclusion in the study, at the Erasmus University Medical Centre as described previously [1-3]. VWF propeptide (VWFpp) was centrally measured at the Leiden University Medical Centre (Leiden, the Netherlands) [3]. VWF multimers and ratios as well as ADAMTS13 activity were assessed as previously described [4, 5].

### PF4 plasma levels

To measure PF4 plasma levels, a PF4 ELISA kit (DY795, R&D Systems) was employed according to the manufacturer's protocol with some adaptations to minimize analytical variation. Between all steps, ELISA plates (Corning, cat#CLS3590) were washed 3x in PBS containing 0.05% Tween-20. Plates were first coated in 2 µg/ml capture antibody in PBS (mouse anti-human PF4) overnight and stored at 4°C until use. Plates were then blocked in PBS + 1% bovine serum albumin (BSA, Sigma, cat#A1470)(PBS/BSA) for 1 hour at RT, after which samples and standard curves were added in duplicate. For standards, we used the recombinant human PF4 provided by the manufacturer (0-4000 pg/ml) as well as a plasma standard based on Normal Pooled Plasma from healthy donors (Sanquin, dilutions ranging from 1:25-1:1600). Each plate had standard curves of both. Patient plasma samples were added in 3 dilutions per sample in PBS/BSA for 2 hours at RT, followed by incubation with 200 ng/ml primary antibody (biotinylated goat anti-human PF4) in PBS/BSA for 2 hours at RT, and finally 1:200 secondary antibody (streptavidin-HRP) in PBS/BSA for 20 min at RT. Ultimately, plates were developed with TMB substrate (Fisher Scientific, cat#10076433) for 5 minutes, stopping the reaction with 2 N H<sub>2</sub>SO<sub>4</sub>. Absorbance was measured on a spectrophotometer (Victor X4, Perkin Elmer) at 480 nm (signal) and 560 nm (background).

PF4 plasma levels in NPP were then determined using the recombinant PF4 standard, by using the aggregate of all plates (n=58) to correct for potential variability across plates. NPP curves were then used to calculate patient PF4 values of the multiple dilutions. Values that did not correspond to a linear section of these plasma curves were omitted.

### Statistics

Continuous data are presented as median and interquartile range [IQR], whereas categorical data are presented as number and proportion (%). Normality of data was assessed with four normality tests, which showed that PF4 was not normally distributed. Prior to analysis, outliers were defined as PF4 levels higher than  $\pm 2$  standard deviations from the mean (Supplemental Figure S1).

Comparison of PF4 levels between VWD types was analyzed using the Kruskal-Wallis test with a post-hoc analysis that was corrected for multiple comparisons using Dunn's test. Correlation between PF4 and VWF levels was assessed with Spearman's correlation analysis. Comparisons of mutations and thrombocytopenia in type 2A and type 2B patients were performed using Mann-Whitney U tests as an explorative analysis. The association between PF4 and total bleeding score was analyzed with linear regression analysis, while the association between PF4 and bleeding requiring treatment in the year prior to inclusion in the study was analyzed with binary logistic regression analysis. Regression analyses were adjusted for age, sex and BMI.

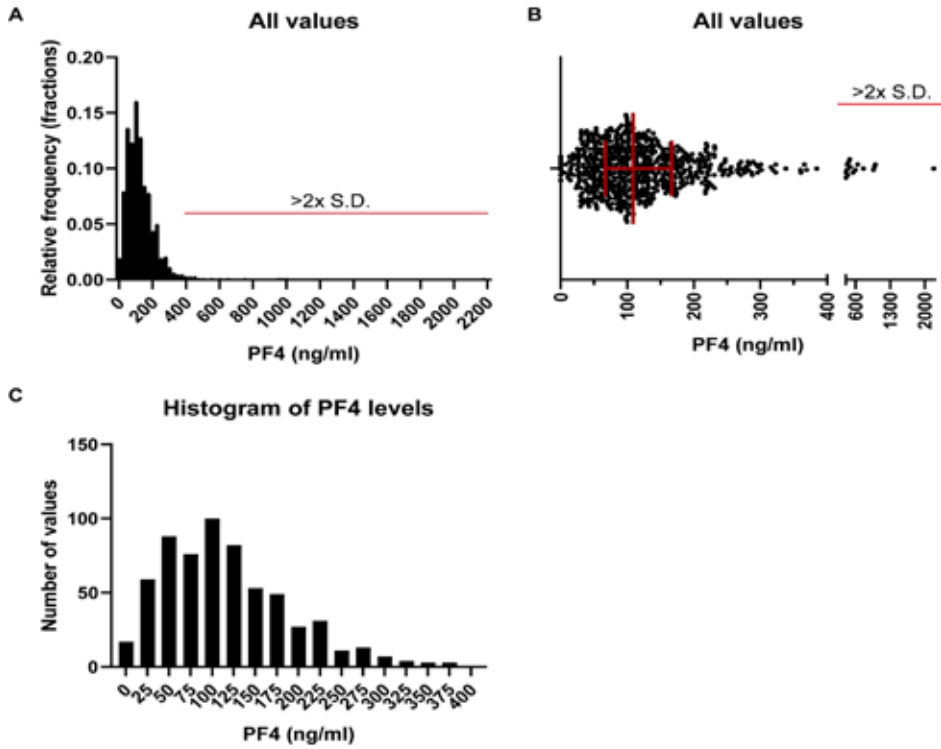
Outcomes of linear regression analyses are presented as unstandardized beta ( $\beta$ ) and 95% confidence interval (CI), whereas outcomes of logistic regression analysis are presented as odds ratio (OR) and 95%CI. In the linear regression analyses and logistic regression analysis with bleeding as dependent variable, PF4 was proportioned in quartiles. A p-value below 0.05 was considered as significant. All analyses were performed with SPSS version 25 (IBM Statistics).

## Supplementary Figures

	VWD (n=594)			
	Total (n=594)	Type 1 (n=368)	Type 2 (n=207)	Type 3 (n=19)
Age (years)	44 [31-58]	45 [32-57]	44 [31-59]	26 [12-54]
Female sex	373 (62.8%)	249 (67.7%)	114 (55.1%)	10 (52.6%)
Blood group O	361 (61.1%)	252 (69.0%)	101 (48.8%)	8 (42.1%)
VWF:Ag (IU/ml)	0.29 [0.17-0.45]	0.36 [0.21-0.53]	0.24 [0.16-0.35]	0.00 [0.00-0.01]
VWF:Ab (IU/ml)	0.22 [0.08-0.53]	0.43 [0.21-0.70]	0.08 [0.03-0.15]	0.00 [0.00-0.00]
VWF:CB (IU/ml)	0.22 [0.07-0.52]	0.41 [0.19-0.66]	0.07 [0.06-0.13]	0.00 [0.00-0.00]
FVIII:C (IU/ml)	0.51 [0.32-0.74]	0.65 [0.46-0.87]	0.36 [0.27-0.47]	0.01 [0.01-0.03]
VWFpp/VWF:Ag	2.79 [1.87-4.96]	2.17 [1.73-3.35]	4.51 [3.31-5.91]	
FVIII:C/VWF:Ag	1.73 [1.38-2.28]	1.81 [1.47-2.36]	1.56 [1.24-2.03]	
Bleeding score	11 [6-17]	9 [5-15]	13 [9-20]	20 [16-27]
Bleeding requiring treatment in the year prior to inclusion in the study	176 (31.1%)	77 (21.8%)	86 (44.1%)	13 (76.5%)
Data are presented as median with interquartile range in brackets or number and proportion (%).				

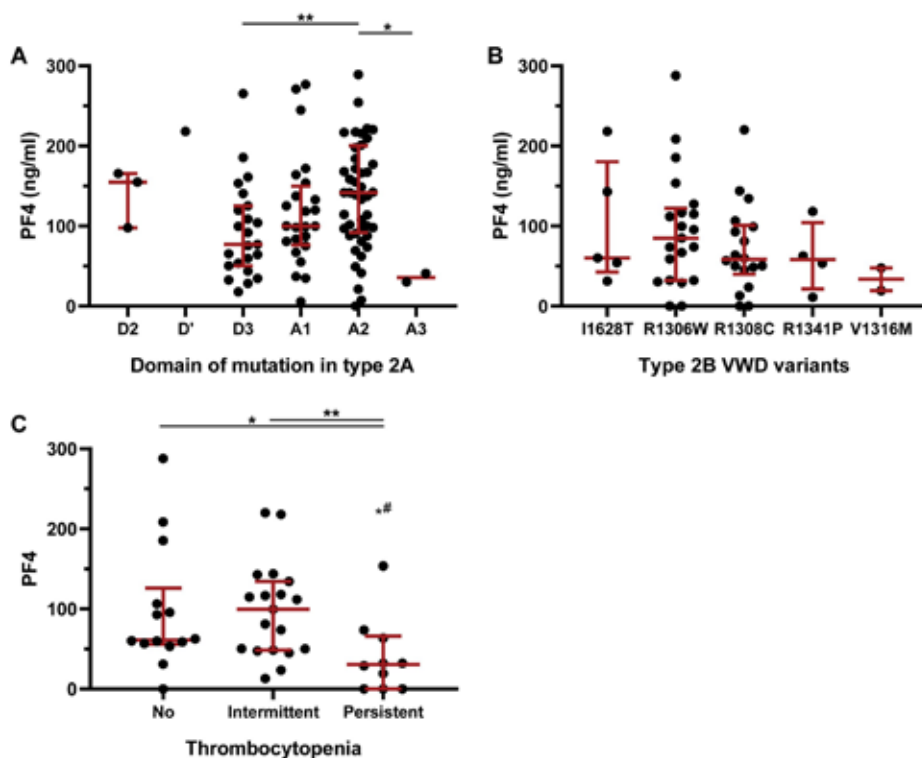
Supplementary Table 1. Patient characteristics.

Samples from the WiN studies were available from 615 adult VWD patients, where we measured PF4 in a total of 594. Five patients were excluded due to a treatment with VWF concentrate or DDAVP less than 72 hours prior to blood draw, or pregnancy. Sixteen patients were excluded as outliers (PF4 levels >2x SD, Supplemental Figure S1). The largest group was type 1 VWD (n=368), followed by type 2 VWD, which was subdivided in type 2A (n=125), type 2B (n=50), type 2M (n=20) and type 2N (n=12). Finally, a small group had type 3 VWD (n=19).



Supplemental Figure S1. Outlier handling and data distribution.

All PF4 data points were analyzed for outliers prior to further analysis, represented as frequency distribution (A) and singular data points (B). Values that were larger than 2x S.D. were excluded (red line), which were 16 data points in total. Data distribution of included PF4 values is also shown (C).



Supplemental Figure S2. PF4 levels in type 2A and 2B patients.

PF4 levels in VWD patients with different mutations in type 2A- (A) and type 2B patients (B). PF4 levels in type 2B patients with no-, intermittent or persistent thrombocytopenia (C). Data shown as median  $\pm$  interquartile range. \* =  $p < 0.05$ , \*\* =  $p < 0.01$ .

## References

1. de Wee EM, Sanders YV, Mauser-Bunschoten EP, van der Bom JG, Degenaar-Dujardin ME, Eikenboom J, et al. Determinants of bleeding phenotype in adult patients with moderate or severe von Willebrand disease. *Thromb Haemost.* 2012;108(4):683-92.
2. Sanders YV, Eikenboom J, de Wee EM, van der Bom JG, Cnossen MH, Degenaar-Dujardin ME, et al. Reduced prevalence of arterial thrombosis in von Willebrand disease. *J Thromb Haemost.* 2013;11(5):845-54.
3. Sanders YV, Groeneveld D, Meijer K, Fijnvandraat K, Cnossen MH, van der Bom JG, et al. von Willebrand factor propeptide and the phenotypic classification of von Willebrand disease. *Blood.* 2015;125(19):3006-13.
4. Boender J, Nederlof A, Meijer K, Mauser-Bunschoten EP, Cnossen MH, Fijnvandraat K, et al. ADAMTS-13 and bleeding phenotype in von Willebrand disease. *Res Pract Thromb Haemost.* 2020;4(8):1331-9.
5. Boender J, Atiq F, Cnossen MH, van der Bom JG, Fijnvandraat K, de Meris J, et al. Von Willebrand Factor Multimer Densitometric Analysis: Validation of the Clinical Accuracy and Clinical Implications in Von Willebrand Disease. *Hemasphere.* 2021;5(3):e542.

# Chapter 5

## Quantitative 3D Microscopy Highlights Altered VWF $\alpha$ -granule Storage in Patients with VWD with Distinct Pathogenic Mechanisms

Maurice Swinkels, Ferdows Atiq, Petra E. Bürgisser, Johan A. Slotman, Adriaan B. Houtsmuller, Cilia de Heus, Judith Klumperman, Frank W. G. Leebeek, Jan Voorberg, Arend Jan Gerard Jansen, Ruben Bierings

Research and Practice in Thrombrosis and Haemostasis. 2021 Sep  
14;5(6):e12595

## Abstract

*Background:* Platelets play a key role in hemostasis through plug formation and secretion of their granule contents at sites of endothelial injury. Defects in von Willebrand factor (VWF), a platelet  $\alpha$ -granule protein, are implicated in von Willebrand disease (VWD), and may lead to defective platelet adhesion and/or aggregation. Studying VWF quantity and subcellular localization may help us better understand the pathophysiology of VWD. *Objective:* Quantitative analysis of the platelet  $\alpha$ -granule compartment and VWF storage in healthy individuals and VWD patients.

*Patients/Methods:* Structured illumination microscopy (SIM) was used to study VWF content and organization in platelets of healthy individuals and patients with VWD in combination with established techniques.

*Results:* SIM capably quantified clear morphological and granular changes in platelets stimulated with proteinase-activated receptor 1 (PAR-1) activating peptide and revealed a large intra- and interdonor variability in VWF-positive object numbers within healthy resting platelets, similar to variation in secreted protein acidic and rich in cysteine (SPARC). We subsequently characterized VWD platelets to identify changes in the  $\alpha$ -granule compartment of patients with different VWF defects, and were able to stratify two patients with type 3 VWD arising from different pathological mechanisms. We further analyzed VWF storage in  $\alpha$ -granules of a patient with homozygous p.C1190R using electron microscopy and found discrepant VWF levels and different degrees of multimerization in platelets of patients with heterozygous p.C1190 in comparison to VWF in plasma.

*Conclusions:* Our findings highlight the utility of quantitative imaging approaches in assessing platelet granule content, which may help to better understand VWF storage in  $\alpha$ -granules and to gain new insights in the etiology of VWD.

**Keywords:** blood platelets, optical imaging, type 3, von Willebrand disease, von Willebrand factor

### Essentials

- Characterizing platelet granule content is essential to better understand platelet disorders.
- Structured illumination microscopy (SIM) allows quantitative study of platelet cargo like von Willebrand factor (VWF).
- SIM identifies different VWF alterations in platelets of patients with type 3 von Willebrand disease.
- Electron microscopy and multimer analysis implicates defective VWF storage in patients with p.C1190.

## Introduction

Platelets are circulating, anucleate cells that play a key role in the hemostatic system. Platelets bud off from megakaryocytes into the circulation and contain several different types of granules [1]. The most abundant organelle in platelets is the  $\alpha$ -granule, which contains many important hemostatic and inflammatory proteins such as von Willebrand factor (VWF), fibrinogen, and platelet factor 4 [1]. Other proteins such as secreted protein acidic and rich in cysteine (SPARC; or osteonectin) have less well-defined roles in hemostasis but are nevertheless abundant in platelet  $\alpha$ -granules [2-5].

Upon tissue injury, platelets adhere to damaged endothelium through extracellular matrix collagen and VWF via various glycoprotein receptors on the platelet membrane, followed by secretion of their granular contents into the thrombus environment [6]. This further enhances the hemostatic response through release of adhesion proteins (like VWF and fibrinogen) and potent signaling molecules, that is, thrombin, ADP, and thromboxane A<sub>2</sub> [1,7]. Regulation of platelet granule biogenesis and release is essential for normal hemostasis, as defects in these pathways can lead to bleeding problems [6,8]. Mechanisms that control these biological processes have been gradually elucidated, yet routine techniques often fail to identify the underlying defects in patients.

With the advent of super-resolution light microscopy techniques, we are able to image platelets with sufficient resolution to discern individual granule cargo while obtaining high-throughput quantitative light microscopy data [9]. Structured illumination microscopy (SIM) is a relatively quick and easy-to-use super-resolution method, which makes it suitable to image platelets of a large number of healthy individuals and patients. A previous study has successfully used SIM-based quantification of dense-granule content to identify Hermansky-Pudlak syndrome patients [10]. However, quantitative studies of platelet  $\alpha$ -granule content and subcellular localization are lacking and will be essential to better understand bleeding disorders where platelet  $\alpha$ -granules or their content are affected [10,11].

Von Willebrand disease (VWD) is the most common inherited bleeding disorder, hallmarked by defects of VWF that may consequently lead to defective platelet adhesion and/or aggregation [12,13]. VWD is classified in subtypes based on either a quantitative (type 1 or 3) or qualitative (type 2) defect of VWF, determined through diagnostic assays that measure circulating levels and function [14]. However, mutations can also cause intracellular defects that lead to inadequate synthesis, secretion, or multimerization [12]. Patients with the same type of VWD and similar circulating VWF levels can have a very different bleeding phenotype [13], suggesting VWF in cellular compartments like platelet  $\alpha$ -granules may play a role in the pathogenesis of VWD.

Patient	Family	Age	Sex	Blood group	VWD type	Platelet count <sup>b</sup>	BS	Mutation	DNA
1	-	33	M	O	3	302	34	Δexon 4-5 +p.L2306R fs*4 compound het	Del exon4-5 +c.6917delT, exon 40
2	2 + 3 + 4	14	F	B	3	328	20	p.C1190R hom	c.3568T>C, exon 27
3	2 + 3 + 4	18	M	A	2A	294	4	p.C1190R het	c.3568T>C, exon 27
4	2 + 3 + 4	43	F	O	2A	261	3	p.C1190R het	c.3568T>C, exon 27
5	-	57	F	O	2A	316	10	p.C1190Y het	c.3569G>A, exon 27

Patient	VWF:Ag <sup>a</sup> [0.60 -1.40]	VWF:Ab <sup>a</sup> [0.60 -1.40]	VWF:CB <sup>a</sup> [0.60 -1.40]	FVIII:C <sup>a</sup> [0.60 -1.40]	VWFpp [150 -400]
1	0.00	0.00	0.00	0.00	0.00
2	0.05	0.04	-	0.04	0.00
3	0.29	0.12	-	0.52	0.39
4	0.24	0.05	0.10	0.42	0.45
5	0.84	0.25	0.23	0.57	0.89

Table 1. Characterization of patients with VWD

Note: Clinical and laboratory data is shown for all five patients with VWD included in this study.

Reference values are shown in brackets.

Abbreviations: BS, bleeding score as determined by the ISTH Bleeding Assessment Tool [53]; FVIII:C, factor VIII activity (IU/mL); het, heterozygous, hom, homozygous; VWF:Ab, von Willebrand factor activity (IU/mL); VWF:Ag, von Willebrand factor antigen (IU/mL); VWF:CB, von Willebrand factor collagen binding (IU/mL); VWFpp, von Willebrand factor propeptide levels (IU/mL).

<sup>a</sup>Historically lowest levels. <sup>b</sup>Average over last four most-recent measurements (\*10<sup>9</sup>/L).

To study VWF in  $\alpha$ -granules, we have developed an analysis tool based on SIM imaging of platelets of healthy individuals and people with VWD. Large data sets of immunofluorescence-based data were processed simultaneously through an analysis workflow that facilitates quantitative study of platelet  $\alpha$ -granule content. We quantified morphological shape change and  $\alpha$ -granule content release in proteinase-activated receptor 1 (PAR-1) stimulated platelets and assessed the variability in  $\alpha$ -granule constituents across healthy individuals. We then focused on patients with VWD with severe quantitative defects (type 3) and qualitative multimerization defects (type 2A) in VWF and assessed changes in their platelet compartment. We generated quantitative

platelet  $\alpha$ -granule cargo data in conjunction with electron microscopy (EM) and VWF multimer analysis, showing the viability of a SIM-based approach in the characterization of the platelet  $\alpha$ -granule compartment and VWF storage in  $\alpha$ -granules in VWD.

## Methods

A full description of flow cytometry, VWF multimer analysis, and EM are available in the Supporting Information (Methods).

### Patients and healthy donors

Peripheral blood was obtained from consenting healthy donors and patients with VWD. Patients were included at the Department of Hematology in the Erasmus University Medical Center, Rotterdam, via the Prospective Von Willebrand Disease in the Netherlands Study (WiN-Pro). This is an ongoing nationwide prospective-observational cohort study (NCT03521583), performed according to the Declaration of Helsinki, and approved by the institutional ethics board. Clinical data shown here was collected as part of the WiN-Pro study protocol or obtained retrospectively from patient files (Table 1).

### Platelet preparation

Whole blood was spun for 20 minutes at 120 g without brake to generate platelet-rich plasma (PRP). Any subsequent centrifugation steps to wash platelet suspensions were performed at 2000 g for 8 minutes as detailed below. PRP was immediately fixed in 1% formaldehyde for 5 minutes, then washed three times in washing buffer (36 mM citric acid, 103 mM NaCl, 5 mM KCl, 5 mM EDTA, 5.6 mM glucose, pH 6.5). For activation experiments, PRP was first incubated with either phosphate buffered saline (PBS) or 10  $\mu$ M PAR-1 AP (Peptides International, Louisville, KY, USA; cat# PAR-3676-PI) for 30 minutes at 37°C, without stirring or agitation.

### Immunofluorescent staining

All incubations were done at room temperature unless otherwise stated. 9 mm<sup>2</sup> 1.5H high-precision coverslips (Paul Marienfeld, Lauda-Königshofen, Germany; cat#OTMS20B) were coated with poly-l-lysine (Sigma-Aldrich, St. Louis, MO, USA; cat#P0899; 100  $\mu$ g/mL in PBS) and seeded with 3 million platelets per sample. Platelets were permeabilized in Perm/Quench (50 mM NH<sub>4</sub>Cl, 0.1% saponin), washed three times in PGAS (PBS with 0.2% gelatin, 0.02% azide, and 0.02% saponin), and finally stored in PGAS at 4°C until immunostaining [15]. Samples were stained and imaged within 1 week. Coverslips containing platelets were probed with antibodies (Table S1) and washed three times with PGAS in between steps. Initial staining setups were controlled using primary or secondary antibodies only and did not yield any immunopositivity. Finally, slides were dipped in PBS, mounted in mowiol (Sigma-Aldrich; cat# 214590), and sealed with nail polish before imaging.

## Structured illumination and confocal microscopy

SIM images were acquired on an Elyra PS1 (Zeiss, Jena, Germany) microscope through a 63× plan-apochromat DIC 1.4 NA lens, using five phases and five rotations of the illumination pattern. Diode lasers (100 mW) with a wavelength of 488, 561, and 633 nm were used with an appropriate emission filter (BP 420–480 +LP750, BP 495–575 +LP 750, LP 655, respectively) in the light path. Laser power and gain were optimized per sample to ensure reconstruction quality. At least three representative fields of view with full Z-stacks were collected per donor, using an interval of 110 nm between slices ( $\approx 50$  slices per Z-stack, or 5.5  $\mu\text{m}$ ). After image acquisition, samples were reconstructed with state-of-the-art SIM reconstruction using Zen Software (Zeiss). From the same sections, confocal images were taken at standardized laser settings. Multiple Z-stacks were taken per sample on a SP5 confocal microscope (Leica, Wetzlar, Germany).

## Image analysis

For analysis of reconstructed SIM data, we applied a semi-automated analysis method using Fiji software [16] in combination with published plugins as well as in-house written macro code (Figure S1). Quality of reconstruction was assessed with the SIM-check plugin [17] while lateral resolution was calculated to be  $\approx 120$  nm using Fourier ring correlation [18] (Figure S2).

In the analysis, single platelets were first segmented on the basis of  $\alpha$ -tubulin staining in a two-dimensional average intensity projection and thresholded on the basis of the Li algorithm [19], excluding platelets that were not completely in the field of view. Baseline correction was performed by subtracting a fixed value (determined by reconstruction software) from the whole image. Background correction for granular staining was then performed for all images individually by normalizing the whole image to the highest background level in the stack (determined by finding an area of background in the slice with the lowest average signal, usually in the middle of a stack).

Next, we segmented unique immunopositive structures, termed objects, per granular channel in full three-dimensional (3D) voxel space using a 3D maxima finder and 3D watershed [20] and applied Moments thresholding [21]. Noise parameters were determined by selecting the best fit (highest derivative point of a plot of threshold parameter vs number of objects) to filter out any quantification of residual noise. Three-dimensional morphometrics were calculated from the segmented immunopositive objects with relative volume sizes represented in voxels [20].

We also quantified unique immunopositive objects in 2D space on an average-intensity projection of each granular channel to assess spatial distribution. Similarly, we used a 2D maxima finder and determined noise parameters through best fit (highest derivative point of a plot of threshold parameter vs number of objects). For each unique 2D object we then calculated minimal distances to the nearest object using the in-house Nearest Neighbour plugin, or minimal distances to the  $\alpha$ -tubulin mask (Nearest Edge)

(code available at <https://github.com/ErasmusOIC/NearestNeighbour>). Finally, we assessed colocalization of separate granular stains using an object-based method by calculating minimal distances of unique objects in channel 1 (eg, VWF) to the nearest object in channel 2 (eg, SPARC) [22-25].

Analysis and quantification of unique objects in confocal images was largely similar but adapted to a 2D approach using maximum intensity projections for all channels. In brief, segmentation of single platelets using  $\alpha$ -tubulin was performed using the Otsu thresholding algorithm [26]. Spatial distributions were calculated as described for reconstructed SIM images. Confocal mean fluorescence intensity (MFI) measurements were performed on an average of three sequential slices.

A detailed description of all parameters measured per platelet and per sample is presented in Table S2.

### Statistical analysis

Continuous variables are presented as mean  $\pm$  standard deviation, whereas categorical variables are presented as number and proportion. To compare two or more groups, we used nested t test or analysis of variance using a mixed-effects model (Prism version 8; GraphPad Software, La Jolla, CA, USA). Correlation was performed using Spearman's ranked correlation. Poisson regression was used in regression analysis. A P value  $<.05$  was considered significant.

## Results

### Quantitative imaging of alpha-granule content by super-resolution microscopy

To quantitatively study platelets and their  $\alpha$ -granule cargo, we used SIM imaging and compared it to standard confocal imaging (Figure 1A). For the analysis, we developed a semi-automated workflow in Fiji software to annotate and quantify unique intracellular structures (termed objects) in full 3D voxel space from reconstructed SIM images (Table S2). In this 3D-SIM workflow, of which one field of view is shown (Figure 1B), platelets were stained for  $\alpha$ -tubulin to depict their unique marginal band (Figure 1C), while VWF and SPARC were immunolabeled to study the  $\alpha$ -granule compartment (Figure 1D,E). We found that SPARC stained more diffusely, while VWF staining was concentrated into discrete volumes (Figure 1D). Additionally, we detected VWF-positive volumes predominantly in close proximity to SPARC-positive staining or in an outline of SPARC-positive objects through the Z-axis (Figure 1E). This was also evident from a 3D perspective (Video S1). Unique objects were quantified per granular staining and per platelet (Figure 1C,D), and we found that the number of VWF- and SPARC-positive structures per platelet was slightly different but correlated closely (Figure 1D,F). Our quantification of unique objects is two- to fourfold lower than  $\alpha$ -granule numbers estimated from historical EM stereology approaches [27-30]. The total cargo volume, which is independent of optimal segmentation

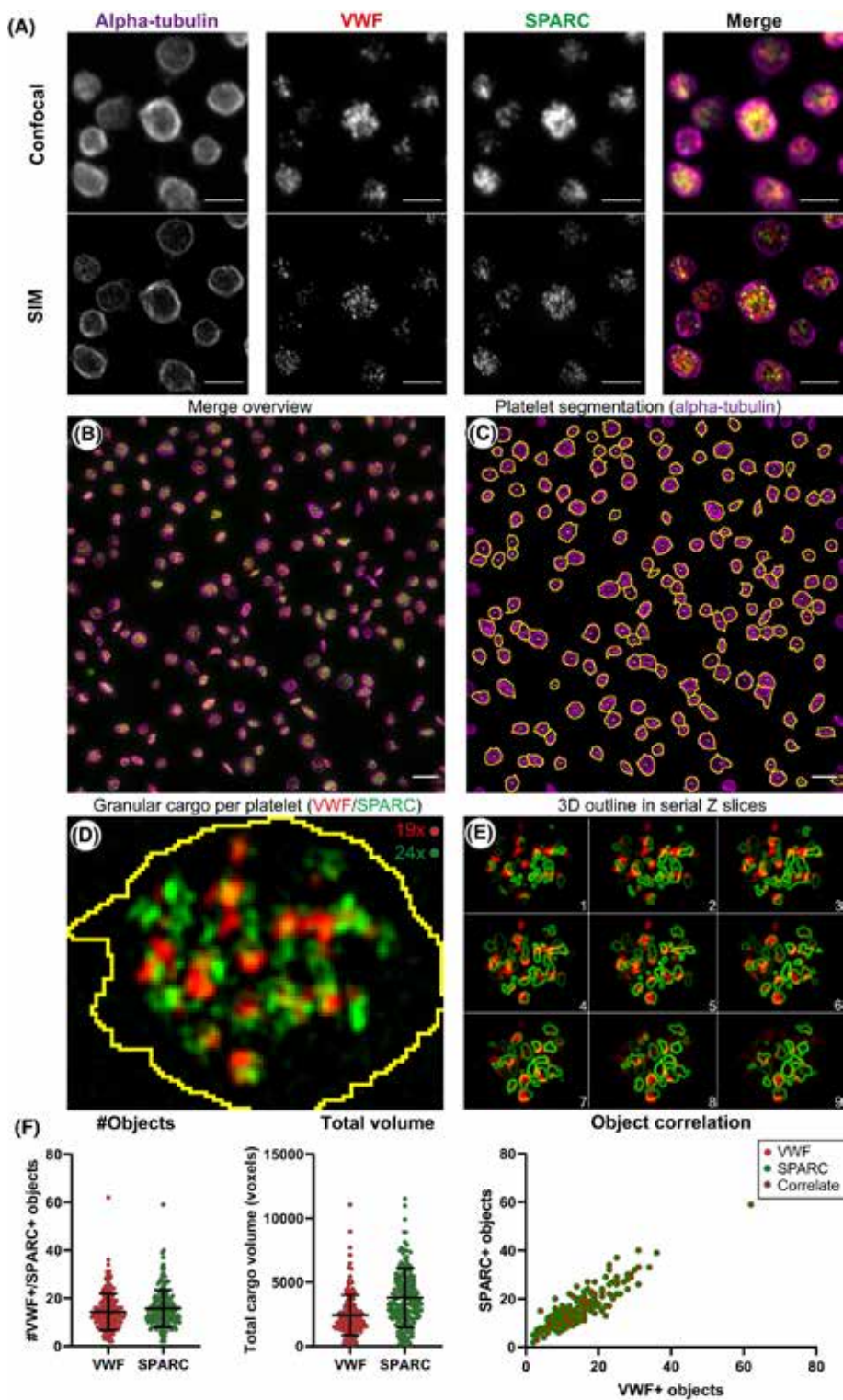


*Figure 1. Differences between confocal and structured illumination microscopy (SIM) imaging, and analysis workflow of platelet and granule morphometrics.*

Resolution differences between confocal and SIM are illustrated in resting platelets. (A). Shown are the four main steps (B-D) for ImageJ-based processing of super-resolution data. One field of view is shown (B). First, platelets are segmented through automated thresholding on alpha-tubulin staining, shown in magenta, segmentation line in yellow (C). Each individual platelet (n=205) is then assessed for granular staining using von Willebrand factor (VWF) (D; shown in red) and secreted protein acidic and rich in cysteine (SPARC) (D; shown in green). Overlap between VWF (object) and SPARC (outline) is shown in serial slices in (E). VWF-or SPARC-positive volumes of fluorescence are then separated in 3D through 3D-based plugins, counted and processed for morphometry (F). Scale bar is 3 $\mu$ m in panel (A), 5 $\mu$ m in panel (B-C); both show an average intensity projection. One slice is shown for panel (D). Brightness and contrast were adjusted to enhance visibility of the design. Quantification of unique VWF-positive (red) and SPARC-positive (green) objects their total volume, and correlation per platelet is illustrated in (F) for one image. Data are represented as mean  $\pm$  standard deviation.

of unique structures, showed a slightly larger discrepancy between VWF and SPARC (Figure 1F). These staining and volume differences are likely due to the reported eccentric localization of VWF within the  $\alpha$ -granule, as opposed to most other  $\alpha$ -granule proteins like SPARC [29-31]. As SPARC occupies a larger area inside  $\alpha$ -granules, this explains the larger volume measurements in comparison with VWF. Some studies have previously argued that VWF and other proteins may be stored in subpopulations of  $\alpha$ -granules [32,33], potentially representing subpopulations with distinct functions. However, recent EM work of whole platelets has shown that VWF is present in every  $\alpha$ -granule, but due to its eccentric localization this becomes only apparent in 3D-EM reconstructions [29](Figure 1E). Morphological SIM analysis of VWF and SPARC staining with fibrinogen or P-selectin yields a similar pattern (Figure S3).

In a quantitative confocal microscopy-based analysis of the same data set, we detected less VWF-positive objects (SIM, 14.4; confocal, 8.1) and less SPARC-positive objects (SIM, 15.8; confocal, 8.4) (Figure S4A). In similar fashion, we observed an overestimation of the total volume by 2.5x in confocal images (Figure S4B), indicating that SIM is more capable to segregate individual objects as well as to better estimate the volume of granule constituents.

### **Platelet stimulation by PAR-1 activating peptide triggers VWF+ granule release, marginal band compression, and $\alpha$ -granule content reorganization**

Next, we tested whether our analysis was able to identify clear changes in platelet morphology and  $\alpha$ -granule content after platelet activation in vitro. Activation of platelets with PAR-1 activating peptide (PAR-1- AP), a strong agonist of the PAR-1 receptor, led to a reduction of VWF-positive objects (rest 14.04 vs PAR-1-AP 7.43,  $P=.03$ ) that signified  $\alpha$ -granule release (Figure 2A,B). Degranulation was confirmed through assessment of P-selectin exposure by flow cytometry, which also showed no signs of platelet aggregation (Figure S5). Confocal 2D analysis found only a trend toward lower levels (Figure S6A,B), which is most likely due to the lower dynamic range in which we can detect granular structures in confocal microscopy. Additionally, we were able to quantify compression of the marginal band area in activated platelets (rest 7.21 $\mu$ m<sup>2</sup> vs PAR-1-AP 5.69 $\mu$ m<sup>2</sup>,  $P=.03$ )

(Figure 2C), which is thought to play a role in  $\alpha$ -granule exocytosis [34]. Finally, we detected a decrease in total VWF-positive volume in stimulated platelets, albeit not significant due to a high variation across experiments (Figure 2D).

Poisson regression analysis showed that the relation between object numbers and marginal band area was significantly different between both conditions (Figure S6C). We were also able to detect changes in the spatial distribution of unique objects in relation to each other or to the marginal band in PAR-1-stimulated platelets (Figure S6D). Combined, these findings are in accordance with an  $\alpha$ -granule release phenotype and may even suggest some degree of granule reorganization in response to PAR-1-AP triggering. Potentially, granule reorganization signifies some degree of compound exocytosis as described previously [35], but this cannot be concluded from our data alone.

### Intra- and interindividual variability in $\alpha$ -granule cargo of healthy donor platelets

We subsequently applied SIM analysis on the alpha-granule compartment in platelets of healthy donors, generating data on >5000 platelets and 100 000 granular objects (per

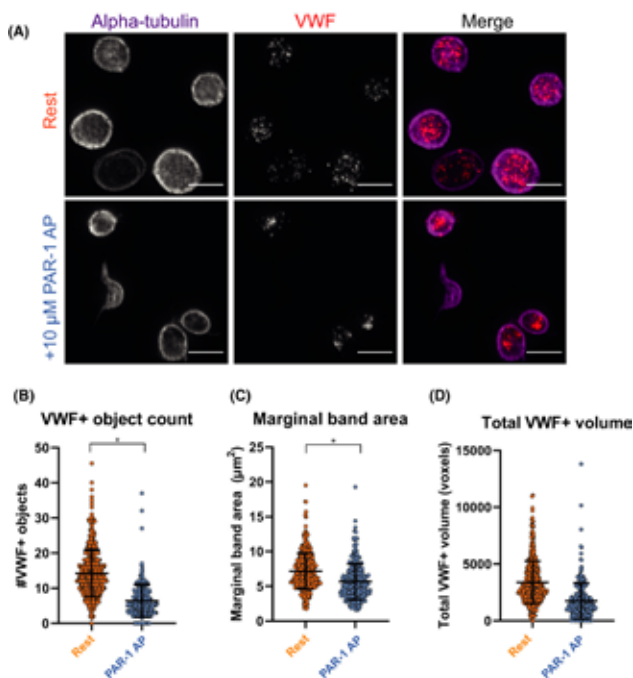


Figure 2. Quantification of granular and morphological changes in activated platelets using structured illumination microscopy.

Platelets were incubated with 10 $\mu$ M proteinase-activated receptor 1 activating peptide (PAR-1-AP; blue) or phosphate buffered saline (PBS; orange, “rest”) for 10 min at 37°C, imaged and processed through our analysis workflow. One representative image of several platelets is shown per condition (A). VWF-positive object numbers (B) and marginal band area were quantified and compared between resting (n=663) and stimulated platelets (n=429) (C). Total VWF-positive volume was assessed in (D). Data is represented as mean  $\pm$  standard deviation. Scale bar is 3 $\mu$ m in panel (A); brightness and contrast were equally amplified for both panels to enhance visibility. \*P < .05.

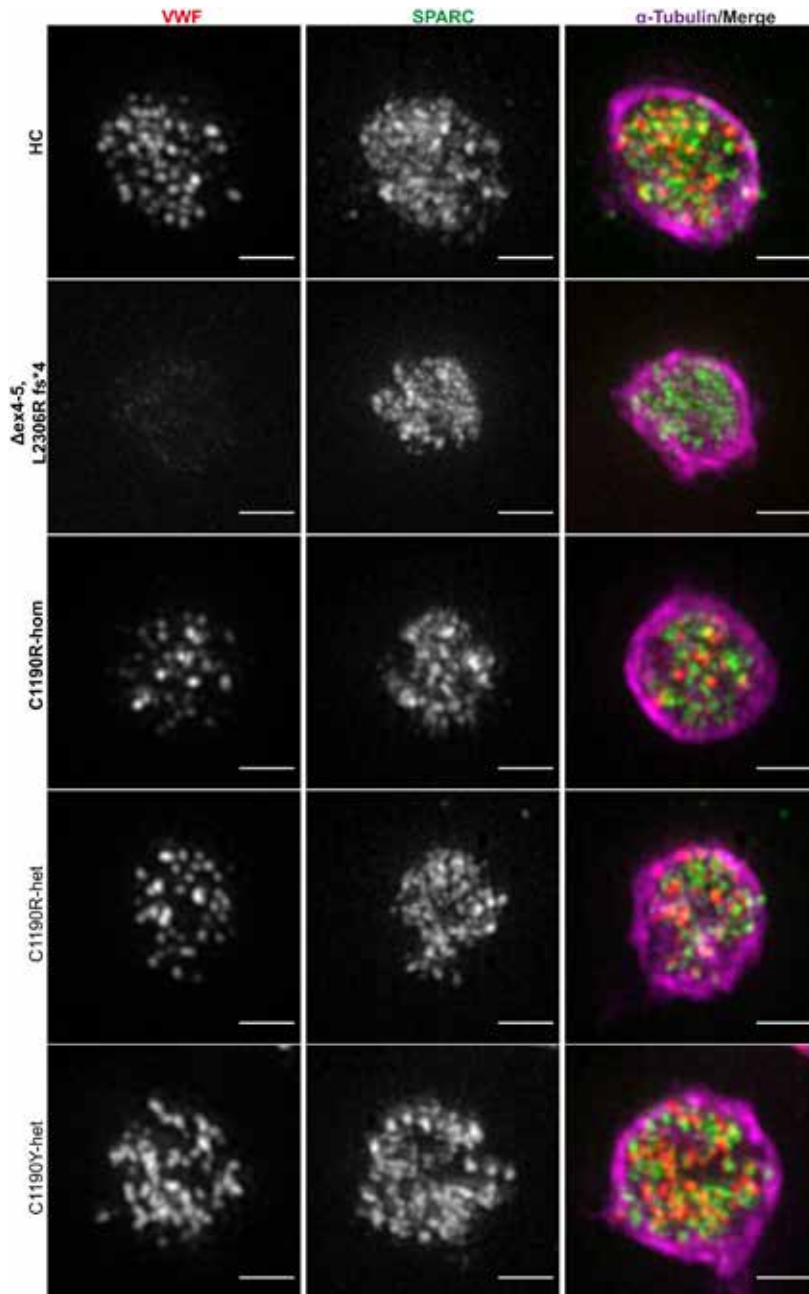


Figure 3. Detailed super-resolution images of representative platelets from patients with von Willebrand disease (VWD).

Platelets from healthy controls (HC), patients with type 3 VWD ( $\Delta$ ex4-5, L2306R fs\*4; C1190R-hom; in bold) and type 2A VWD (C1190R-het, C1190Y-het) were stained for VWF (red), SPARC (green), and  $\alpha$ -tubulin (magenta) and were imaged through structured illumination microscopy. Scale bar is 1 $\mu$ m.

staining) over five individuals (Figure 3; Figure S7, healthy control [HC]). We observed a large variation in the number of VWF- and SPARC-positive objects in healthy, resting platelets (VWF,  $18.0 \pm 8.9$ ; SPARC,  $21.6 \pm 12.1$ ) (Figure 4A). VWF- and SPARC-positive total volume similarly varied across individuals (Figure 4B). Furthermore, object numbers and volumes were correlated to marginal band area in all donors (Figure S8A-D), in line with earlier studies that showed that the number of  $\alpha$ -granules is related to platelet size [29]. Together, our data provide quantitative evidence for a highly heterogeneous storage capacity of individual healthy platelets, which is proportional to platelet size.

### Quantitative differences in platelet VWF storage in type 3 and 2A VWD platelets

To address whether quantitative or qualitative defects in VWF lead to abnormalities in platelet  $\alpha$ -granule cargo we applied our analysis to patients with VWD (Table 1, Figures 3 and 4), analyzing more than 500 platelets and 10 000 granular objects per individual patient (in all but one with  $>250$  platelets). We first studied a compound heterozygous patient with type 3 VWD with complete absence of plasma VWF due to a deletion of exons 4 and 5 and a frameshift mutation (c.6917delT p.L2306Rfs\*4) in the other allele, both leading to early termination signals. In endothelial cells, ablation of VWF expression leads to absence of their VWF-containing secretory organelles, the Weibel-Palade bodies [36-38]. As expected, we did not detect any VWF-positive objects (Figure 4A;  $\Delta$ ex4-5, L2306R fs\*4), which is also evident from the overview images (Figure 3,  $\Delta$ ex4-5, L2306R fs\*4). However, SPARC-positive objects were still present ( $\Delta$ ex4-5, L2306R fs\*4 14.5), and the total SPARC-positive volume was similar to healthy individuals (HC 8285 voxels vs  $\Delta$ ex4-5, L2306R fs\*4 8524 voxels) (Figure 4A,B), indicating that despite the absence of VWF, other  $\alpha$ -granule proteins are organized normally in this patient.

We also analyzed another patient with type 3 VWD with a homozygous missense mutation at p.C1190 in the D3 domain (c.3568T>C; p.C1190R), which is thought to affect VWF multimerization (Figure 3) [39,40]. Interestingly, in this patient we found a relatively normal number of VWF- and SPARC-positive objects (HC 18.0 vs C1190R-hom 14.7) (Figure 4A). This was not apparent from confocal MFI measurements, in which patients with type 3 were very close to baseline intensities ( $\Delta$ ex4-5, L2306R fs\*4 5.66 vs C1190R-hom 6.27) (Figure 4C, Figure S9). Quantification of unique VWF-positive objects through confocal microscopy seemed to correlate directly to staining intensity rather than accurately reflecting the number of objects/granular structures (Figure 4D). This suggests that p.C1190R homozygous platelets probably contain some residual VWF, and it highlights that our workflow is capable of discriminating these patients with type 3 VWD stemming from distinct molecular defects.

Additionally, we investigated three patients with type 2A VWD with a heterozygous mutation at the same position p.C1190 into R or Y (Table 1), two of whom are part of the same family as the homozygous p.C1190R patient. We found that two patients with the heterozygous p.C1190R mutation had relatively normal VWF- and SPARC-positive object numbers and total volumes compared to healthy individuals (Figures 3 and 4A,B).

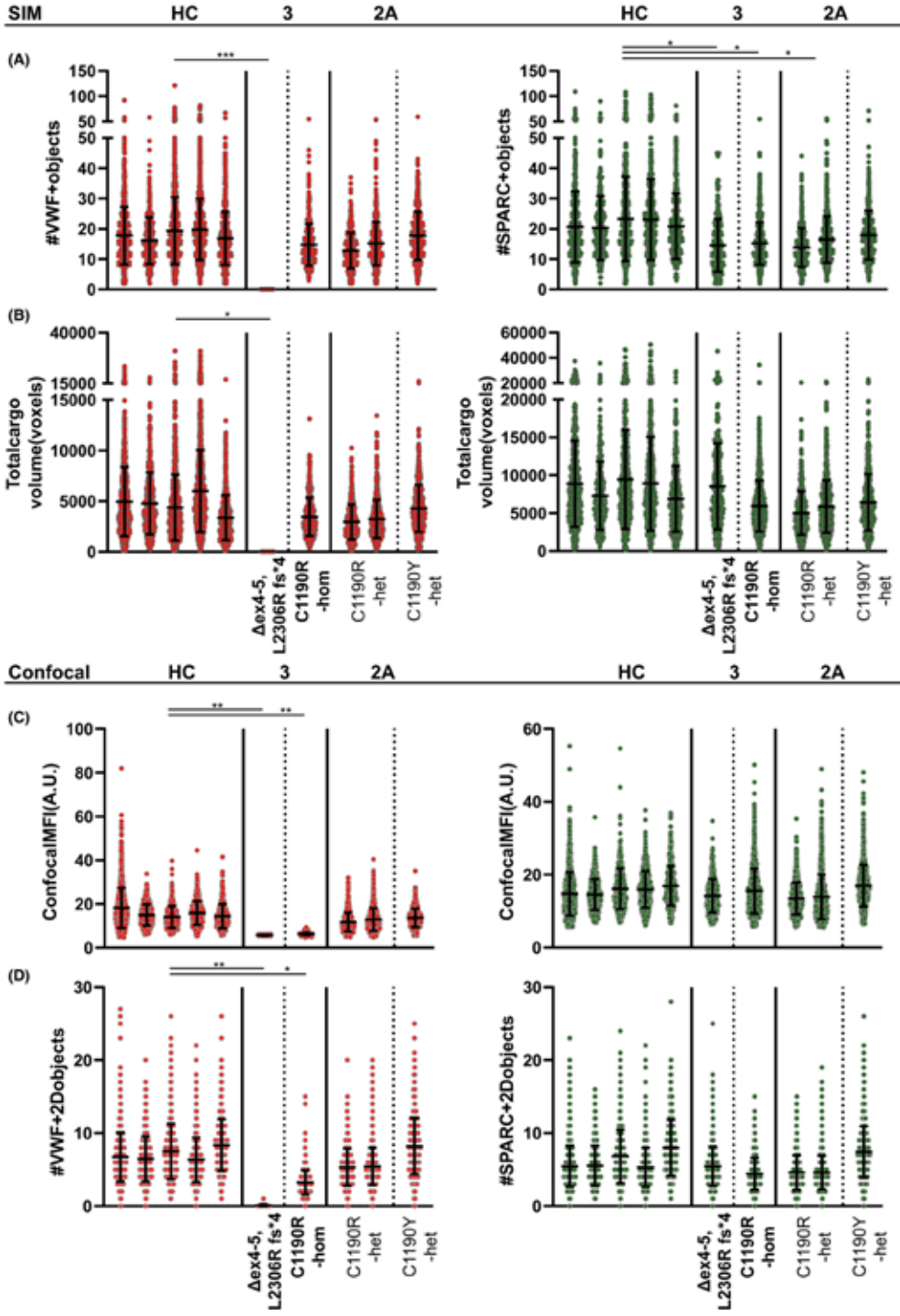


*Figure 4. Quantification of  $\alpha$ -granule content of von Willebrand disease (VWD) platelets using super-resolution and confocal microscopy.*

Von Willebrand factor (red) and secreted protein acidic and rich in cysteine (SPARC; green)  $\alpha$ -granule cargo was quantified for all patients through 3D structured illumination microscopy (A-B) and 2D confocal (C-D) workflows and compared to healthy control platelets (n=5310 platelets over five donors). Patients with type 3 VWD are marked in bold text ( $\Delta$ ex4-5, L2306R fs\*4; n=290; homozygous C1190R-hom, n=578 platelets), while patients with type 2A are nonbold (C1190R-het (n=535/921) and C1190Y-het (n=749)). Object numbers (A/D) were assessed through both techniques while total volume (B) and mean fluorescence intensity (C) were exclusively measured through SIM and confocal microscopy, respectively. Data are represented as mean  $\pm$  standard deviation. \*P < .05, \*\*P < .01, \*\*\*P < .001.

Although the number of SPARC-positive objects was significantly lower in the patients (HC 21.6; C1190R-het 15.1, P=.03), the biological implications of such minor differences are unclear. Interestingly, object numbers were closer to those of healthy individuals (and not significantly different) in the patient with a heterozygous p.C1190Y mutation (VWF, 17.7; SPARC, 17.91). Parallel confocal analysis to obtain information on average protein levels (Figure 4C,D) showed that the decrease in MFI (HC 15.52; C1190R-hom 6.27; C1190R-het 12.30; C1190Y-het 13.71) and VWF-positive object numbers (HC 7.56; C1190R-hom 2.75; C1190R-het 5.32; C1190Y-het 8.2) followed the same pattern as the plasma VWF levels in these patients (Table 1). In contrast to VWF, SPARC levels were not significantly different across any of the patients, which is in line with the minimal differences observed by SIM (Figure 4C,D). We found no evidence of altered VWF-SPARC colocalization across controls and patients (Figure S10).

### **Normal $\alpha$ -granules but reduced VWF content in p.C1190R homozygous platelets**

To assess whether the residual VWF observed in p.C1190R homozygous platelets is in fact localized in  $\alpha$ -granules, we studied platelet VWF and  $\alpha$ -granules by immuno-EM (Figure 5A). VWD platelets and  $\alpha$ -granules looked morphologically normal as assessed through thin sections. In line with our SIM analysis, we found similar numbers of morphologically identifiable  $\alpha$ -granules between HC and VWD platelets (HC 10.6 vs C1190R-hom 9.3) (Figure 5B). In healthy platelets, VWF immuno-gold labeling was mostly confined to  $\alpha$ -granules, and, as reported earlier [31], on one side of the  $\alpha$ -granule (Figure 5A \*). VWF in homozygous p.C1190R platelets was also found in  $\alpha$ -granules but in much lower quantities (Figure 5A). Some labeling was also observed in areas outside  $\alpha$ -granules, but whether this is mislocalization of VWF or low-level aspecific background labeling (from the antibody or secondary protein A gold-labeled reagent) remains unclear. Semiquantitative analysis of VWF labeling in morphologically identifiable  $\alpha$ -granules identified a strong reduction of VWF present in p.C1190R homozygous platelets compared to HCc, both in total and per  $\alpha$ -granule (Figure 5C). Occasionally, we observed VWF labeling in structures that resemble the open canalicular system (Figure 5A #), although this did not appear to differ between patient and control platelets.

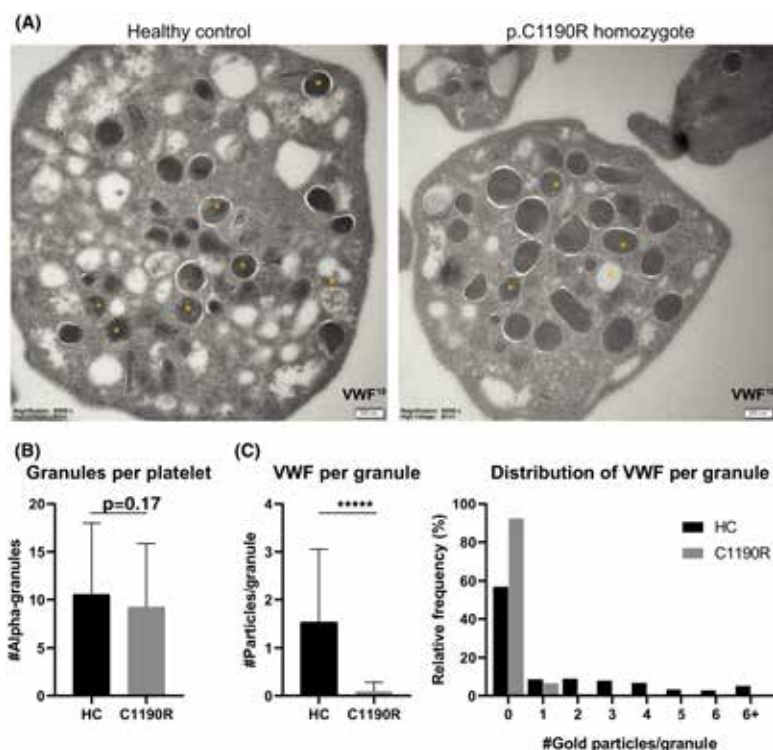


Figure 5. Morphological evaluation of  $\alpha$ -granules and von Willebrand factor (VWF) localization in the p.C1190R homozygous patient.

Platelets from a healthy control (HC; n=73) and homozygous p.C1190R patient (C1190R, n=75) were assessed through immuno-electron microscopy for  $\alpha$ -granule numbers and subcellular localization of VWF (A). Immuno-gold labeling for VWF is shown in  $\alpha$ -granules (\*) and open canalicular system (#). Morphologically identifiable  $\alpha$ -granules were quantified (B) and scored for VWF staining inside these granules (C). Data are represented as mean  $\pm$  standard deviation. \*\*\*\* $P < 0.0001$ .

### Intracellular and extracellular defects in VWF multimers caused by mutations at p.C1190

Finally, we analyzed VWF multimers in plasma and platelets (Figure 6). Consistent with the strong reduction of VWF content that we observed via platelet imaging, we were able to detect very little VWF in platelets of the patient with homozygous p.C1190R (Figure 6A, lane 2). A similar pattern was observed in plasma (Figure 6A, lane 7). Any residual VWF in platelets and plasma of this patient consisted of low-molecular-weight multimers, which points to reduced multimerization of VWF that most probably already occurs intracellularly (Figure 6B,C). Platelet VWF from all three patients with type 2A showed a normal multimer pattern similar to HCs (Figure 6B; lanes 1, 3–5), while plasma VWF was lacking high-molecular-weight (HMW) multimers in patients with p.C1190R and p.C1190Y heterozygotes (Figure 6A,C; lanes 6, 8–10). Intriguingly, platelet and plasma VWF migrated differently through the gel, which may point at significant molecular differences such as differential glycosylation or processing between megakaryocytes and endothelial cells [41,42].

## Discussion

We report the application of a quantitative methodology to assess platelet  $\alpha$ -granule content in platelets from healthy individuals and patients with VWD based on super-resolution microscopy. Using a semiautomated analysis workflow, we generated quantitative data sets of platelet  $\alpha$ -granule proteins of hundreds of platelets per donor. We validated our approach in vitro measuring PAR-1-AP-induced degranulation of activated platelets, and assessed variation of  $\alpha$ -granule cargo in and across healthy individuals. Finally, we quantitatively characterized the  $\alpha$ -granule compartment of a subset of patients with VWD. SIM data revealed distinct alterations between and within different VWD subtypes that we ultimately characterized through EM and VWF multimer analysis. Our findings illustrate the utility of quantitative imaging approaches to study and pinpoint platelet  $\alpha$ -granule alterations in patients with VWD.

We found a large inter- and intraindividual variability in  $\alpha$ -granule cargo across healthy individuals, which demonstrates the heterogeneity of platelets in circulation, as platelets gradually release granule content and undergo morphological changes during aging [43-45]. Our findings also highlight the importance of generating large data sets when interpreting platelet morphology or granule cargo data and the caveat of drawing conclusions based on limited sample sizes. In contrast, detailed analysis of thin sections generated through EM-based methods may yield data of even higher resolution than our current approach but is labor intensive, which limits the cell volume and numbers that can be analyzed simultaneously. As such, SIM-based quantitative granule cargo studies will play an important role in parallel to established methods to further unravel  $\alpha$ -granule biology and processes that affect platelet  $\alpha$ -granule content.

While SIM provides powerful quantitative immunofluorescence-based data of platelet granule cargo, the separation of unique structures is not optimal due to its resolution limitations, particularly in the Z-axis [9]. For example, the average object numbers we quantified in our studies are two- to fourfold lower than estimated by EM [29].  $\alpha$ -granules can be found in 30 nm proximity of one another [29], which is below the resolution level of SIM ( $\sim 100$  nm in XY). Therefore, differences between the EM and SIM approaches may be explained by the incomplete separation of unique cargo-containing  $\alpha$ -granules in SIM, thereby leading to lower quantifiable object numbers. Nevertheless, we have presented data in our work that strongly correlates with previous SIM and EM findings [29,46], showing that our estimation of unique granular structures defined by unique volumes of fluorescence can accurately distinguish changes in the  $\alpha$ -granule compartment of platelets. We were able to identify more unique objects by SIM than by confocal microscopy, implying that our approach is an improvement of previous light microscopy-based methods to discern individual granular structures. While confocal microscopy provides more linear intensity data that is suitable for direct comparison of labeling density, SIM is more capable of defining unique structures independently of signal intensity. Thus, we think using both imaging modalities in tandem is a powerful tool to

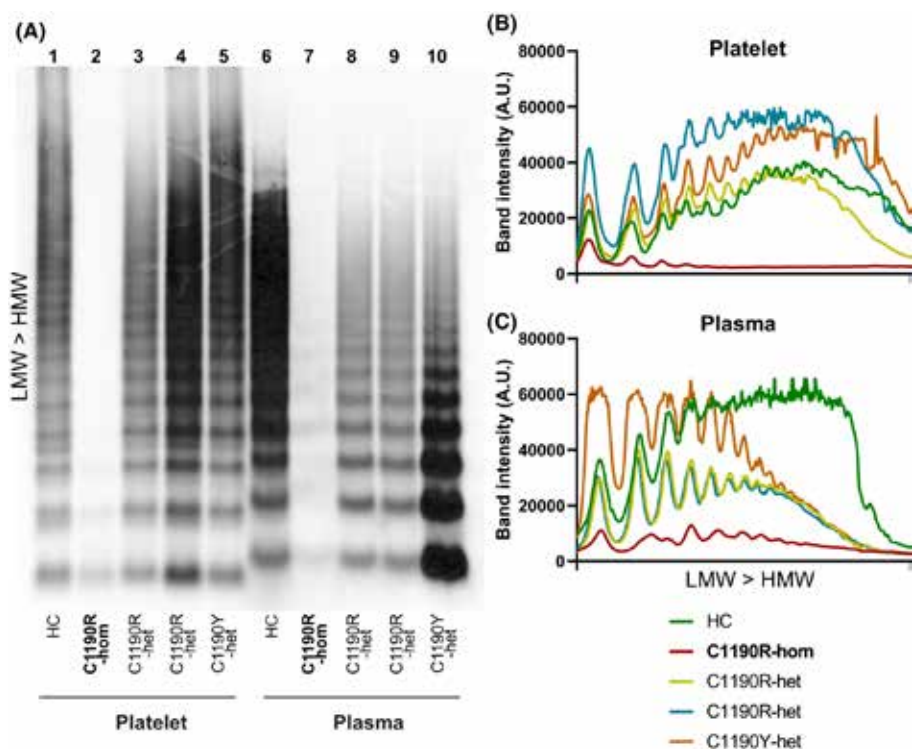


Figure 6. Von Willebrand factor (VWF) multimer analysis of patients with p.C1190.

Platelets (lanes 1-5) and plasma (lanes 6-10) from a healthy control (HC) all patients with p.C1190 were analyzed for VWF multimer patterns (A). Patient with type 3 VWD (C1190R-hom) is marked as bold text to distinguish from heterozygous C1190R (C1190R-het) and C1190Y (C1190Y-het). Line intensity plots were generated and plotted separately for platelet lysates (B) and plasma (C), with each individual color coded. Patterns were illustrated from low-molecular-weight (LMW) to high-molecular-weight (HMW) VWF multimers (B-C), which is bottom to top on the blot (A).

assess  $\alpha$ -granule content. For those applications in which demands for increased resolution outweigh quantitative advantages or speed of SIM, super-resolution microscopy approaches with even higher resolving power such as stimulated emission depletion and stochastic optical reconstruction microscopy may be more applicable [47,48].

We used a SIM-based technique to assess the  $\alpha$ -granule compartment in patients with VWD, as the role that platelet VWF has in this disease is still elusive [49-57]. Our quantitative analysis showed that platelets of both patients with type 3 VWD contained normal numbers and regular distribution of SPARC-positive objects, which indicates that in these patients  $\alpha$ -granule formation and storage of other  $\alpha$ -granule proteins was not disturbed. This is in support of an earlier EM study that showed that  $\alpha$ -granules in patients with type 3 VWD appear morphologically normal [56]. Taken together, this shows that unlike endothelial Weibel-Palade bodies, whose biogenesis is driven by VWF biosynthesis [36,38,58], defective or severely reduced VWF synthesis does not impact the formation of its storage organelles in platelets.

SIM-based quantitative analysis of platelet VWF content, in contrast to SPARC, highlighted profound differences between the two patients with type 3 VWD. These patients have severe quantitative VWF deficiencies that are underpinned by different pathogenic mechanisms. In one patient, compound heterozygous for two separate null alleles ( $\Delta\text{ex4-5}$ , L2306Rfs\*4), we were unable to detect any VWF in platelets, consistent with an absence of protein synthesis because of early termination signals in both alleles. Conversely, VWF-positive objects were found in platelets of the other patient with type 3 VWD with a homozygous missense mutation at p.C1190R in the D3 domain. Heterozygous mutations at this position [40,59,60] and at other cysteine residues within this domain have been previously linked to type 2A VWD, a subtype that is characterized by low platelet binding activity of VWF due to loss of HMW multimers (also Figure 6). Lower multimers in type 2A VWD arise from either intracellular trafficking and/or multimerization defects during VWF biosynthesis (group I) or an increased sensitivity to extracellular proteolysis by ADAMTS-13 (group II) [61]. The cysteines in the D3 domain form a complex network of intra- and interchain disulfide bonds that support the alignment and N-terminal oligomerization of pro-VWF dimers [62]. The contribution of intrachain disulfide bonds, including the one formed by C1190, are not clearly defined, except that heterologous expression of various type 2A missense mutants at D3 cysteines in this region invariably leads to low-molecular-weight multimers [40,60,63,64]. This is reflected by the absence of medium-molecular-weight and HMW VWF multimers in the platelets of the patient with homozygous p.C1190R, which also points to a defect occurring during VWF biosynthesis. Despite the strongly reduced synthesis of VWF and its apparent loss of multimerization, our combined SIM and EM data (Figures 4A,C and 5A) points toward targeting of homozygous p.C1190R VWF to a normal number of  $\alpha$ -granules, albeit in reduced quantities. These data are in line with a previous study that showed that platelets of patients with type 3 VWD with the P2808Lfs\*24 mutation, which presumably impairs VWF dimerization, still contained VWF in granular structures that could be mobilized by platelet activation [57]. From this study it remained unclear whether VWF was incorporated in  $\alpha$ -granules and whether the lack of VWF multimers in plasma also manifested in platelets. Regardless, both this previous and our current study suggest that multimerization per se is not a prerequisite for VWF to enter platelet  $\alpha$ -granules.

Despite the reduction of HMW VWF multimers in their plasma, patients heterozygous for p.C1190R or p.C1190Y had platelet VWF multimers that were indistinguishable from healthy controls. De Jong et al [59] recently tested a single nucleotide polymorphism-based approach to specifically silence expression of an autosomal dominant VWD allele in blood outgrowth endothelial cells of the same patient with type 2A with p.C1190Y included in our study. VWF multimers from heterozygous p.C1190Y endothelial cells showed an overabundance of dimeric VWF and pronounced retention of VWF in the endoplasmic reticulum (ER), both of which were alleviated by specific silencing of the p.C1190Y allele. Accumulation of dimeric VWF, which possibly consists of ER-retained mutant wild-type heterodimers [65], was not observed in platelets in our current work. This discrepancy may be explained by retention of this pool in megakaryocytes during

proplatelet formation. However, we cannot exclude the possibility that this is the result of differences in disulfide exchange or posttranslational modifications of VWF between megakaryocytes and endothelial cells. Similarly, we found that platelet- and plasma-derived VWF migrated differently through a multimer gel, suggestive of altered processing between both cell types. Judging by the presence of HMW multimers in platelets as well as endothelial cells of this patient, reduction of VWF multimer size in plasma cannot be fully explained by biosynthetic defects alone but potentially also by a reduced half-life of circulating HMW multimers. Finally, we also observed a discrepancy between VWF levels in platelets of the patients with p.C1190Y and p.C1190R heterozygotes, which was consistent with their plasma VWF levels (Table 1). This is in line with previous observations suggesting that missense mutations at p. C1190 can have differential effects based on the substitution [40].

The potential diagnostic utility of our approach was demonstrated by the quantification of granular abnormalities in patients with VWD with different etiologies. Currently, we are collecting and analyzing platelet data from additional patients with VWD to answer follow-up questions. For example, studying the distribution of VWF in platelets may provide an easily accessible way of studying VWF synthesis defects. Additionally, tools to explain variability in bleeding phenotypes of patients with VWD are lacking, for which studies in larger groups need to be done to address the link between platelet VWF and bleeding severity. The possibility to rapidly image and analyze large numbers of platelets in 3D in a large field of view with SIM will be an important advantage versus other super-resolution methods when analyzing platelet content and morphology in large cohort studies [48] and may also be useful to study inherited platelet storage pool disorders stemming from variants such as GFI1b, NBEAL2, or GATA1. We envision SIM in parallel to confocal imaging to be considered as a diagnostic tool for complex cases, such as unexplained storage pool disease, similar to current EM-based diagnostics.

One promising example to better characterize the bleeding phenotype in patients stems from our current study in relation to the Bowman study [57]. Patients with the p.P2808Lfs\*24 mutation had very low VWF plasma levels, but their bleeding scores were relatively low (median, 8.5) compared to other patients with type 3 VWD, or the patient with  $\Delta$ ex4-5 described in our study (bleeding score = 34, Table 1). Similarly, the p.C1190R homozygote in our work had but a moderate bleeding phenotype (score=20, Table 1). It remains to be determined whether (release of) residual platelet VWF contributes to the milder phenotype of p.P2808Lfs\*24 and p.C1190R homozygous patients in comparison to other patients with type 3 VWD, or whether it potentially is a surrogate marker of VWD severity. However, our combined findings suggest that studying VWF content in platelets of patients with VWD could have predictive value in telling apart patients with severe VWD with severe and mild bleeding phenotypes.

In summary, we developed a quantitative methodology to evaluate alpha-granule constituents through super-resolution imaging which can be used for the characterization

of the platelet  $\alpha$ -granule compartment and VWF storage in healthy individuals and patients with VWD.

### Acknowledgments

We thank I. van Moort for on-site blood collection.

### Relationship Disclosure

The authors declare no conflicts of interest related to the subject of this study.

### Author Contributions

MS performed in vitro experiments and imaging and designed the Fiji-based analysis. FA included patients for the study and obtained clinical and laboratory data. PEB performed VWF multimer analysis. JAS and ABH helped design the imaging setup and analysis. CdH and JK performed immuno-EM imaging and analysis. FWGL, JV, AJG J, and RB supervised experimental design, analysis design, and selection of patients. All authors provided input and made suggestions for improvement of the manuscript.

### ORCID

Maurice Swinkels <https://orcid.org/0000-0002-6667-9031>

Ferdows Atiq <https://orcid.org/0000-0002-3769-9148>

Johan A. Slotman <https://orcid.org/0000-0001-9705-9620>

Adriaan B. Houtsmuller <https://orcid.org/0000-0003-0967-0740>

Cilia de Heus <https://orcid.org/0000-0001-8618-8451>

Judith Klumperman <https://orcid.org/0000-0003-4835-6228>

Frank W. G. Leebeek <https://orcid.org/0000-0001-5677-1371>

Jan Voorberg <https://orcid.org/0000-0003-4585-2621>

Arend Jan Gerard Jansen <https://orcid.org/0000-0002-2612-1420>

Ruben Bierings <https://orcid.org/0000-0002-1205-9689>

## References

1. Yadav S, Storrie B. The cellular basis of platelet secretion: emerging structure/function relationships. *Platelets*. 2017;28:108-118.
2. Kelm RJ Jr, Mann KG. Human platelet osteonectin: release, surface expression, and partial characterization. *Blood*. 1990;75:1105-1113.
3. Breton-Gorius J, Clezardin P, Guichard J, et al. Localization of platelet osteonectin at the internal face of the alpha-granule membranes in platelets and megakaryocytes. *Blood*. 1992;79:936-941.
4. Chen CI, Federici AB, Cramer EM, et al. Studies of multimerin in patients with von Willebrand disease and platelet von Willebrand factor deficiency. *Br J Haematol*. 1998;103:20-28.
5. Hayward CP, Cramer EM, Kane WH, et al. Studies of a second family with the Quebec platelet disorder: evidence that the degradation of the alpha-granule membrane and its soluble contents are not secondary to a defect in targeting proteins to alpha-granules. *Blood*. 1997;89:1243-1253.
6. Karampini E, Bierings R, Voorberg J. Orchestration of primary hemostasis by platelet and endothelial lysosome-related organelles. *Arterioscler Thromb Vasc Biol*. 2020;40:1441-1453.
7. Heemskerk JW, Mattheij NJ, Cosemans JM. Platelet-based coagulation: different populations, different

- functions. *J Thromb Haemost.* 2013;11:2-16.
8. Ambrosio AL, Di Pietro SM. Storage pool diseases illuminate platelet dense granule biogenesis. *Platelets.* 2017;28:138-146.
  9. Schermelleh L, Ferrand A, Huser T, et al. Super-resolution microscopy demystified. *Nat Cell Biol.* 2019;21:72-84.
  10. Westmoreland D, Shaw M, Grimes W, et al. Super-resolution microscopy as a potential approach to diagnosis of platelet granule disorders. *J Thromb Haemost.* 2016;14:839-849.
  11. Pluthero FG, Kahr WHA. Imaging platelets and megakaryocytes by high-resolution laser fluorescence microscopy. *Methods Mol Biol.* 2018;1812:13-31.
  12. de Jong A, Eikenboom J. Von Willebrand disease mutation spectrum and associated mutation mechanisms. *Thromb Res.* 2017;159:65-75.
  13. Leebeek FW, Eikenboom JC. Von Willebrand's disease. *N Engl J Med.* 2016;375:2067-2080.
  14. Leebeek FWG, Atiq F. How I manage severe von Willebrand disease. *Br J Haematol.* 2019;187:418-430.
  15. Schillemans M, Karampini E, van den Eshof BL, et al. Weibel-Palade body localized syntaxin-3 modulates Von Willebrand factor secretion from endothelial cells. *Arterioscler Thromb Vasc Biol.* 2018;38:1549-1561.
  16. Schindelin J, Arganda-Carreras I, Frise E, et al. Fiji: an open-source platform for biological-image analysis. *Nat Methods.* 2012;9:676-682.
  17. Ball G, Demmerle J, Kaufmann R, Davis I, Dobbie IM, Schermelleh L. SIMcheck: a toolbox for successful super-resolution structured illumination microscopy. *Sci Rep.* 2015;5:15915.
  18. Banterle N, Bui KH, Lemke EA, Beck M. Fourier ring correlation as a resolution criterion for super-resolution microscopy. *J Struct Biol.* 2013;183:363-367.
  19. Sezgin M, Sankur B. Survey over image thresholding techniques and quantitative performance evaluation. *J Electron Imaging.* 2004;13:146-168.
  20. Ollion J, Cochennec J, Loll F, Escude C, Boudier T. TANGO: a generic tool for high-throughput 3D image analysis for studying nuclear organization. *Bioinformatics.* 2013;29:1840-1841.
  21. Tsai WH. Moment-preserving thresholding – a new approach. *Comput Vision Graph.* 1985;29:377-393.
  22. Aaron JS, Taylor AB, Chew TL. Image co-localization -co- occurrence versus correlation. *J Cell Sci.* 2018;131(3):jcs211847.
  23. Coltharp C, Yang X, Xiao J. Quantitative analysis of single-molecule superresolution images. *Curr Opin Struct Biol.* 2014;28:112-121.
  24. Nicovich PR, Owen DM, Gaus K. Turning single-molecule localization microscopy into a quantitative bioanalytical tool. *Nat Protoc.* 2017;12:453-460.
  25. Lagache T, Sauvonnnet N, Danglot L, Olivo-Marin JC. Statistical analysis of molecule colocalization in bioimaging. *Cytometry A.* 2015;87:568-579.
  26. Otsu N. Threshold selection method from gray-level histograms. *IEEE T Syst Man Cyb.* 1979;9:62-66.
  27. Harrison P, Savidge GF, Cramer EM. The origin and physiological relevance of alpha-granule adhesive proteins. *Br J Haematol.* 1990;74:125-130.
  28. King SM, Reed GL. Development of platelet secretory granules. *Semin Cell Dev Biol.* 2002;13:293-302.
  29. Pokrovskaya ID, Yadav S, Rao A, et al. 3D ultrastructural analysis of alpha-granule, dense granule, mitochondria, and canalicular system arrangement in resting human platelets. *Res Pract Thromb Haemost.* 2020;4:72-85.
  30. van Nispen tot Pannerden H, de Haas F, Geerts W, Posthuma G, van Dijk S, Heijnen HF. The platelet interior revisited: electron tomography reveals tubular alpha-granule subtypes. *Blood.* 2010; 116: 1147-1156.
  31. Cramer EM, Meyer D, le Menn R, Breton-Gorius J. Eccentric localization of von Willebrand factor in an internal structure of platelet alpha-granule resembling that of Weibel-Palade bodies. *Blood.* 1985;66:710-713.
  32. Battinelli EM, Thon JN, Okazaki R, et al. Megakaryocytes package contents into separate alpha-granules that are differentially distributed in platelets. *Blood Adv.* 2019;3:3092-3098.
  33. Italiano JE Jr, Richardson JL, Patel-Hett S, et al. Angiogenesis is regulated by a novel mechanism: pro-and antiangiogenic proteins are organized into separate platelet alpha granules and differentially released. *Blood.* 2008;111:1227-1233.
  34. Diagouraga B, Grichine A, Fertin A, Wang J, Khochbin S, Sadoul K. Motor-driven marginal band coiling promotes cell shape change

- during platelet activation. *J Cell Biol.* 2014;204:177-185.
35. Eckly A, Rinckel JY, Proamer F, et al. Respective contributions of single and compound granule fusion to secretion by activated platelets. *Blood.* 2016;128:2538-2549.
  36. Groeneveld DJ, van Bekkum T, Dirven RJ, et al. Angiogenic characteristics of blood outgrowth endothelial cells from patients with von Willebrand disease. *J Thromb Haemost.* 2015;13:1854-1866.
  37. Schillemans M, Karampini E, Kat M, Bierings R. Exocytosis of Weibel-Palade bodies: how to unpack a vascular emergency kit. *J Thromb Haemost.* 2019;17:6-18.
  38. Schillemans M, Kat M, Westeneng J, et al. Alternative trafficking of Weibel-Palade body proteins in CRISPR/Cas9-engineered von Willebrand factor-deficient blood outgrowth endothelial cells. *Res Pract Thromb Haemost.* 2019;3:718-732.
  39. Springer TA. von Willebrand factor, Jedi knight of the bloodstream. *Blood.* 2014;124:1412-1425.
  40. Schneppenheim R, Michiels JJ, Obser T, et al. A cluster of mutations in the D3 domain of von Willebrand factor correlates with a distinct subgroup of von Willebrand disease: type 2A/IIe. *Blood.* 2010;115:4894-4901.
  41. McGrath RT, van den Biggelaar M, Byrne B, et al. Altered glycosylation of platelet-derived von Willebrand factor confers resistance to ADAMTS13 proteolysis. *Blood.* 2013;122:4107-4110.
  42. McGrath RT, McRae E, Smith OP, O'Donnell JS. Platelet von Willebrand factor—structure, function and biological importance. *Br J Haematol.* 2010;148:834-843.
  43. Rijkers M, van den Eshof BL, van der Meer PF, et al. Monitoring storage induced changes in the platelet proteome employing label free quantitative mass spectrometry. *Sci Rep.* 2017;7:11045.
  44. Rijkers M, van der Meer PF, Bontekoe IJ, et al. Evaluation of the role of the GPIb-IX-V receptor complex in development of the platelet storage lesion. *Vox Sang.* 2016;111:247-256.
  45. Shrivastava M. The platelet storage lesion. *Transfus Apher Sci.* 2009;41:105-113.
  46. Sehgal S, Storrie B. Evidence that differential packaging of the major platelet granule proteins von Willebrand factor and fibrinogen can support their differential release. *J Thromb Haemost.* 2007;5:2009-2016.
  47. Ronnlund D, Yang Y, Blom H, Auer G, Widengren J. Fluorescence nanoscopy of platelets resolves platelet-state specific storage, release and uptake of proteins, opening up future diagnostic applications. *Adv Healthc Mater.* 2012;1:707-713.
  48. Montague SJ, Lim YJ, Lee WM, Gardiner EE. Imaging platelet processes and function-current and emerging approaches for imaging in vitro and in vivo. *Front Immunol.* 2020;11:78.
  49. Casonato A, Cattini MG, Daidone V, Pontara E, Bertomoro A, Prandoni P. Diagnostic value of measuring platelet von Willebrand factor in von Willebrand disease. *PLoS One.* 2016;11:e0161310.
  50. Gralnick HR, Rick ME, McKeown LP, et al. Platelet von Willebrand factor: an important determinant of the bleeding time in type I von Willebrand's disease. *Blood.* 1986;68:58-61.
  51. Rodeghiero F, Castaman G, Ruggeri M, Tosetto A. The bleeding time in normal subjects is mainly determined by platelet von Willebrand factor and is independent from blood group. *Thromb Res.* 1992;65:605-615.
  52. Verhenne S, Denorme F, Libbrecht S, et al. Platelet-derived VWF is not essential for normal thrombosis and hemostasis but fosters ischemic stroke injury in mice. *Blood.* 2015;126:1715-1722.
  53. Nurden P, Chretien F, Poujol C, Winckler J, Borel-Derlon A, Nurden A. Platelet ultrastructural abnormalities in three patients with type 2B von Willebrand disease. *Br J Haematol.* 2000;110:704-714.
  54. Nurden P, Debili N, Vainchenker W, et al. Impaired megakaryocytopoiesis in type 2B von Willebrand disease with severe thrombocytopenia. *Blood.* 2006;108:2587-2595.
  55. Nurden P, Gobbi G, Nurden A, et al. Abnormal VWF modifies megakaryocytopoiesis: studies of platelets and megakaryocyte cultures from patients with von Willebrand disease type 2B. *Blood.* 2010;115:2649-2656.
  56. Nurden P, Nurden AT, La Marca S, Punzo M, Baronciani L, Federici AB. Platelet morphological changes in 2 patients with von Willebrand disease type 3 caused by large homozygous deletions of the von Willebrand factor gene. *Haematologica.* 2009;94:1627-1629.
  57. Bowman ML, Pluthero FG, Tuttle A, et al. Discrepant platelet and plasma von Willebrand factor in von Willebrand disease patients with p.Pro2808Leufs\*24. *J Thromb Haemost.* 2017;15:1403-1411.
  58. Denis CV, Andre P, Saffaripour S, Wagner DD. Defect in regulated secretion of P-selectin affects leukocyte

- recruitment in von Willebrand factor-deficient mice. *Proc Natl Acad Sci U S A*. 2001;98:4072-4077.
59. de Jong A, Dirven RJ, Boender J, et al. Ex vivo improvement of a von Willebrand disease type 2A phenotype using an allele-specific small-interfering RNA. *Thromb Haemost*. 2020;120:1569-1579.
60. Jacobi PM, Gill JC, Flood VH, Jakab DA, Friedman KD, Haberichter SL. Intersection of mechanisms of type 2A VWD through defects in VWF multimerization, secretion, ADAMTS-13 susceptibility, and regulated storage. *Blood*. 2012;119:4543-4553.
61. Lyons SE, Bruck ME, Bowie EJ, Ginsburg D. Impaired intracellular transport produced by a subset of type IIA von Willebrand disease mutations. *J Biol Chem*. 1992;267:4424-4430.
62. Dong X, Leksa NC, Chhabra ES, et al. The von Willebrand factor D'D3 assembly and structural principles for factor VIII binding and concatemer biogenesis. *Blood*. 2019;133:1523-1533.
63. Eikenboom JC, Matsushita T, Reitsma PH, et al. Dominant type 1 von Willebrand disease caused by mutated cysteine residues in the D3 domain of von Willebrand factor. *Blood*. 1996;88:2433-2441.
64. Tjernberg P, Vos HL, Castaman G, Bertina RM, Eikenboom JC. Dimerization and multimerization defects of von Willebrand factor due to mutated cysteine residues. *J Thromb Haemost*. 2004;2:257-265.
65. Bodo I, Katsumi A, Tuley EA, Eikenboom JC, Dong Z, Sadler JE. Type 1 von Willebrand disease mutation Cys1149Arg causes intracellular retention and degradation of heterodimers: a possible general mechanism for dominant mutations of oligomeric proteins. *Blood*. 2001;98:2973-2979.

## Appendix

### Supplementary Methods

#### Flow cytometry

Fixed platelet preparations for flow cytometry were stained for both a platelet-specific marker (CD61-APC, BD Biosciences, 1:100) as well as a marker of (alpha-)granule release (CD62P-PE, clone AK4, BD Biosciences, 1:100) for 15 min at RT. Samples were washed once in washing buffer before acquisition on a FACS Canto II (BD Biosciences). Platelets were gated on a logarithmic FSC/SSC plot and single cell characteristics. Compensation was calculated based on single stains as necessary. Percentage of positive cells was calculated based on isotype controls and data was analyzed in FlowJo software.

#### VWF multimer analysis

Platelet lysates were prepared by washing PRP three times in WB containing respectively 111, 11 and 0 $\mu$ M prostaglandin E1 (Sigma-Aldrich). Finally, platelets were resuspended in cold lysis buffer (1% (v/v) Triton X-100, 10% (v/v) glycerol, 50 mM Tris-HCl, 100 mM NaCl, 1 mM EDTA, pH 7.4; containing 1:100 Complete Protease Inhibitor Cocktail (Sigma-Aldrich)) at 1,000,000 platelets/ $\mu$ l for 1 hour at 4 degrees. Debris were removed by spinning 15 min at 16,000 x g and lysates were stored at -20 degrees until use.

Equivalent volumes of platelet lysate (1 in 2) or plasma (1 in 3) were incubated at 60 degrees with loading buffer (10 mM Tris, 1 mM EDTA, 2% SDS, 0.5 mM bromophenolblue, pH 6.9) and loaded on a 0.9% agarose gel. The gel ran for 5 hours at 75 V to allow optimal separation of VWF multimers, and was then chemically reduced with  $\beta$ -mercapto-ethanol. Proteins were carefully transferred on a nitrocellulose membrane through overnight capillary blotting in blot buffer (20 mM Tris, 10 mM acetate, 0.5 mM EDTA, 10% SDS, pH 8.0). Transferred proteins were blocked in 10% milk (Biorad) for 1 hour at RT, stained with a VWF-HRP polyclonal antibody (DAKO, 1:1000) for 3 hours at RT, washed, and developed using ECL (Pierce). Imaging was done on an Amersham Imager 600 (GE Healthcare) and line-plots were generated using ImageJ software.

#### Immuno-gold electron microscopy

Electron microscopy samples were generated by washing PRP three times with WB containing prostaglandin E1 as described above. Platelets were then fixed at RT by adding 1:1 (v/v) 4% FA plus 0.4% glutaraldehyde (GA) in 0.1M Phosphate Buffer (PB) for 10 min, replaced by fresh fixative for 2 hours, and stored in 1% FA in 0.1M PB until further processing as previously described [1]. In short, fixed cells were washed three times with PBS, incubated for 10 min in 0.15% Glycine/PBS and 10 min at 37 $^{\circ}$ C in 12% gelatin, spun down at 4000g and left on ice for 30 min. The solidified pellet was cut into small blocks and placed overnight in 2.3M sucrose. Gelatin blocks were mounted on aluminum pins and frozen in liquid nitrogen. Ultrathin cryosections of 70 nm were sectioned at -110 $^{\circ}$ C

using a Leica ultracut 6 ultramicrotome and placed in a 1:1 mixture of 2.3M sucrose and 1.8% methylcellulose. To rinse away the gelatin, grids were transferred section-down on droplets of PBS at 37°C for 30 min, transferred to RT and washed 3 x 2 min with 0.15% Glycin/PBS. For labeling, grids were incubated 3 min on 0.5% fish-gelatin/1% bovine serum albumin-C blocking buffer and then with VWF-antibody solution (DAKO, cat#: A0082) for 1 hour, followed by Protein A gold 10 nm (Cell Microscopy Core, UMC Utrecht) for 15 min. Final staining of the grids was performed with uranyl acetate (UAc) followed by a UAc-methylcellulose mixture.

Semi-quantitative analysis of electron microscopy images was performed by scoring blinded images for the number of alpha-granules and the number of gold particles per alpha-granule, by three independent researchers (M.S., P.B. and R.B.). Only platelets that were entirely in the field of view were considered for quantification.

## Supplementary Figures

Antigen	Species (Isotype)	Label	Supplier	Cat. Nr.	Dilution
Alpha-tubulin	<u>Mouse (IgG2b)</u>	-	Abcam	ab56676	1:500
Alpha-tubulin	Mouse (IgG1)	-	Sigma	DM1A	1:500
SPARC	<u>Mouse (IgG1)</u>	-	SantaCruz	sc-73472	1:500
<u>Von Willebrand factor</u>	<u>Rabbit</u>	-	<u>DAKO</u>	<u>A0082</u>	<u>1:500</u>
Von Willebrand factor	Mouse (IgG2b)	-	Sanquin	CLB-Rag20	1:500
Fibrinogen	Rabbit	-	DAKO	A0080	1:500
CD62P	Mouse (IgG1)	AF 488	AbD Serotec	MCA796	1:400
Mouse IgG1	Goat	CF 647	Biotium	20252	1:1000
Mouse IgG2b	Goat	CF 488	Biotium	20266	1:1000
Rabbit IgG (H+L)	Donkey	AF 568	ThermoFisher	A11042	1:400
Underlined primary antibodies were used in all primary experiments. Other primary antibodies were used for Supplemental Figure S3.					

Supplementary Table S1. Antibodies used in immunofluorescence studies.

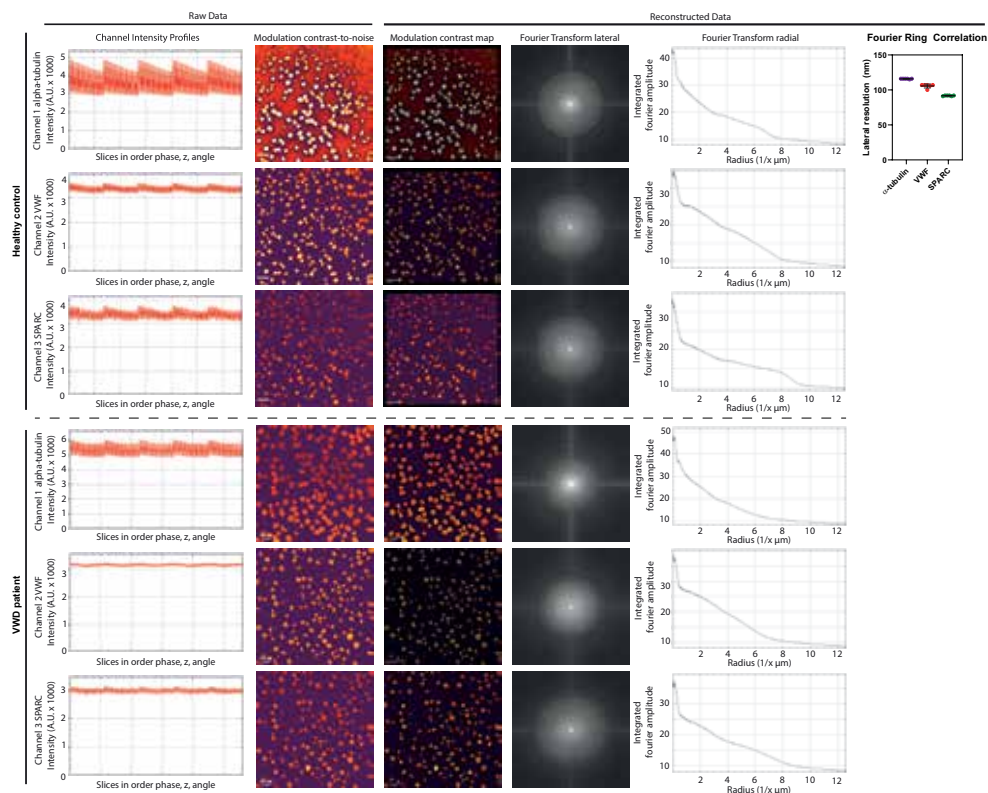
Parameter measured	Description
Marginal band size ( $\mu\text{m}^2$ )	Surface area measured based on alpha-tubulin staining on 2D average intensity projection. Segmentation and thresholding was based on the Li algorithm for automated thresholding [2], excluding platelets that were not completely in the field of view.
Number of VWF+/SPARC+ objects	Unique volumes of fluorescence measured through 3D maxima detection and watershedding, based on VWF- or SPARC-staining, or 2D maxima detection for distance measurements. Thresholds for these maxima were determined by iterating noise parameters over the resulting amount of unique spots and selecting the best fit, filtering out background signal. Objects were then segmented through a watershed algorithm in 3D for granule morphometrics [3]. Background correction for alpha-granule stainings was performed for all images individually by dividing all Z-stacks by the highest background level in the stack. Adapted to 2D for confocal images.
Total volume (voxels)	Total voxel value of all unique volumes summed per platelet
Minimal distance between granules (nm)	Minimal distance from a unique cargo-positive object to its nearest neighbor in 2D
Minimal distance to membrane (nm)	Minimal distance from a unique cargo-positive object to the marginal band in 2D
Colocalization (nm)	Minimal distance between unique VWF-positive and SPARC-positive objects in 2D
MFI (A.U.)	Mean fluorescence intensity averaged over three sequential slices in the middle of a platelet. Quantified only in confocal microscopy images.

*Supplementary Table S2. Overview of main parameters measured in platelets through SIM and confocal analysis.*

*Supplementary Video SV1. 3D rendering of VWF and SPARC granular staining.*

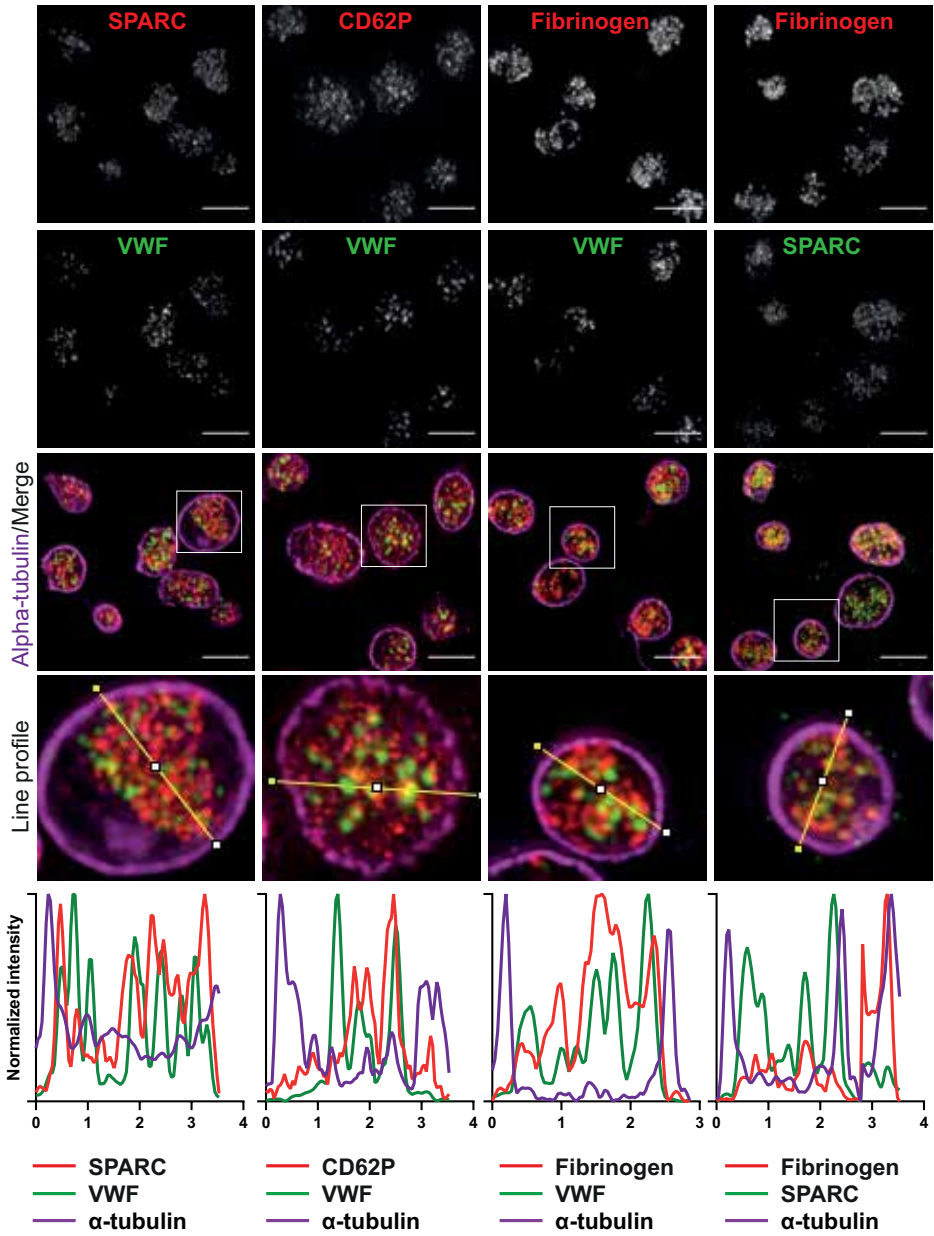
Shown are VWF (red), SPARC (green), composite VWF/SPARC and composite VWF/SPARC/alpha-tubulin (magenta) staining of the platelet example shown in in Figure 1. The video rotates around the Y-axis. Video can be found online.





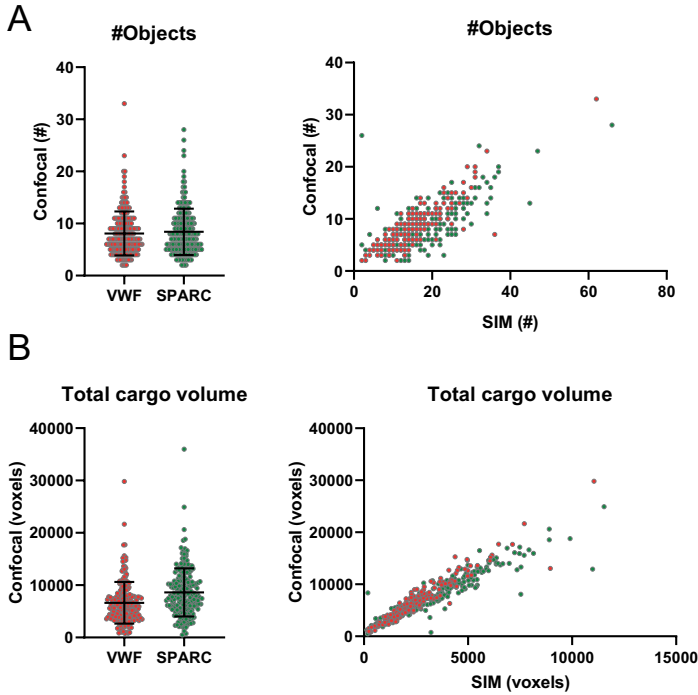
Supplementary Figure S2. SIMCheck analysis of raw and reconstructed SIM data of healthy control and VWD platelets.

Data is shown as X(HC)/Y(VWD). First column: channel intensity profiles show a variation of 34.9% (HC) and 17.0% (VWD) for alpha-tubulin, 9.12% and 4.10% for VWF, 15.2% and 9.32% for SPARC; where less than 50% is considered good. Second column: modulation contrast-to-noise for the raw images has an average of 19.0 (HC) and 5.96 (VWD) for alpha-tubulin, 13.9 and 5.55 for VWF, 6 and 4.32 for SPARC; where 8-12 is good and >12 is excellent. Third column: modulation contrast map shows the modulation contrast related to the reconstruction image where orange/yellow is considered good, white is excellent. Fourth and fifth column: Fourier transformation of the reconstructed images indicating the enhanced resolution, both laterally (XY, fourth column) and in a radial plot (fifth column) averaging over the angles. Sixth column: lateral resolution calculated through Fourier Ring Correlation. All graphs are based on experimental imaging data that was used in the manuscript.



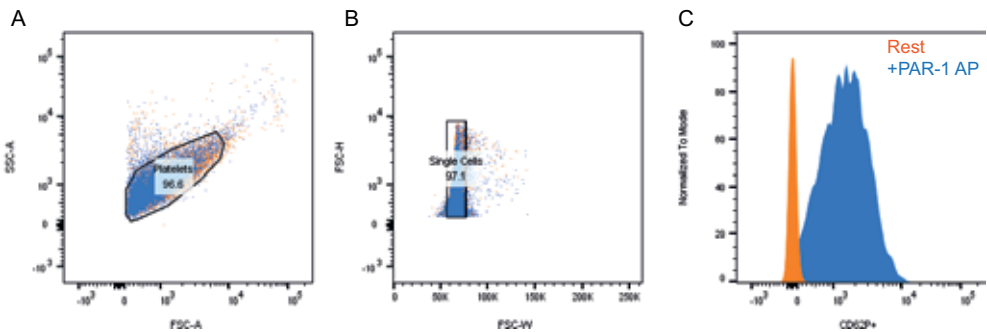
Supplementary Figure S3. Alpha-granule stainings in healthy resting platelets.

Healthy platelets were stained for various alpha-granule proteins and overlap between different stainings was visualized through relative line intensity profiles. For each combination of stained proteins, one zoomed-in platelet is shown as an example. Line plots are in the direction from yellow to white square. Scale bar is 3 $\mu$ m.



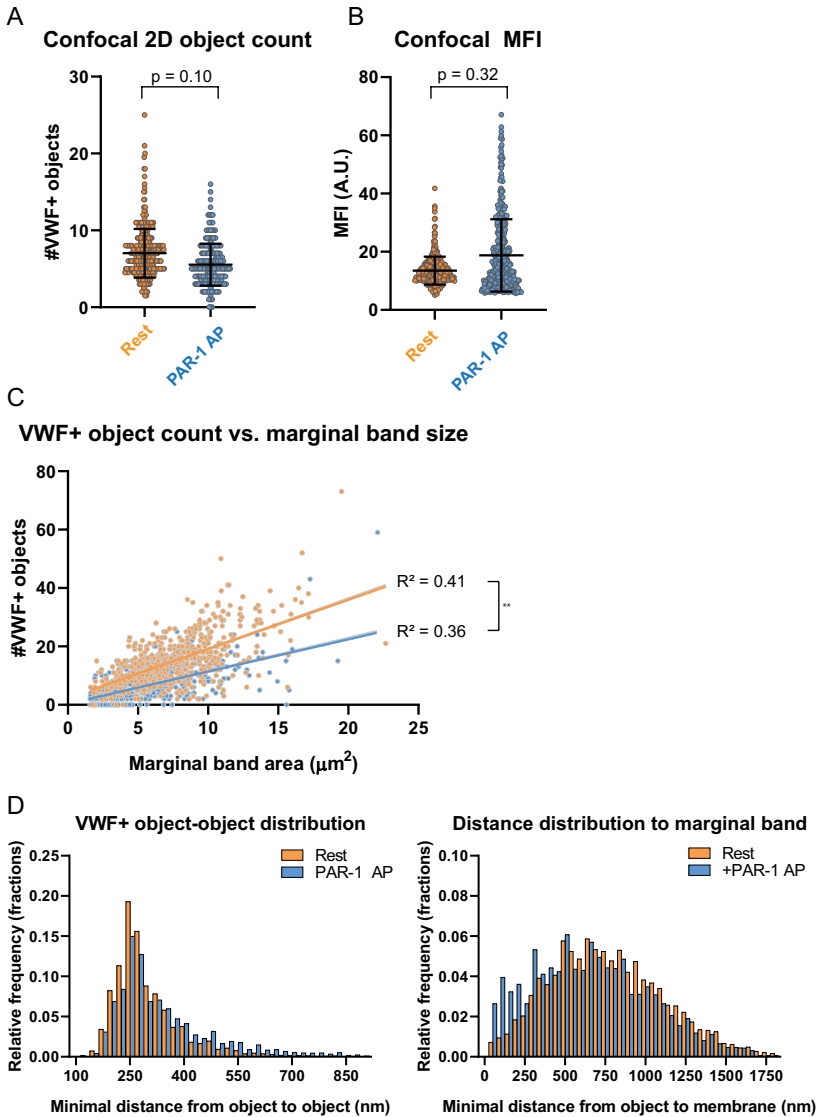
Supplementary Figure S4. Comparison of SIM and confocal analysis workflows.

VWF (red) and SPARC (green) signals were quantified as unique structures (A) and as total volume per platelet (B). Both the distribution of the data in confocal images (left graph) and correlation between SIM and confocal data (right graph) is shown. Data is represented as mean  $\pm$  standard deviation.



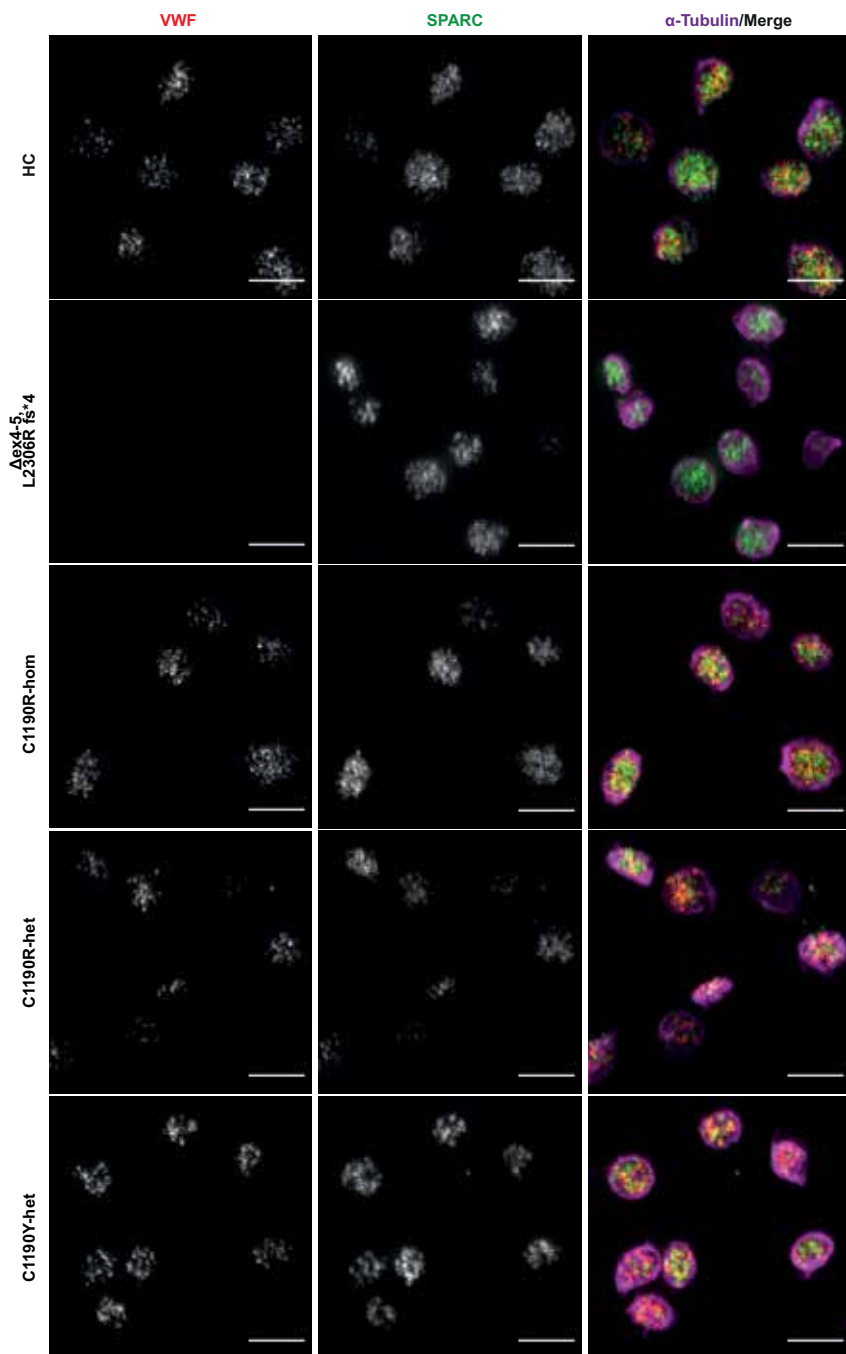
Supplementary Figure S5. Flow cytometry controls of resting and activated platelets.

Platelets were stimulated with PAR-1 AP (10 $\mu$ M) or vehicle control (PBS) for 30 minutes at 37°C and assessed for CD62P+ exposure as a marker of alpha-granule release. Platelets were gated based on a logarithmic FSC/SSC scale (A). Single cells were gated (B) and assessed for CD62P+ exposure (C). Resting (orange) and activated (blue) platelets are shown in all graphs.



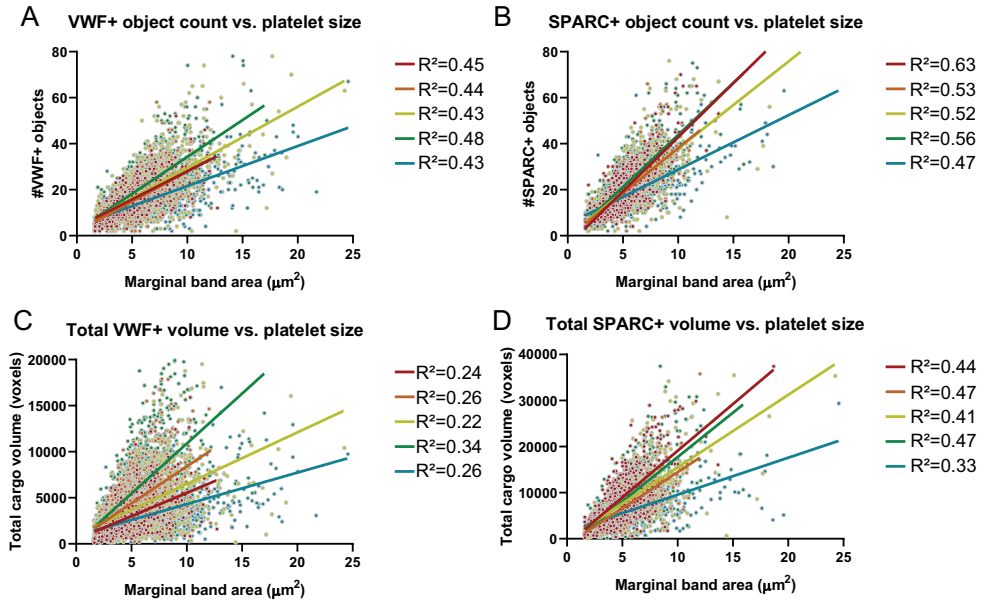
Supplementary Figure S6. Detailed SIM- and confocal analysis of PAR-1 stimulated platelets.

Resting (orange) and PAR-1 stimulated (blue) platelets were assessed for VWF-positive objects (A) and MFI (B) by confocal microscopy. Relation between VWF-positive objects and marginal band area of SIM data was assessed through linear regression in (C). Spatial distribution of VWF-positive objects in relation to other objects or to marginal band was quantified in (D). Data is represented as mean  $\pm$  standard deviation. \*\* =  $p < 0.01$



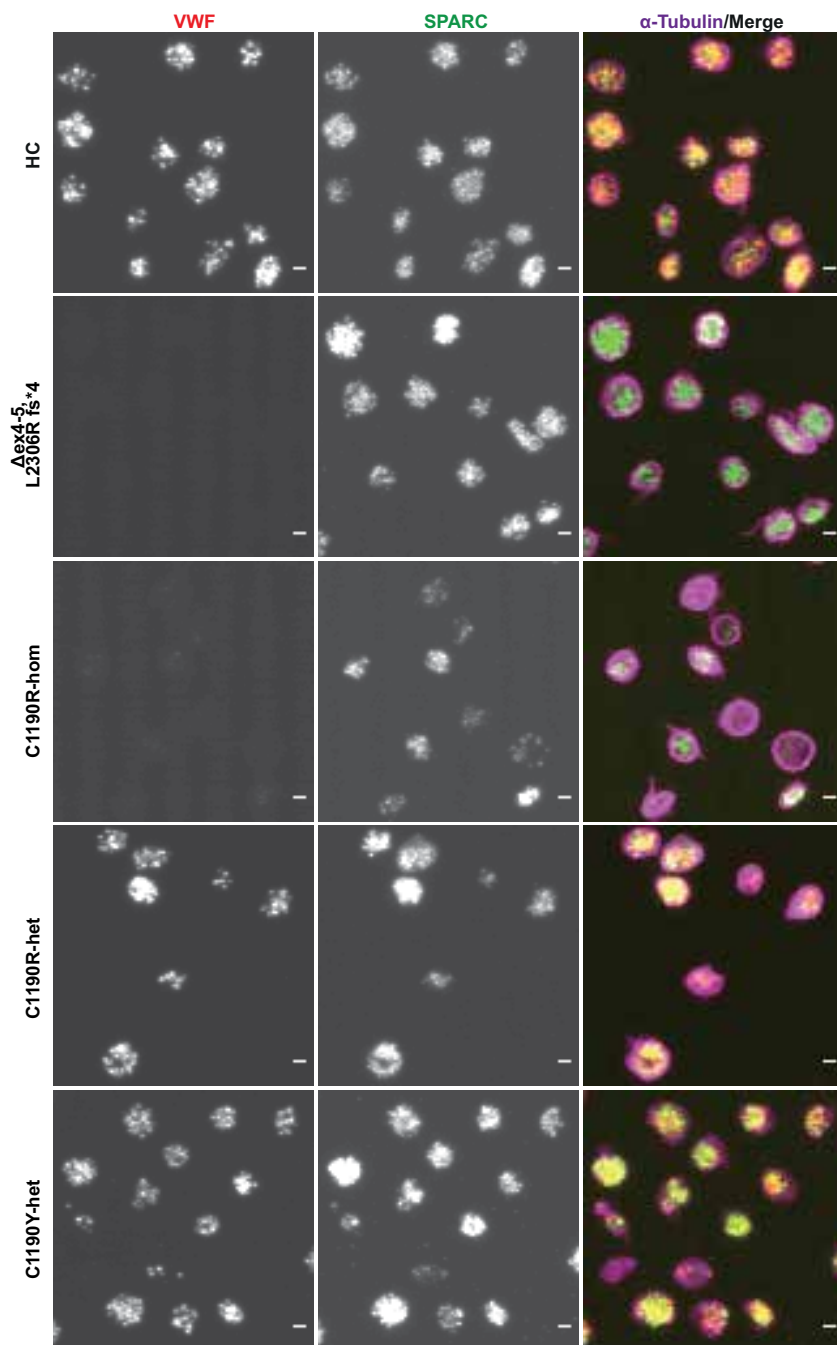
Supplementary Figure S7. SIM images of VWD patients.

Resting platelets from healthy individuals (HC), type 3 ( $\Delta$ ex4-5, C1190R-hom) and type 2A (C1190R-het, C1190Y-het) VWD patients were imaged for VWF (red), SPARC (green) and alpha-tubulin (magenta). Representative overview images are shown. Scale bar is 3 $\mu$ m.



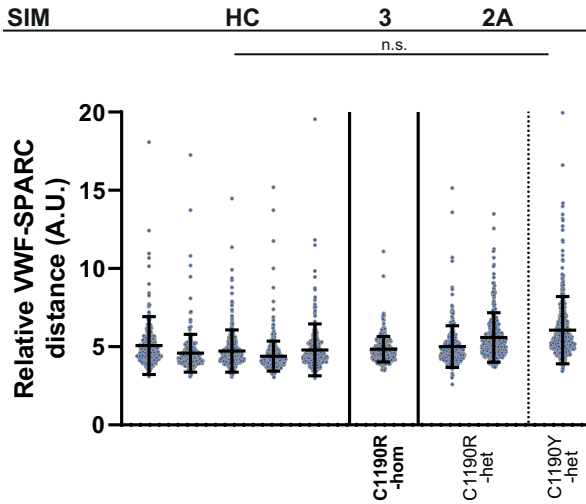
Supplementary Figure S8. Correlation between alpha-granule proteins and platelet size in healthy individuals.

VWF- and SPARC-positive objects and total volumes were assessed in five different healthy donors (illustrated by different colors), and correlated to relative platelet size as measured by marginal band area. Correlation lines are shown per donor.



Supplementary Figure S9. Confocal images of VWD patients.

Resting platelets from healthy individuals (HC), type 3 ( $\Delta$ ex4-5, C1190R-hom) and type 2A (C1190R-het, C1190Y-het) VWD patients were imaged for VWF (red), SPARC (green) and alpha-tubulin (magenta). Representative overview images are shown. Scale bar is 1  $\mu$ m.



Supplemental Figure S10. Co-localization of VWF and SPARC across healthy controls and VWD patients.

Degree of co-localization between VWF and SPARC was assessed in platelets based on distance measurements between unique VWF-positive and SPARC-positive objects. Co-localization analysis could not be performed for one type 3 VWD patient as they did not have any VWF-positive objects. n.s. = non significant

## References

1. Slot JW, Geuze HJ. Cryosectioning and immunolabeling. *Nat Protoc.* 2007; 2: 2480-91.
2. Sezgin M, Sankur B. Survey over image thresholding techniques and quantitative performance evaluation. *J Electron Imaging.* 2004; 13: 146-68.
- 3 Ollion J, Cochenne J, Loll F, Escude C, Boudier T. TANGO: a generic tool for high-throughput 3D image analysis for studying nuclear organization. *Bioinformatics.* 2013; 29: 1840-1.

# Chapter 6

## Quantitative Super-resolution Imaging of Platelet Degranulation Reveals Differential Release of VWF and VWF-Propeptide from $\alpha$ -granules

Maurice Swinkels, Sophie Hordijk, Petra E. Bürgisser, Johan A. Slotman, Tom Carter, Frank W. G. Leebeek, A. J. Gerard Jansen, Jan Voorberg, Ruben Bierings

Journal of Thrombosis and Haemostasis 2023 Jul;21(7):1967-1980

## Abstract

*Background:* Von Willebrand factor (VWF) and VWF propeptide (VWFpp) are stored in eccentric nanodomains within platelet alpha-granules. VWF and VWFpp can undergo differential secretion following Weibel-Palade body exocytosis in endothelial cells; however, it is unclear if the same process occurs during platelet alpha-granule exocytosis. Using a high-throughput 3-dimensional super-resolution imaging workflow for quantification of individual platelet alpha-granule cargo, we studied alpha-granule cargo release in response to different physiological stimuli.

*Objectives:* To investigate how VWF and VWFpp are released from alpha-granules in response to physiological stimuli.

*Methods:* Platelets were activated with protease-activated receptor 1 (PAR-1) activating peptide (PAR-1 ap) or collagen-related peptide (CRP-XL). Alpha-tubulin, VWF, VWFpp, secreted protein acidic and cysteine rich (SPARC), and fibrinogen were imaged using 3-dimensional structured illumination microscopy, followed by semiautomated analysis in FIJI. Uptake of anti-VWF nanobody during degranulation was used to identify alpha-granules that partially released content.

*Results:* VWFpp overlapped with VWF in eccentric alpha-granule subdomains in resting platelets and showed a higher degree of overlap with VWF than SPARC or fibrinogen. Activation of PAR-1 (0.6-20  $\mu$ M PAR-1 ap) or glycoprotein VI (GPVI) (0.25-1  $\mu$ g/mL CRP-XL) signaling pathways caused a dose-dependent increase in alpha-granule exocytosis. More than 80% of alpha-granules remained positive for VWF, even at the highest agonist concentrations. In contrast, the residual fraction of alpha granules containing VWFpp decreased in a dose-dependent manner to 23%, whereas SPARC and fibrinogen were detected in 60% to 70% of alpha-granules when stimulated with 20  $\mu$ M PAR-1 ap. Similar results were obtained using CRP-XL. Using an extracellular anti-VWF nanobody, we identified VWF in postexocytotic alpha-granules.

*Conclusion:* We provide evidence for differential secretion of VWF and VWFpp from individual alpha-granules.

**Keywords:**

blood platelets, exocytosis, hemostasis, secretory vesicles, von Willebrand factor

**Essentials**

- Activated platelets secrete hemostatic proteins from alpha-granules.
- We investigated how von Willebrand factor (VWF) and VWF propeptide (VWFpp) are released from platelet alpha-granules.
- VWF and VWFpp are localized in the same eccentric alpha-granule subdomain in resting platelets.
- VWF and VWFpp are differentially secreted from individual alpha-granules upon activation.

## Introduction

During thrombopoiesis, several types of secretory granules from bone marrow megakaryocytes are packaged into budding platelets. Release of their content enables platelets to rapidly respond to changes in their environment, such as during injury, inflammation, or when encountering pathogens. Alpha-granules are the most abundant platelet secretory organelle and contain various proteins and molecules involved in the hemostatic response [1,2]. Among these is von Willebrand factor (VWF), a key hemostatic adhesive glycoprotein whose main roles are to facilitate platelet adhesion to vascular injury sites and to stabilize coagulation factor VIII in the circulation [3]. VWF is also produced by endothelial cells and stored in Weibel-Palade bodies (WPBs), where it can be released via exocytosis following cellular activation. Circulating VWF levels in plasma are primarily maintained through basal secretion of WPBs from the endothelium [4].

Our knowledge of VWF biosynthesis primarily comes from studies utilizing endothelial cells and heterologous expression systems as cellular models. As it progresses through the secretory pathway, VWF undergoes several posttranslational processing steps, which include dimerization, glycosylation, and multimerization into long platelet-adhesive concatemers [3]. Within the acidifying milieu of the Golgi, VWF multimers condense into helical VWF tubules that lend WPBs their characteristic rod-like shape [5]. Here, a large N-terminal moiety called VWF propeptide (VWFpp) is proteolytically cleaved from the mature VWF chain. In endothelial cells, cleaved VWFpp remains noncovalently associated with VWF due to prevailing conditions in the Golgi and beyond (low pH and high Ca<sup>2+</sup>), leading to its copackaging in the developing WPBs [6]. VWFpp is essential for VWF multimerization, tubulation, and WPB biogenesis [7–9] and becomes an integral part of VWF tubules *in vitro* and *in vivo* [10,11]. During exocytosis, the vesicle interior neutralizes, leading to rapid decondensation of VWF tubules [12,13] and loss of noncovalent association between VWF and VWFpp [14]. Depending on the type of exocytosis (full fusion, lingering kiss, or compound fusion) [4] and extracellular environment, VWF, VWFpp, and other WPB cargo molecules undergo divergent fates postrelease [14–17].

In platelets, VWF is zonally packaged within eccentric alphagranule nanodomains, which also contain short VWF tubules [18–20], and can be released upon stimulus [21]. Platelets also contain VWFpp [22] and are able to secrete the protein following stimulation with various agonists that induce alpha-granule release [23]. However, the organization of VWFpp in alpha-granules or its release from alpha-granules has not been documented in detail. Similar to endothelial WPBs, platelet alpha-granules can undergo single and compound exocytosis depending on the type and magnitude of stimulus [24,25]. Following activation, alpha-granule cargo such as VWF, fibrinogen, chemokines, and other mediators are not released uniformly but can vary significantly between proteins in terms of release kinetics and in the proportions that are released or retained after degranulation [26–28]. Many of these cargo proteins are nonhomogeneously distributed within alpha-granules

[20,27,29–31], which has led to the hypothesis that their differential release is the result of uneven solubilization of alpha-granule cargo clusters [26]. It is unclear how these processes influence the efficiency of release of VWF and VWFpp specifically or whether VWF and VWFpp release from platelet alpha-granules is comparable to their release from endothelial cell storage organelles.

In this study, we investigated the storage and release of VWF and VWFpp in platelets using 3 dimensional structured illumination microscopy (3D-SIM). We show that VWF and VWFpp reside in a distinct alpha-granule subdomain not occupied by other alpha-granule proteins such as fibrinogen. Using quantitative 3D-SIM analysis of residual VWF and VWFpp in activated platelets, we demonstrate that VWFpp is efficiently released from platelets in a dose-dependent manner and, even at maximal activation, the bulk of VWF remains associated with platelets in postfusion structures. Our study sheds new light on divergent outcomes of VWF and VWFpp following release from platelet alpha-granules.

## Methods

### Platelet isolation

All steps were performed at room temperature (RT) unless otherwise stated. Whole blood was drawn from consenting healthy donors in citrate tubes. Washed platelets were prepared as described previously [20]. In brief, platelet-rich plasma was generated by centrifugation at 120 x g for 20 minutes with low acceleration (maximum 5) and low brake (maximum 3). Platelet-rich plasma was washed once in 10% acid-citrate dextrose buffer (85 mM Na<sub>3</sub>-citrate, 71 mM citric acid, and 111 mM glucose) with 111 μM prostaglandin E<sub>1</sub> (Sigma) and twice in washing buffer (36 mM citric acid, 103 mM NaCl, 5 mM KCl, 5 mM EDTA, and 5.6 mM glucose, pH 6.5) with 11 μM and 0 μM prostaglandin E<sub>1</sub>, respectively, and then resuspended at 250 x 10<sup>3</sup> platelets/μL in assay buffer (10 mM HEPES, 140 mM NaCl, 3 mM KCl, 0.5 mM MgCl<sub>2</sub>, 10 mM glucose, and 0.5 mM NaHCO<sub>3</sub>, pH 7.4).

### Platelet activation

Washed platelets at 250 x 10<sup>3</sup> platelets/μL were stimulated with 0 to 20 μM of protease-activated receptor 1 activating peptide (PAR-1 ap, Peptides International) or 0 to 1 μg/mL of collagen-related peptide (CRP-XL, CambCol Labs) for 30 minutes at 37 °C. Reactions were stopped by adding 1% paraformaldehyde (final concentration) for 5 minutes and then quenched with 50 mM NH<sub>4</sub>Cl for 5 minutes. Samples were diluted in a large volume of washing buffer, washed once, and resuspended in assay buffer at approximately 250 x 10<sup>3</sup>/μL.

### VWF nanobody internalization assay

Washed platelets were incubated with nanobodies directed against the VWF C-terminal cystine knot domain or control nanobodies (s-VWF and R2, respectively [32]; kindly supplied by Dr Coen Maas, UMCU, The Netherlands) at a final concentration of 1 μg/mL

and were stimulated as described above. Internalized nanobodies were detected using goat anti-Alpaca IgG-AF488 (Jackson ImmunoResearch).

### Flow cytometry

Small aliquots were used for quality control of platelet activation by flow cytometry. Samples were stained with CD61-APC (BD Biosciences, 1:400) and CD62P-PE (BD Biosciences, 1:100) or with secondary anti-Alpaca IgG-AF488 (Jackson ImmunoResearch, 1:400) for 15 minutes at RT, diluted in assay buffer, and immediately read on a FACS Canto II flow cytometer (BD Biosciences). In some cases, fixed platelets were permeabilized with 0.05% saponin before staining. Forward scatter (FSC) and side scatter (SSC) parameters were used to gate platelets and single cells, whereas single stains and isotype controls were used to determine fluorescence gating.

### Platelet seeding and immunofluorescence

Seeding and staining were performed as described previously [20]. In brief, all unique sample conditions were seeded on poly-D-lysine coated 9-mm diameter 1.5H high-precision coverslips (Marienfeld), permeabilized, and stored in PBS supplemented with 0.2% gelatin, 0.02% azide, and 0.02% saponin (PGAS). Primary and secondary antibody staining was performed in PGAS for 30 minutes at RT and washed 3 times with PGAS following incubations. The antibodies used are listed in Supplementary Table S1. Finally, slides were dipped in PBS, mounted in Mowiol, and imaged within 1 week.

### Structured illumination and confocal microscopy and image analysis

All samples were imaged with SIM (Elyra PS.1, Zeiss) and confocal microscopy (SP8, Leica). Three representative fields of view were collected per donor, using 40 Z-slices with an interval of 110 nm (4.4 $\mu$ m in total). Raw SIM images were reconstructed with state-of-the-art Zen Software (Zeiss). Due to very bright alpha-tubulin signals and relatively broad emission filters, crosstalk between far-red and red channels was observed, which was corrected equally in all applicable images by subtracting the far-red channel (alpha-tubulin) from the red channel. The number of 3D granular structures per platelet was separately quantified for VWF, VWFpp, secreted protein acidic and cysteine rich (SPARC), and Fbg. SIM images were analyzed through ImageJ-based processing workflows as described in detail previously [20]. In brief, individual platelets were segmented based on alpha-tubulin staining, and individual 2D and 3D granular structures were quantified based on individual staining (eg, VWF/VWFpp) by automated thresholding. Platelets in which 2D and 3D granule counts within the same channel differed by more than 15 were excluded from analysis.

For analyzing the nanobody internalization assay, images without alpha-tubulin were segmented in individual platelets based on local differences in signal intensity using in-house written macro-code (available from our <https://github.com/Clotterdam> repository). VWF+ granules were identified with 3D Object Counter [33] and converted

into a mask in which the presence of VWFpp and/or VWF nanobody was measured.

### **Immunoblotting**

Human umbilical vein endothelial cells (grown as previously described[34]) and washed platelets were lysed in NP-40 buffer (0.5% NP-40, 150 mM NaCl, 10 mM Tris, and 5 mM EDTA, pH 8.5). Lysate samples, normalized for VWF concentration, were separated on 4% to 12% Bis-Tris NuPAGE gels (Invitrogen) under reducing conditions and transferred to 0.2  $\mu$ m nitrocellulose membranes. Membranes were probed with rabbit anti-VWF (DAKO) and rabbit anti-VWFpp [17], followed by LT680-labeled donkey anti-rabbit secondary antibodies (Li-COR). The membranes were scanned on an Odyssey scanner (Li-COR).

### **Platelet secretion assay and VWF and VWFpp ELISA**

Washed platelets ( $5.6 \times 10^6$  platelets in a final volume of 200  $\mu$ L) of 4 independent, healthy donors were stimulated with 0 to 20  $\mu$ M of PAR-1 activating peptide (Peptides International) or 0 to 1  $\mu$ g/mL collagen-related peptide (CRP-XL, CambCol Labs) for 30 minutes at 37 °C. Releasates and platelets were separated by centrifugation (13 000 x g), after which platelet pellets were lysed in 50  $\mu$ L lysis buffer (1% Triton X-100, 10% glycerol, 50 mM Tris-HCL, 100 mM NaCl, and 1mM EDTA, pH 7.4). VWF and VWFpp secretion was determined using sandwich ELISA as described earlier [35], using rabbit polyclonal anti-human VWF (DAKO; 0.5  $\mu$ g/well) or mouse monoclonal anti-human VWFpp (CLBPro35; 1.0  $\mu$ g/well) as coating antibodies and horseradish peroxidase (HRP)-conjugated rabbit polyclonal anti-human VWF (DAKO; 0.5  $\mu$ g/mL) or HRP-conjugated mouse monoclonal anti-human VWFpp (CLBPro14-3; 0.125  $\mu$ g/mL) for detection. Blocking, washing, and detection steps were performed in PBS supplemented with 0.1% Tween-20, 0.2% gelatin and 1 mM EDTA. HRP activity was measured by colorimetric detection of 3,3',5,5'-tetramethylbenzidine conversion using a Victor X4 microplate reader (Perkin Elmer). All samples were measured in duplicate in 3 different dilutions. Concentrated conditioned media from HEK293Ts stably expressing human wildtype VWF and VWFpp [36], which was calibrated against a normal plasma pool of >30 donors, was used as a standard.

### **Statistical analysis**

Individual stimulation conditions were compared with resting platelets by 2-way analysis of variance (ANOVA). Multiple comparisons were corrected using Sidak's multiple comparisons test. All statistical analyses were performed using GraphPad Prism (version 8). Data are presented as mean  $\pm$  95% CI unless stated otherwise. A P value of <.05 was considered statistically significant.

## **Results**

### **VWFpp colocalizes with mature VWF in eccentric alpha-granule nanodomains**

Localization of VWF and VWFpp in resting platelets was studied using 3D-SIM [20].

VWF- and VWFpp-immunoreactivity were localized to discrete regions within the platelet (Figure 1A, Supplementary Figure S1) that were encapsulated by a P-selectin-positive membrane (Supplementary Figure S2). In the presence of SPARC and fibrinogen, these regions were identified as alpha-granules within platelet cytoplasm (Figure 1B, C). Consistent with previous ultrastructural studies [18–20,31], close inspection of our images showed that VWF and VWFpp were colocalized in a subdomain within the alpha granule (Figure 1A), whereas SPARC or fibrinogen showed a more homogenous distribution and appeared to be excluded from these VWF containing nano-domains (Figure 1B, C). Colocalization analysis confirmed striking overlap between VWF- and VWFpp immunoreactivity within individual alpha-granules (Pearson's colocalization coefficient ( $PCC_{VWFpp}$ : 0.521; Manders' colocalization coefficient ( $MCC1_{VWFpp}$ : 0.590;  $MCC2_{VWFpp}$ : 0.548), (Figure 1D), whereas the overlap between VWF and SPARC or fibrinogen was lower, as expected (SPARC:  $PCC_{SPARC}$  0.336,  $MCC1_{SPARC}$  0.386,  $MCC2_{SPARC}$  0.498; fibrinogen:  $PCC_{Fibrinogen}$  0.369,  $MCC1_{Fibrinogen}$  0.467,  $MCC2_{Fibrinogen}$  0.571) (Figure 1D–E). In these experiments, a rabbit polyclonal antibody that specifically recognizes the cleaved and processed carboxyterminal octapeptide of VWFpp was used to visualize endogenous VWFpp [17]. Immunoblot analysis confirmed that in both endothelial and platelet lysates, this VWFpp antibody exclusively recognizes a 100 kDa protein corresponding to the size of VWFpp (Supplementary Figure S3). Probing for VWF, it was clear that platelets, unlike endothelial cells, contain only mature VWF and no detectable proVWF (Supplementary Figure S3), suggesting that proteolytic processing of proVWF into mature VWF and VWFpp is completed before or during the formation of alpha-granules in megakaryocytes and does not continue after budding of platelets. Thus, the striking overlap of VWF and VWFpp in our SIM analysis suggests that both proteins are incorporated into the same supramolecular structures within alpha-granules and are not the result of cross-reaction of the VWFpp antibody with unprocessed proVWF.

### Differential loss of VWF and VWFpp from post-exocytotic alpha granules of activated platelets

We next investigated VWF and VWFpp secretion from individual platelet alpha granules following strong activation of PAR-1 (20  $\mu$ M PAR-1 ap) or GPVI (1  $\mu$ g/mL CRP-XL) signaling pathways to drive a high level of platelet activation and degranulation (Supplementary Figures S4 and S5). We quantified the number of VWF+ and VWFpp+ structures (alpha-granules) before and after stimulation using 3D-SIM. After PAR-1 stimulation, we observed little change in the number of VWF+ structures; however, there was a dramatic reduction in VWFpp+ structures consistent with secretion of VWFpp (Figure 2A). The remaining VWF staining was confined to P-selectin (CD62P) labeled structures, suggesting that the protein mostly resides in postexocytotic alpha-granules (Supplementary Figure S6). Stimulation with 1 $\mu$ g/mL CRP-XL gave similar results to PAR-1 ap (Figure 2C). These data suggest that VWF and VWFpp may be differentially released by activated platelets despite their close proximity within alpha-granules in resting platelets.

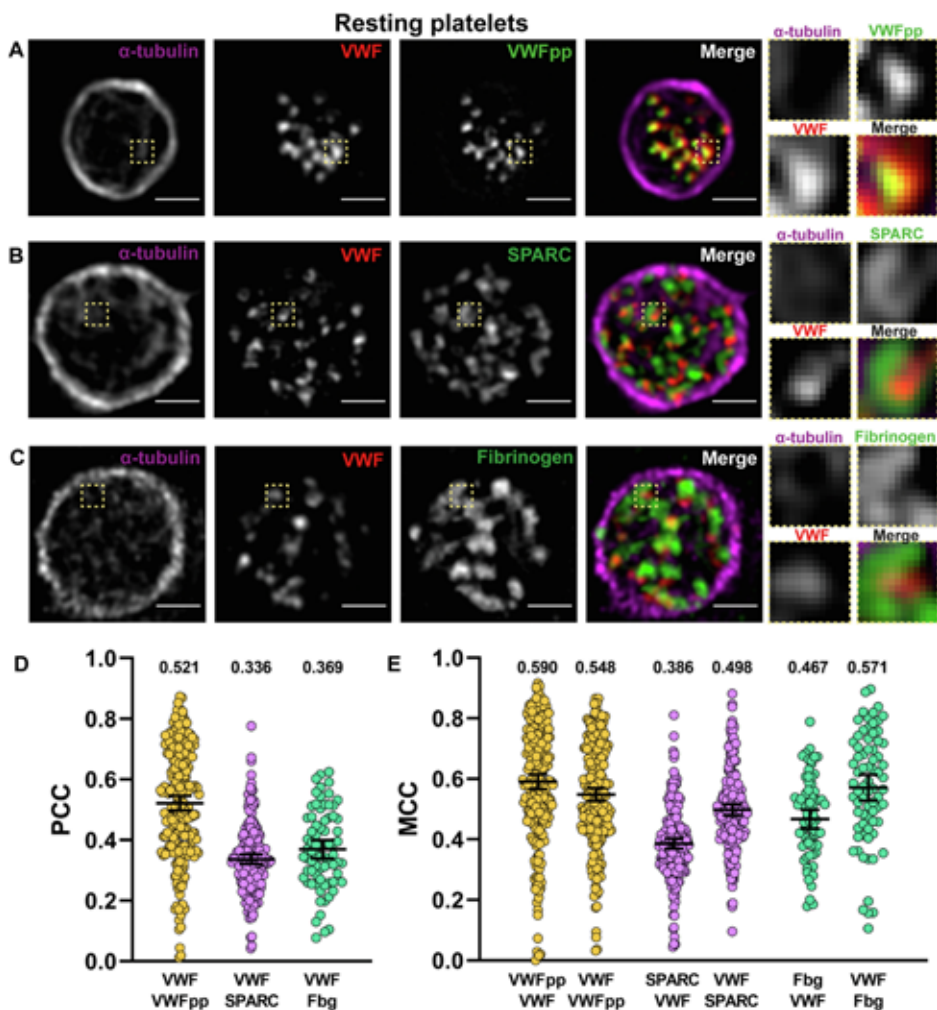


Figure 1. VWF and VWFpp localization in resting platelets.

(A, B) Resting platelets were stained for alpha-tubulin (magenta), VWF (red, mouse monoclonal anti-VWF, CLB-RAg20), and (A) VWFpp (green), or (B) fibrinogen (green). (C) Resting platelet stained for alpha-tubulin (magenta), VWF (red, rabbit polyclonal anti-VWF, DAKO), and SPARC (green). Imaging was performed by SIM, and representative high resolution single-plane, magnified images are shown. Areas within yellow squares that contain single granules are magnified on the right (yellow square). The scale bar represents 1  $\mu$ m. (D, E) Colocalization analysis for VWF with alpha-granule proteins VWFpp, SPARC, and fibrinogen. (D) Pearson's colocalization coefficients (PCC) and (E) pairwise Manders' colocalization coefficients (MCC) for individual platelet images (VWF-VWFpp  $n = 239$ , VWF-SPARC  $n = 199$ , VWF-Fibrinogen  $n = 73$ ) show VWF has a higher overlap with VWFpp than with SPARC or fibrinogen. Bars indicate means with 95% CIs and mean PCC and MCC values are at the top of the graph. SIM, structured illumination microscopy; SPARC, secreted protein acidic and cysteine rich; VWF, von Willebrand factor; VWFpp, VWF propeptide.

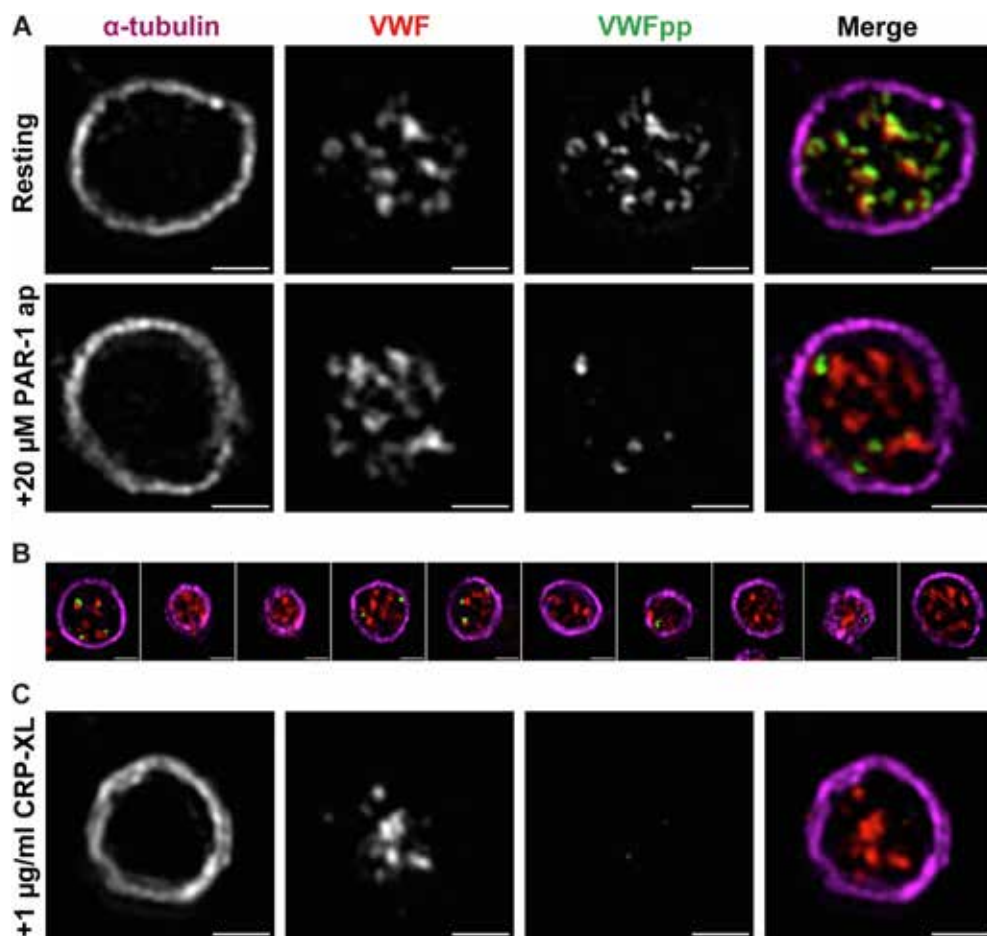


Figure 2. Release of VWF and VWFpp from alpha granules.

Platelets were stimulated for 30 minutes with vehicle or 20 $\mu$ M PAR-1 ap (A, B) or 1  $\mu$ g/mL CRP (C) and stained for alpha-tubulin (magenta), VWF (red, CLB-RAg20) and VWFpp (green). Single-plane magnified images are shown (A, C), as well as a panel of single-plane magnified images of 10 random platelets (B). The scale bar represents 1  $\mu$ m. CRP, collagen related peptide; PAR-1 ap, protease-activated receptor 1 activating peptide; VWF, von Willebrand factor; VWFpp, VWF propeptide.

Differences in VWF and VWFpp release in relation to agonist responsiveness may be explained by the large differences in size between VWF and VWFpp (VWFpp is a 100-kDa protein, whereas ultralarge VWF multimers can be in excess of 100 MDa), but we also looked at exocytosis of other alpha-granule constituents. SPARC (40kDa) immunoreactivity was decreased more extensively than for VWF (Figure 3A); however, changes in fibrinogen (340 kDa) immunoreactivity were qualitatively similar to that of VWF (Figure 3B). This would suggest that additional factors other than protein size play a role in facilitating differential agonist responsiveness of VWF vs VWFp.

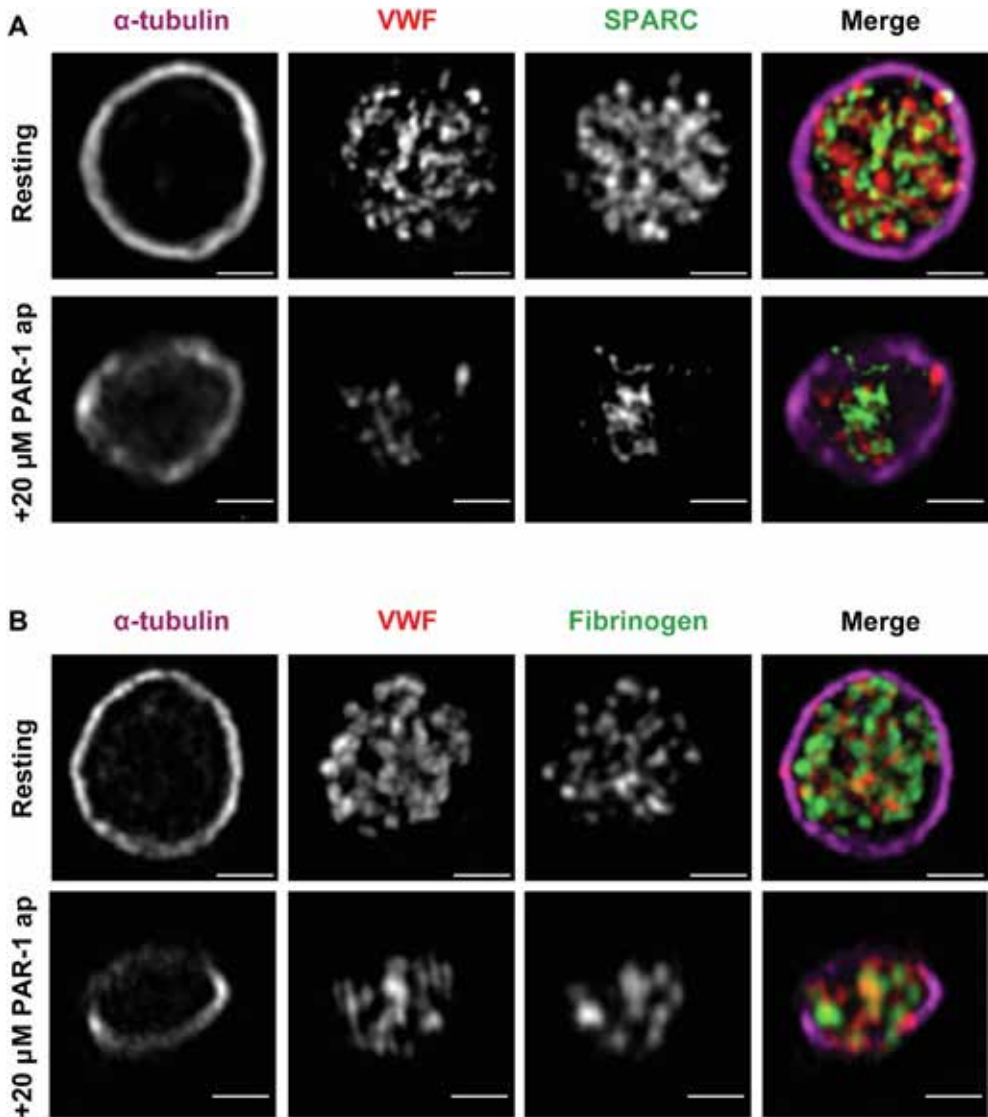


Figure 3. Release of SPARC and fibrinogen from alpha-granules.

Platelets were stimulated with 20  $\mu$ M PAR-1 and compared with resting platelets for release of alpha-granule proteins. Immunofluorescent staining for alpha-tubulin (magenta) in combination with (A) VWF (red, DAKO) and SPARC (green) or (B) VWF (red, CLB-RAg20) and fibrinogen (green). Single-plane, representative magnified images are shown. The scale bars represent 1  $\mu$ m. PAR-1, protease-activated receptor 1; SPARC, secreted protein acidic and cysteine rich; VWF, von Willebrand factor; VWFpp, VWF propeptide.

### Differential release of VWF and VWFpp relates to agonist responsiveness

Having established that strong platelet stimulation results in differential release of VWF and VWFpp, we next asked whether this phenomenon was influenced by stimulus strength. For this, we used a semiautomated quantitative workflow on 3D-SIM images [20] of platelets activated with a broad concentration range of PAR-1 and CRP-XL that partially or fully trigger alpha-granule release (Supplementary Figure S4). We found that differential release of VWF and VWFpp was apparent at all stimulus concentrations of PAR-1 ap (Figure 4A); however, it was clear that less VWFpp was retained in postexocytotic alpha-granules as the stimulus strength was increased. At 0.625  $\mu\text{M}$  PAR-1 ap, the fraction of VWFpp+ alpha granules was 76.8% compared with control platelets ( $p < .0001$ , 2-way ANOVA), and this fraction reduced to 23.4% at 20 $\mu\text{M}$  PAR-1 ap ( $p < .0001$ , 2-way ANOVA). In contrast, for 20  $\mu\text{M}$  PAR-1 ap, the fraction of VWF+ alpha granules was 80.9% of the control ( $p < 0.0001$ , 2-way ANOVA). This difference between the retention of VWF and VWFpp was significant at all stimulus strengths. Similar findings were obtained using CRP-XL (Supplementary Figure S7A, B). Consistent with our 3D-SIM-based exocytosis assay, biochemical analysis showed that VWFpp and VWF were differentially secreted following dose dependent activation of PAR-1 or GPVI signaling (Figure 4C, D, Supplementary Figure S7C, D).

The release of SPARC and fibrinogen from alpha-granules showed a different pattern (Supplementary Figure S8). The fraction of SPARC+ or fibrinogen+ alpha granules present in stimulated platelets was reduced to 60.7% and 67.6% of the control at 20  $\mu\text{M}$  PAR-1 ap, respectively. The data illustrated that the extent of cargo release was protein specific.

In conclusion, we observed a large disparity in alpha-granule release of VWF versus VWFpp, where the former was partially retained in alpha-granules, even under strong stimulatory conditions. In contrast, VWFpp release was sensitive to lower agonist concentrations.

### Anti-VWF nanobody incorporates in postexocytotic VWF<sup>+</sup> structures in degranulation dependent manner

Finally, we wanted to study how and when individual alpha-granule structures differentially release VWF versus VWFpp. As we clearly identified granule populations that contained residual VWF but no more VWFpp, this would suggest that individual alpha-granules could perform a kiss-and-run type of exocytosis that facilitates release of selective alpha-granule cargo. To investigate this theory further, we performed a platelet degranulation experiment with an anti-VWF nanobody added in suspension, assuming that opening an alpha-granule during exocytosis would facilitate uptake of the nanobody. We found that uptake of the nanobody was directly dependent on the degree of platelet stimulation and, thus, degranulation, whereas a control R2 nanobody nonspecific for VWF did not show any signal by flow cytometry (Supplementary Figure S10A). Additionally, permeabilized platelets showed an increasingly higher mean fluorescent intensity at higher doses of PAR-1, suggesting increasing amounts of nanobody specifically inside platelets (Supplementary Figure S10A). We further confirmed

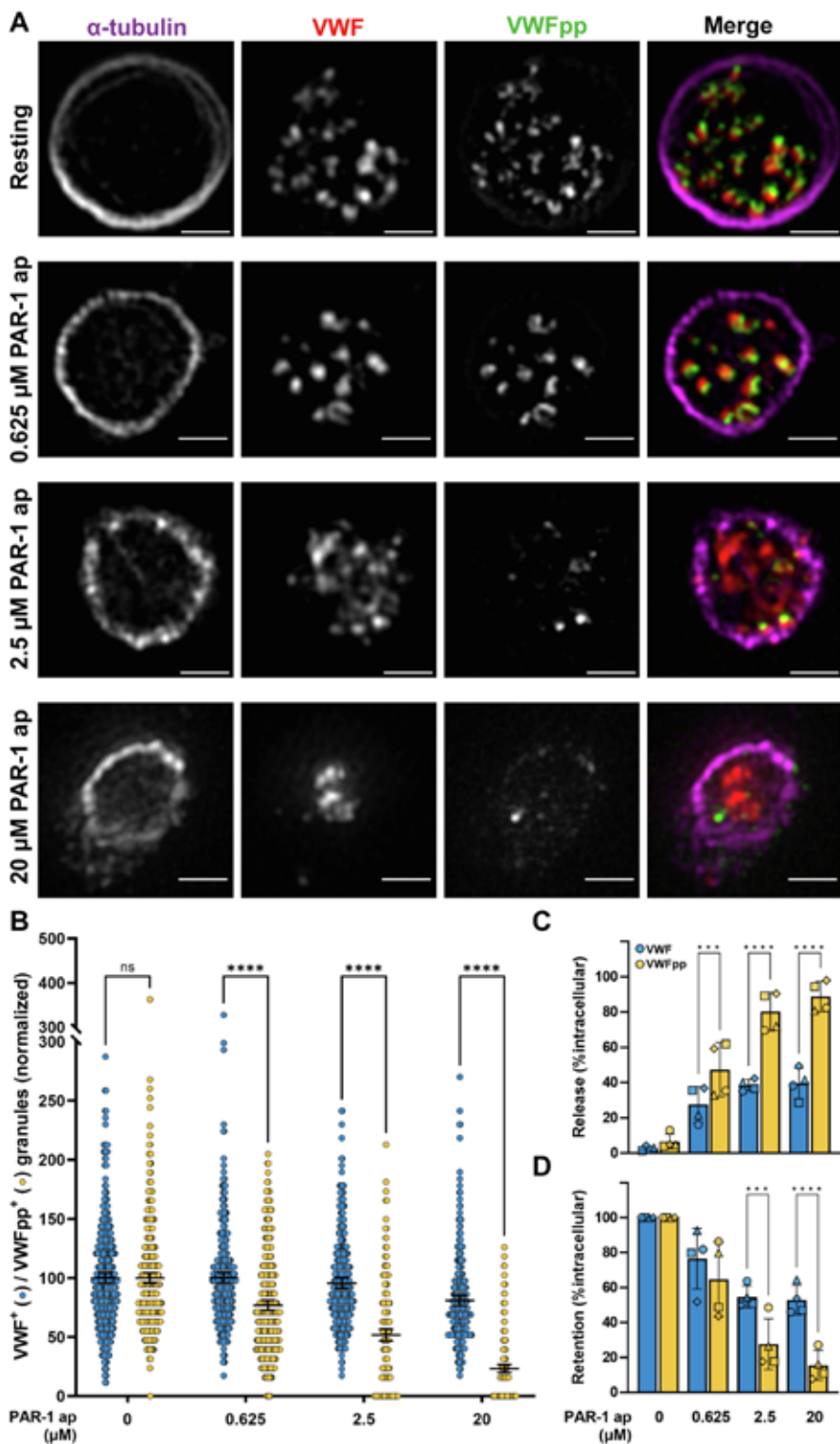


*Figure 4. Dose-response release of VWF and VWFpp.*

(A) Platelets were stimulated with 0 to 20  $\mu\text{M}$  PAR-1 ap and stained for alphas-tubulin (magenta), VWF (red, CLB-RAG20), and VWFpp (green). Representative single-plane, magnified images are shown. Scale bars represent 1  $\mu\text{m}$ . (B) VWF and VWFpp release was assessed by quantification of residual VWF<sup>+</sup> or VWFpp<sup>+</sup> structures in platelets normalized to resting platelets. Counts are pooled from 3 independent, healthy donors: 0  $\mu\text{M}$  PAR-1 ap n = 435; 0.625  $\mu\text{M}$  PAR-1 ap n = 365; 2.5  $\mu\text{M}$  PAR-1 ap n = 318; and 20  $\mu\text{M}$  PAR-1 ap n = 280 platelets. Absolute platelet counts per donor are stated in Supplementary Figure S9. The release (C) and retention (D) of VWF and VWFpp in PAR-1 ap stimulated platelets were measured by ELISA and normalized to resting intracellular content. Statistical analysis was performed by 2-way ANOVA with Sidak's multiple comparisons test at significance levels of \*\*\*p < .001 and \*\*\*\*p < .0001. The bars show means with 95% CIs. PAR-1 ap, protease-activated receptor 1 activating peptide; VWF, von Willebrand factor; VWFpp, VWF propeptide.

this with confocal imaging, where we observed accumulation of the nanobody inside the tubulin ring at 20  $\mu\text{M}$  PAR-1 ap but not in resting platelets (Supplementary Figure S10B).

Additionally, the nanobody colocalized completely with residual VWF<sup>+</sup> structures, suggesting that all VWF<sup>+</sup> granules are postexocytotic under these conditions. Together, these findings show that the uptake of the VWF nanobody is degranulation dependent. Ultimately, we analyzed individual alpha-granules that were able to take up the VWF nanobody through 3D-SIM. In accordance with flow cytometry and confocal data, we found an increasing population of VWF nanobody<sup>+</sup> structures colocalizing with residual VWF that was directly related to the degree of stimulation. Most resting platelets contained granules with overlapping VWF and VWFpp signals (Figure 5A). At a low dose of PAR-1 ap (Figure 5B), only a minority of granules was strongly positive for the nanobody. However, most granules were VWF<sup>+</sup> and VWFpp<sup>+</sup> but revealed weak staining for the nanobody. At a maximum dose of PAR-1 ap, we found a majority of VWF nanobody<sup>+</sup> and VWF<sup>+</sup> granules, but these did not contain any VWFpp (Figure 5A, B), suggesting that this content has been released during granule opening. Taken together, our findings imply that increasing doses of PAR-1 ap trigger large-scale release of VWFpp from alpha-granules, whereas VWF is partially retained in such postexocytotic granules as evidenced by PAR-1-dependent accumulation of VWF nanobody in VWFpp-VWF<sup>+</sup> structures. Our cumulative findings show that alpha-granules may exclusively release content like VWFpp while maintaining other cargo, like VWF, under the conditions described in our work.

## Discussion

Important biochemical and functional differences exist between platelet and endothelial (plasma) VWF [37] that suggest dissimilarities in biosynthesis of VWF between endothelial cells and megakaryocytes: platelet VWF is composed of higher molecular weight multimers and carries different N-linked glycan structures, which makes it more resistant to proteolysis by ADAMTS13 [38] and has higher binding affinity for alphaIIb $\beta$ 3 integrin [39]. In this study, we investigated the storage and exocytosis of VWF and VWFpp from platelet alpha

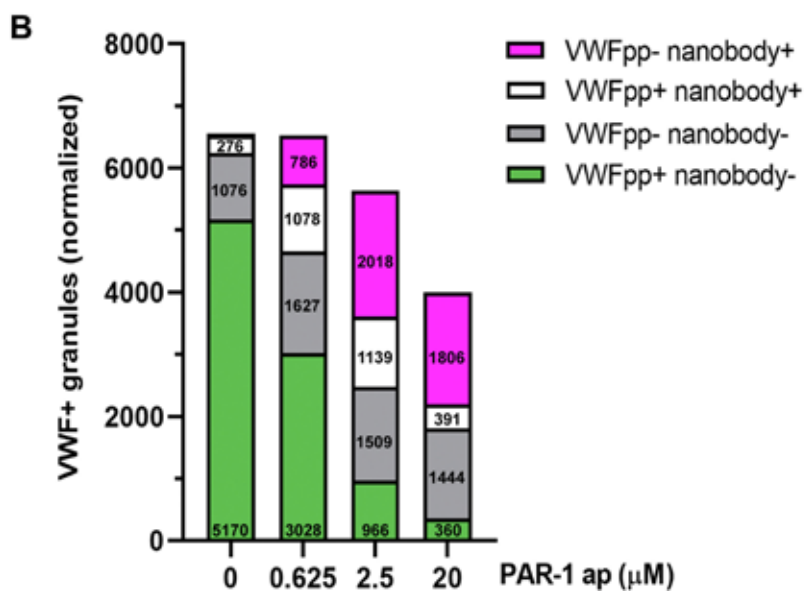
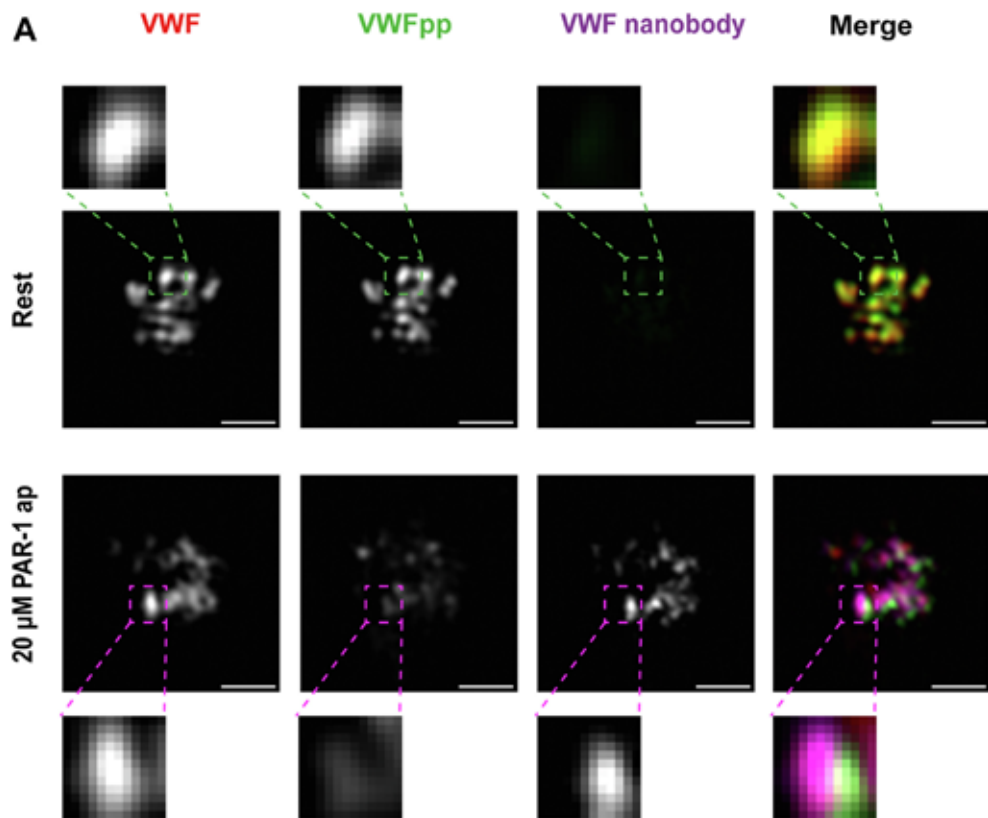


Figure 5. SIM analysis of VWF nanobody uptake during alpha granule release.

(A) Platelets were stimulated with 0 to 20  $\mu\text{M}$  of PAR-1 ap in the presence of 1  $\mu\text{g}/\text{mL}$  VWF nanobody (magenta) and stained for VWF (red, CLB-RAG20) and VWFpp (green). A single-plane, representative magnified image of granule content of a resting and maximum stimulated platelet. The magnified region shows single granule content. Scale bar represents 1  $\mu\text{m}$ . (B) Granule populations of positive VWF/VWFpp/VWF-nanobodies were quantified for each stimulus condition. Platelet counts are pooled from 4 independent, healthy donors: 0  $\mu\text{M}$  PAR-1 ap n = 835; 0.625  $\mu\text{M}$  PAR-1 ap n = 696; 2.5  $\mu\text{M}$  PAR-1 ap n = 748; and 20  $\mu\text{M}$  PAR-1 ap n = 620 platelets. Granule counts were normalized to the number of platelets that were analyzed and indicated within their respective boxes within the stacked bar graph. PAR-1 ap, protease-activated receptor 1 activating peptide; SIM, structured illumination microscopy; VWF, von Willebrand factor; VWFpp, VWF propeptide.

granules through quantitative super-resolution microscopy. Our results showed that VWFpp was eccentrically localized within alpha granules in close proximity to mature VWF. In endothelial cells, VWFpp was integrated into tubules composed of helically condensed VWF multimers found within WPBs. Given that similar tubules, albeit shorter in length, have been observed in platelet alpha-granules [19], we speculated that VWFpp is similarly arranged within VWF tubules as in endothelial WPBs.

In contrast to WPBs, where the tubular arrangement of VWF is essential for its rapid and efficient release upon exocytosis, alpha-granules only released a limited amount of their VWF, even at agonist concentrations that elicited maximum surface exposure of P-selectin and led to incorporation of anti-VWF nanobody into practically all the remaining VWF-positive structures. The latter is important because it implies that all these granules have undergone a granule fusion event that generated a fusion pore in contact with the extracellular space. Additionally, we found evidence for differential release of VWFpp and VWF, showing that individual alpha-granules can preferentially release their VWFpp cargo while retaining VWF. Differential release was dependent on stimulus strength but not related to the type of agonist we used in our study. This contrasts sharply with the 1:1 stoichiometry between VWF and VWFpp released from endothelial cells [14].

What could explain the difference in secretion efficiency between VWF and VWFpp from alpha-granules? Earlier studies on the organization and exocytosis of different types of alpha-granule cargo have resulted in several models of how platelets can (differentially) release their content. Based on the localization of several alpha-granule cargo proteins, including VWF, fibrinogen, and several proangiogenic and antiangiogenic mediators, it was postulated that subpopulations of alpha-granules exist based on the inclusion of cargo with opposing functions [29,40]. Preferential mobilization of one of these subpopulations by specific agonists would then lead to differential release of distinct functional classes of alpha-granule cargo, allowing platelets to direct their secretory response in a context-specific manner. However, this hypothesis was significantly challenged by quantitative, high-resolution imaging showing that alpha-granule cargo is stochastically packaged in alpha granules but segregated within subdomains of the granule matrix [27,30,31]. Kinetic release studies also showed little evidence of specific alpha-granule subpopulations but instead identified 3 classes of cargo release based on their rate constants (fast, intermediate, and slow) in which alpha-granule cargo distribution is random [26].

Several nonmutually exclusive mechanisms have been proposed that can achieve differential release of VWF and other cargo from the same granule, such as exocytotic fusion mode (direct vs lingering kiss vs compound fusion) [41,42] from WPBs, or differences in cargo solubilization such as the polar release of nonhomogeneously distributed cargo from one side of the alpha granule [26]. The nearly perfect overlap between VWF and VWFpp that we observed in resting platelets (Figures 1 and 2, Supplementary Figure S2) suggests that both proteins are localized in the same alpha granules and occupy the same granule subdomains, which rules out that the differences in their release were reflective of granule subpopulations or could have been the result of polar release of cargo from one end of the granule. Differential release through premature closure of the fusion pore, such as in lingering kiss exocytosis [41], is also unlikely to serve as an explanation since the size of VWFpp (~100 kDa) would require the fusion pore to fully expand before release. Indeed, we did not find an obvious correlation between releasability and size, as SPARC (40kDa) was less sensitive to low-concentration stimulation and achieved lower maximal release than VWFpp (Supplementary Figure S8).

In line with previous reports by others [25,43], we frequently observed a clustering of VWF-positive structures in the central area of activated platelets that were negative for VWFpp, especially at higher agonist concentrations (Figure 4, Supplementary Figure S7). In some cases, a continuous P selectin staining enveloping several VWFpositive structures (Supplementary Figure S6) was present, reminiscent of several alpha granules that had engaged in compound fusion. This exocytotic fusion mode likely poses no obstacle for VWFpp but does not favor the release of bulky, multimeric cargo, such as VWF, for instance by preventing the orderly unfurling of VWF tubules [42,44]. This may indirectly also relate to differences in solubility of VWF and VWFpp, such as previously observed during loss from the cell surface of endothelial cells following release from WPBs [15]. As a result, VWF remains stuck in postfusion alpha granules, whereas VWFpp is efficiently released.

While traces of VWFpp may stick to the D'D3 region of VWF postrelease [45], it is likely that after exocytosis, its extracellular course is primarily VWF-independent, as attested by the large difference in plasma survival between VWF and VWFpp [46]. However, despite the well-documented pleiotropic roles of VWF, the biological function of extracellular VWFpp remains unclear. Several *in vitro* studies have demonstrated that bovine VWFpp can bind to collagen type I [47], and this interaction can block collagen-induced platelet aggregation [48]. VWFpp also contains an arginine-glycine-aspartic acid (RGD) sequence, a motif that can serve as a ligand for a subfamily of integrins that contain alpha-5, alpha-8, alpha-V, and alpha-IIb subunits. The VWFpp RGD motif is not strongly conserved between species [49]; the integrin receptor for this site has not been identified, and its significance remains uncertain as the RGD sequence appears unfavorably arranged within the native conformation to support adhesive interactions [48]. Bovine VWFpp can bind alpha4β1 and alpha9β1 integrins, which are expressed on lymphocytes, monocytes, and neutrophils via a sequence within the VWD2 domain conserved in humans [50–52]. Another ligand for these integrins, coagulation factor FXIII, has been shown to crosslink

VWFpp to the extracellular matrix protein laminin [52–54]. Focused release of VWFpp from degranulating platelets during initial thrombus formation and incorporation in the adhesive surface via laminin and collagen possibly provides a mechanism to influence the adhesive properties of the exposed extracellular matrix and direct hemostatic and immune responses following vascular injury. Recent reports have emerged that VWFpp can contribute to platelet adhesion to collagen surfaces and enhance thrombus mass in a glycan-dependent manner [55], and in a murine model of deep vein thrombosis, VWFpp incorporates in venous thrombi near regions of active thrombus formation [56].

We have recently shown that platelet factor 4 (PF4) levels in plasma are positively correlated with the current severity of bleeding phenotype in patients with VWD type 1 [57]. PF4 is a chemokine that is mainly produced by megakaryocytes and stored in platelet alpha-granules, which means that systemic PF4 levels are reflective of platelet degranulation. One possible explanation for the observed association with bleeding severity in this group is that apart from a quantitative deficiency of VWF in plasma, hemostatic contribution of platelets is impaired by premature release of alpha-granules. This could lead to insufficient delivery of their hemostatic content, such as platelet VWF and other alpha-granule cargo, to sites of vascular injury. A number of studies have focused on the role of platelet derived VWF in hemostasis [58–62]. Patients with mild and severe circulating VWF deficiencies with residual platelet VWF show a milder clinical phenotype [20,63]. Platelet VWF has also been reported to be important for DDAVP-related amelioration of bleeding times in subgroups of patients with type 1 VWD [64]. Together, this leads to the notion that release of platelet VWF helps to establish hemostasis in these patients. Our data suggest that following activation, most mature VWF remains within the platelets, not supporting any interactions that can contribute to the hemostatic functions of platelets, such as adhesion or aggregation. This is in contrast to its proteolytic cleavage product VWFpp, which is efficiently released from platelet alpha-granules following activation and has its own capabilities to interact with components of the extracellular matrix, cellular adhesion receptors, and the thrombus. The question thus arises how much of the perceived role of platelet VWF in hemostasis can be attributed to mature VWF and how much (if not more) is actually dependent on VWFpp. More studies that focus on the extracellular role(s) of VWFpp, from endothelial and platelet origin, are urgently needed.

### **Acknowledgments**

We thank Dr Coen Maas (University Medical Center Utrecht, The Netherlands) for the generous supply of Alpaca anti-VWF C-terminal cystine knot nanobodies. We thank Titus Lemmens (Maastricht University Medical Center+, The Netherlands) for stimulating discussion and experimental assistance.

### **Author Contributions**

M.S., S.H., P.E.B., J.A.S., and R.B. performed experiments and analyzed the data. T.C. and F.W.G.L. provided essential reagents and expertise. M.S., S.H., A.J.G.J., J.V., and R.B. designed the research and wrote the paper. All authors critically revised and approved the

final version of the manuscript.

## Declaration of Competing Interests

F.W.G.L. received research support from CSL Behring, Takeda, uniQure, and Sobi and is a consultant for uniQure, Biomarin, CSL Behring, and Takeda, of which the fees go to the institute. He was a DSMB member for a study sponsored by Roche. A.J.G.J. received speaker fees and travel cost payments from 3SBio, Amgen, and Novartis, is on the international advisory board at Novartis, and received research support from CSL Behring, Principia, and Argenx. None of the other authors have conflicts of interest to declare.

## References

1. Yadav S, Storrie B. The cellular basis of platelet secretion: emerging structure/function relationships. *Platelets*. 2017;28:108–18.
2. Karampini E, Bierings R, Voorberg J. Orchestration of primary hemostasis by platelet and endothelial lysosome-related organelles. *Arterioscler Thromb Vasc Biol*. 2020;40:1441–53.
3. Springer TA. Von Willebrand factor, Jedi knight of the bloodstream. *Blood*. 2014;124:1412–26.
4. Schillemans M, Karampini E, Kat M, Bierings R. Exocytosis of Weibel–Palade bodies: how to unpack a vascular emergency kit. *J Thromb Haemost*. 2019;17:6–18.
5. Valentijn KM, Sadler JE, Valentijn JA, Voorberg J, Eikenboom J. Functional architecture of Weibel-Palade bodies. *Blood*. 2011;117:5033–43.
6. Vischer U, Wagner D. Von Willebrand factor proteolytic processing and multimerization precede the formation of Weibel-Palade bodies. *Blood*. 1994;83:3536–44.
7. Wagner DD, Saffari-pour S, Bonfanti R, Sadler JE, Cramer EM, Chapman B, Mayadas TN. Induction of specific storage organelles by von Willebrand factor propolypeptide. *Cell*. 1991;64:403–13.
8. Voorberg J, Fontijn R, Calafat J, Janssen H, van Mourik JA, Pannekoek H. Biogenesis of von Willebrand factor-containing organelles in heterologous transfected CV-1 cells. *EMBO J*. 1993;12: 749–58.
9. Haberichter SL, Fahs SA, Montgomery RR. Von Willebrand factor storage and multimerization: 2 independent intracellular processes. *Blood*. 2000;96:1808–15.
10. Huang R-H, Wang Y, Roth R, Yu X, Purvis AR, Heuser JE, Egelman EH, Sadler JE. Assembly of Weibel Palade body-like tubules from N-terminal domains of von Willebrand factor. *Proc Natl Acad Sci U S A*. 2008;105:482–7.
11. Berriman JA, Li S, Hewlett LJ, Wasilewski S, Kiskin FN, Carter T, Hannah MJ, Rosenthal PB. Structural organization of Weibel-Palade bodies revealed by cryo-EM of vitrified endothelial cells. *Proc Natl Acad Sci U S A*. 2009;106:17407–12.
12. Michaux G, Abbitt KB, Collinson LM, Haberichter SL, Norman KE, Cutler DF. The physiological function of von Willebrand's factor depends on its tubular storage in endothelial Weibel-Palade bodies. *Dev Cell*. 2006;10:223–32.
13. Conte IL, Cookson E, Hellen N, Bierings R, Mashanov G, Carter T. Is there more than one way to unpack a Weibel-Palade body? *Blood*. 2015;126:2165–7.
14. Wagner DD, Fay PJ, Sporn LA, Sinha S, Lawrence SO, Marder VJ. Divergent fates of von Willebrand factor and its propolypeptide (von Willebrand antigen II) after secretion from endothelial cells. *Proc Natl Acad Sci U S A*. 1987;84:1955–9.
15. Hannah MJ, Skehel P, Erent M, Knipe L, Ogden D, Carter T. Differential kinetics of cell surface loss of von Willebrand factor and its propolypeptide after secretion from Weibel-Palade bodies in living human endothelial cells. *J Biol Chem*. 2005;280:22827–30.
16. Babich V, Knipe L, Hewlett L, Meli A, Dempster J, Hannah MJ, Carter T. Differential effect of extracellular acidosis on the release and dispersal of soluble and membrane proteins secreted from the Weibel-Palade body. *J Biol Chem*. 2009;284:12459–68.
17. Hewlett L, Zupančić G, Mashanov G, Knipe L, Ogden D, Hannah MJ, Carter T. Temperature-dependence

- of Weibel-Palade body exocytosis and cell surface dispersal of von Willebrand factor and its propolypeptide. *PLoS One*. 2011;6:e27314.
18. Cramer E, Meyer D, le Menn R, Breton-Gorius J. Eccentric localization of von Willebrand factor in an internal structure of platelet alpha-granule resembling that of Weibel-Palade bodies. *Blood*. 1985;66:710–3.
  19. van Nispen tot Pannerden H, de Haas F, Geerts W, Posthuma G, van Dijk S, Heijnen HFG. The platelet interior revisited: electron tomography reveals tubular  $\alpha$ -granule subtypes. *Blood*. 2010;116:1147–56.
  20. Swinkels M, Atiq F, Bürgisser PE, Slotman JA, Houtsmuller AB, de Heus C, Klumperman J, Leebeek FWG, Voorberg J, Jansen AJG, Bierings R. Quantitative 3D microscopy highlights altered von Willebrand factor  $\alpha$ -granule storage in patients with von Willebrand disease with distinct pathogenic mechanisms. *Res Pract Thromb Haemost*. 2021;5:e12595.
  21. Koutts J, Walsh PN, Plow EF, Fenton JW II, Bouma BN, Zimmerman TS. Active release of human platelet factor VIII-related antigen by adenosine diphosphate, collagen, and thrombin. *J Clin Invest*. 1978;62:1255–63.
  22. Montgomery RR, Zimmerman TS. Von Willebrand's disease antigen II. A new plasma and platelet antigen deficient in severe von Willebrand's disease. *J Clin Invest*. 1978;61:1498–507.
  23. Scott J, Montgomery R. Platelet von Willebrand's antigen II: active release by aggregating agents and a marker of platelet release reaction in vivo. *Blood*. 1981;58:1075–80.
  24. Morgenstern E, Neumann K, Patscheke H. The exocytosis of human blood platelets. A fast freezing and freeze-substitution analysis. *Eur J Cell Biol*. 1987;43:273–82.
  25. Eckly A, Rinckel J-Y, Proamer F, Ulas N, Joshi S, Whiteheart SW, Gachet C. Respective contributions of single and compound granule fusion to secretion by activated platelets. *Blood*. 2016;128:2538–49.
  26. Jonnalagadda D, Izu LT, Whiteheart SW. Platelet secretion is kinetically heterogeneous in an agonist-responsive manner. *Blood*. 2012;120:5209–16.
  27. Sehgal S, Storrle B. Evidence that differential packaging of the major platelet granule proteins von Willebrand factor and fibrinogen can support their differential release. *J Thromb Haemost*. 2007;5:2009–16.
  28. Wijten P, van Holten T, Woo LL, Bleijerveld OB, Roest M, Heck AJR, Scholten A. High precision platelet releasate definition by quantitative reversed protein profiling—brief report. *Arterioscler Thromb Vasc Biol*. 2013;33:1635–8.
  29. Italiano JE, Richardson JL, Patel-Hett S, Battinelli E, Zaslavsky A, Short S, Ryeom S, Folkman J, Klement GL. Angiogenesis is regulated by a novel mechanism: pro- and antiangiogenic proteins are organized into separate platelet  $\alpha$  granules and differentially released. *Blood*. 2008;111:1227–33.
  30. Kamykowski J, Carlton P, Sehgal S, Storrle B. Quantitative immunofluorescence mapping reveals little functional coclustering of proteins within platelet  $\alpha$ -granules. *Blood*. 2011;118:1370–3.
  31. Pokrovskaya ID, Yadav S, Rao A, McBride E, Kamykowski JA, Zhang G, Aronova MA, Leapman RD, Storrle B. 3D ultrastructural analysis of  $\alpha$ -granule, dense granule, mitochondria, and canalicular system arrangement in resting human platelets. *Pract Thromb Haemost*. 2020;4:72–85.
  32. de Maat S, Clark CC, Barendrecht AD, Smits S, van Kleef ND, El Otmani H, Waning M, van Moorsel M, Szardenings M, Delaroque N, Vercruyse K, Urbanus RT, Sebastian S, Lenting PJ, Hagemeyer C, Renne T, Vanhoorelbeke K, Tersteeg C, Maas C. Microlyse: a thrombolytic agent that targets VWF for clearance of microvascular thrombosis. *Blood*. 2022;139:597–607.
  33. Bolte S, Cordeliès FP. A guided tour into subcellular colocalization analysis in light microscopy. *J Microsc*. 2006;224:213–32.
  34. Karampini E, Bürgisser PE, Olins J, Mulder AA, Jost CR, Geerts D, Voorberg J, Bierings R. Sec22b determines Weibel-Palade body length by controlling anterograde ER-Golgi transport. *Haematologica*. 2021;106:1138–47.
  35. Schillemans M, Karampini E, van den Eshof BL, Gangaev A, Hofman M, van Breevoort D, Meems H, Jansen H, Mulder AA, Jost CR, Escher JC, Adam R, Carter T, Koster AJ, van den Biggelaar M, Voorberg J, Bierings R. Weibel-Palade body localized syntaxin-3 modulates von Willebrand factor secretion from endothelial cells. *Arterioscler Thromb Vasc Biol*. 2018;38:1549–61. [36] van den Biggelaar M, Bierings R, Storm G, Voorberg J, Mertens K. Requirements for cellular co-trafficking of factor VIII and von Willebrand factor to Weibel-Palade bodies. *J Thromb Haemost*. 2007;5:2235–42.
  37. McGrath RT, McRae E, Smith OP, O'Donnell JS. Platelet von Willebrand factor—structure, function and biological importance. *Br J Haematol*. 2010;148:834–43.
  38. McGrath RT, van den Biggelaar M, Byrne B, O'Sullivan JM, Rawley O, O'Kennedy R, Voorberg J, Preston RJS,

- O'Donnell JS. Altered glycosylation of platelet-derived von Willebrand factor confers resistance to ADAMTS13 proteolysis. *Blood*. 2013;122: 4107–10.
39. Williams SB, McKeown LP, Krutzsch H, Hansmann K, Gralnick HR. Purification and characterization of human platelet von Willebrand factor. *Br J Haematol*. 1994;88:582–91.
40. Battinelli EM, Thon JN, Okazaki R, Peters CG, Vijey P, Wilkie AR, Noetzli LJ, Flaumenhaft R, Italiano JE. Megakaryocytes package contents into separate  $\alpha$ -granules that are differentially distributed in platelets. *Blood Adv*. 2019;3:3092–8.
41. Babich V, Meli A, Knipe L, Dempster JE, Skehel P, Hannah MJ, Carter T. Selective release of molecules from Weibel-Palade bodies during a lingering kiss. *Blood*. 2008;111:5282–90.
42. Stevenson NL, White IJ, McCormack JJ, Robinson C, Cutler DF, Nightingale TD. Clathrin-mediated post-fusion membrane retrieval influences the exocytic mode of endothelial Weibel-Palade bodies. *J Cell Sci*. 2017;130:2591–605.
43. Stenberg PE, Shuman MA, Levine SP, Bainton DF. Redistribution of alpha-granules and their contents in thrombin-stimulated platelets. *J Cell Biol*. 1984;98:748–60.
44. Mourik MJ, Valentijn Ja, Voorberg J, Koster aj, Valentijn KM, Eikenboom J. von Willebrand factor remodeling during exocytosis from vascular endothelial cells. *J Thromb Haemost*. 2013;11:2009–19.
45. Madabhushi SR, Shang C, Dayananda KM, Rittenhouse-Olson K, Murphy M, Ryan TE, Montgomery RR, Neelamegham S. von Willebrand factor (VWF) propeptide binding to VWF DcD3 domain attenuates platelet activation and adhesion. *Blood*. 2012;119: 4769–78.
46. van Mourik JA, Boertjes R, Huisveld IA, Fijnvandraat K, Pajkrt D, van Genderen PJ, Fijnheer R. Von Willebrand factor propeptide in vascular disorders: a tool to distinguish between acute and chronic endothelial cell perturbation. *Blood*. 1999;94:179–85.
47. Takagi J, Kasahara K, Sekiya F, Inada Y, Saito Y. A collagen-binding glycoprotein from bovine platelets is identical to propolypeptide of von Willebrand factor. *J Biol Chem*. 1989;264:10425–30.
48. Takagi J, Sekiya F, Kasahara K, Inada Y, Saito Y. Inhibition of plateletcollagen interaction by propolypeptide of von Willebrand factor. *J Biol Chem*. 1989;264:6017–20.
49. Janel N, Ribba A-S, Che´ rel G, Kerbiriou-Nabias D, Meyer D. Primary structure of the propeptide and factor VIII-binding domain of bovine von Willebrand factor. *Biochim Biophys Acta*. 1997;1339:4–8.
50. Takagi J, Sudo Y, Saito T, Saito Y. Beta 1-integrin-mediated adhesion of melanoma cells to the propolypeptide of von Willebrand factor. *Eur J Biochem*. 1994;222:861–8.
51. Isobe T, Hisaoka T, Shimizu A, Okuno M, Aimoto S, Takada Y, Saito Y, Takagi J. Propolypeptide of von Willebrand factor is a novel ligand for very late antigen-4 integrin. *J Biol Chem*. 1997;272:8447–53.
52. Takahashi H, Isobe T, Horibe S, Takagi J, Yokosaki Y, Sheppard D, Saito Y. Tissue transglutaminase, coagulation factor XIII, and the pro-polypeptide of von Willebrand factor are all ligands for the integrins  $\alpha 9\beta 1$  and  $\alpha 4\beta 1$ . *J Biol Chem*. 2000;275:23589–95.
53. Usui T, Takagi J, Saito Y. Propolypeptide of von Willebrand factor serves as a substrate for factor XIIIa and is cross-linked to laminin. *J Biol Chem*. 1993;268:12311–6.
54. Takagi J, Aoyama T, Ueki S, Ohba H, Saito Y, Lorand L. Identification of factor-XIIIa-reactive glutaminy residues in the propolypeptide of bovine von Willebrand factor. *Eur J Biochem*. 1995;232:773–7.
55. Rawley O, Lillicrap D. Functional roles of the von Willebrand factor propeptide. *Hamostaseologie*. 2021;41:63–8.
56. Rawley O, Dwyer C, Nesbitt K, Notley C, Michels A, Lillicrap D. The VWF propeptide is a novel component of venous thrombi in a mouse model of DVT. *Res Pract Thromb Haemost*. 2022;6:(Abstract PB0802).
57. Swinkels M, Atiq F, Bürgisser PE, Moort I, Meijer K, Eikenboom J, Fijnvandraat K, Galen KPM, Meris J, Schols SEM, Bom JG, Cnossen MH, Voorberg J, Leebeek FWG, Bierings R, Jansen AJG, Fijnvandraat K, Coppens M, Meris J, Nieuwenhuizen L, et al. Platelet degranulation and bleeding phenotype in a large cohort of Von Willebrand disease patients. *Br J Haematol*. 2022;197:497–501.
58. Gralnick HR, Rick ME, McKeown LP, Williams SB, Parker RI, Maisonneuve P, Jenneau C, Sultan Y. Platelet von Willebrand factor: an important determinant of the bleeding time in type I von Willebrand's disease. *Blood*. 1986;68:58–61.
59. Fressinaud E, Baruch D, Rothschild C, Baumgartner H, Meyer D. Platelet von Willebrand factor: evidence for its involvement in platelet adhesion to collagen. *Blood*. 1987;70:1214–7.

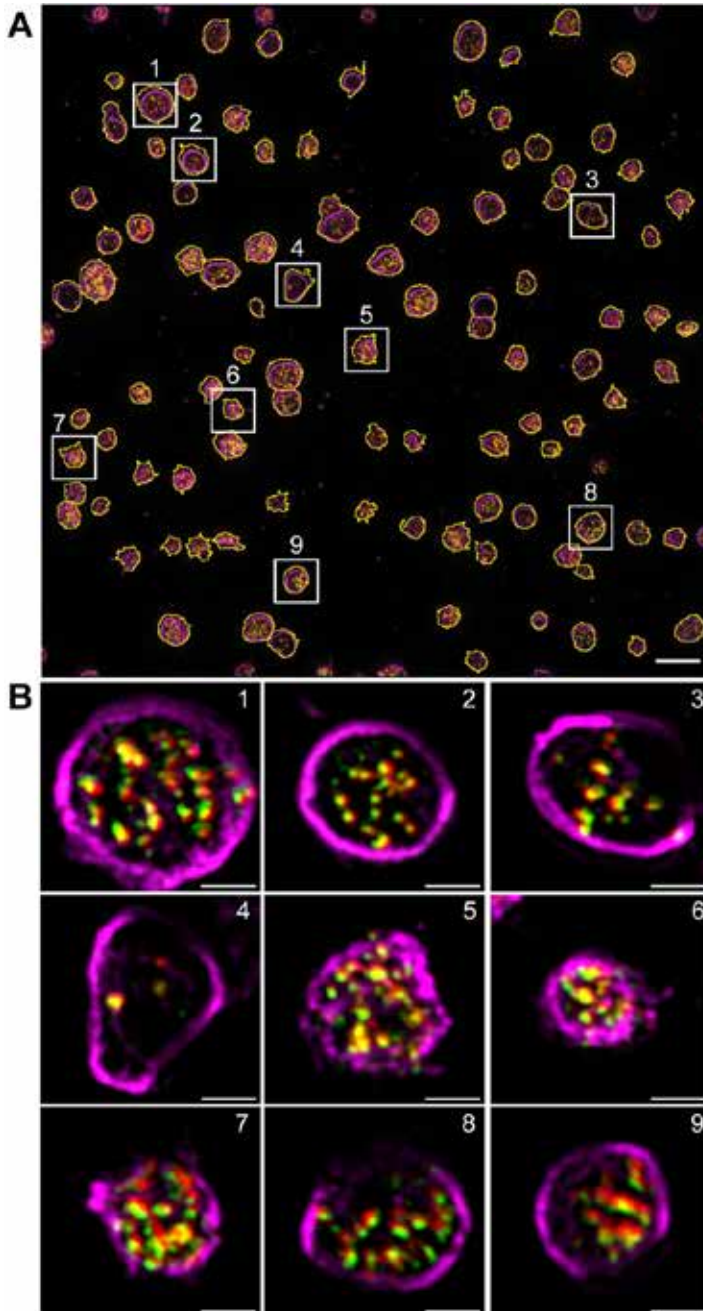
60. Rodeghiero F, Castaman G, Ruggeri M, Tosetto A. The bleeding time in normal subjects is mainly determined by platelet von Willebrand factor and is independent from blood group. *Thromb Res.* 1992;65: 605–15.
61. Kanaji S, Fahs SA, Shi Q, Haberichter SL, Montgomery RR. Contribution of platelet vs. endothelial VWF to platelet adhesion and hemostasis. *J Thromb Haemost.* 2012;10:1646–52.
62. Verhenne S, Denorme F, Libbrecht S, Vandembulcke A, Pareyn I, Deckmyn H, Lambrecht A, Nieswandt B, Kleinschnitz C, Vanhoorelbeke K, De Meyer SF. Platelet-derived VWF is not essential for normal thrombosis and hemostasis but fosters ischemic stroke injury in mice. *Blood.* 2015;126:1715–22.
63. Bowman ML, Pluthero FG, Tuttle A, Casey L, Li L, Christensen H, Robinson KS, Lillicrap D, Kahr WHA, James P. Discrepant platelet and plasma von Willebrand factor in von Willebrand disease patients with p.Pro2808Leufs\*24. *J Thromb Haemost.* 2017;15: 1403–11.
64. Mannucci PM, Lombardi R, Bader R, Vianello L, Federici AB, Solinas S, Mazzucconi MG, Mariani G. Heterogeneity of type I von Willebrand disease: evidence for a subgroup with an abnormal von Willebrand factor. *Blood.* 1985;66:796–802.

# Appendix

## Supplementary Figures

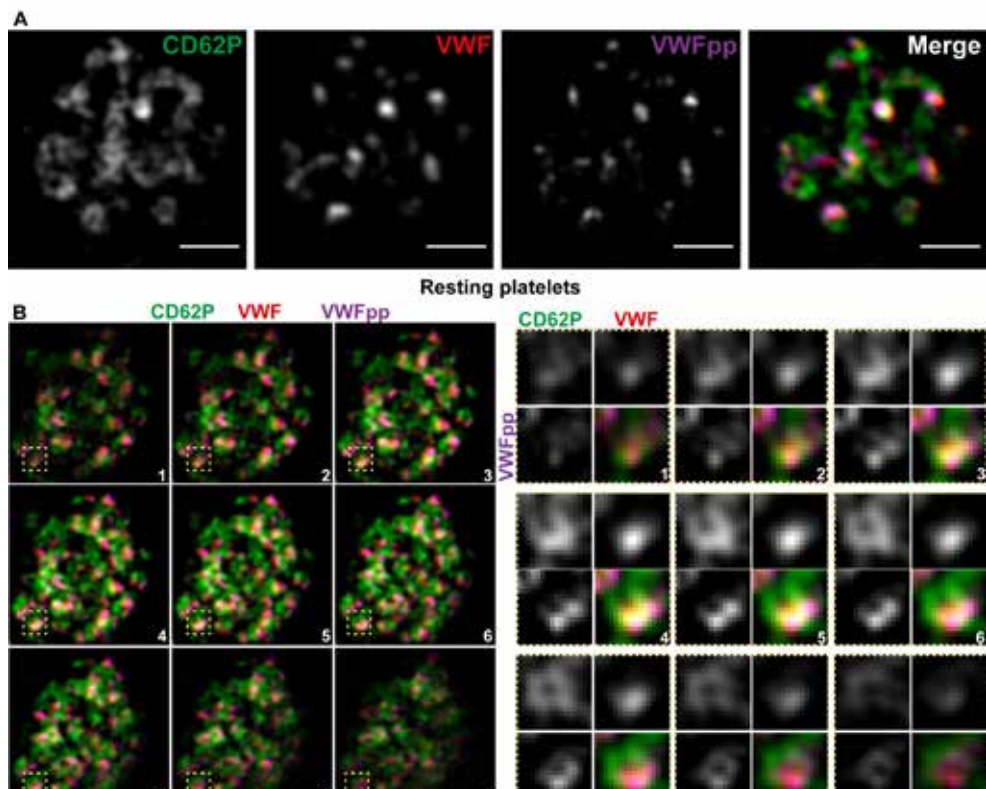
Antigen	Species (Iso-type)	Label	Supplier	Cat. Nr.	Dilution
Von Willebrand factor propeptide	Rabbit	-	Prof. Tom Carter, SGUL	-	1:500
Von Willebrand factor	Rabbit	-	DAKO	A0082	1:500
Von Willebrand factor	Mouse (IgG2b)	-	Sanquin	CLB-RAg20	1:500
Alpha-tubulin	Mouse (IgG2b)	-	Abcam	ab56676	1:500
Alpha-tubulin	Mouse (IgG1)	-	Sigma	DM1A	1:500
SPARC	Mouse (IgG1)	-	SantaCruz	sc-73472	1:500
Fibrinogen	Rabbit	-	DAKO	A0080	1:500
CD62P	Mouse (IgG1)	-	Bio-Rad	MCA796	1:500
Mouse IgG1	Goat	CF488A	Biotium	20246	1:1000
Mouse IgG1	Goat	CF568	Biotium	20248	1:1000
Mouse IgG1	Goat	CF647	Biotium	20252	1:1000
Mouse IgG2b	Goat	CF647	Biotium	20272	1:1000
Rabbit IgG (H+L)	Goat	CF488	Biotium	20012	1:1000
Rabbit IgG (H+L)	Donkey	AF 568	ThermoFisher	A11042	1:400
Alpaca IgG	Goat	AF 488	Jackson ImmunoResearch	128-545-230	1:400

Supplementary Table S1. Antibodies used in immunofluorescent staining.

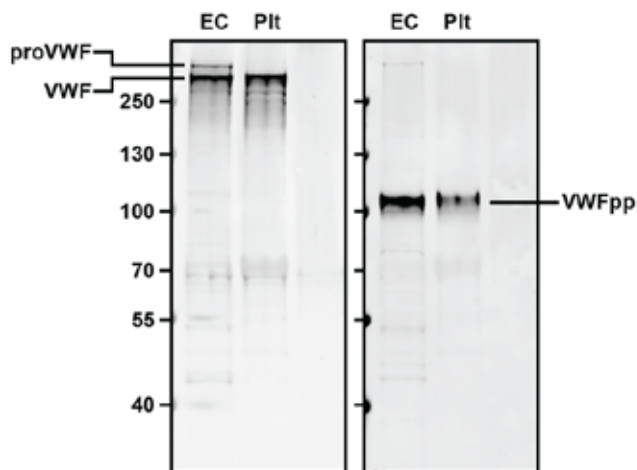


Supplemental Figure 1. VWF and VWFpp localization in resting platelets.

Full field of view of resting platelets segmented based on alpha-tubulin staining (magenta) and stained for VWF (red) and VWFpp (green) (A). Highlighted platelets are randomly selected and presented as single plane zoom-in images in (B). Scale bar represents 5  $\mu\text{m}$  in (A) and 1  $\mu\text{m}$  in (B).

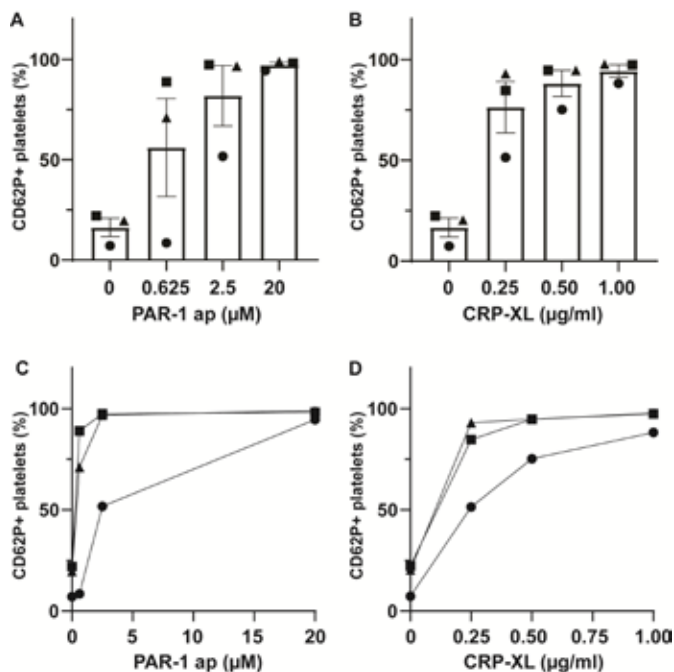


*Supplemental Figure 2. 3D VWF and VWFpp localization in CD62P-defined alpha-granular structures.* Resting platelets were stained for CD62P (green), VWF (red, CLB-RAg20) and VWFpp (magenta). Representative platelets are shown as single plane zoom-in image (A) or in serial planes of a zoom-in image (B) to illustrate 3D localization of the stained proteins. Single granule details of CD62P/VWF/VWFpp (yellow squares) are shown. Scale bar represents 1  $\mu$ m.



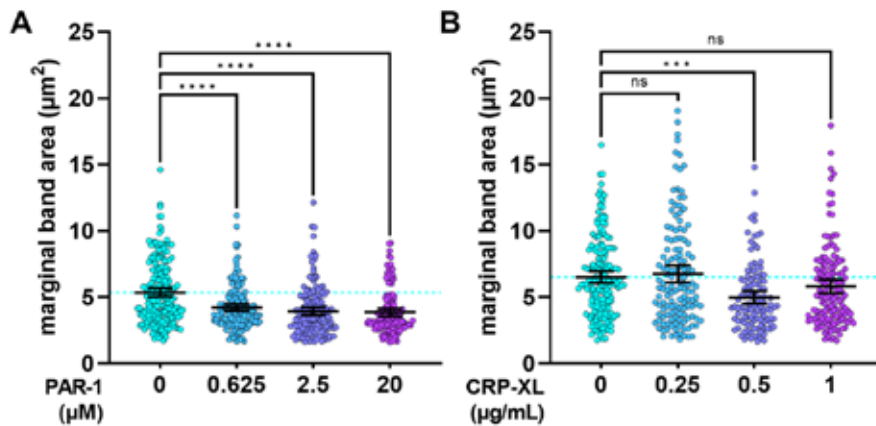
Supplemental Figure 3. VWF and VWFpp immunoblots of endothelial- and platelet lysates.

Endothelial and platelet lysates were separated on a 4-12% Bis-Tris gel and probed for VWF (left, DAKO) or VWFpp (right). Bands corresponding to proVWF, mature VWF (VWF) and VWFpp are indicated.



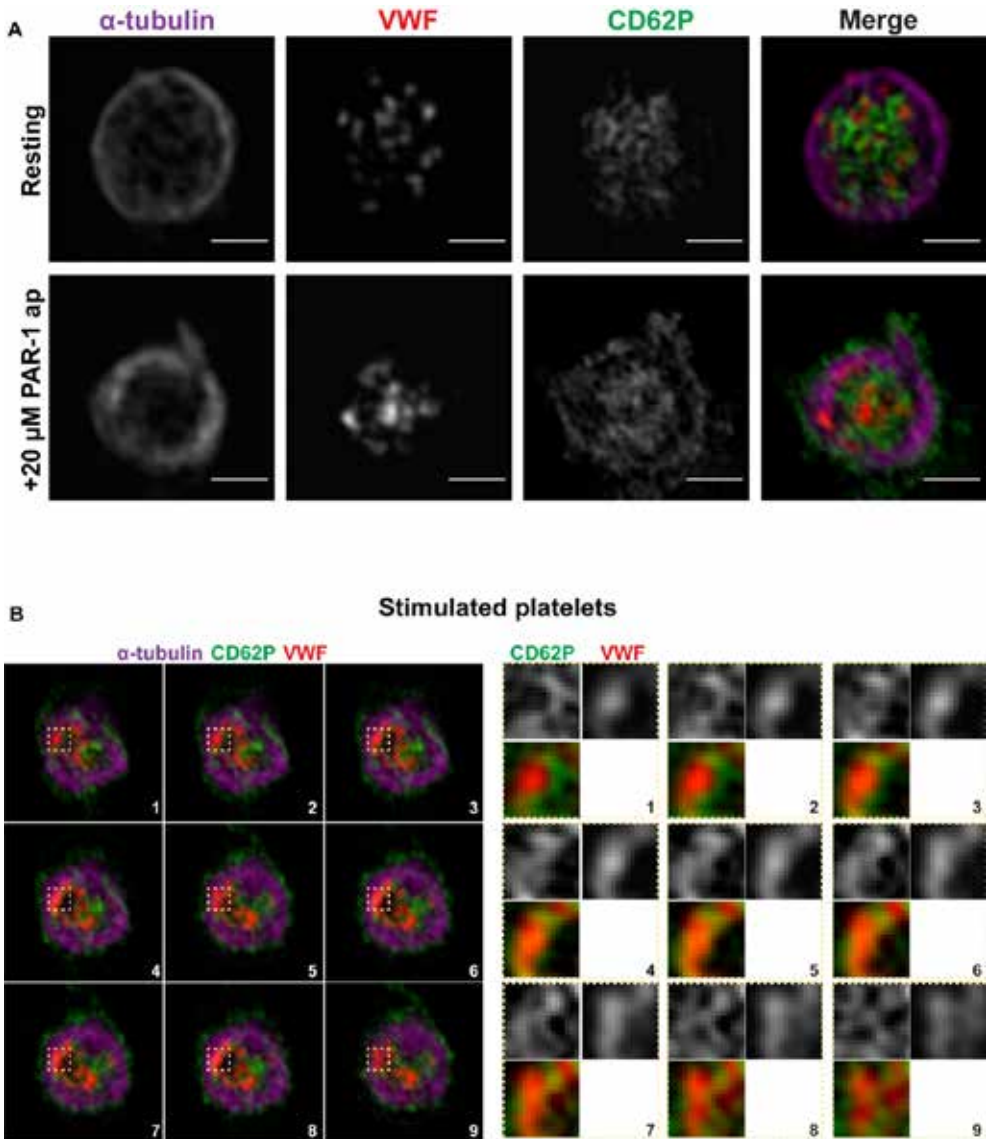
Supplemental Figure 4. Alpha-granule release assessed by FACS analysis of P-selectin exposure.

Platelets were stimulated with increasing doses of PAR-1 ap (A) or CRP-XL (B) and quantified for CD62P+ cell surface exposure by flow cytometry. Symbols represent individual donors (n=3). Individual dose response curves are shown in C (PAR-1 ap) and D (CRP-XL) with symbols representing unique donors. Data presented as mean  $\pm$  SD.



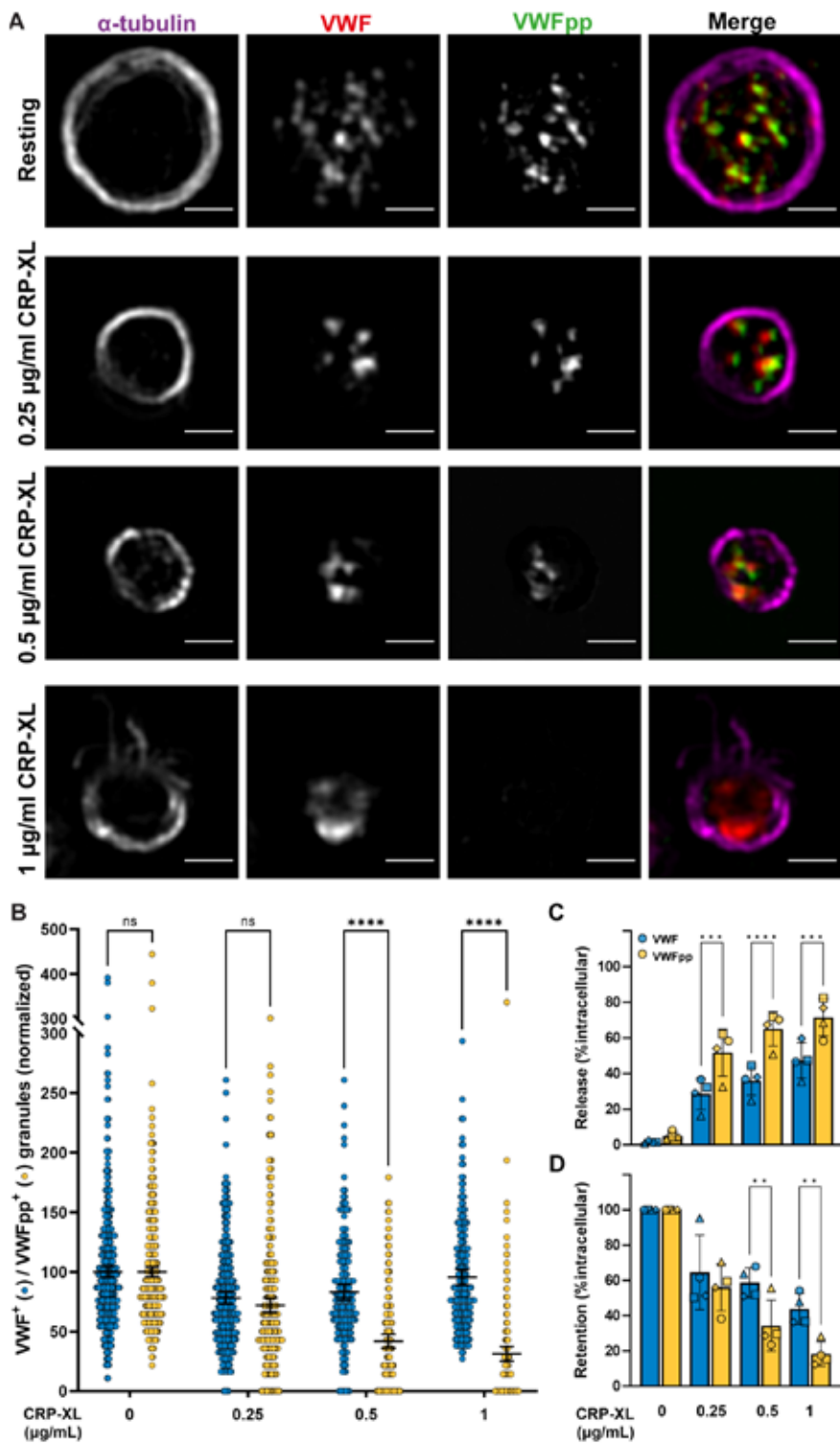
Supplemental Figure 5. Compression of marginal band area in PAR1- and GPVI-activated platelets.

Platelets were incubated with vehicle or increasing doses of PAR-1 or CRP-XL (B). Marginal band area was determined based on the delineation by the alpha-tubulin immunofluorescent staining of the ring structure in the middle Z-slice. Data shown are derived from platelets from 3 independent healthy control donors (PAR1 0  $\mu\text{M}$ , n=208; PAR1 0.625  $\mu\text{M}$ , n=166; PAR1 2.5  $\mu\text{M}$ , n=157; PAR1 20  $\mu\text{M}$ , n=128; CRP-XL 0  $\mu\text{g/mL}$ , n=179; CRP-XL 0.25  $\mu\text{g/mL}$ , n=137; CRP-XL 0.5  $\mu\text{g/mL}$ , n=113; CRP-XL 1.0  $\mu\text{g/mL}$ , n=139). Bars represent means and 95% confidence interval. \*\*\*  $p < 0.001$ , \*\*\*\*  $p < 0.0001$  by 1-way ANOVA with Dunnett's post hoc test for multiple comparison.



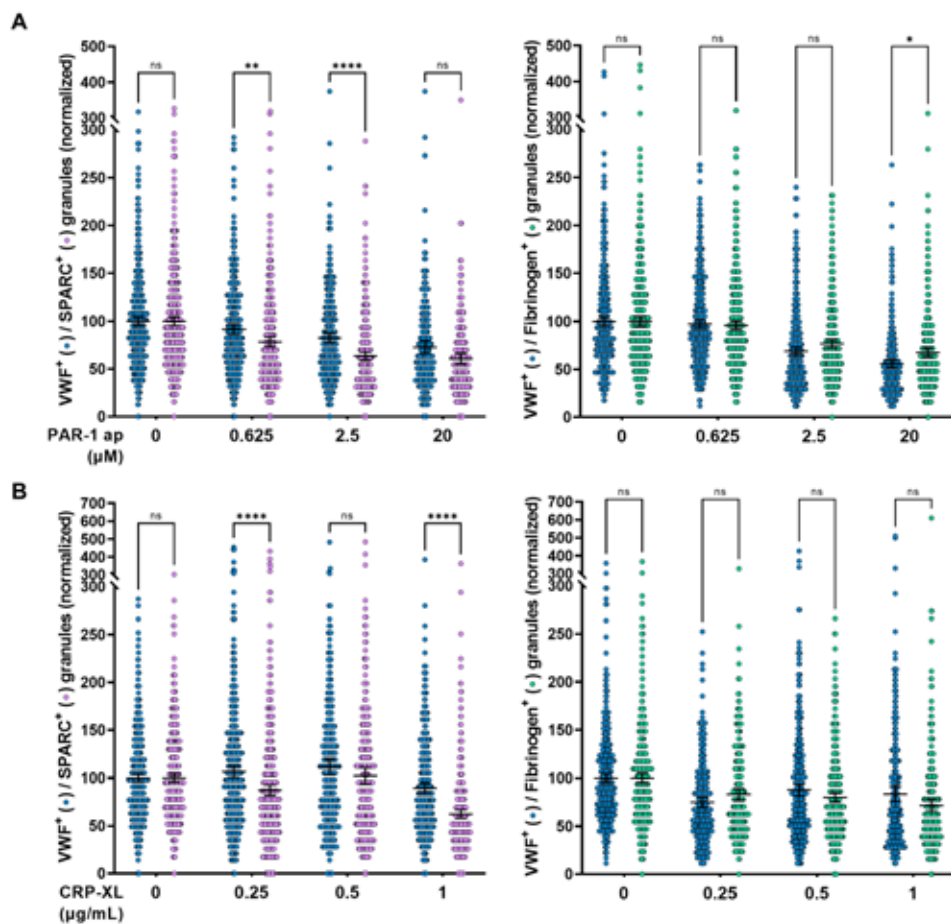
Supplemental Figure 6. 3D VWF localization in stimulated platelets.

Platelets stimulated with 20  $\mu$ M PAR-1 ap were stained for CD62P (green), VWF (red, DAKO) and  $\alpha$ -tubulin (magenta) and compared to resting platelets (A). Serial planes of a zoom-in image are shown with granule details on the right (yellow squares) to illustrate 3D localization of CD62P and VWF (B). Scale bar represents 1  $\mu$ m.



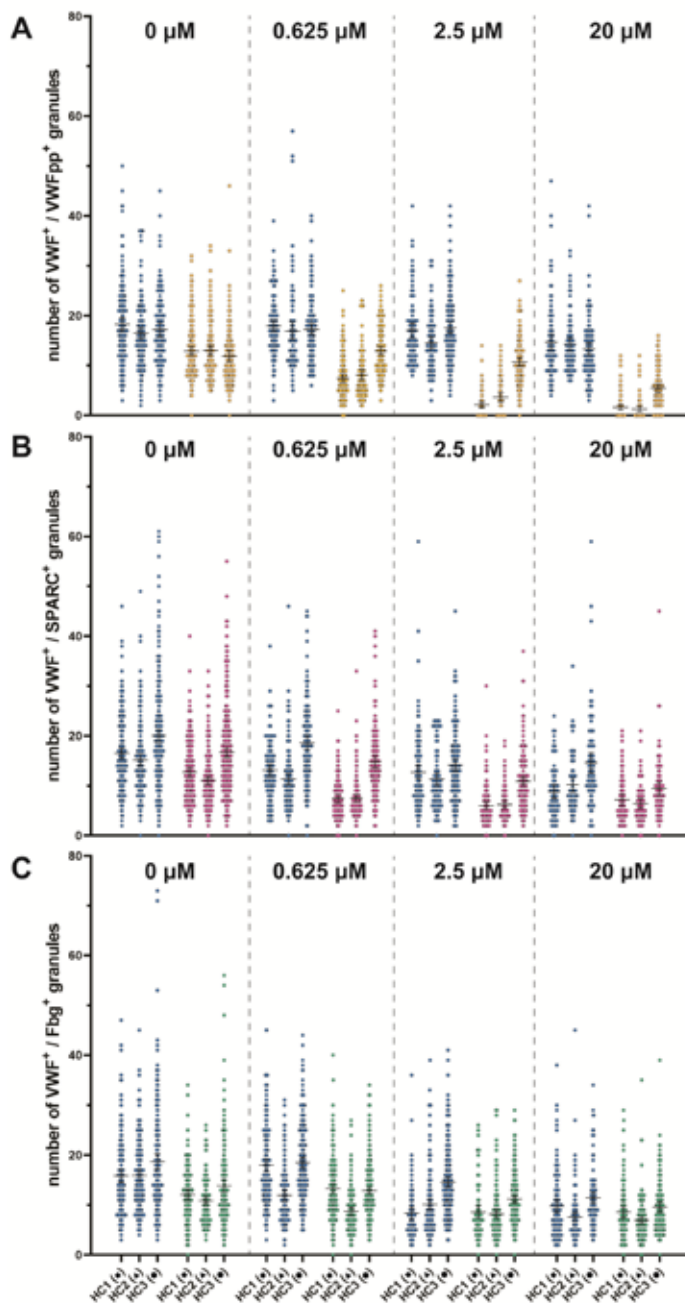
*Supplemental Figure 7. Dose-response release of VWF and VWFpp.*

Platelets were stimulated with 0-1  $\mu\text{g/ml}$  CRP-XL and stained for  $\alpha$ -tubulin, VWF (CLB-RAg20) and VWFpp (A). Representative single plane zoom-in images are shown. Scale bar represents 1  $\mu\text{m}$ . (B) VWF and VWFpp release were assessed by quantification of their residual levels in platelets normalized to resting platelets. N=498, 305, 187 and 191 respectively. Counts are pooled from 3 independent healthy donors. The release (C) and retention (D) of VWF and VWFpp in CRP-XL stimulated platelets was measured by ELISA and normalized to resting intracellular content. Symbols represent 4 healthy donors (N=4). Statistical analysis was two-way ANOVA with Sidak multiple comparisons test and significance levels of \*\* =  $p < 0.01$ , \*\*\* =  $p < 0.001$ , \*\*\*\* =  $p < 0.0001$ . Data is presented as mean with 95% confidence interval.



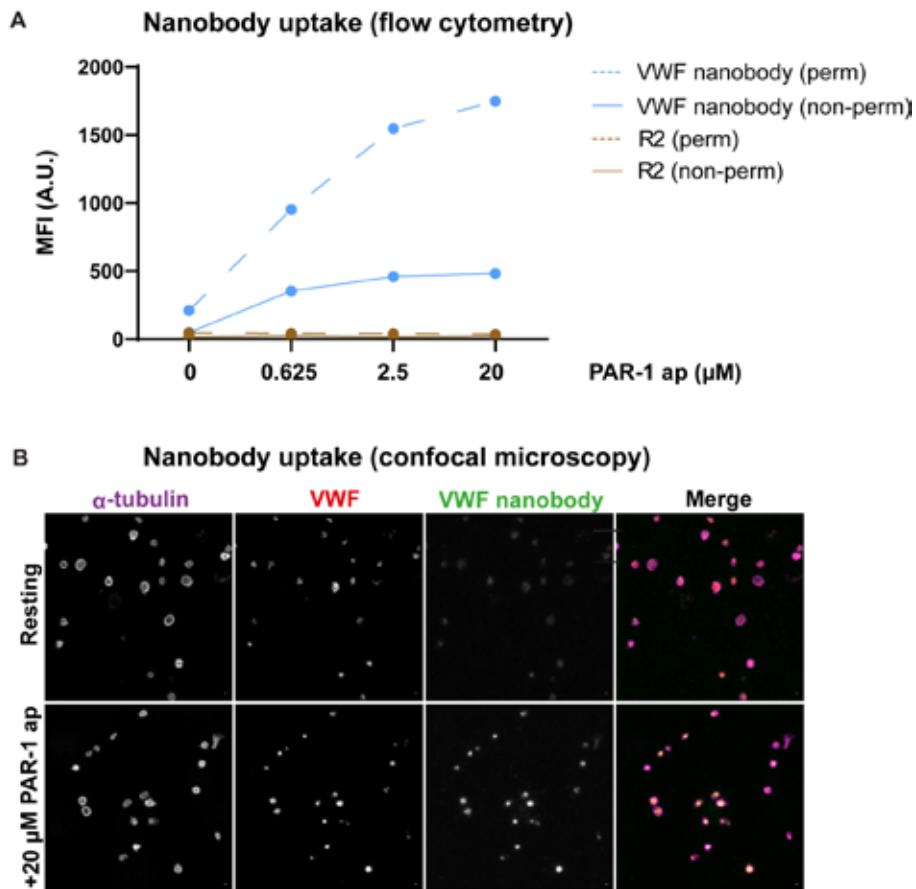
Supplemental Figure 8. Dose-response release of VWF compared to SPARC and Fibrinogen.

Platelets were stimulated with 0-20  $\mu\text{M}$  PAR-1 ap (A) or 0-1  $\mu\text{g/mL}$  CRP-XL (B). VWF (blue), SPARC (pink) and fibrinogen (green) release was assessed by quantification of their residual levels in platelets normalized to resting platelets. (SPARC PAR1 0  $\mu\text{M}$ , n=512; PAR1 0.625  $\mu\text{M}$ , n=376; PAR1 2.5  $\mu\text{M}$ , n=355; PAR1 20  $\mu\text{M}$ , n=218; CRP-XL 0  $\mu\text{g/mL}$ , n=512; CRP-XL 0.25  $\mu\text{g/mL}$ , n=480; CRP-XL 0.5  $\mu\text{g/mL}$ , n=263; CRP-XL 1.0  $\mu\text{g/mL}$ , n=401) (Fibrinogen PAR1 0  $\mu\text{M}$ , n=549; PAR1 0.625  $\mu\text{M}$ , n=499; PAR1 2.5  $\mu\text{M}$ , n=437; PAR1 20  $\mu\text{M}$ , n=342; CRP-XL 0  $\mu\text{g/mL}$ , n=430; CRP-XL 0.25  $\mu\text{g/mL}$ , n=255; CRP-XL 0.5  $\mu\text{g/mL}$ , n=355; CRP-XL 1.0  $\mu\text{g/mL}$ , n=292) \* =  $p < 0.1$ , \*\* =  $p < 0.01$ , \*\*\*\* =  $p < 0.0001$ , as analyzed by two-way ANOVA with Sidak multiple comparison test. Data presented as mean with 95% confidence interval.



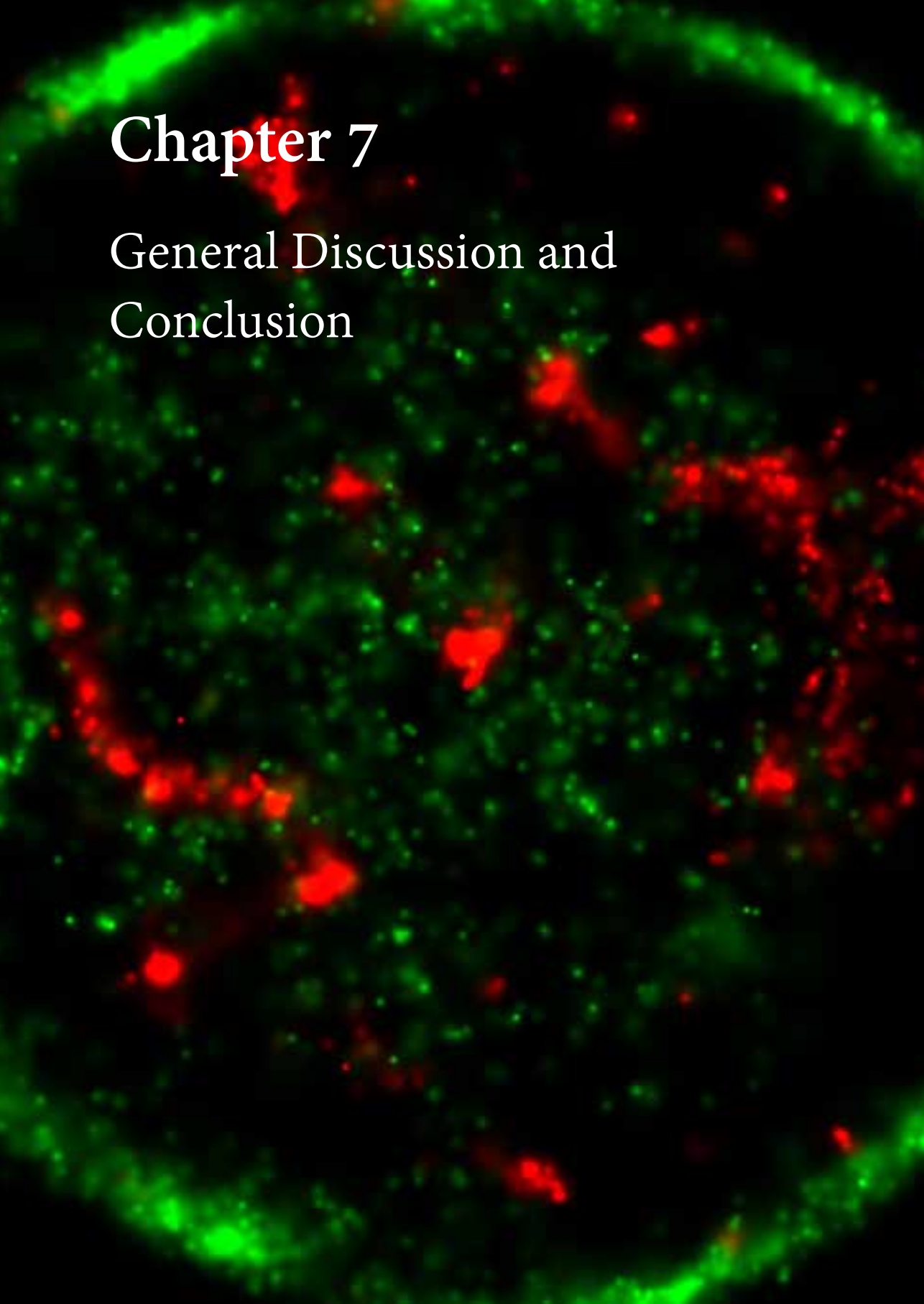
Supplemental Figure 9. Healthy donor variation in dose-response release.

Platelets of healthy donors were stimulated with 0-20  $\mu$ M PAR-1 ap and imaged by SIM. Absolute counts of VWF and VWFpp (A), SPARC (B) and fibrinogen (C) positive granules are shown per donor. The symbol for each individual donor corresponds to the one that is used in Supplemental Figure 4.



Supplemental Figure 10. VWF nanobody bulk uptake in platelets.

Platelets were stimulated for 30 minutes with 0-20  $\mu\text{M}$  PAR-1 in the presence of 1  $\mu\text{g}/\text{ml}$  VWF nanobody or R2 control nanobody and were analyzed for nanobody uptake by flow cytometry (A) and confocal microscopy (B).

A fluorescence microscopy image of a cell. The cell is roughly circular and filled with a complex network of green and red signals. The green signal is more widespread, forming a dense, somewhat diffuse pattern. The red signal is more localized, appearing as several distinct, bright spots or clusters. The overall appearance is that of a cell with specific organelles or structures highlighted in different colors. The background is black, making the green and red signals stand out prominently.

# Chapter 7

## General Discussion and Conclusion

## General Discussion and Conclusion

Platelets take the centre stage in primary hemostasis by rapidly transforming their adhesive properties in response to vascular injury [1]. Platelets perform this role in close collaboration with VWF, which originates from the circulation and from intracellular reservoirs in platelets and endothelial cells. VWF assembles into multimers through a complex biosynthetic pathway that is presumably shared by endothelial cells and megakaryocytes [2]. Another key aspect of platelet function is the array of hemostatic and procoagulant molecules, like VWF, that are released upon platelet activation and degranulation [3]. Yet, the post-release fates of many of these molecules as well as their contribution to hemostasis are not yet fully characterized [4,5]. Defects in components of the hemostatic system lead to bleeding problems in affected patients. In this thesis the role of platelets was studied in the context of two hemostatic disorders (ITP and VWD) with a particular focus on platelet dynamics, the platelet-VWF axis, and the role of platelet cargo release.

### **Platelet numbers and ITP - "*Measuring is knowing*"**

Thrombopoiesis is carefully regulated by the number of platelets in circulation, TPO, and the availability of TPO to megakaryocytes to produce new platelets [6]. When platelets physiologically end their life cycle, they can be cleared via the Ashwell-Morrell receptor on hepatic cells (and by the spleen), which subsequently leads to new TPO production. In turn, TPO is regulated by the number of circulating platelets [7,8]. This careful balance is disturbed in hemostatic disorders like ITP, as both enhanced platelet destruction and reduced platelet production in the bone marrow can be at play [9-11]. As a result, platelet numbers can sometimes vary considerably in patients and proper monitoring is essential.

However, there have been only a few studies in adult ITP patients that have (retrospectively) gathered observational data on platelets counts at multiple time points [12-14]. Therefore, the variability of an individual ITP patient's platelet counts remains mostly unexplored, also considering that ITP status is frequently established in relation to a large variety of causes (e.g. infections, various auto-immune disorders). As most studies have relied on a limited number of platelet counts, contradictory findings have been reported [15]. One topic that remains unresolved is whether or not vaccination events may act as a trigger for the onset of ITP, and what the effects of vaccination may be on platelet counts in ITP patients [9,10,16]. In particular, case reports during the recent COVID-19 pandemic implicated various COVID-19 vaccines to cause severe (and sometimes fatal) thrombocytopenia in ITP patients or even de novo [17,18]. To further study this phenomenon and the effect of vaccinations in ITP patients in a systematic approach, we analyzed a large group of adult ITP patients and as control population healthy donors undergoing vaccination in Chapter 3. We prospectively measured platelet counts at several time points, both before and after vaccination, to assess the effect of vaccination on platelet counts over time.

In this study, we employed a mixed-effects analysis, that takes into account intra- and interindividual variability. Combined with the long observation period and multiple measurements before and after vaccination, we can firmly conclude that there was no significant difference between ITP patients and healthy individuals in terms of platelet count changes over the course of two vaccination events. This strongly suggests that the susceptibility to platelet count changes as a result of (COVID-19) vaccination is similar between ITP patients and healthy individuals. In line with our observation, another study found that ITP patients receiving the BNT162b2 vaccine similarly did not develop decreased platelets counts [19]. Whether or not specific vaccines (also other than COVID-19) may elicit a stronger response in ITP patients remains to be further investigated, ideally using similar methods of prospective monitoring.

Another important point to consider is the variability within the cohort of ITP patients, as the disease is still diagnosed as thrombocytopenia per exclusion of other causes, which leads to a heterogenous population of patients [9,15,16]. We observed that platelet count changes were most evident in patients that were under active treatment, required rescue medication, or that had a previous splenectomy. This suggests that patients that are on treatment, or in an active phase of the disease, may be more susceptible to platelet count changes and thrombocytopenia compared to a group of adult ITP patients currently not requiring treatment. These findings illustrate that it is important to specify and adequately characterize ITP subgroups, with the potential to identify which patients are more prone to platelet count changes and more at risk for exacerbation of disease.

Considering that ITP stems from differential effector mechanisms leading to low platelet counts (platelet destruction and inhibited platelet production), tools that are able to predict platelet age in vivo would be highly useful to better separate these mechanisms and thus lead to a better classification (see further below). Additionally, the current clinical classification would report immune-related triggering events like infections as secondary ITP. However, as postulated in Chapter 2, infections could very well act as a trigger for chronic ITP, similar to other autoimmune disorders. This inconsistency between the clinical classification and underlying pathophysiology needs to be resolved. Ultimately, a structured approach of platelet monitoring combined with ITP subgroup stratification based on biological mechanisms instead of clinical classification (aided by predictive tools) would help us better resolve which patients are actually suffering from an autoimmune origin versus thrombocytopenia from other causes. This will also help to better understand how vaccination may affect platelet counts in individual ITP patients.

### **Quantitative SIM - "It's a number's game"**

Besides variability in platelet number, the circulating population of platelets is also variable in itself due to the age-related changes that gradually occur [20–22]. This is an important consideration in platelet function-, morphology- and granule studies. In particular, quantitative data of platelet granule imaging studies are needed to objectively capture the entire population of platelets with a gradient of age-related granular changes [20,23].

However, quantitative platelet imaging has long been hampered by resolution limits in light microscopy [3,23]. With the rapid and continuous development of super-resolution microscopy, it is feasible to generate large scale light microscopy data on a resolution level that can resolve individual organelles like alpha-granules [23]. The importance of such data is evident from previous studies on alpha-granule organization, in which initial studies led to the premature conclusion that there were populations of alpha-granules with different cargo identities. Based on qualitative thin section electron microscopy or the limited resolution of confocal microscopy, cargo proteins appeared to reside in different granules [24,25]. Later studies, using quantitative light microscopy on hundreds of granules and platelets illustrated that alpha-granule cargo proteins are distributed stochastically. Additionally, 3D electron microscopy firmly demonstrated that proteins previously thought to be located in different granule populations (VWF and fibrinogen) reside in each alpha-granule [26-28].

In this thesis, we describe a methodology to quantitatively assess platelet components using SIM, which allows quantification of alpha-granule cargo, dense-granule cargo and structural proteins on a organelle-level of resolution. One of the main considerations to have opted for SIM over other super-resolution techniques with higher resolving power is that SIM is a relatively high-throughput technique, capable of simultaneously imaging hundreds of platelets within single fields of view [29]. SIM is therefore ideally suited to study patient groups or multiple conditions of biological experiments, due to a large field of view, ease of use, and uncomplicated imaging data. While this may make SIM the most promising technique to be employed as a diagnostic tool or in automated quantitative analyses [30], studies that may want to further characterize sub-granule biological processes like compound fusion events in platelets will likely need the increased resolution of STED and/or STORM [23,29].

Additionally, one of the caveats of SIM is the non-linearity of the reconstructed data [31]. In our work, we focused on an object-based analysis of granular structures to avoid a direct dependency on labelling density. Secondly, we performed parallel studies with confocal microscopy to also obtain linear fluorescent intensities in the same samples of interest. Ideally, future developments in SIM algorithms such as those by Smith et al. circumvent this problem, by generating a natural noise appearance [31]. Applying standardized thresholds and analysis settings instead of user-adjusted reconstruction parameters will greatly improve the objectivity of automated SIM-based analyses. Altogether, this should make SIM a highly promising technique to identify platelet defects in hemostatic disorders, as further discussed below.

One of the applications of the SIM-based methodology demonstrated in this thesis is the stratification of VWD patients. VWD is clinically diagnosed in various subtypes, but within these subtypes the molecular mechanisms of disease may differ [32,33]. One highly illustrative example is presented in Chapter 5, where we stratified two type 3 VWD patients with a compound heterozygous deletion and homozygous missense

mutation in the VWF gene, respectively, which results in distinct pathogenic mechanisms underpinning their loss of circulating VWF in plasma. Based on SIM - but not on confocal microscopy - we were able to distinguish these patients that, despite their similar circulating VWF levels, differed in storage of VWF in platelet alpha-granules. Adequate stratification in such complex cases may help us better understand VWD pathology but may also have direct clinical implications, as type 3 VWD patients with residual platelet- (and possibly endothelial-) VWF could potentially benefit from DDAVP treatment [32,34]. Effectively, SIM could particularly play a role in rapidly analyzing (the severity of) cellular VWF defects, not only in type 3 but also other subtypes.

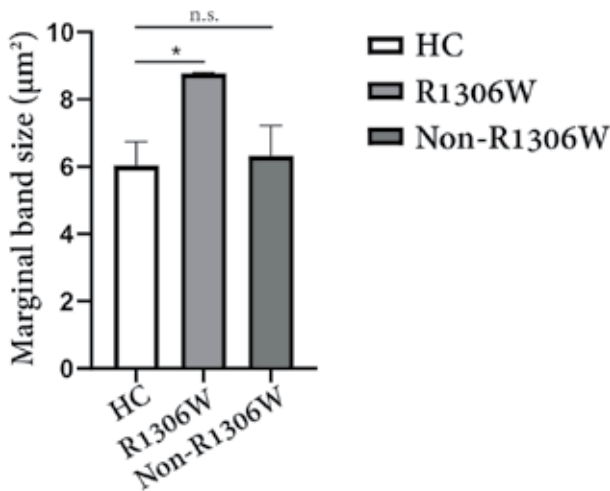


Figure 1. Marginal band size of healthy controls and type 2B VWD patients.

Alpha-tubulin size was quantified across healthy controls (n=6) and type 2B VWD patients (n=6) from the WiN-Pro study, separated in those with the p.R1306W mutation (n=2) and those with other type 2B mutations: p.R1306N (n=1) and p.R1308C (n=3). Mean±standard deviation is shown. \* = p<0.05; n.s. = non significant. Unpublished work.

SIM-based analysis may also be used in type 2B VWD, where gain-of-function mutations in VWF lead to disruption of thrombopoiesis in the bone marrow through the spontaneous interaction of VWF and megakaryocytes [35,36]. As a result, patients present with a varying degree of both megakaryocyte and platelet defects, depending on the mutation. Nurden and colleagues have characterized morphological changes in platelets as a result of different mutations in type 2B VWD patients using electron microscopy [35,37]. In follow-up work from Chapter 5, we also applied quantitative SIM on type 2B VWD patients. Using the staining combination of alpha-tubulin, VWF and SPARC on additional VWD patients, we were able to identify larger tubulin rings in a subset of type 2B patients with the p.R1306W mutation that constitutes giant platelets, while direct granular changes were not evident (Figure 1). Further analysis of both morphological and granular changes in a more quantitative setting using a SIM-based approach would be merited to better understand how VWF mutations affect thrombopoiesis in type 2B VWD. Ultimately, those defects can

also affect platelets in the circulation and determine to what extent patients experience bleeding problems [35].

A final potential application for SIM-based, quantitative imaging as described in this thesis is the study of platelet disorders characterized by defects in the formation of lysosome-related organelles such as alpha- and dense-granules [30,38,39], and in certain acquired platelet disorders that occasionally constitute storage pool deficiency like in myeloproliferative neoplasms or ITP [40]. Quantitative imaging of platelets could simultaneously yield information on a structural protein, an alpha-granule cargo protein, and a dense-granule cargo marker. This would provide a rapid screening test not only to assess platelet morphology but also on the morphology and number of platelet storage organelles. As current diagnostic tests mostly assess this indirectly by measuring platelet secretion or aggregation, a microscopy-based approach would also constitute a novel approach in the diagnostic toolkit. Another consideration would be to incorporate imaging of both resting- and stimulated platelets to include further simultaneous information on platelet secretion. Finally, the quantitative nature of a SIM-based approach allows rapid screening of hundreds of platelets which is much less labour-intensive than established methods and allows identification of more subtle defects. As such, it could directly be applied for the quantification of dense granule numbers [30], which is currently done by whole-mount EM [41].

### **Platelet imaging and neural networks - *"This Is The World Now. Logged On, Plugged In, All The Time"***

Another field where the heterogenous nature and rapid degradation of platelets plays a major role is in the storage of platelet transfusion products [20-22]. Here, it is important to fully characterize platelet dynamics, in order to be able to predict the quality of transfusion products to be used in the clinic. Proteomic, functional and morphological changes in stored platelets have been elaborately characterized but accurate prediction tools are lacking [20-22]. Generating imaging datasets of many different platelet states in combination with advanced analytical tools derived from the rapidly expanding field of AI-based learning might be a new approach in quality prediction of platelet transfusion products.

Imaging datasets are a prime candidate to train neural networks to recognize specific, well-characterized cell states, and both histological and fluorescent images are increasingly used via AI recognition in pathology and research laboratories, such as for recognition of platelet spreading [42]. As an extension of the quantitative work presented in Chapter 5, a default staining of several key platelet components was used to generate training and validation datasets of in vitro-aged platelets in an ongoing project (Figure 2). A neural network was trained to identify sections of platelets under well-characterized different conditions that resemble younger and older platelets based on confocal microscopy images. The convolutional network was then applied to platelet transfusion products stored over several time points [43]. Based on these platelet images, the algorithm was able to predict

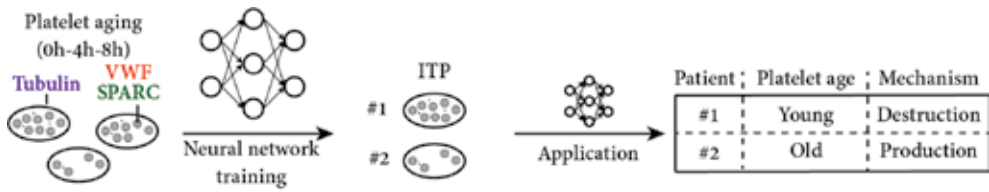


Figure 2. Platelet aging and neural network application.

Platelets were aged in vitro for 0, 4 or 8 hours; and used as training and validation sets for neural network development. A potential application for ITP patients is illustrated, as predicting platelet age as successfully done in transfusion products may also be applied here. Predicting ITP platelet age will help stratify between effector mechanisms at work in ITP.

the correct platelet age in blood products stored for 1, 3, 6 or 10 days. Other combinations of stainings should be tested to further optimize prediction accuracy and single platelet information.

A direct application of this approach is to rapidly assess the quality of platelet transfusion bags using a standardized protocol after further development and validation. Secondly, AI-based interpretation of a platelet imaging dataset may be used as a diagnostic toolkit to rapidly analyse platelet states in individuals. For example, the differential platelet states present in ITP patients that stem from either platelet destruction or reduced platelet production likely elicit a shift in the ratio between young and old platelets (Figure 2).

As described in Chapter 2, ITP is caused by differential effector mechanisms for which the current therapeutic approach is trial-and-error based [10,15]. Having a tool that can segregate patients based on platelet production defects versus platelet clearance would be useful in further dissecting the disease into well-characterized therapeutic and potentially even immunological subtypes. After validation, future steps in the project therefore would be to screen well-characterized ITP patients for potentially different platelet states and correlate this to their active treatment, platelet counts over time, and clinical condition.

### VWD and platelet degranulation – “Correlation is no causation”

Besides the microscopic approaches presented in this thesis that have a particular focus on platelet granular cargo like VWF in selective patients, we also performed a large explorative cohort study of platelet degranulation in VWD. In Chapter 4, we analysed the correlations between platelet degranulation and VWF- and clinical parameters in a large cohort of VWD patients for the first time, in an effort to pinpoint interesting targets for further investigation of the platelet compartment in VWD.

One of the most prominent findings in this study was the association between higher PF4 plasma levels and the current bleeding phenotype, particularly in type 1 VWD. This type of VWD is a heterogeneous collection of patients with synthesis or clearance defects, or other causes that lead to low VWF levels, with around 30% where no mutation can be identified in the VWF gene [32,44]. Therefore, it is intriguing that a marker for platelet cargo

release could warrant such an association with bleeding. While this may have multiple causes, elevated PF4 levels as we found in this subtype could be indicative of constitutive platelet activation. Pre-activated platelets are less likely to adequately respond to hemostatic challenges [3], which is in line with a previous correlative study that suggests that type 1 VWD patients with a relatively adequate hemostatic response (signified by DDAVP response) have a lower bleeding score [45]. Considering that platelet-derived VWF levels can also be reduced in type 1 VWD or low-VWF patients [46,47], often pointing to biosynthesis defects, studies on the platelet alpha-granule compartment and its secretion competence in well-characterized type 1 VWD patients is warranted to better identify the contribution of platelets and their cargo release such as VWF in type 1 VWD and its subgroups.

We also found that type 2B patients had lower PF4 levels in plasma, which may signify the inability of platelets to release PF4, a reduced synthesis of PF4 as a result of defective thrombopoiesis and/or a lower platelet pool that is capable of releasing PF4. However, platelet count alone may not explain lower PF4 levels in type 2B patients, considering that non-thrombocytopenic type 2B patients also had lower PF4 levels compared to other VWD types. Nurden et al. suggested that VWF has an important modulatory effect on megakaryopoiesis and platelet production, as evidenced by the fact that various type 2B mutations affect megakaryocyte production, platelet function and morphology [35,36]. While all type 2B patients tested had some degree of altered production or platelet abnormalities, some mutations like p.V1316M showed more severe defects than others. Finally, PF4 plasma levels may be an indicator for type 2B severity as we found lower PF4 levels in those patients with persistent thrombocytopenia. Regardless, further biological work on thrombopoiesis and the role of VWF therein will be essential to better understand how type 2B VWD modulates platelet biogenesis.

### **VWF and VWFpp in the megakaryocyte lineage - "You Never Clot Alone"**

Most of the work on VWF biosynthesis has been performed in cultured endothelial cell systems and heterologous expression systems. Although a handful of studies have illustrated that VWF in megakaryocytes and endothelial cells appears similar [48], there is still a significant lack of knowledge on VWF biosynthesis and trafficking in and from megakaryocytes. Further studies on platelet VWF from VWD patients may help us understand how VWF synthesis works in megakaryocytes. There may be differences in VWF dimerization, multimerisation, storage in- and exocytosis from WPBs versus alpha-granules as a result of specific mutations, which is currently unexplored. Parallel studies with endothelial cells will be paramount to assess cellular differences and to better understand when and how mutations affect patients. Bowman et al. showed that a specific type 3 mutation was less severe due to the contributions of residual endothelial- and platelet-derived VWF, signifying the importance of resolving the contributions and differences of cellular sources of VWF [34].

On a similar note, it is unclear how VWF is organized in the megakaryocyte

lineage in relation to its associated VWFpp, which is essential for VWF biosynthesis in endothelial cells [2]. In Chapter 6, we explored the distribution of VWF and VWFpp from megakaryocyte origin in platelets and compared this to findings from endothelial cell systems. We found that VWF and VWFpp are both present in close proximity in the eccentric part of alpha-granules [49]. As we know that platelet VWF is organized in tubular structures that are shorter in length than WPBs, it is likely that VWFpp is also present in these tubular structures [50]. However, advanced 3D electron microscopy will be necessary to fully disclose how VWFpp is incorporated in these structures and how this may differ from WPBs, where VWFpp is critical for the condensation of VWF tubules [5,51].

### **VWF and VWFpp exocytosis - "Secreted, not Stirred"**

We also studied the events triggering VWF and VWFpp release from platelet alpha-granules in Chapter 6. Studying platelet secretion events without the physical forces that are extended during platelet plug formation and aggregation allows one to discern the individual roles of cargo proteins in platelet organelles during the initial phase of cargo release. While one can precisely interrogate and compare granule release events, one of the caveats is that physical forces that may be necessary for complete release of alpha-granule cargo are not taken into account in this model [3].

Using quantitative 3D SIM, we found that VWFpp was released in much higher quantities than VWF despite their close proximity in alpha-granules. These findings are in contrast to release from endothelial cells, where VWF and VWFpp exit WPBs in a 1:1 stoichiometry [52]. It has been well established that VWF is partially retained in platelets [53]. We found that VWF-positive residual structures were often clustered together, which suggests that compound fusion events take place on a large scale during alpha-granule release [54]. We confirmed that such structures were post-exocytotic by using an anti-VWF nanobody that co-stained nearly all such structures. Together, this may indicate that VWF is unable to exit compound-fused granules while VWFpp can be adequately released. Alternatively, additional physical forces such as those in a thrombus environment are necessary to fully release platelet VWF, considering that platelets differentially release their content depending on their position in a thrombus [55].

### **VWF and VWFpp in thrombus formation - "Not All Those Who Wander Are Lost"**

In an effort to characterize the role of post-release VWFpp in a thrombus, we generated both thrombi in the absence of plasma and whole blood thrombi in a microfluidic device and analysed the 3D structural mapping of VWF and VWFpp at different time points of thrombus formation [56]. In particular, in thrombi that developed core and shell structures, we found a majority of VWFpp at the core whereas VWF could be predominantly found in the thrombus shell (Figure 3). This was the case in both plasma-depleted and whole blood thrombi, indicating that the presence or absence of plasma-derived VWF and VWFpp did not alter the distribution of these proteins. Additionally, the size of released cargo may determine its distribution in the thrombus environment and thus may affect VWF and

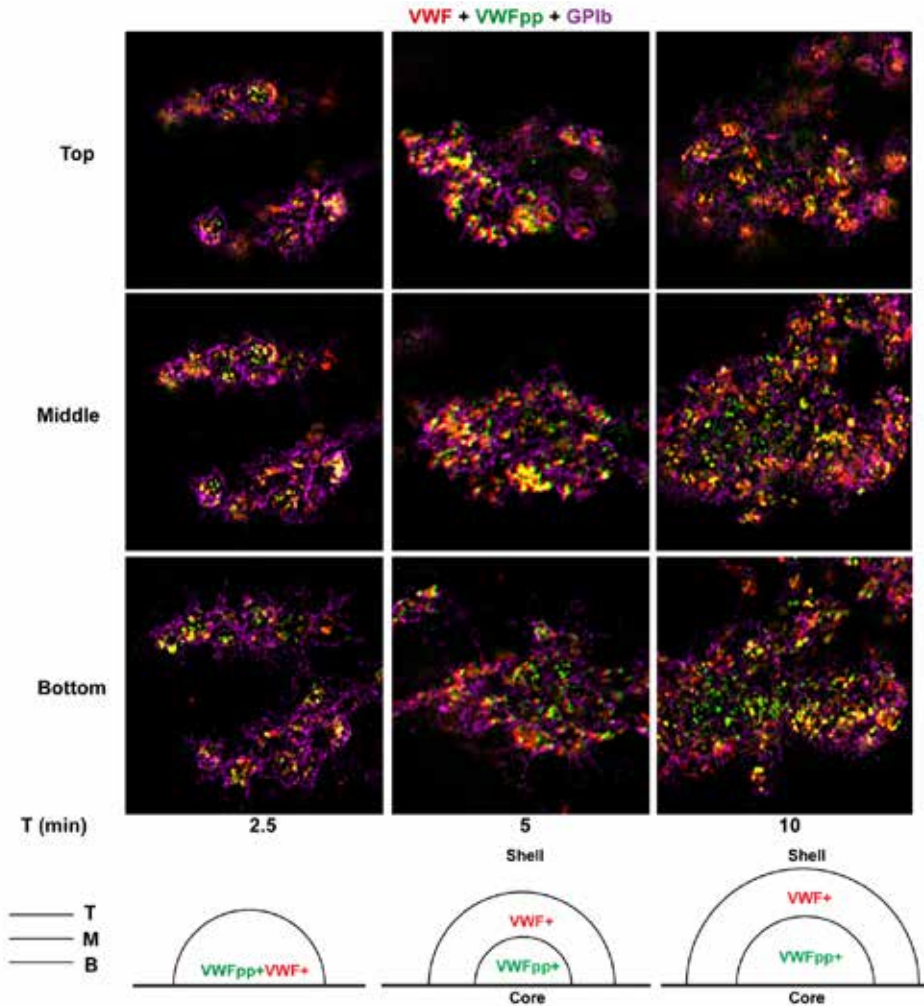


Figure 3. Thrombus generation under flow and VWF/VWFpp immunolocalization.

Thrombi were generated in a microfluidic model by flowing platelets and erythrocytes over a collagen type I layer for 2.5 / 5 / 10 minutes. Whole blood thrombi were similarly generated and showed similar immunolocalization. Top, middle and bottom sections of thrombi are depicted as stained for GPIb (magenta), VWF (red) and VWFpp (green). Cartoon illustrates the differential distribution of VWF and VWFpp in larger thrombi consisting of a core and shell. Samples were prepared by Titus Lemmens (and imaged by Maurice Swinkels) as part of a collaboration with dr. Judith Cosemans at MUMC. Unpublished work.

VWFpp differentially considering their size difference [55]. Further experiments are needed in order to identify whether the differential localization of VWFpp and VWF in thrombi results from differential exocytosis of alpha granules, as a result of thrombus dynamics, or a combination of these factors.

As Scott and Montgomery already posed in 1981: is VWFpp a platelet antigen while VWF is an endothelial antigen [57]? In Chapter 6, we speculate about a potential role of VWFpp as a platelet-derived component of VWF-related function that may be rapidly released at sites of tissue injury. The current findings are in line with emerging studies of VWFpp in mice [5], [58], where VWFpp appears to stimulate platelet-rich thrombus formation. It is unclear whether this phenomenon is a separate, or rather synergistic mechanism in relation to the differential distribution and release of VWF and VWFpp observed in our work. Further studies in mice and potentially also in human thrombectomy samples would be useful to establish the *in vivo* role of VWFpp in primary hemostasis. These are intriguing questions that hopefully will be answered in future experiments that interrogate the megakaryocyte- and endothelial VWF lineages before- and during thrombus formation and in the different pathological conditions of VWD.

In particular, the importance of VWFpp for megakaryocyte VWF biosynthesis and platelet VWF organization is yet unknown. Studying the effect of VWFpp mutations in VWD patient platelets [51], such as through iPSC-derived primary MK cultures, may help us better understand how these proteins are regulated in megakaryocytes and platelets.

### **Conclusions and future perspectives – “Merging is complete”**

The studies presented in this thesis highlight the potential of studying platelets in two distinct hematological disorders. One avenue where more rigorous platelet studies are needed is in ITP. Adequate monitoring of platelet counts is essential in both clinical and biological studies on ITP patients, in combination with an improved stratification of this heterogeneous disease. Hopefully, this will allow us to step away from the diagnosis of ‘thrombocytopenia without a known cause’.

Another avenue is the future development of unbiased, automated analyses of quantitative platelet imaging data, that will be an important stepping stone to move away from qualitative assessments of the highly heterogeneous population of circulating platelets. This discussion described three ongoing projects with a particular focus on quantitative imaging that prove to be interesting topics for future study.

Finally, platelets present an easy to access target to study the end product of VWF biosynthesis, which is particularly applicable in a translational setting to study VWD subtypes suffering from cellular VWF defects. This may help to better predict and understand the therapeutic efficacy of platelet transfusions (with functional cellular VWF) and DDAVP (releasing functional cellular VWF). With continuous developments in super-resolution microscopy, the way is open to quantitatively assess a cellular form of VWF in the diagnostic pipeline. Zooming in on platelet may provide us with novel insights to unravel the role of platelet-derived VWF and VWFpp in VWD pathogenesis.

## References

1. Broos K, Feys HB, De Meyer SF, Vanhoorelbeke K, Deckmyn H. Platelets at work in primary hemostasis. *Blood Rev* 2011; 25: 155–67.
2. Springer TA. Von Willebrand factor, Jedi knight of the bloodstream. *Blood* 2014; 124: 1412–25.
3. Yadav S, Storrie B. The cellular basis of platelet secretion: Emerging structure/function relationships. *Platelets* Taylor & Francis; 2017; 28: 108–18.
4. Yadav S, Storrie B. The cellular basis of platelet secretion: Emerging structure/function relationships. *Platelets* Taylor & Francis; 2017; 28: 108–18.
5. Rawley O, Lillicrap D. Functional Roles of the von Willebrand Factor Propeptide. *Hamostaseologie* 2021; 41: 63–8.
6. Kaushansky K. The molecular mechanisms that control thrombopoiesis. *J Clin Invest* 2005; 115: 3339–47.
7. Grozovsky R, Begonja AJ, Liu K, Visner G, Hartwig JH, Falet H, Hoffmeister KM. The Ashwell-Morell receptor regulates hepatic thrombopoietin production via JAK2-STAT3 signaling. *Nat Med* 2015; 21: 47–54.
8. Fielder PJ, Gurney AL, Stefanich E, Marian M, Moore MW, Carver-Moore K, De Sauvage FJ. Regulation of thrombopoietin levels by c-mpl - Mediated binding to platelets. *Blood* 1996; 87: 2154–61.
9. Cines DB, Cuker A, Semple JW. Pathogenesis of immune thrombocytopenia. *Press Medicale* 2014; 43.
10. Zufferey A, Kapur R, Semple JW. Pathogenesis and therapeutic mechanisms in immune thrombocytopenia (ITP). *J Clin Med* 2017; 6.
11. Nelson VS, Jolink ATC, Amini SN, Zwaginga JJ, Netelenbos T, Semple JW, Porcelijn L, de Haas M, Schipperus MR, Kapur R. Platelets in ITP: Victims in charge of their own fate? *Cells* 2021; 10.
12. Schifferli A, Holbro A, Chitlur M, Coslovsky M, Imbach P, Donato H, Elalfy M, Graciela E, Grainger J, Holzhauser S, Riccheri C, Rodeghiero F, Ruggeri M, Tamary H, Uglova T, Wu R, Kühne T. A comparative prospective observational study of children and adults with immune thrombocytopenia: 2-year follow-up. *Am J Hematol* 2018; 93: 751–9.
13. Stasi R, Stipa E, Masi M, Cecconi M, Scimò MT, Oliva F, Sciarra A, Perrotti AP, Adomo G, Amadori S, Papa G. Long-Term observation of 208 adults with chronic idiopathic thrombocytopenic purpura. *Am J Med* 1995; 98: 436–42.
14. Sailer T, Lechner K, Panzer S, Kyrle PA, Pabinger I. The course of severe autoimmune thrombocytopenia in patients not undergoing splenectomy. *Haematologica* 2006; 91: 1041–5.
15. Neunert C, Terrell DR, Arnold DM, Buchanan G, Cines DB, Cooper N, Cuker A, Despotovic JM, George JN, Grace RF, Kühne T, Kuter DJ, Lim W, McCrae KR, Pruitt B, Shimanek H, Vesely SK. American Society of Hematology 2019 guidelines for immune thrombocytopenia. *Blood Adv* 2019; 3: 3829–66.
16. Cines DB, Bussel JB, Liebman HA, Luning Prak ET. The ITP syndrome: Pathogenic and clinical diversity. *Blood* 2009; 113: 6511–21.
17. Greinacher A, Thiele T, Warkentin TE, Weisser K, Kyrle PA, Eichinger S. Thrombotic Thrombocytopenia after ChAdOx1 nCov-19 Vaccination. *N Engl J Med* 2021; 384: 2092–101.
18. Beltrami Moreira M, Bussel JB, Lee E-J. Sars-Cov-2 Vaccination in Pre-Existing and De Novo ITP: A Single Center Experience with Long-Term Follow-up. *Blood* 2022; 140: 8495–6.
19. Crickx E, Moulis G, Ebbo M, Terriou L, Briantais A, Languille L, Limal N, Guillet S, Michel M, Mahevas M, Godeau B. Safety of anti-SARS-CoV-2 vaccination for patients with immune thrombocytopenia. *Br J Haematol* 2021; 195: 703–5.
20. Shrivastava M. The platelet storage lesion. *Transfus Apher Sci* 2009; 41: 105–13.
21. Rijkers M, van der Meer PF, Bontekoe IJ, Daal BB, de Korte D, Leebeek FWG, Voorberg J, Jansen AJG. Evaluation of the role of the GPIb-IX-V receptor complex in development of the platelet storage lesion. *Vox Sang* 2016; 111: 247–56.
22. Rijkers M, Van Den Eshof BL, Van Der Meer PF, Van Alphen FPJ, De Korte D, Leebeek FWG, Meijer AB, Voorberg J, Jansen AJG. Monitoring storage induced changes in the platelet proteome employing label free quantitative mass spectrometry. *Sci Rep* 2017; 7.
23. Montague SJ, Lim YJ, Lee WM, Gardiner EE. Imaging Platelet Processes and Function—Current and Emerging Approaches for Imaging in vitro and in vivo. *Front Immunol* 2020; 11.
24. Italiano JE, Richardson JL, Patel-Hett S, Battinelli E, Zaslavsky A, Short S, Ryeom S, Folkman J, Klement GL.

- Angiogenesis is regulated by a novel mechanism: Pro- and antiangiogenic proteins are organized into separate platelet  $\alpha$  granules and differentially released. *Blood* 2008; 111: 1227–33.
25. Sehgal S, Storrie B. Evidence that differential packaging of the major platelet granule proteins von Willebrand factor and fibrinogen can support their differential release. *J Thromb Haemost* 2007; 5: 2009–16.
  26. Kamykowski J, Carlton P, Sehgal S, Storrie B. Quantitative immunofluorescence mapping reveals little functional coclustering of proteins within platelet  $\alpha$ -granules. *Blood* 2011; 118: 1370–3.
  27. Pokrovskaya ID, Yadav S, Rao A, McBride E, Kamykowski JA, Zhang G, Aronova MA, Leapman RD, Storrie B. 3D ultrastructural analysis of  $\alpha$ -granule, dense granule, mitochondria, and canalicular system arrangement in resting human platelets. *Res Pract Thromb Haemost* 2020; 4: 72–85.
  28. Jonnalagadda D, Izu LT, Whiteheart SW. Platelet secretion is kinetically heterogeneous in an agonist-responsive manner. *Blood* 2012; 120: 5209–16.
  29. Schermelleh L, Ferrand A, Huser T, Eggeling C, Sauer M, Biehlmaier O, Drummen GPC. Super-resolution microscopy demystified. *Nat Cell Biol* 2019; 21: 72–84.
  30. Westmoreland D, Shaw M, Grimes W, Metcalf DJ, Burden JJ, Gomez K, Knight AE, Cutler DF. Super-resolution microscopy as a potential approach to diagnosis of platelet granule disorders. *J Thromb Haemost* 2016; 14: 839–49.
  31. Smith CS, Slotman JA, Schermelleh L, Chakrova N, Hari S, Vos Y, Hagen CW, Müller M, van Cappellen W, Houtsmuller AB, Hoogenboom JP, Stallinga S. Structured illumination microscopy with noise-controlled image reconstructions. *Nat Methods* 2021; 18: 821–8.
  32. De Gopegui RR, Feldman BF. von Willebrand's disease. *Comp Clin Path* 1997; 7: 187–96.
  33. de Jong A, Eikenboom J. Von Willebrand disease mutation spectrum and associated mutation mechanisms. *Thromb Res* 2017; 159: 65–75.
  34. Bowman ML, Pluthero FG, Tuttle A, Casey L, Li L, Christensen H, Robinson KS, Lillicrap D, Kahr WHA, James P. Discrepant platelet and plasma von Willebrand factor in von Willebrand disease patients with p. Pro2808Leufs\*24. *J Thromb Haemost* 2017; 15: 1403–11.
  35. Nurden P, Gobbi G, Nurden A, Enouf J, Youyouz-Marfak I, Carubbi C, La Marca S, Punzo M, Baronciani L, De Marco L, Vitale M, Federici AB. Abnormal VWF modifies megakaryocytopoiesis: Studies of platelets and megakaryocyte cultures from patients with von Willebrand disease type 2B. *Blood* 2010; 115: 2649–56.
  36. Nurden P, Debili N, Vainchenker W, Bobe R, Bredoux R, Corvazier E, Combrie R, Fressinaud E, Meyer D, Nurden AT, Enouf J. Impaired megakaryocytopoiesis in type 2B von Willebrand disease with severe thrombocytopenia. *Blood* 2006; 108: 2587–95.
  37. Nurden P, Chretien F, Poujol C, Winckler J, Borel-Derlon A, Nurden A. Platelet ultrastructural abnormalities in three patients with type 2B von Willebrand disease. *Br J Haematol* 2000; 110: 704–14.
  38. Karampini E, Bierings R, Voorberg J. Orchestration of Primary Hemostasis by Platelet and Endothelial Lysosome-Related Organelles. *Arterioscler Thromb Vasc Biol* 2020; 40: 1441–53.
  39. Lentaigne C, Freson K, Laffan MA, Turro E, Ouwehand WH. Inherited platelet disorders: Toward DNA-based diagnosis. *Blood* 2016; 127: 2814–23.
  40. Casari C, Bergmeier W. Acquired platelet disorders. *Thromb Res* 2016; 141: S73–5.
  41. Brunet JG, Iyer JK, Badin MS, Graf L, Moffat KA, Timleck M, Spitzer E, Hayward CPM. Electron microscopy examination of platelet whole mount preparations to quantitate platelet dense granule numbers: Implications for diagnosing suspected platelet function disorders due to dense granule deficiency. *Int J Lab Hematol* 2018; 40: 400–7.
  42. Pike JA, Simms VA, Smith CW, Morgan N V., Khan AO, Poulter NS, Styles IB, Thomas SG. An adaptable analysis workflow for characterization of platelet spreading and morphology. *Platelets* 2021; 32: 54–8.
  43. Slotman J, Swinkels M, Burgisser PE, Bestebroer J, Klei TRL, Houtsmuller AB, Leebeek FWG, Bierings R, Jansen AJG. Predicting Platelet Age Using Artificial Intelligence Techniques. *Blood* 2022; 140: 2656–7.
  44. Flood VH, Christopherson PA, Gill JC, Friedman KD, Haberichter SL, Bellissimo DB, Udani RA, Dasgupta M, Hoffmann RG, Ragni M V., Shapiro AD, Lusher JM, Lentz SR, Abshire TC, Leissing C, Hoots WK, Manco-Johnson MJ, Gruppo RA, Boggio LN, Montgomery KT, et al. Clinical and laboratory variability in a cohort of patients diagnosed with type 1 VWD in the United States. *Blood* 2016; 127: 2481–8.
  45. Atiq F, Schütte LM, Looijen AEM, Boender J, Cnossen MH, Eikenboom J, de Maat MPM, Kruip MJHA, Leebeek FWG. Von Willebrand factor and factor VIII levels after desmopressin are associated with bleeding

phenotype in type 1 VWD. *Blood Adv* 2019; 3: 4147–54.

46. Casonato A, Cattini MG, Daidone V, Pontara E, Bertomoro A, Prandoni P. Diagnostic value of measuring platelet von Willebrand factor in von willebrand disease. *PLoS One* 2016; 11.

47. Lavin M, Aguila S, Schneppenheim S, Dalton N, Jones KL, O'Sullivan JM, O'Connell NM, Ryan K, White B, Byrne M, Rafferty M, Doyle MM, Nolan M, Preston RJS, Budde U, James P, Di Paola J, O'Donnell JS. Novel insights into the clinical phenotype and pathophysiology underlying low VWF levels. *Blood* 2017; 130: 2344–53.

48. Sporn LA, Chavin SI, Marder VJ, Wagner DD. Biosynthesis of von Willebrand protein by human megakaryocytes. *J Clin Invest* 1985; 76: 1102–6.

49. Cramer EM, Meyer D, Le Menn R, Breton-Gorius J. Eccentric localization of von Willebrand factor in an internal structure of platelet  $\alpha$ -granule resembling that of Weibel-Palade bodies. *Blood* 1985; 66: 710–3.

50. Van Nispen Tot Pannerden H, De Haas F, Geerts W, Posthuma G, Van Dijk S, Heijnen HFG. The platelet interior revisited: Electron tomography reveals tubular  $\alpha$ -granule subtypes. *Blood* 2010; 116: 1147–56.

51. Haberichter SL. Von Willebrand factor propeptide: Biology and clinical utility. *Blood* 2015; 126: 1753–61.

52. Wagner DD, Fay PJ, Sporn LA, Sinha S, Lawrence SO, Marder VJ. Divergent fates of von Willebrand factor and its propolypeptide (von Willebrand antigen II) after secretion from endothelial cells. *Proc Natl Acad Sci U S A* 1987; 84: 1955–9.

53. Koutts J, Walsh PN, Plow EF, Fenton II and JW, Bouma BN, Zimmerman TS. Active release of human platelet factor VIII related antigen by adenosine diphosphate, collagen, and thrombin. *J Clin Invest* 1978; 62: 1255–63.

54. Eckly A, Rinckel JY, Proamer F, Ulas N, Joshi S, Whiteheart SW, Gachet C. Respective contributions of single and compound granule fusion to secretion by activated platelets. *Blood* 2016; 128: 2538–49.

55. Stalker TJ, Welsh JD, Brass LF. Shaping the platelet response to vascular injury. *Curr Opin Hematol* 2014; 21: 410–7.

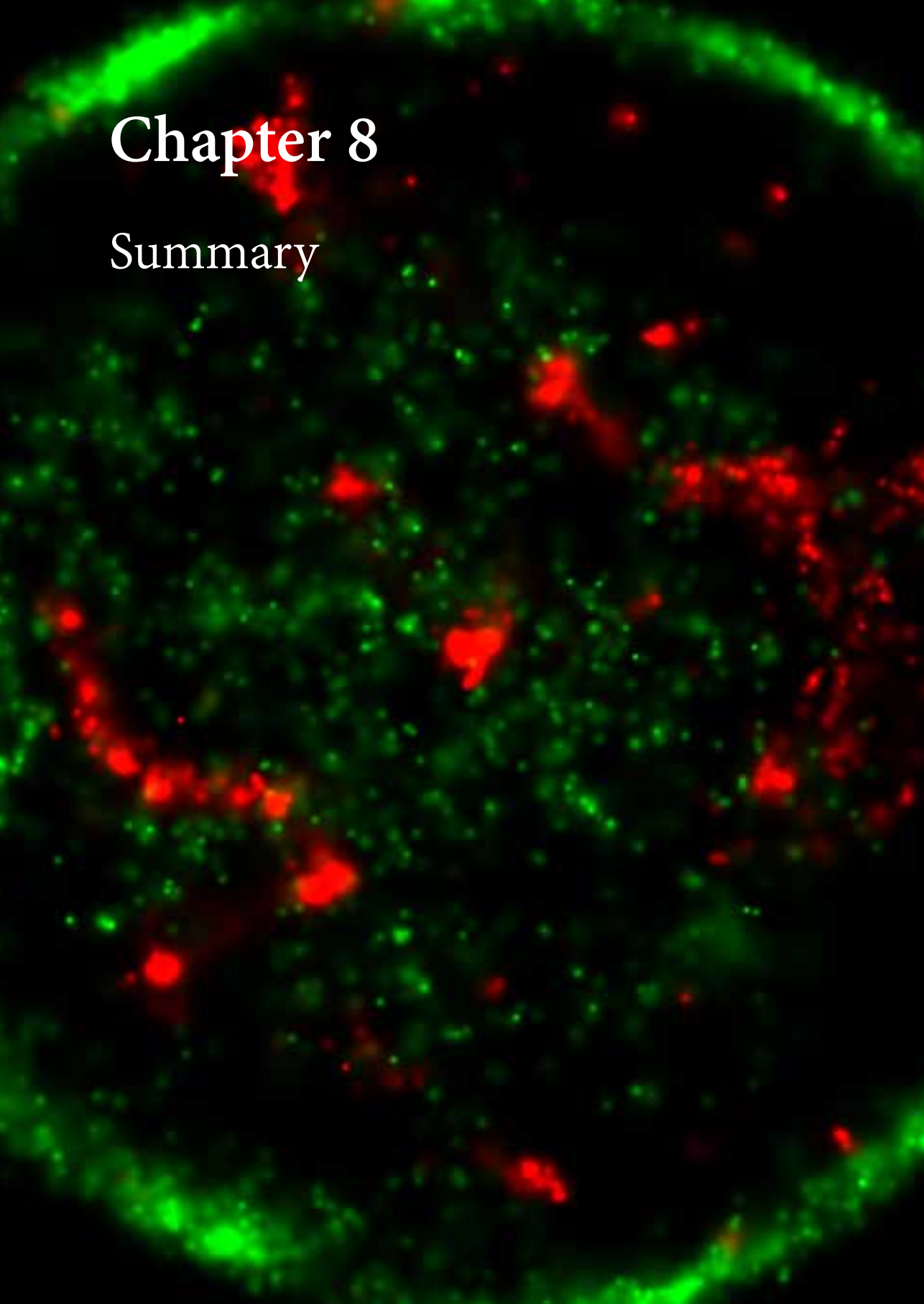
56. Oral Communication abstracts. *Res Pract Thromb Haemost* 2022; 6: e12787.

57. Scott JP, Montgomery RR. Platelet von Willebrand's antigen II: Active release by aggregating agents and a marker of platelet release reaction in vivo. *Blood* 1981; .

58. Rawley O, Dwyer C, Nesbitt K, Notley C, Michels A, Lillicrap D. The VWF Propeptide Is A Novel Component Of Venous Thrombi In A Mouse Model Of DVT. *Res Pr Thromb Haemost* 2022; 6: e12788.

# Chapter 8

## Summary



## Summary

Platelets play a central role in the hemostatic system, and platelet defects are found in various hemostatic disorders. The aim of this thesis was to study the dynamics and function of platelets in the hemostatic disorders immune thrombocytopenia (ITP) and von Willebrand Disease (VWD). As platelets are heterogeneous cells with a short lifespan, quantitative methodologies were an important part of the approach for each chapter. The background biology of platelets, pathobiology of ITP and VWD, and quantitative methodologies presented in this thesis are part of Chapter 1. The subsequent parts of the thesis focused on platelet aspects in ITP (Chapter 2 and 3) and in VWD (Chapter 4, 5 and 6). Finally, a general discussion that outlines the research presented in this thesis in a broader perspective is part of Chapter 7. Future perspectives and preliminary data of follow-up studies are also discussed.

### Part 1: Platelets in ITP: Opportunities and Challenges

In Chapter 2, we reviewed several emerging concepts in the pathophysiology of ITP with the aim to summarize our current mechanistical knowledge on ITP and to provide suggestions on the conceptual approach of ITP pathophysiology. The anti-platelet response in ITP patients is characterized by autoantibodies and cytotoxic CD8+ T cells, which may enhance platelet clearance and/or inhibit platelet production in the bone marrow. We proposed a novel model for ITP pathogenesis, where onset of the disease relies on a trigger leading to exposure of platelet surface antigens. Additionally, loss of tolerance is essential for chronic auto-immunity against platelets. These concepts are in line with other auto-immune diseases, but are not used in ITP, where classification of ITP is primarily based on clinical aspects. We finally speculated that post-translational modifications of platelet antigens may contribute to ITP pathogenesis.

In Chapter 3, we presented a systematic study of platelet counts in ITP patients and healthy individuals undergoing COVID-19 vaccination, with the aim to assess the safety and effect of vaccination on platelets counts. The systematic approach entailed platelet counts measured before and after first- and second vaccination events, which enabled mixed-effects modelling to analyse platelet counts over time and differentiation from natural platelet fluctuations. Vaccination leads to a decrease in platelet counts in ITP patients and healthy controls, but there was no significant difference in the decrease between these groups. A subgroup of ITP patients at risk, due to lower baseline platelet counts or those requiring active ITP treatment, were found to have relatively more ITP exacerbations. We found that COVID-19 vaccination was safe for ITP patients but close monitoring of platelet counts is important for subgroups at risk of exacerbation. Additionally, this study illustrated that a systematic approach is needed to differentiate platelet fluctuations that are also present in healthy individuals from platelet changes in ITP patients at risk.

## Part 2: Platelet and VWF: Key Partners in Disease and Health

In Chapter 4, we explored the role of platelet degranulation in the context of VWD, with the aim to explore VWD subtypes where the contribution of platelet derived VWF may need to be more intensively studied. Platelet degranulation was measured based on plasma PF4 samples in a large cohort of VWD patients to identify possible associations with VWF- and clinical parameters from this population. We found that PF4 levels were lower in type 2B VWD, particularly in patients with persistent thrombocytopenia. Another observation was that PF4 levels were correlated to a current bleeding phenotype in type 1 patients. Whether these cumulative findings are indicative of platelet (degranulation) defects in these subtypes is currently unclear. However, the associations found in this study suggest that platelet function and degranulation may play a unique role in specific VWD subtypes and provide a basis for further studies on platelets in VWD.

In Chapter 5, we developed a quantitative super-resolution imaging methodology based on SIM to study platelet granular structures, with the aim to tackle the heterogeneity of platelets in the circulation, and particularly the heterogeneity of their granular content. This methodology was applied to study VWF in platelets from healthy individuals and VWD patients in comparison to a control alpha-granule cargo protein, SPARC. SIM-based imaging highlighted a large intra- and interindividual variability in VWF and SPARC-positive structures in healthy individuals. Despite this variability, we were able to accurately quantify alpha-granular release of VWF and SPARC upon platelet stimulation with the developed methodology. Furthermore, we were able to stratify two type 3 VWD patients caused by distinct pathogenic mechanisms that could not be distinguished by their diagnostic VWF values. Stratification was successful using SIM, but not when using standard confocal microscopy, illustrating the added value of a SIM-based approach. Finally, we studied VWD patients with heterozygous or homozygous p.C1190 mutations in VWF with SIM and traditional approaches, and found that platelet- and plasma-VWF multimerization differed in patients with a p.C1190 mutation. We demonstrated that a quantitative imaging approach helps to better understand VWF storage in alpha-granules and how VWF biosynthesis defects in VWD may lead to VWF defects in platelets.

In Chapter 6, we studied the localization and contribution of platelet-derived VWF and its propeptide in hemostasis during platelet cargo release with the aim to characterize their release profiles in response to physiological stimuli. Quantitative super-resolution imaging as developed in Chapter 5 revealed that VWF and VWFpp occupy the same alpha-granular nanodomains in resting platelets. Various stimuli and dosages demonstrated that the release of VWF and VWFpp from individual granule nanodomains occurs in a differential fashion. VWFpp exits alpha-granules even at low stimulus conditions while VWF requires a strong stimulus to be released, and even then is partially retained. VWFpp was the major antigen to be released from a large number of individual alpha-granules, both in reference to VWF and to fibrinogen and SPARC, two other alpha-granule cargo proteins. Considering the unexplored function of VWFpp in the circulation, these findings

hopefully help unravel the contribution of VWF and VWFpp, differentially derived from either endothelium or platelets, in the formation of hemostatic platelet plugs.

Finally, the findings from this thesis were discussed in view of the general literature in Chapter 7, with additional suggestions for future research. We relate the published findings from this thesis to preliminary data from additional ongoing studies of platelet imaging in A) additional VWD patients, B) the application of AI on platelet images and C) in vitro-generated thrombi to further study VWF and VWFpp in hemostasis. Finally, we re-iterate the importance of quantitative platelet studies in order to accurately capture their heterogeneity in terms of platelet numbers and granular content. Future studies on ITP (numbers), VWD (granular content) and beyond should always consider the heterogeneity of platelets.

# Samenvatting

Bloedplaatjes spelen een centrale rol in het hemostatische systeem, en defecten in bloedplaatjes worden gevonden in verschillende hemostatische ziektes. Het doel van het onderzoek in dit proefschrift was om de dynamiek en functie van bloedplaatjes te bestuderen in de hemostatische ziektes immuun trombocytopenie (ITP) en von Willebrandziekte (VWZ). Omdat bloedplaatjes heterogene cellen zijn met een korte levensduur, waren kwantitatieve methodologieën een belangrijk onderdeel in de aanpak van elk hoofdstuk. De achtergrondkennis van de onderliggende biologie van bloedplaatjes in ITP en VWZ, als ook de kwantitatieve methodologieën die gebruikt zijn in dit proefschrift worden beschreven in hoofdstuk 1. De volgende delen van het proefschrift richten zich op de aspecten van bloedplaatjes in ITP (hoofdstuk 2 en 3) en in VWZ (hoofdstuk 4, 5 en 6). Hoofdstuk 7 sluit af met een algemene discussie die betrekking heeft op het uitgevoerde onderzoek in een breder kader. Toekomstperspectieven en preliminaire data van vervolgonderzoek worden hier ook bediscussieerd.

## Deel 1: Bloedplaatjes in ITP: kansen en uitdagingen

In hoofdstuk 2 wordt er gereflecteerd op enkele nieuwe ideeën en concepten op het gebied van de pathofysiologie van ITP, met als doel om suggesties te doen in de conceptuele aanpak van ITP en onze huidige mechanistische kennis van ITP samen te vatten. De immuunreactie tegen bloedplaatjes in ITP patiënten wordt gekarakteriseerd door autoantistoffen en cytotoxische CD8<sup>+</sup> T-cellen, die de opruiming van bloedplaatjes versnellen of de productie van nieuwe bloedplaatjes in het beenmerg afremmen. We hebben een nieuw model voor de pathogenese van ITP voorgesteld waar de aanleiding van de ziekte afhangt van een trigger die leidt tot de blootstelling van oppervlakte antigenen op bloedplaatjes. Daarnaast is het verlies van immuuntolerantie essentieel om chronische auto-immuniteit tegen bloedplaatjes te ontwikkelen. Deze concepten komen overeen met die van andere auto-immuunziektes, maar worden nu niet toegepast voor ITP, waar de classificatie voornamelijk afhangt van klinische eigenschappen. Ten slotte speculeren we dat post-translationele modificaties van antigenen op bloedplaatjes een rol kunnen spelen in de ITP pathogenese.

In hoofdstuk 3 hebben we een systematische studie gedaan naar bloedplaatjes aantallen in ITP patiënten en gezonde donoren die gevaccineerd werden tegen COVID-19, met als doel de veiligheid en het effect van deze vaccinatie op bloedplaatjes aantallen vast te stellen. Als onderdeel van de systematische aanpak werd het aantal bloedplaatjes gemeten voor- en na de eerste- en tweede vaccinatie, waardoor met behulp van mixed-effect modellering het aantal bloedplaatjes in de loop van de tijd en los van natuurlijke afwijkingen kon worden bepaald. Vaccinatie leidde tot een afname in bloedplaatjes in ITP patiënten en gezonde donoren, maar er was geen significant verschil in deze afname tussen deze twee groepen. Een subgroep van ITP patiënten die een verhoogd risico op bloedingen hadden

vanwege een verlaagd standaard aantal bloedplaatjes of omdat ze intensieve medicatie nodig hadden, hadden ook relatief vaker een verergering van de ziekte. COVID-19 vaccinatie is veilig voor ITP patiënten maar bloedplaatjes aantallen moeten goed gemonitord worden in subgroepen die een verhoogd risico hebben. Daarnaast liet deze studie zien dat een systematische aanpak nodig is om natuurlijk afwijkingen in het aantal bloedplaatjes, die ook in gezonde donoren kunnen voorkomen, te kunnen onderscheiden van afwijkingen in ITP patiënten met een verhoogd risico.

## **Deel 2: Bloedplaatjes en VWF: compagnons in ziekte en gezondheid**

In hoofdstuk 4 hebben we een oriënterende studie gedaan naar de rol van bloedplaatjes degranulatie binnen VWZ, met het doel om VWZ subtypes te bekijken waar de bijdrage van bloedplaatjes afkomstig-VWF mogelijk beter moet worden onderzocht. Bloedplaatjes degranulatie werd gemeten op basis van plasma PF4 waardes in monsters van een groot cohort van VWZ patiënten om te kijken naar mogelijk associaties met VWF en klinische parameters. PF4 levels waren lager in type 2B VWZ, met name in patiënten met een persistente trombocytopenie. Daarnaast waren PF4 waardes gecorreleerd aan een huidig bloedingsfenotype in type 1 patiënten. Of deze bevindingen indicatief zijn voor bloedplaatjes (degranulatie) defecten in deze subtypes is onduidelijk. Desalniettemin suggereren de associaties in deze studie dat bloedplaatjes functie en degranulatie een unieke rol kan spelen in specifieke VWZ subtypen en vormen een basis voor verdere studie van bloedplaatjes binnen VWZ.

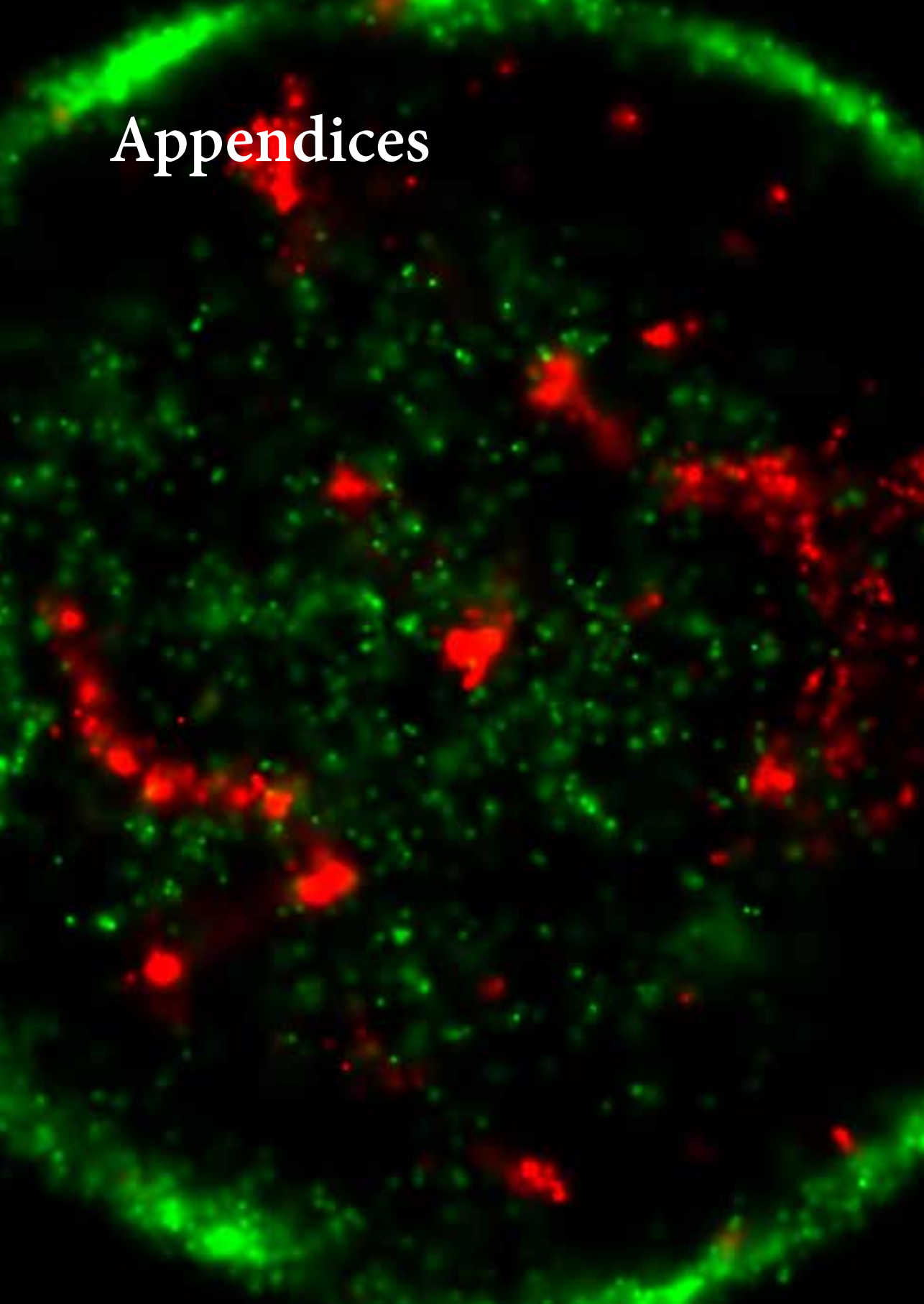
In hoofdstuk 5 hebben we een kwantitatieve super-resolutie microscopie methodologie ontwikkeld op basis van SIM om granulaire structuren van bloedplaatjes te kunnen bekijken, met als doel om de heterogeniteit van bloedplaatjes in de circulatie, en met name van diens granulaire inhoud, goed te kunnen bestuderen. Hiermee is er gekeken naar de organisatie van VWF in bloedplaatjes van gezonde donoren en VWZ patiënten in vergelijking met een controle alfa-granule eiwit, SPARC. Met SIM-gebaseerde imaging was het mogelijk om grote intra- en interindividuele afwijkingen te meten in VWF- en SPARC-positieve structuren in gezonde donoren. Ondanks deze variatie was het mogelijk om de release van VWF en SPARC vanuit alfa-granules als gevolg van bloedplaatjes stimulatie accuraat te kwantificeren. Het was ook mogelijk om twee verschillende type 3 VWZ patiënten met een verschillend onderliggend pathogeen mechanisme te onderscheiden, die niet te onderscheiden waren op basis van hun diagnostische lab waardes. Dit onderscheid lukte wel met SIM, maar niet met een standaard aanpak op basis van confocale microscopie, wat de meerwaarde van een op SIM-gebaseerde aanpak onderstreept. Ten slotte zijn VWZ patiënten met een heterozygote of homozygote p.C1190 mutatie onderzocht met SIM en traditionele technieken. Hiermee werd gevonden dat de multimerisatie van bloedplaatjes- en plasma-VWF afweek in p.C1190 patiënten. In dit hoofdstuk hebben we laten zien dat een kwantitatieve imaging aanpak bij kan dragen om beter te begrijpen hoe VWF wordt opgeslagen in alfa-granules en hoe defecten in de biosynthese van VWF in VWD patiënten kunnen leiden tot VWF defecten in bloedplaatjes.

In hoofdstuk 6 hebben we de lokalisatie en contributie van bloedplaatjes afkomstig VWF en VWF-propeptide (VWFpp) in hemostase en gedurende bloedplaatjes degranulatie bestudeerd, met als doel om het degranulatie profiel als gevolg van verschillende fysiologische stimuli in kaart te brengen. De kwantitatieve imaging methodologie van hoofdstuk 5 liet zien dat VWF en VWFpp in hetzelfde nanodomein van alfa-granules zitten. De release van VWF en VWFpp uit deze zelfde nanodomeinen is verschillend onder variërende stimuli en doseringen. VWFpp komt snel vrij uit alfa-granules, ook bij lage doseringen, terwijl VWF een sterke stimulus nodig heeft om vrij te komen, en zelfs dan niet volledig vrij komt. In vergelijking met VWF maar ook met fibrinogeen en SPARC, twee andere eiwitten uit alfa-granules, is VWFpp een antigeen wat in grote mate uit alfa-granules vrij komt als gevolg van stimulatie. Omdat het nog onduidelijk is wat VWFpp doet in de circulatie, helpen deze bevindingen hopelijk hoe de verschillende release van VWF en VWFpp uit zowel endotheel als bloedplaatjes bijdragen aan de vorming van bloedstolsels.

Ten slotte zijn de bevindingen in dit proefschrift bediscussieerd in de context van de bekende literatuur in hoofdstuk 7, met suggesties voor verder onderzoek. We hebben de gepubliceerde bevindingen gerelateerd aan preliminaire data van aanvullende lopende studies op het gebied van bloedplaatjes imaging in A) extra VWZ patiënten, B) de toepassing van kunstmatige intelligentie op afbeeldingen van bloedplaatjes, en C) in-vitro gegenereerde trombi om de rol van VWF en VWFpp in hemostase verder te bestuderen. Ten slotte blijft het belangrijk om kwantitatieve studies van bloedplaatjes te doen om goed met hun heterogeniteit in aantal- en granulaire inhoud om te kunnen gaan. Verdere studies op het gebied van ITP (aantallen) en VWD (granulaire inhoud) zullen altijd de heterogeniteit van bloedplaatjes in acht moeten houden.



# Appendices



## List of publications

**Swinkels M**, Hordijk S, Bürgisser PE, Slotman JA, Carter T, Leebeek FWG, Jansen AJG, Voorberg J, Bierings R. “Quantitative super-resolution imaging of platelet degranulation reveals differential release of von Willebrand factor and von Willebrand factor propeptide from alpha-granules.” *J Thromb Haemost.* 2023 Jul;21(7):1967-1980.

Bura A, de Matteis MA, Bender M, **Swinkels M**, Versluis J, Jansen AJG, Jurak Begonja A. “Oculocerebrorenal syndrome of Lowe protein controls cytoskeletal reorganisation during human platelet spreading.” *Br J Haematol.* 2023 Jan;200(1):87-99.

**Swinkels M**, Atiq F, Bürgisser PE, van Moort I, Meijer K, Eikenboom J, Fijnvandraat K, van Galen KPM, de Meris J, Schols SEM, van der Bom JG, Cnossen MH, Voorberg J, Leebeek FWG, Bierings R, Jansen AJG; WiN study group. “Platelet degranulation and bleeding phenotype in a large cohort of Von Willebrand disease patients.” *Br J Haematol.* 2022 May;197(4):497-501.

Visser C, **Swinkels M**, van Werkhoven ED, Croles FN, Noordzij-Nooteboom HS, Eefting M, Last-Koopmans SM, Idink C, Westerweel PE, Santbergen B, Jobse PA, Baboe F; RECOVAC-IR Consortium; Te Boekhorst PAW, Leebeek FWG, Levin MD, Kruij MJHA, Jansen AJG. “COVID-19 vaccination in patients with immune thrombocytopenia.” *Blood Adv.* 2022 Mar 22;6(6):1637-1644.

**Swinkels M**, Atiq F, Bürgisser PE, Slotman JA, Houtsmuller AB, de Heus C, Klumperman J, Leebeek FWG, Voorberg J, Jansen AJG, Bierings R. “Quantitative 3D microscopy highlights altered von Willebrand factor  $\alpha$ -granule storage in patients with von Willebrand disease with distinct pathogenic mechanisms.” *Res Pract Thromb Haemost.* 2021 Sep 14;5(6):e12595.

Van Dijck R, Lauw MN, **Swinkels M**, Russcher H, Jansen AJG. “COVID-19-associated pseudothrombocytopenia.” *EJHaem.* 2021 Jun 6;2(3):475-477.

**Swinkels M**, Rijkers M, Voorberg J, Vidarsson G, Leebeek FWG, Jansen AJG. “Emerging Concepts in Immune Thrombocytopenia.” *Front Immunol.* 2018 Apr 30;9:880.

**Swinkels M**, Zhang JH, Tilakaratna V, Black G, Perveen R, McHarg S, Inforzato A, Day AJ, Clark SJ. “C-reactive protein and pentraxin-3 binding of factor H-like protein 1 differs from complement factor H: implications for retinal inflammation.” *Sci Rep.* 2018 Jan 26;8(1):1643.

## About the Author

Maurice Swinkels was born in Asten on the 11th of August, 1993. He finished his VWO at the Varendonck College in Asten in 2010. He went to study Molecular Life Sciences in Nijmegen (Bachelor degree in 2014 and Master degree in 2016). His Bachelor internship was done at the Radboud Institute for Molecular Life Sciences under Dr. Koenderink. Master Internships were taken under Prof. Van der Vlag, Department of Nephrology, at the same institute; and at the University of Manchester, under Dr. Simon Clark. Due to his interests in innate response systems, Maurice went to study for his PhD on blood platelets at the Department of Hematology at the Erasmus MC in Rotterdam. Afterwards, he stepped into the family business of Primasta B.V., where he uses his biological expertise in the technical aspects of the company.

## PhD Portfolio

<b>Courses</b>	<b>ECTS</b>	<b>Year</b>
Scientific Integrity	0.3	2017
Biostatistics	5.7	2017
CPO	0.3	2017
BROK	1.5	2017
Flow Cytometry course	1	2017
NVTH PhD course	0.6	2017
Photoshop/InDesign course	0.3	2019
Image Analysis course	0.6	2019
<b>Scientific meetings</b>	<b>ECTS</b>	<b>Year</b>
Work discussions hemostasis (weekly)	10.8	2017-2021
Work discussions platelets (weekly)	18	2017-2021
Friday Floor meetings (weekly)	7.8	2017-2021
Hematology lectures + PhD lunch (monthly)	1.8	2017-2021
Journal Club (monthly)	1.8	2017-2021
<b>Symposia and congresses</b>	<b>ECTS</b>	<b>Year</b>
NVTH Symposium	1.8	2017, 2019, 2020
COEUR Symposia	1.6	2017-2020
ISTH Congress	5.4	2017, 2020-2022
NVB Symposium	0.6	2017
Platelets Symposium	1.2	2018
COEUR PhD Day	3	2017-2019
ExCOEURsions	0.8	2018-2019
ASH Congress	1.2	2019
DHC Congress	0.1	2020
<b>Scientific presentations</b>	<b>ECTS</b>	<b>Year</b>
ASH Congress (Poster)	1.5	2019
DHC Congress (Oral)	0.9	2020
ISTH Congress (Virtual Poster)	0.9	2020
ISTH Congress (Oral)	1.5	2022
<b>Supervision</b>	<b>ECTS</b>	<b>Year</b>
Systematic Reviews for Medicine students	1.2	2017-2019
Clinical Technology Bachelor Project	2	2018
<b>Total ECTS</b>	<b>74.2</b>	

**Committees**

Lab Day committee

**Year**

2017-2018

COEUR PhD committee

2017-2019

**Awards**

RPTH Editor's Award for Early Career Researchers

2022

ISTH Early Career Award

2022

## Dankwoord

**Frank:** toen ik begon in jouw toch redelijke klinische groep was het allemaal nog nieuw. Het was ontzettend leuk om in het begin de polibespreking, het stolrapport en zelfs een keer de ochtendbespreking van de kliniek mee te maken. In het begin was het geloof ik voor ons allen nog een beetje onduidelijk wat ik allemaal ging doen met bloedplaatjes, flow cytometrie en imaging, maar op een gegeven moment hebben we een mooie draai weten te maken naar VWF en VWD. Bedankt voor alle feedback, hulp en begeleiding gedurende de afgelopen jaren.

**Jan:** de maandagochtend werd stevast begonnen met een strakke resultatenbespreking over Skype/Zoom en soms een kritische noot, maar er was ook altijd ruimte voor wat droge humor over bijvoorbeeld de eeuwige rivaliteit tussen Amsterdam en Rotterdam. Je constante roep om deadlines hielp ontzettend om in de eerste jaren om goed door te schakelen naar meer succesvolle projecten. Bedankt voor deze uitstekende samenwerking.

**Gerard:** je karakteristieke loopje naar het kantoor in het lab kenmerkte weer een mooi gesprek (ook wel eens midden in een experiment) over alle lopende projecten, met vaak nieuwe ideeën en soms ook behoorlijke discussie. We filosofeerden ook graag over carrière, verschillen tussen medici en postdocs, en meer. Het was erg fijn dat je me overal bij betrok, bij de zeer diverse projecten - al dan niet met succes: een moeizaam case report of juist een mooie paper in samenwerking met Kroatië. Zo was het bezoek aan Platelets in Israël kenmerkend voor onze fijne samenwerking; altijd weer nieuwe ideeën met enthousiasme voor het bloedplaatje voorop. Bedankt hiervoor en voor je betrokkenheid.

**Ruben:** jij was de zeer welkome biologische powerhouse in mijn promotieteam. Zeker in de tweede helft waarin we meer indoken op bijvoorbeeld alpha-granules is jouw intensieve begeleiding van veel waarde geweest; van het tackelen van de commentaren van reviewer 3 tot de discussie en de implicatie van verschillende microscopische analyses. Het was ook leuk dat ik mocht aansluiten bij het endotheel-VWF team en de werkbesprekingen om zo een bredere blik te krijgen. Bedankt voor al je hulp, begeleiding en fijne samenwerking.

Ik zou ook graag de leden van de kleine commissie bedanken voor hun deelname hierin.

**Moniek,** het was altijd leuk om mee te denken over de diagnostiek van bloedplaatjes tijdens de instuurronde en jouw waardevolle input op diverse projecten tijdens de werkbespreking of in de wandelgangen.

**Judith,** het was erg leerzaam om in Maastricht op bezoek te komen en nog een erg leuk experiment met thrombi uit te voeren in mijn laatste jaar. Helaas is dit niet meer in de paper gekomen maar toch in ieder geval in de discussie van dit proefschrift.

**Prof. Langerak**, beste **Ton**, bedankt voor het deelnemen in de kleine commissie en ook voor de kans om in mijn allereerste jaar een keer mee te kijken op het lab voor de isolatie van B-cellen.

De leden van de grote commissie, **Marjon**, **Gestur** en **Johan** zou ik ook erg willen bedanken voor hun deelname hierin.

Ik ben ook heel veel andere collega's van de afdeling Hematologie dankbaar voor hun feedback, hulp en advies: hematologen, professoren, groepsleiders, het secretariaat, de klinici waar ik hulp van had, en nog veel meer mensen.

Alle co-auteurs ben ik ook zeer dankbaar voor jullie feedback, ideeën en hulp bij de diverse artikelen – thank you to all co-authors for your valuable feedback, ideas and help in various publications.

Alle collega's van het Optical Imaging Center (OIC) en specifiek Johan (nogmaals) enorm bedankt voor alle hulp met de verschillende microscopische technieken. Johan voor al je feedback om de SIM methodiek mee op te zetten, het vele brainstormen over hoe het SIM algoritme precies werkt, en het meewerken aan de diverse publicaties. Ook was het erg leuk om een keer te snuffelen aan STED en STORM.

Judith en Titus bedankt voor de mooie thrombi studies, die helaas buiten de discussie niet in dit boekje zijn gekomen.

Bedankt ook Judith en Cilia voor jullie hulp en feedback op het gebied van elektronenmicroscopie.

Thank you to all people from Sanquin I have briefly or intensively collaborated with, especially Maaïke at the start of my PhD. And thanks to Gestur, David & Remco for allowing me to work on ITP B cells in your lab.

### “De 8e”

Voor mij een toch onbekende wereld met veel artsen, klinische studies, correlaties, etc. Hierin ben ik heel prettig opgevangen in het eerste jaar dankzij alle collega PhD's met behulp van de gezellige NVTH's, koffie, en meer. Speciale dank richting Ferdows vanwege jouw ontzettende daadkracht (getuige je eigen dikke boekwerk) en de fijne samenwerking voor diverse hoofdstukken. Natuurlijk ook Chantal voor je leuke studie naar ITP en dat ik hieraan mee kon helpen.

### Office 1330b

Heimwee naar het biologische lab bracht mij naar de 13e; bedankt Leonie (sorry voor mijn macro-flitsen) en Patricia (helaas ben je voor die andere club) als ervaren academici die ik van alles kon vragen. Daarna grafisch expert Dorien, (hardloop-)enthousiasteling

Emma en op het einde ook “praatgroepguru” Sanne voor alle discussies over Friday Floors, koffiemomenten, etc. Zal ik nog eens koffie komen zetten?

### **VWF Lab Ee13**

Thank you all for the fruitful collaborations, always nice to hear about the BOECs and VWF work in parallel. Big thanks especially to Petra for all your help as well as Sophie for the exocytosis work and finally Iris for your help and ever-positive attitude. Isabel and Bas, thank you as well - it was a fantastic treat to go to ISTH 2022 one last time with you all.

### **13th floor**

Thanks to everybody for small-talk in the lab, crazy experiments, quick-and-dirty blood draw, borrels, etc. Particularly grateful towards the technicians for helping with equipment and questions; maybe especially Onno as our techniques overlapped the most and you were closest to bombard with questions initially and later through our shared affinity with imaging.

**Bestuursuitje 5.0** voor de escape rooms en het altijd gezellige bijkletsen alsof we nog steeds allemaal bij Akris spelen. **Omnoms** voor de mooie momenten in Nijmegen en Rotterdam. **Varendonckse Vrinden** voor een gezonde dosis Brabantse gezelligheid. **Kolonisten van d’End** – iemand zin in Risk? **Klusteam #2** - thank you for good times.

**Berlijn** – in mooie en moeilijke tijden, altijd fijn met jullie. Bellen, skypen, bommen ontmantelen, Vitamins, kerstdiners, creepy Agatha Christie verfilmingen, Kuip-bezoekjes en nog veel meer.

**Levensgenieters/Swinkels & Co.** – we zijn nooit zo van de bedankjes en de woorden, maar de onvoorwaardelijke steun en liefde van naaste familie moet toch ooit benoemd worden. Bedankt.

**Inge** – niet alleen ben je mijn nuchtere Brabantse wederhelft, mijn voice of reason, maar ook heb je me ontzettend geholpen bij mijn boekje en om het af te maken. Dankjewel voor alles (ik zal niet té complimenteus doen want daar kan je niet tegen).